

NATURAL VENTILATION OF BUILDINGS

Ralph Edward Bilsborrow,

M.A., Dip. Arch.

A thesis submitted to fulfil the
requirements for the degree of

Doctor of Philosophy

at the

Department of Building Science,

University of Sheffield.

October 1973

SUMMARY

NATURAL VENTILATION OF BUILDINGS

RALPH EDWARD BILSBORROW

The method of ventilation of a building is of considerable importance as it affects many aspects of the design. In order to compare the performance of different ventilation methods, likely ventilation rates need to be accurately predicted. The assessment of realistic rates of natural ventilation, in most buildings, is complex and the value of the current methods available to the designer is dubious.

A survey of previous studies of natural ventilation and infiltration was carried out and it was concluded that most design recommendations are based on the results of digital analogue studies. As the natural ventilation rate calculation methods reviewed make a number of simplifying assumptions which have not been experimentally verified studies were carried out to investigate the validity of these methods. A computer programme, which assumed the normally used simplifications, was written and used in a series of comparative studies. Results from a full-scale study were inconclusive, due to errors in the experimental observations. Consequently a number of controlled model-scale experiments were carried out. Calculated ventilation rates were up to 30% higher than the corresponding observed model ventilation rates. The observed and calculated pressure difference distributions

were also different. The observed pressure drops across the windward faces were, relatively, much larger than their theoretical values. It was shown that the differences between the observed and computed results were caused by reductions in operating efficiency of the ventilation openings with respect to their calibrated efficiencies. Corrected ventilation rates, allowing for changes in efficiency due to pressure fluctuations and lateral air flows over the model surfaces, showed close agreement with the observed results.

Finally, current methodologies for predicting infiltration and natural ventilation rates are discussed and alternative methods of predicting infiltration heat losses and likely ventilation rates are suggested.

LIST OF CONTENTS

List of Illustrations

Nomenclature

Acknowledgements

Chapter	Page
1. Natural Ventilation of Buildings - Introduction	1
2. Natural Ventilation of Buildings - Theory and Practice	9
3. A Critical Appraisal of Previous Studies of Natural Ventilation	44
4. Air Flow Characteristics of Ventilation Openings	89
5. Description of the Digital Analogue Developed to Predict Building Infiltration Rates	112
6. Results of Comparative Full-Scale Ventilation Studies	129
7. Model Ventilation Studies - Experimental Apparatus and Techniques	150
8. Model Ventilation Studies - Results and Discussion	192
9. A Discussion on Design Methodologies	246
10. Conclusions	270

Appendices

Page

- | | | |
|-----|---|-----|
| A1. | A Print-out of the Digital Analogue Programme Developed to Determine Building Ventilation Rates | 281 |
| A2. | An Estimation of the Rate of Loss of Helium Through the Building Openings by Diffusion in Tamura's Full-Scale Ventilation Studies | 294 |
| A3. | Calibration Measurements for the Ventilation Openings Used in the Comparative Model Studies | 299 |
| A4. | Measured External Pressure Coefficients Used in the Comparative Model Studies | 310 |
| A5. | Model Ventilation Studies - Detailed Results | 316 |
| A6. | A Suggested Function to Describe the Variation of Mean Pressure Coefficient with Angle of Incidence | 326 |
| A7. | The Use of the Digital Analogue in Analysing a Simple Combined Natural and Mechanical Ventilation System | 331 |

References

LIST OF ILLUSTRATIONS

The illustrations are placed at the end of each chapter to which they are relevant.

Figure	Title
Pages 38-43	
2.1	Relation between comfort and peak temperature for schools after Langdon and Loudon.
2.2	Theoretical comfort zones after Humphreys.
2.3	Relation between comfort and variability of internal temperature, after Humphreys and Nicol.
2.4	Comfort zones for offices, after Wise.
2.5	Comfort zones for offices, after Wise.
2.6	Sound reduction indices for partially open single and double glazing, after Ford and Kerry.
2.7	Spectrum of horizontal wind speed near the ground, after Van den Hoven.
2.8	Mean wind velocity profiles for surfaces of different roughness, after Davenport.
2.9	Variation of velocity gradient exponent, α , with wind speed and temperature gradient in open country in the first 20 m., after Johnson.
Pages 80-88	
3.1	The effect of wind speed and direction on the air change rate of a house, after Dick.
3.2	The effect of wind speed on the air change rate in a house with a temperature difference of 5.56°C. (10°F.) acting, after Dick.

Figure	Title
3.3	Relationship between observed ventilation rates, wind speeds and temperature differences for two houses, after Bahnfleth et al.
3.4	Schematic building forms assumed representative of typical building types, after Harrison.
3.5	Theoretical ventilation rates in a ten storey building, after Jackman and den Ouden.
3.6	Nomogram for calculating basic infiltration rate in buildings, from the I.H.V.E. Guide, 1970.
3.7	A comparison of measurements of pressure coefficients on a model building with estimates from B.R.S. Digest 119 and A.S.H.P.A.E. Infiltration Algorithm.
3.8	A summary of the variables used in the digital analogue ventilation studies discussed previously.
3.9	The effect of variation of exponent, n , and coefficient reference pressure difference on air flow rates through windows over an assumed working range of 1-6 mm.wg. pressure difference.

Pages 106-111

4.1	Infiltration through window gaps, after Dick and Thomas.
4.2	Orifice discharge coefficients for narrow slit openings at different Reynolds numbers, after Lenkei.
4.3	Variation of air flow rate with pressure difference for a simple opening, after Dick and Thomas, and Lenkei.
4.4	Infiltration through window gaps, after Lenkei.

Figure	Title
4.5	Variation of infiltration coefficient, C, and flow exponent reciprocal, after Lenkei, and Dick and Thomas.
4.6	Infiltration rates for standard windows: design figures, and variability, after Jackman.
Pages 124-128	
5.1	Flow chart for building ventilation prediction program, BT5VENT4.
5.1(a)	Calculation of ventilation rates due to wind alone, floors considered in isolation.
5.1(b)	Calculation of neutral zone height.
5.1(c)	Calculation of combined ventilation rates.
5.2	Typical plan forms suitable for analysis by BT5VENT4.
Pages 145-149	
6.1	Plan of house No. 1, after Tamura and Wilson.
6.2	Comparison of observed ventilation rate with wind speed, after Tamura and Wilson.
6.3	Assumed pressure coefficients based on B.R.S. Digest 119.
6.4	Comparison of computed ventilation rate with wind speed.
6.5	Comparison of lines of best fit for observed and computed results assuming an exponential relationship between wind speed and ventilation rate.
Pages 179-191	
7.1	Wind tunnel details.

Figure	Title
7.2	Section through internal pressure measurement model; 2.5 mm. diameter openings.
7.3	Exploded view of internal pressure measurement model, showing external pressure measuring positions and ventilation opening grid.
7.4	Section through orifice plate model.
7.5	Detail section through orifice plate.
7.6	Schematic layout of orifice plate calibration equipment.
7.7	Calibration of standard orifice plate.
7.8	Calibration of orifice plate model, showing the effect of the model front plate.
7.9	Calibration of orifice plate model, with model back plate in position.
7.10	Orifice plate model mounted in the wind tunnel with the surface roughness in position.
7.11	Variation of velocity and turbulence intensity with height in model tests.
7.12	Experimental apparatus used with the orifice plate model.
7.13	Schematic layout of model ventilation rate measurement apparatus.

Pages 224-245

8.1	Observed model pressure coefficients at different angles of incidence.
8.2	Opening positions used to evaluate variation of internal pressure with opening configuration.
8.3	Observed and computed internal pressures, opening configuration A, boundary layer I.

Figure	Title
8.4	Observed and computed internal pressures, opening configuration B, boundary layer I.
8.5	Observed and computed internal pressures, opening configuration C, boundary layer I.
8.6, 8.7	Variation of observed and computed mean internal pressures with angle of incidence of air flow, opening configuration C, 9 x 2.5 mm. openings/face.
8.8, 8.9	Variation of observed and computed mean internal pressures with angle of incidence of air flow, opening configuration C, 3 x 2.5 mm. openings/face.
8.10, 8.11	Variation of observed and computed mean internal pressures with angle of incidence of air flow, opening configuration C, 1 x 2.5 mm. openings/face.
8.12, 8.13	Variation of observed and computed mean internal pressures with angle of incidence of air flow, opening configuration C, 36 x 1.0 mm. openings/face.
8.14, 8.15	Variation of observed and computed mean internal pressures with angle of incidence of air flow, opening configuration C, 12 x 1.0 mm. openings/face.
8.16, 8.17	Variation of observed and computed mean internal pressures with angle of incidence of air flow, opening configuration C, 4 x 1.0 mm. openings/face.
8.18	Variation of pressure difference ratio, and relative orifice operating efficiency, with angle of incidence, 2.5 mm. openings.
8.19	Variation of pressure difference ratio, and relative orifice operating efficiency, with angle of incidence, 1.0 mm. openings.

Figure	Title
8.20	Variation of observed and computed ventilation rates with air velocity, opening configuration C, 9 and 15 x 2.5 mm. openings/face, boundary layer I.
8.21	Variation of observed and computed ventilation rates with air velocity, opening configuration C, 9 and 15 x 2.5 mm. openings/face, boundary layer II.
8.22	Variation of observed and computed ventilation rates with air velocity, opening configuration C, 36 and 60 x 1.0 mm. openings/face, boundary layer I.
8.23	Variation of observed and computed ventilation rates with air velocity, opening configuration C, 36 and 60 x 1.0 mm. openings/face, boundary layer II.
8.24	Variation of relative ventilation rate with angle of incidence, 2.5 mm. openings.
8.25	Variation of relative ventilation rate with angle of incidence, 1.0 mm. openings.
8.26	Variation of non-dimensional ventilation rate, with angle of incidence.
8.27	Variation of computed orifice operating efficiency with magnitude of pressure fluctuations.
8.28	Variation of average R.M.S. pressure coefficient with angle of incidence.
8.29	Variation of orifice operating efficiency with lateral flow velocity.
8.30	Variation of mean lateral flow velocities, with angle of incidence.

Pages 265-269

9.1	Variation of design wind speed with external temperature at Abbots Langley.
-----	---

Page

Title

- 2.2 Nomogram for predicting wind induced infiltration.
- 2.3 Nomogram for predicting stack induced infiltration.
- 2.4 Variation of maximum combined ventilation rate with position and relative magnitude of wind and stack effects.
- 2.5 Suggested nomogram for estimation of maximum ventilation rates available for environmental control in summertime.

NOMENCLATURE

A list of the nomenclature used in the thesis is given below. The list covers the nomenclature used in the main part of the thesis and the appendices, apart from Appendix A1. In this appendix a separate list describing the variable names used in the digital analogue for calculating natural ventilation in buildings is given.

The units used are given in the listing. Throughout the thesis air flow rates and pressures are presented in units of $\text{m}^3/\text{hr.}$ and mm.wg. respectively, as these types of unit are most commonly used in work on ventilation in buildings. These units may be converted to the appropriate S.I. units using the conversion factors:

$$1 \text{ m}^3/\text{hr.} \equiv 0.278 \text{ l/s.}$$

$$1 \text{ l/s.} \equiv 3.60 \text{ m}^3/\text{hr.}$$

$$1 \text{ mm.wg.} \equiv 9.81 \text{ N/m}^2$$

$$1 \text{ N/m}^2 \equiv 0.102 \text{ mm.wg.}$$

List of Nomenclature

Symbol		Unit
A	Area	m^2
A'	Total leakage coefficient for windward face of building, at 1 mm.wg. pressure difference.	$\text{m}^3/\text{hr.}$
B'	Total leakage coefficient for leeward face of building, at 1 mm.wg. pressure difference.	$\text{m}^3/\text{hr.}$
C	Window crack air leakage coefficient, at 1 mm.wg. pressure difference.	$\text{m}^3/\text{hr/m.}$

Symbol		Unit
C_D	Mean difference in pressure acting across a building, expressed as a pressure coefficient, (proportion of the dynamic head of the air velocity, P_v).	
C_p	External pressure, expressed as a pressure coefficient.	
C_{pd}	Difference in mean pressures on opposite building faces, expressed as a pressure coefficient.	
C_{pm}	Average of mean pressures on opposite building faces, expressed as a pressure coefficient.	
C_{p_i}	Internal pressure expressed as a pressure coefficient.	
C_{p_l}	Mean pressure on leeward face expressed as a pressure coefficient.	
C_{p_w}	Mean pressure on windward face expressed as a pressure coefficient.	
C_Z	Orifice plate coefficient of discharge.	
c	Equilibrium tracer gas concentration, proportion by volume.	
c_0	Initial tracer gas concentration, proportion by volume.	
c_t	Tracer gas concentration after time t , proportion by volume.	
D	Orifice plate, pipeline diameter.	mm.
D_o	Orifice plate, orifice diameter.	mm.
ΔP	Pressure difference.	mm.wg.
ΔT	Temperature difference.	$^{\circ}C$.
E	Coefficient for estimating flow similarity in model studies.	m^2/s .
e_l	Mean ventilation opening operating efficiency relative to calibrated efficiency, openings in leeward face.	
e_w	Mean ventilation opening operating efficiency relative to calibrated efficiency, openings in windward face.	

		Unit
V_o	Orifice plate velocity of approach factor.	
g	Gravitational constant.	m/s^2 .
H	Height	m.
h_o	Roughness height.	m.
h_g	Gradient height.	m.
I	Infiltration rate or ventilation rate through a building.	$hr.^{-1}$
K	von Karman's constant.	
L	Window crackage length.	m.
l	Flow length of air path through section of window crack.	mm.
n	Number of ventilation openings/model face.	
n	Reciprocal of exponent value used in estimating air leakage through ventilation openings.	
P_v	Dynamic head of free stream air velocity at a height equal to the building roof height.	mm.wg.
p	Air pressure	mm.wg.
q	Perimeter of exposed building face past which air flows.	m.
q_c	Rate of release of tracer gas, proportion by volume.	$hr.^{-1}$
q_t	Total quantity of tracer gas released at a reference position, proportion by volume.	
Re	Reynolds number.	
R_h	Hydraulic radius.	mm.
r	Opening radius.	mm.
T	Temperature.	$^{\circ}C$.
t_a	Air temperature.	$^{\circ}C$.

Symbol		Unit
t_{ei}	Environmental temperature.	$^{\circ}\text{C}$.
t_{eq}	Equivalent temperature.	$^{\circ}\text{C}$.
t_g	Globe temperature.	$^{\circ}\text{C}$.
t_r	Mean radiant temperature.	$^{\circ}\text{C}$.
u	Air velocity in wind tunnel tests.	m/s.
V	Volumetric air flow rate.	m^3/hr .
V_m	Molecular velocity.	m/s.
V_o	Volume.	m^3
W	Wind speed.	m/s.
W'	Air velocity.	m/s.
W_g	Gradient wind speed.	m/s.
W_h	Wind speed at a height h above ground level.	m/s.
W^*	Friction velocity.	m/s.
\bar{w}	Window crackage width.	mm.
α	Exponent value in logarithmic wind velocity profile.	
ϵ	Orifice plate expansibility factor.	
λ	Mean free path length of helium molecules at N.T.P.	m.
μ	Dynamic viscosity of air.	$\text{N}\cdot\text{s}/\text{m}^2$.
ρ	Density.	kg/m^3 .
τ_o	Surface shear stress.	N/m^2 .
θ	Angle of incidence between mean air flow direction and a normal to the building face being considered.	degrees

ACKNOWLEDGEMENTS

I would like to thank Dr. F.R. Fricke, my supervisor for the greater part of the time during which I was carrying out this work, for his sympathetic guidance. In particular I would like to thank Dr. Fricke for his advice and constructive criticism during the execution of the model studies and the writing of the thesis.

In the initial period of the research my supervisor was Dr. T.D. Brown. I would like to thank him for his help and encouragement, especially in relation to the development of the digital analogue.

I want also to express my gratitude to Professor J.K. Page and the other staff and students of the Department of Building Science for their valuable suggestions, and to the technical staff, Mr. R. Webster, Mr. A. Shale, Mr. C. Hardwick, Mr. D. Laycock, Mr. M. Broady and Mr. T. Thomas for their assistance in constructing models and altering the wind tunnel used in the comparative studies.

Miss L. Millar typed this thesis and I would particularly like to acknowledge the care and diligence with which she carried out this work.

The help of the Science Research Council who provided the research studentship is also gratefully acknowledged.

Finally, I should like to thank my wife for her patience, understanding and encouragement during the period of my research.

1. NATURAL VENTILATION OF BUILDINGS - INTRODUCTION

1.1 The importance of ventilation

1.1.1 It was stated at the 1972 R.I.B.A. Conference that about 40% of the energy used in this country is used in the construction and operation of its buildings. A considerable proportion of this expenditure is concerned with controlling the internal environment of buildings, and environmental conditions are inevitably affected by the nature of the ventilation which is available. Some ventilation is required in all occupied spaces in order to control the levels of undesirable contaminants. In many cases much greater rates of ventilation are needed to control internal temperatures by removing excess heat. At other times, in cold weather, the amounts of ventilation occurring in many buildings may be considerably in excess of the minimum requirements. These conditions alter the costs of operating any building both directly, by affecting the heat requirements in winter and the need for artificial environmental control in summer, and indirectly by affecting the comfort of the occupants.

1.1.2 The building designer today has a rapidly expanding field of technology to assist him in solving his problems. However the complexity of the situations which he must control in his design work are greater than ever before because of the higher requirements of

performance, the often more difficult external environment with which he has to contend and even because of the presence of this more powerful technology. The availability of this technological ability implies that the designer has a considerably greater degree of choice in the method with which he may attempt to balance his design constraints. Furthermore he must be able to provide a solution which is demonstrably able to provide the standards of comfort, economy and performance which are required. Consequently it is often necessary to provide accurate comparisons of the likely performance of different methods for solving the same problems, and so the importance of methods for assessing, quantitatively, the performance of building systems has increased significantly in recent years. This type of comparison is often of the greatest importance when considering the alternative methods of ventilating a building.

2.1.3 A building can be ventilated using natural ventilation, mechanical ventilation or air conditioning. The choice of technique used to control the internal climate of the building is of fundamental importance as this decision normally affects many of the other characteristics of a solution. The type of ventilation used often dictates permissible building depth, and this in turn, will affect many other principles of design on which the building may be based. The type of

ventilation may also influence the degree of sophistication with which the internal environment can be controlled. Air conditioning and mechanical ventilation present the user with much more closely controllable internal conditions; natural ventilation is dependent upon external conditions which are highly variable and so such close control of internal conditions is not possible. Finally air conditioning and mechanical ventilation also represent additional capital and running costs which must be added to other costs. With some types of building this cost may be wholly or partially recovered because of the possible alterations which can be made in other aspects affecting the economy of the design. There are many types of building where air conditioning or natural ventilation may be obvious choices because of the overriding influence of other design constraints, such as noise or building cost limits. However there are many types of building where an adequately controlled internal environment may be economically produced using any of several methods, and in these cases quantitative comparisons must be made.

1.1.4 As has been shown above the decision on a method of ventilation for a building may have a great influence on many other aspects of the final design. Quantitative estimates of likely ventilation rates under different conditions may be required for several reasons,

some of which are:

- a) to determine more accurately the design constraints, such as building depth, or maximum glazed area, imposed by the assumption of the use of natural ventilation with a specified quality of environmental control;
- b) to enable the quality of environmental control possible in a naturally ventilated solution to be estimated, so that a comparison of environmental quality can be made between naturally ventilated and mechanically ventilated or air conditioned solutions, as well as a comparison of capital costs;
- c) to evaluate likely running costs due to infiltration, so that decisions on such features as facade design may be made. Capital cost of window units must be correlated with running costs due to infiltration heat losses, in order to decide logically the desirable window air-tightness standards;
- d) to assist in the development of new ventilation systems, practical experience of which may not be available.

Although the principles of natural ventilation are simple to understand, the prediction of realistic rates in complex buildings under varying design conditions is much more difficult. Far less assistance is available

of the designer to help him predict appropriate ventilation rates under such conditions than is available for other aspects of environmental design. Consequently in this thesis, in an attempt to improve the quality of the information available, the methods suitable for predicting natural ventilation conditions in buildings have been investigated.

1.2 The pattern of investigation

1.2.1 In the first part of the thesis, chapters 2 - 4, the predictive techniques that are currently available and the knowledge on which they are based is reviewed. This work was carried out in order to establish the most useful techniques and the accuracy of the information available for use with the techniques, so that estimates could be made of the accuracy of these methods and the areas in which there is most uncertainty. In Chapter 2 ventilation theory, as it is used in practical design methods, is reviewed. The ventilation requirements of buildings are established, the forces which produce ventilation considered, and the recommended methods for establishing ventilation rates presented. In Chapter 3 the studies which have been carried out in order to attempt to verify or contribute to ventilation theory are reviewed. The studies are classified broadly into full scale studies on existing buildings and various analogue studies, and

a comparison of the accuracy and validity of the studies is made. In the fourth chapter the information available, describing the air leakage characteristics of building construction, is reviewed. The most useful ways of expressing leakage characteristics, and the dependability of the information available are considered.

1.2.2 The results of the work carried out in the first section of the thesis suggest that the predictive techniques which are currently available are being increasingly based on digital analogue methods of predicting ventilation rates. These methods assume that quasi-static pressures act over the surfaces of a building and produce steady rates of natural ventilation. Analyses of the internal flow patterns and rates of flow in the building are then carried out, assuming the building to consist of a network of cells each presenting specific values of flow resistance. The accuracy of the assumptions made in this type of analysis have not been verified in any comparative experiments, a serious omission which, it was thought, required investigation before design recommendations could validly be made using such techniques. Consequently in the second section of the thesis, Chapters 5 - 8, an attempt was made to investigate the inherent accuracy of the assumptions made in these methods. From this analysis an attempt

was made to establish the likely accuracies of these predictive methods and consequently the degree of sophistication required in the analysis and its data requirements.

1.2.3 A simple computer programme for determining flow patterns in multi-storey buildings, which uses the assumptions made in the similar programmes from which predictive techniques are being established, was written. The programme is described fully in Chapter 5. The programme was then used in a number of controlled comparative studies. In Chapter 6 a comparison between the results of a full-scale study and the digital method are presented and discussed. In Chapters 7 and 8 the results of a series of comparative model and theoretical studies are described and discussed. Because of the need to use model studies to obtain strictly controlled conditions it was necessary to restrict the comparisons to those concerning wind induced ventilation only, as stack-induced ventilation could not be adequately modelled. From these experiments conclusions concerning the accuracy and the data requirements of these analogue techniques were drawn.

1.2.4 In the final section of the thesis consideration was given to the development of design methods most appropriate to the prediction of natural ventilation of buildings. The present design methods were considered

and suggested improvements to the design methodologies made. Finally in Chapter 10 the conclusions reached in the thesis were summarised and the areas in which most uncertainty exists, and their relevance to present predictive methods, discussed.

2. NATURAL VENTILATION OF BUILDINGS - THEORY AND PRACTICE

2.1 Introduction

2.1.1 Ventilation occurs in all types of buildings; some takes place by design, because of the deliberate provision of openings in the building fabric, and some by chance, because of cracks in the fabric. Where ventilation is caused by natural motive forces, normally differential wind pressures or differences in air density between the air inside the building and that outside it, acting across openings in the building, it is known as natural ventilation. When the ventilation is produced by mechanical systems it may be known as mechanical ventilation or air conditioning. Some ventilation will also normally occur when all the openings through which ventilation normally takes place are nominally closed. This type of ventilation, the natural ventilation occurring under extreme conditions of maximum practical air-tightness of the building, is usually referred to as infiltration.

2.1.2 The general principles which operate to produce natural ventilation in buildings have been appreciated for a considerable time. The natural forces of wind or buoyancy act to produce pressure differences across elements of the building. The relative resistances to flow of the various openings through which flow can occur, dictate the pattern of air flow through the

building. The magnitude of the pressure differences and the flow resistances dictate the rates of air flow through the building. In practice the predictions of detailed quantitative air flow rates for a particular example can often be very complex. As the forces which act to cause natural ventilation occur naturally they are likely to be variable and difficult to represent accurately. The complexity of possible patterns of ventilation which might occur becomes very considerable in a large building and the effects of various inaccuracies in the predictive method become correspondingly more difficult to evaluate. Furthermore, the amount and effectiveness of the ventilation will normally vary over a large range in a building of any complexity.

2.1.3 The techniques used to describe quantitatively the ventilation in any space must also be complex if they are to describe adequately the effectiveness of the ventilation. The simplest measure of ventilation used is the volume of the ventilating air supplied. This measure is more often expressed as an air change rate; a volume flow rate expressed in terms of the room or building volume being considered. A crude measure of this type may be of use in simple cases, such as the calculation of total thermal loads for a building, but for more complex requirements, for example the evaluation of comfort conditions and detailed thermal

loads for individual spaces, air change rates in many parts of the building will be required. Even this level of information is far from ideal as a full description of the ventilation occurring in a building. In particular, ventilating air which enters a space from another part of the building may be very different in its physical properties, especially its thermal and hygienic condition, to air entering the room from outdoors. This aspect is particularly important in hospitals where control of bacterial content may be of the utmost importance.

2.1.4 In enclosed spaces with limited areas for the admission and extraction of ventilating air the ventilation rates throughout the various sections of the space will often vary. Thus the effectiveness of the new air for ventilating a space will depend not only on its flow rate but also on the efficiency of the mixing of the new air with the old. In conditions where the new air being introduced to a space is perfectly mixed with the old air, approximately 63 per cent of the old air in the room will be replaced in unit time when the nominal air change rate is unity. If, with the same rate of supply of fresh air, no mixing takes place there could be no effective replacement of the old air, although the nominal ventilation rate would be the same as in the previous case. In calculations of ventilation requirements or performance, conditions are normally

assumed to approximate to perfect mixing. Accurate theoretical verification of this assumption for any particular situation is not practicable at the present time, and no fully comprehensive studies of intra-room mixing were noted by Hitchin and Wilson (Hitchin, 1967) in a survey of experimental techniques. However, they summarised the results of several workers who had investigated the variation of apparent ventilation rate with positions in naturally ventilated rooms. In most cases the maximum variations were within 10 per cent of the mean rate, which suggested that reasonably good mixing was taking place in the test rooms. The variations tended to be higher in the tests carried out with lower mean ventilation rates, and it is possible, particularly in conditions of relatively low ventilation rate, that significant variations in quality of mixing occur throughout single rooms.

2.1.5 An expression has been developed to describe the effectiveness of a ventilation system with respect to air transfer from one area of a room to another, and is known as the transfer index (Lidwell, 1960 a). The index is defined numerically as:

$$\text{transfer index} = \frac{c}{q_c} \quad \dots \quad (2.1)$$

where c is the equilibrium concentration of
contaminant at a study position

q_c is the rate of continuous release of
contaminant at a reference position.

or alternatively as:

$$\text{transfer index} = 1/q_t \int_0^{\infty} c_t \cdot dt \quad \dots\dots (2.2)$$

where c_t is the contaminant concentration at time t
at a study position

q_t is the total quantity of contaminant
released at the reference position.

The index, which is obviously applicable to tracer gas measurement techniques, refers to the air movement characteristics between any two specific points in a room. The index has been used to describe the results of specialised observation of contamination transfer in operating theatres (Lidwell, 1960 b), but is too specific for general use.

2.1.6 In practice ventilation rates must still be designated in terms of air supply rates or air change rates, as these are the only types of expression which can be assessed sufficiently easily to be of use in quantitative estimates. This type of specification is the simplest technique for describing ventilation conditions. Other factors, in particular the previous history of the supply air, may have to be considered to achieve an accurate assessment of the effectiveness of the ventilation.

2.2. Ventilation requirements in buildings

2.2.1 Some ventilation is necessary in most types of buildings in order to maintain comfortable conditions for human occupation. Replacement of air may be required for four reasons which affect the comfort of the occupants. These are:

- a) to provide adequate oxygen for breathing and to remove excess carbon dioxide;
- b) to remove normal occupation products, generally odours, from the air;
- c) to remove any specific artificial contaminants which may be produced in the environment;
- d) to assist in controlling the thermal conditions in the space.

Statutory regulations concerning the ventilation of buildings are normally based on the provision of adequate means to ensure the minimum amount of ventilation which will satisfy the first three requirements. In many buildings however the use of ventilation to control thermal conditions may be more influential in determining the environmental acceptability of the building under normal conditions.

2.2.2 The provision of ventilation to satisfy requirements for respiration is related directly to the number of occupants in the building. A design figure for this type of ventilation is $3.6 \text{ m}^3/\text{hr./person}$, (I.H.V.E., 1970). This figure is considerably lower

than the requirement for the control of odours at normal occupancy levels and consequently is generally not the determining factor for calculating minimum ventilation rates. The amount of ventilation required for the removal of normal products of occupation, in particular body odours, is more complex to determine. It is taken to be related to the type and level of occupancy (persons/m³) in the space under consideration. Recommended minimum ventilation rates for different conditions of occupancy are given in Table 2.1, the

TABLE 2.1 Recommended minimum ventilation rates to control occupation products, (after I.H.V.E. Guide 1970 and A.S.H.R.A.E. Handbook of Fundamentals), m³/hr./person.

Space allocation m ³ /person	A.S.H.R.A.E. Handbook of Fundamentals, adults of average socio-economic status	I.H.V.E. Guide, non- smoking areas	I.H.V.E. Guide, smoking permitted	Equivalent air change rate,/hr.
3	45.0	40.6	61.0	14 - 20
6	28.8	25.4	38.5	4 - 6
9	21.6	18.6	28.0	2 - 3
12	-	14.4	21.5	1.2 - 1.8
15	12.6	-	-	0.8

figures being taken from the I.H.V.E. Guide 1970, and the A.S.H.R.A.E. Handbook of Fundamentals (A.S.H.R.A.E., 1972). Requirements for removal of specific artificial

contaminants may occur in many specialised types of building (typical examples being kitchens, laundries and certain types of laboratories). These cases must be considered individually in order to lay down suitable minimum ventilation rates.

2.2.3 Ventilation is often used to help control the thermal balance of buildings. Several different comfort criteria are used in describing desirable thermal conditions in buildings. Of these the more important are the air temperature, equivalent temperature, globe temperature and environmental temperature. These indices are described by the following relationships:

Air temperature: t_a

Environmental temperature: $t_{ei} =$

$$0.667t_r + 0.333t_a \quad \dots\dots (2.3)$$

Equivalent temperature: $t_{eq} =$

$$0.522t_a + 0.478t_r - 0.21(37.8 - t_a)W \quad \dots\dots (2.4)$$

$$\text{Globe temperature: } t_g = \frac{t_r + 2.35t_a W}{1 + 2.35 W} \quad \dots\dots (2.5)$$

where t_r represents mean radiant temperature, $^{\circ}\text{C}$

W represents mean air speed, m/s.

Of these criteria the air temperature is the least satisfactory index, but is often used because of its simplicity. The environmental temperature, a modified globe temperature assuming constant air velocity, has been developed recently for use in calculating comfort

conditions in buildings (Loudon, 1968). It has been developed as a compromise index, being sufficiently accurate to give reasonable comfort predictions and sufficiently simple to use in analytical design methods. The equivalent temperature and globe temperature are more complex indices, and are not normally used for specifying building performance requirements. Both these indices are affected by the air movement rate. Under normal conditions the change in either comfort index value directly due to change in air velocity is likely to be much smaller than that due to the change in air temperature caused by replacing old air with cooler outside air (Humphreys, 1970 a). In practice then the effect of the ventilation, in terms of controlling thermal comfort, will normally be assessed by its effect on the internal temperatures.

2.2.4 A considerable number of investigations have been carried out in recent years into comfort conditions in naturally ventilated buildings. This has been done in an attempt to find relevant comfort criteria and to improve prediction methods. It has been shown (Langdon, 1965), (Kibblewhite, 1967) that many occupants of this type of building suffer appreciable discomfort due to overheating. Surveys (Loudon, 1968), (Langdon, 1970) have correlated perceived comfort conditions with calculated peak environmental temperatures (Figure 2.1). Langdon and Loudon suggested from their survey of schools

that a peak environmental temperature of 30°C will result in less than 10% of the building population suffering serious discomfort. Meanwhile more recent work (Humphreys, 1970 a), (Humphreys, 1970 b) suggested that the long-term, monthly, mean internal temperature may be varied over quite large ranges without significantly altering the acceptability of an environment. They showed that over a range of mean globe temperatures between 18°C and 30°C there is little change in perceived comfort. This tolerance, they suggest, is due to the fact that the individual will be able to choose his clothing to suit the mean internal temperatures (Figure 2.2). Humphreys et al also suggested that comfort is much more closely related to the short-term variation in internal temperature and suggest comfort criteria based on this (Figure 2.3). Their suggested criterion is that the monthly standard deviation of the globe temperature, during working hours, should not exceed 1°C. This implies that the globe temperature should be maintained within a range of 4°C for 95% of the working hours for any one month. Wise (Wise, 1973) has extracted, largely from the above work, comfort criteria for naturally ventilated office buildings. These are:

a) for a high environmental standard,

$$t_{ei} = 24^{\circ}\text{C} \pm 2^{\circ}\text{C} \quad \dots (2.6)$$

b) for an acceptable environmental standard,

$$t_{ei} = 25^{\circ}\text{C} \pm 4^{\circ}\text{C} \quad \dots (2.7)$$

The mean temperatures are taken from Humphreys' chart (Figure 2.2), assuming sedentary workers.

2.2.5 The effect of ventilation rates on the likely internal temperatures in buildings can be assessed using the method of calculation derived at the Building Research Station, (Loudon, 1968) and now used in the I.H.V.E. Guide. A series of simple design charts, showing the effect of the major factors affecting internal temperatures for a small office, have been produced (Wise, 1973). Some of these are shown in Figures 2.4 and 2.5. The importance of being able to guarantee a minimum ventilation rate under unfavourable conditions can be clearly seen in the design situations.

2.2.6 The requirements for the sound reduction indices of building facades are of increasing significance in restricting the maximum amount of window opening permissible in naturally ventilated buildings. Road traffic noise was shown to be one of the greatest sources of annoyance to people in the London Noise Survey, 1961-62 (Wilson, 1963) and it is likely that this situation will continue. The sound reduction index of a facade is reduced very considerably by the introduction of quite small open areas, and this phenomenon tends to restrict window opening habits. Some evidence of this effect is shown in the results of a survey of schools by the Building

Research Station, (Langdon, 1970) which are summarised in Table 2.2. Respondents from many schools were asked whether they were "sometimes too hot", and the results were classified with respect to type of ventilation and quietness of the environment. The results show clearly that fewer users from quiet areas suffered from overheating, suggesting that users in noisy areas restricted their window opening habits because of the noise and consequently were liable to become uncomfortably hot.

TABLE 2.2 The effect of noise on comfort in naturally ventilated schools, after Langdon and Loudon.

External conditions	Noisy	Noisy	Quiet	Quiet
Internal conditions	Noisy	Quiet	Noisy	Quiet
Single sided ventilation % sometimes too hot	58	51	57	42
Cross ventilation % sometimes too hot	49	36	38	27

2.2.7 The use of staggered opening double glazing has been suggested as a means of maintaining an acceptable level of sound attenuation, while allowing the use of natural ventilation. The sound reduction indices of single and double glazing for varying amounts of open area are given in Figure 2.6, after measurements made by Ford and Kerry (Ford, 1973). The measurements were made using a spectrum typical of road traffic

noise. The use of this technique allows greater open areas of facade to be used while retaining the same acoustical performance. This advantage is offset to some extent by the greater resistance to flow of this type of window, although the presence of the double glazing will reduce the thermal load on the building.

2.2.8 Ventilation requirements can be seen therefore, to be dependent on many factors. In winter conditions ventilation rates are normally determined by contaminant control requirements, which are related to the type and density of occupation. In summer thermal control is more commonly the determining requirement. In these conditions requirements are related to the thermal mass of the building, the type and amount of glazing and the internal sources of heat, factors which determine the thermal load; and to the acoustical environment of the building which limits the amount of window area which is available to achieve ventilation.

2.3 Factors influencing natural ventilation

2.3.1 The two main factors which produce natural ventilation in buildings are the differential pressures caused by air movement around the building, and the pressures caused by differences in buoyancy of the internal and external air. A third factor which causes ventilation is turbulent diffusion. This effect is normally of secondary importance, but may be

important in some cases, for example in rooms where there is no cross ventilation. In order to accurately assess the pattern of ventilation these pressures and the processes by which they are caused must be accurately described.

2.3.2 The magnitude of the differential pressures caused by wind are determined by the wind speed and direction. Wind speeds and directions vary almost constantly in normal atmospheric conditions, so that they are best described statistically by a mean wind speed and a spectral distribution. A typical spectrum, measured by Van den Hoven (Van den Hoven, 1957) is given in Figure 2.7. It can be seen that the stability of the atmospheric wind is very high in the spectral gap, centred on a period of 10-60 minutes. The performance of ventilation systems is normally specified with relation to removal of contaminants or excess heat, and consequently, is assumed to be unaffected by short-term variations in flow rate; as the resulting variations in contaminant concentration or temperature in the room will normally be imperceptible. Consequently a design wind speed averaged over a time in the spectral gap region is normally used and the effect of turbulence is ignored.

2.3.3 In terms of specifying design wind speeds for ventilation calculations the mean wind speed profile is also required. Wind speed increases with height and

the rate of increase, or the shape of the wind speed profile, is dependent upon the type of terrain over which the wind has flowed and upon the atmospheric stability. This variation in velocity has been studied extensively, (Davenport, 1967; Harris, 1970; Jensen, 1963). Above the layer of frictional influence of the earth, which extends for 300 m. - 600 m., the air moves solely under the influence of the pressure gradients and moves at the 'gradient' velocity. Closer to the ground the air flow is slowed down by the drag forces at the surface and by the turbulent flow conditions, which also create momentum exchanges between the layers of the air flow.

2.3.4 In conditions of neutral stability the variation of velocity with height can normally be adequately modelled by the Prandtl logarithmic profile (Jensen, 1963):

$$\frac{W_h}{W_*} = \frac{1}{k} \cdot \log_e \frac{h}{h_0} \quad \dots\dots (2.8)$$

where W_* is a friction velocity, defined as $\sqrt{\frac{\tau_0}{\rho}}$ (where τ_0 is the shear stress at the surface), and is dependent only upon the roughness of the surface and the free wind speed. h_0 is the roughness height, a parameter descriptive of the heights of the irregularities in the surface and

has been found empirically for different surface roughnesses. k is von Karman's constant, 0.4.

The profile agrees well with experimental measurements for heights up to 50 - 100 m., but over that height or in conditions other than those of neutral stability the observed profiles show significant departures from this form (Davenport, 1965 a).

2.3.5 Under most strong wind conditions it has been shown (Davenport, 1965 a) that an equally reliable prediction of the mean wind conditions can be given using the much simpler, but empirically derived, power law profile:

$$\frac{W_h}{W_{h'}} = \left(\frac{h}{h'} \right)^\alpha \quad \dots\dots (2.9)$$

In particular, relating wind speeds to the gradient wind speed, W_g , and the gradient height, h_g ;

$$\frac{W_h}{W_g} = \left(\frac{h}{h_g} \right)^\alpha \quad \dots\dots (2.10)$$

Empirical measurements have established that the gradient height, h_g , and velocity profile exponent are related to the type of surface over which the flow has travelled. Davenport (Davenport, 1967) has summarised the data from many studies and suggests the values of h_g and α shown in Table 2.3.

TABLE 2.3 Average values of exponent, α , and gradient height, h_g , for use in exponential wind speed profiles, after Davenport.

	α	gradient height, m.
Flat open country	0.16	280
Rough wooded country, Suburban areas.	0.28	400
Heavily built-up urban areas	0.40	430

2.3.6 This type of treatment may be used to estimate approximate relationships for flow above these types of terrain (Figure 2.8) but does not give accurate estimates of flow conditions below the roughness height. In this region flow patterns are more complex, no well-defined general relationships exist and conditions are dependent upon the detailed configuration of the nearest obstacles. Harris, (Harris, 1972) indicates that in heavily built-up areas the velocity gradient can be fitted better by assuming a displaced ground level, or displacement height, which is normally of the same order of height as the mean height of the obstructions. The profile can then be expected to be of exponential form to within approximately 1.5 times this height. Values of the flow characteristics within the displacement height are not well established for urban conditions. Values calculated assuming no displacement height are generally used (I.H.V.E., 1970) as the values so calculated give

conservative values for design wind speeds.

2.3.7 Under conditions of less extreme wind speed the profile of the mean wind speed near the ground also varies with the thermal stability of the atmosphere and the mean wind speed. Observed changes in the velocity gradient near the ground with varying wind speed on a site in open country are shown in Figure 2.9 (Johnson, 1948). Generally the shape of the velocity profile tends to remain constant with wind speed at higher wind speeds. At low wind speeds the steepness of the velocity gradient tends to become greater (Johnson, 1948; Geiger, 1966). The shape of the wind speed profile is also affected by the vertical temperature gradient, and the relationship between profile and temperature gradient for a site in open country is also shown in Figure 2.9 (Johnson, 1948). Over the range of mean monthly temperature gradients for south east England (Best, 1952) for a height range of 1 m. - 47 m. the exponent for open country might be expected to vary between 0.13 and 0.18 due to this effect. Under most conditions this alteration of the velocity profile would probably only be significant in the range 0-50 m. At greater heights, in open country, at least, the temperature is much more stable, and consequently the velocity gradient may be expected to be relatively constant. The effect of these microclimatic influences is likely to be even more complex in the urban situation.

The influence of these factors on the wind climate is usually much less significant than the sheltering effect of the ground roughness. Consequently these factors are not normally taken into account in estimating design mean wind speed; however this is an omission which will lead to additional uncertainties in estimating design speeds, especially in conditions of low wind speed.

2.3.8 Once the mean wind speed and velocity gradient of the wind at a building site is determined, the relative aerodynamically induced pressures over the building must be estimated. The pressures cannot be adequately calculated theoretically but can be estimated from the results of the many studies of pressure distributions which have been carried out on wind tunnel models. The accuracy of model pressure predictions has been well established (Whitbread, 1965; Dalglish, 1967; Newberry, 1968), and the effect of building shape, velocity profile and local obstructions on determining these pressures is fairly well documented (Chien, 1951; Baines, 1965; Bailey, 1943). These pressures are normally expressed as pressure coefficients, C_p , which are defined as:

$$C_p = \frac{(p - p_{ref}) \cdot g \cdot \gamma_w}{\frac{1}{2} \cdot \rho \cdot W^2} \quad \dots (2.11)$$

where p is the external pressure, m.wg.

p_{ref} is a reference pressure, m.wg.

W is a reference wind speed, m/s.

γ_w is the density of water, 1000 kg/m³.

ρ is the air density kg /m³.

g is the gravitational constant, m/s².

In most studies these pressures are expressed as coefficients relative to the pressure caused by the dynamic wind speed at a height equal to the height of the building. Particular pressure coefficient values relevant to design situations are discussed in more detail in Chapter 3.

2.3.9 One further aspect of the effect of wind on the pressure distributions over the surfaces of a building is the influence of turbulence. Typical values of turbulence intensity are dependent upon the type of terrain over which the air flow has passed, and can be described for general types of surface roughness (Harris, 1970). Turbulence levels are of importance because they affect the magnitude of the mean pressures and because they produce large short term dynamic pressure fluctuations. These fluctuations are not considered in current techniques for the calculation of ventilation rates in buildings, and their importance is not known; however it seems possible that they have significant effects particularly in situations where ventilation is obtained using a single window opening.

2.3.10 The second mechanism which produces ventilation is stack effect. Differences in the internal air temperature of a building and the external air temperature

around it produce differences in air density. These differential densities in turn result in variations in pressure within the building and between the interior of the building and the outside air. The density of air is dependent upon humidity as well as air temperature. However under normal ambient conditions the effect of humidity is negligible and air density can be expressed by a relationship which varies in proportion to the absolute temperature:

$$\rho = 1.29 \frac{273}{T} \text{ kg /m}^3 \quad \dots\dots (2.12)$$

where T is the air temperature expressed in $^{\circ}\text{K}$
 1.29 represents normal air density at 0°C ,
 273°K .

The pressure caused by the weight of a column of air of height h metres and temperature $T^{\circ}\text{K}$ is:

$$P = 1.29.h. \frac{273}{T} \text{ mm.wg} \quad \dots\dots (2.13)$$

Consequently in a building the differential pressure due to the differences in weight of air columns of height h metres and internal and external air temperatures T_i and T_o $^{\circ}\text{K}$ will be given by:

$$dP = 1.29.h.273\left(\frac{1}{T_o} - \frac{1}{T_i}\right) \text{ mm.wg} \quad \dots\dots (2.14)$$

Assuming an internal temperature of 20°C and an external temperature in the range 15°C to -5°C equation 2.14 may

be simplified to:

$$\delta P \approx 0.0044.h.(T_i - T_o) \quad \dots\dots (2.15)$$

where T_i and T_o may be expressed in $^{\circ}\text{C}$.

2.3.11 Stack effect produces a constant rate of variation of pressure difference with height, acting over the height of the building. Under conditions where stack effect is operating the mean internal pressure in the building adjusts itself until the flow into the building at the lower levels equates with the flow out in the upper part of the building. The height at which the internal pressure is equal to the corresponding external pressure is known as the neutral zone height. This height is normally about half way up the building, although the precise location depends upon the distribution of the ventilation openings, and on the internal temperature variation throughout the building. In a building with relatively large openings in the lower half of its height the neutral zone height will be less than half way up the building, in one with large openings in the upper half the reverse will occur. As changes in internal and external air temperature are relatively slow the pressures caused by stack effect unlike wind induced pressures show no short term variations in value.

2.3.12 Under most conditions stack effect and wind will be acting together to produce natural ventilation.

The pressures caused by the two effects are added to give the total pressure difference acting at any opening and hence, with a knowledge of the open areas and their discharge coefficients the ventilation rate can be determined.

2.4 Techniques for the prediction of natural ventilation and infiltration

2.4.1 There are two widely used methods of predicting natural ventilation or infiltration rates in buildings; the air change method and the crack method. The air change method assumes an air change rate which is dependent mainly upon the type of building concerned and its exposure. The method is entirely empirical, and relies on the assumption that values in existing buildings adequately represent values in new buildings of the same type. The crack method is used to calculate the ventilation rate from the estimated infiltration characteristics of the building envelope and design external pressure distributions. The crack method is regarded as being more accurate, but is more complex to carry out. For the purposes of estimating infiltration and natural ventilation heat loss the I.H.V.E. Guide (I.H.V.E., 1970) and the A.S.H.R.A.E. Guide (A.S.H.R.A.E., 1972) each quote both methods. For estimating ventilation rates in summer conditions the I.H.V.E. Guide presents a separate set of recommendations.

2.4.2 Recommended design ventilation rates for winter conditions, using the air change method, are classified in the I.H.V.E. Guide with respect to building type. Allowances are made for the degree of exposure of the building and for the area of glazing. The allowances and representative figures for dwellings are presented in Table 2.4. This method may be compared with that given in the A.S.H.R.A.E. Guide which gives values applicable to residences. The figures are classified according to opening distribution with no allowance being made for the shelter of the buildings or the amount of glazing. Representative figures for this method are also given in Table 2.4. The figures given in both cases represent room air change rate allowances. The I.H.V.E. Guide recommends that approximately one half of the total individual room leakage values be taken as the total building infiltration rate, as air entering the building will normally travel through more than one room. The Guide also recommends that the figures in Table 2.4 be halved when the building is unoccupied. The A.S.H.R.A.E. Guide suggests that, for dwellings, the total rate for all rooms should be used to calculate the infiltration heating load for the whole building.

2.4.3 As an alternative method, infiltration rates may be calculated using the crack method. The I.H.V.E. Guide method is based on a design wind speed which

TABLE 2.4 Design infiltration rates for rooms in dwellings using the air change method, from the I.H.V.E. Guide and the A.S.H.R.A.E. Guide, air changes/hr. winter conditions.

I.H.V.E. Guide

<u>Room</u>				
<u>Classification</u>	<u>Sheltered</u>	<u>Normal</u>	<u>Exposed</u>	<u>Allowances</u>
Living rooms	0.7	1.0	1.5	Glazing \geq 25% in one wall x 1.25 Glazing \geq 25% in two or more walls x 1.50
Bedrooms	0.3	0.5	0.8	
Bathrooms	1.3	2.0	3.0	
Lavatories	1.0	1.5	2.3	
Stairs, Entrances	1.0	1.5	2.3	

A.S.H.R.A.E. Guide

<u>Room Classification</u>	<u>All Categories</u>	<u>Allowances</u>
No windows or external doors	0.5	Weatherstripped windows x 0.67
Windows or external doors in one wall	1.0	
Windows or external doors in two walls	1.5	
Windows or external doors in three walls	2.0	
Entrances	2.0	

represents an approximate one-percentile wind speed. This wind speed is corrected for building height and type of terrain. A representative total leakage area is taken which depends upon the window distribution; being one half of the total glazed area for a building glazed on two faces or the area of the vertical diagonal plane through the building for a building uniformly glazed on four sides. Assuming a pressure coefficient of 0.55 across the glazed area, a maximum infiltration rate is calculated. This method is presented in greater detail in paragraph 3.4.13. The A.S.H.R.A.E. Guide presents a method which is based on similar principles. A design wind speed is used with no allowance for shelter or height of the building. The representative area chosen is either the leakage area of the face with the greatest leakage area or one half of the total leakage area of the building, whichever is greater. To calculate the total infiltration rate a pressure difference coefficient of 0.64 is assumed to act across this glazed area.

2.4.4 For the purposes of estimating likely ventilation rates in the summertime general recommendations are made in the I.H.V.E. Guide. The recommended rates are based on window opening distribution and opening times. No allowances for building exposure or open window area are made. The recommended rates are shown in Table 2.5.

TABLE 2.5 Recommended ventilation rates for naturally ventilated buildings on sunny days, air changes/hr.

Time during which windows are opened		Windows in one wall only	Windows in two or more walls
Day	Night		
Closed	Closed	1	2
Open	Closed	3	10
Open	Open	10	30

2.4.5 The techniques for estimating natural ventilation or infiltration rates in buildings show considerable differences in method and resulting recommended air change rates. Design rates for the domestic dwelling used as the subject for Tamura and Wilson's full scale tests in Chapter 5, for example, are 0.71 air changes/hr. by the A.S.H.R.A.E. air change method, 0.24 or 0.48 air changes/hr. (dependent upon whether the house is occupied) by the I.H.V.E. air change method, and 0.46 air changes/hr. by the A.S.H.R.A.E. crack method (assuming the standard 6.7 m/s design wind speed). The air change methods can only be used for producing very broad approximations as they have, in particular, no method of correcting for the amount or airtightness of the glazing used. The crack methods used to calculate building infiltration rates show significant differences in

approach. The A.S.H.R.A.E. figures are rather more conservative in the calculation of their equivalent opening areas and in not allowing for the effects of sheltering on design wind speed. This is compensated to some extent by the I.H.V.E. Guide recommendation that infiltration figures be doubled when the building is occupied, to allow for the effects of normal occupation. Both the crack methods given are suited to estimating maximum infiltration loads for the purposes of heat loss calculations. They are not well suited to predicting infiltration loads under normal conditions, in order to assess running costs when, particularly in sheltered areas, the importance of stack effect may be much greater.

2.4.6 The importance of the assessment of infiltration and ventilation rates in buildings is primarily of significance as a detailed element of building performance. Much less guidance is available on likely possible ventilation rates in naturally ventilated buildings in summer conditions. This information may often be more significant in determining the form of a particular design, as it may dictate the need for mechanical ventilation if results suggest that acceptable comfort conditions could not be maintained in hot weather. The information concerning summertime ventilation rates in buildings in the I.H.V.E. Guide is very general, and makes no

allowance for the exposure of the building, maximum permissible open area of glazing or building depth. The prediction of such ventilation rates is made more difficult because it is dependent upon the pattern of occupation by the users. However a more accurate method of prediction of maximum ventilation rates which is related to these design parameters and appropriate climatic conditions is required in order to be able to ascertain whether acceptable comfort conditions are capable of being maintained in a proposed solution.

Figure 2.1.

Relation between comfort and peak temperature for schools after Langdon and Loudon.

percentage of population being 'sometimes too hot'.

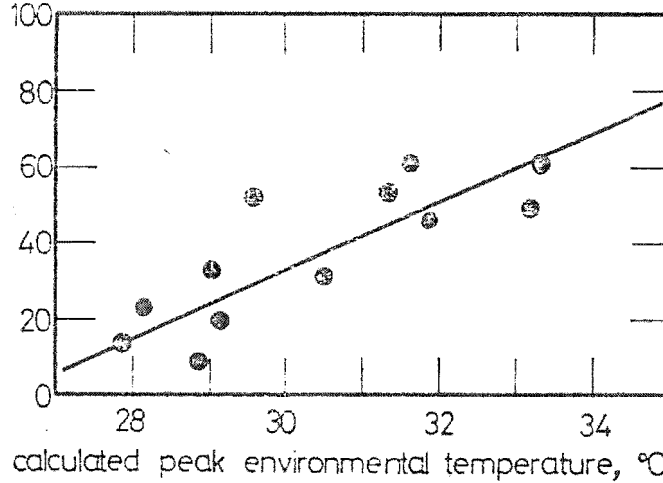


Figure 2.2.

Theoretical comfort zones after Humphreys.

globe temperature, °C.

for air velocity 0.1 m/s.

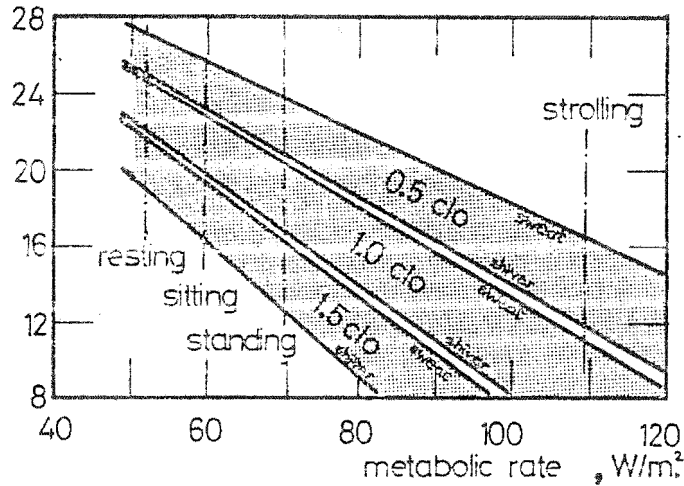


Figure 2.3.

Relation between comfort and variability of internal temperature, after Humphreys and Nicol.

percentage of time comfortable

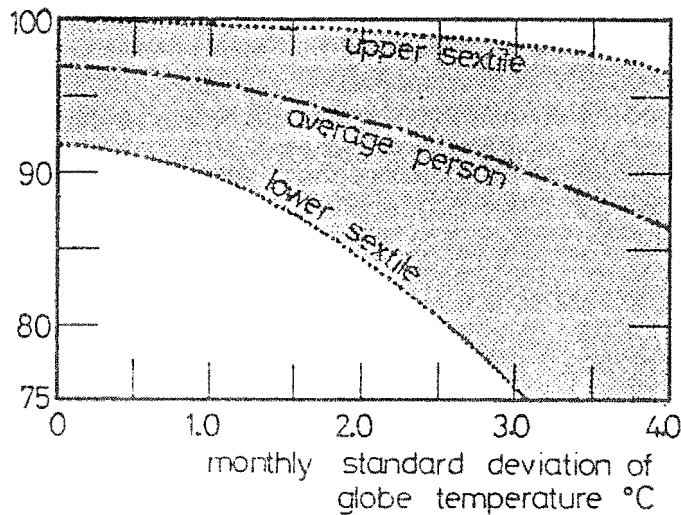


Figure 2.4. Comfort zones for offices after Wise

High comfort standard: $T = 24 \pm 2^\circ\text{C}$
 $T_{\text{max}} = 26^\circ\text{C}$
 $T_{\text{range}} = 4^\circ\text{C}$

Acceptable comfort standard: $T = 25 \pm 4^\circ\text{C}$
 $T_{\text{max}} = 29^\circ\text{C}$
 $T_{\text{range}} = 8^\circ\text{C}$

ventilation rate,
 air changes/hr.

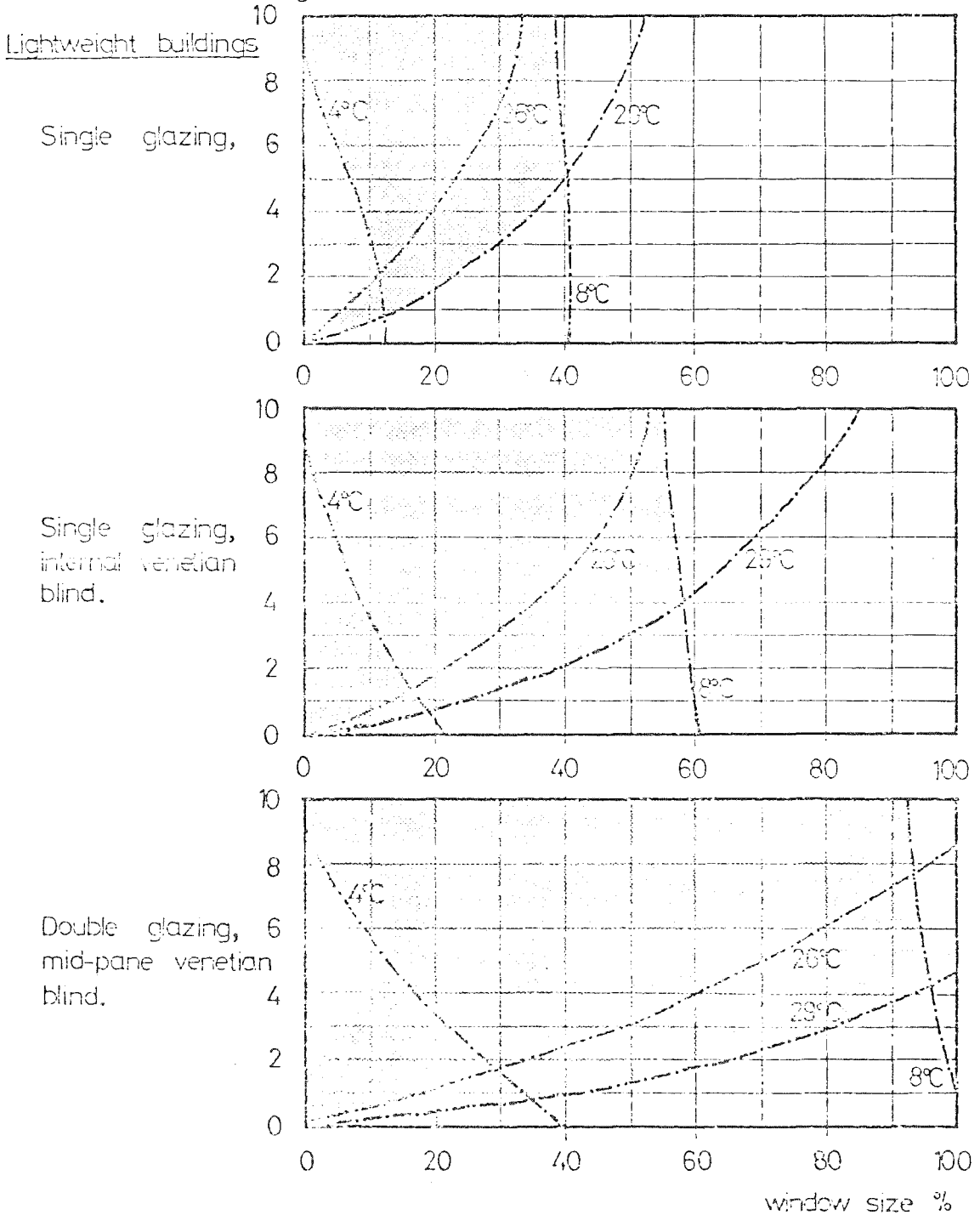


Figure 2.5. Comfort zones for offices after Wise

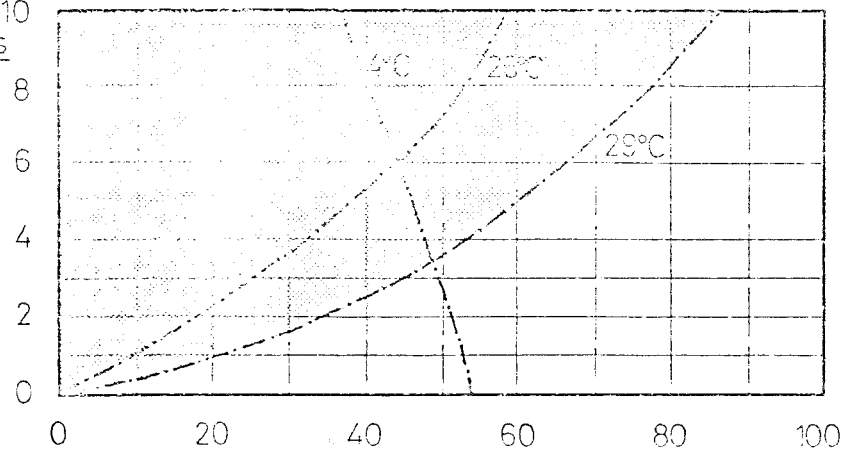
High comfort standard: $T = 24 \pm 2^\circ\text{C}$
 $T_{\text{max}} = 26^\circ\text{C}$
 $T_{\text{range}} = 4^\circ\text{C}$

Acceptable comfort standard: $T = 25 \pm 4^\circ\text{C}$
 $T_{\text{max}} = 29^\circ\text{C}$
 $T_{\text{range}} = 8^\circ\text{C}$

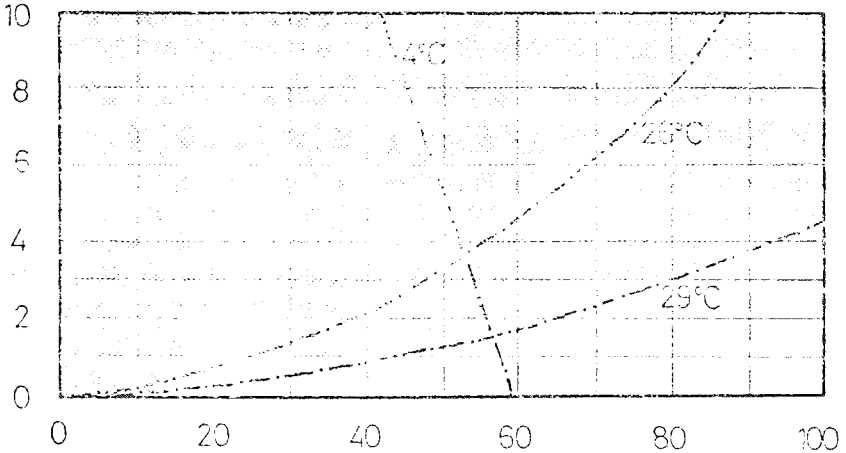
ventilation rate,
air changes/hr.

Heavyweight buildings

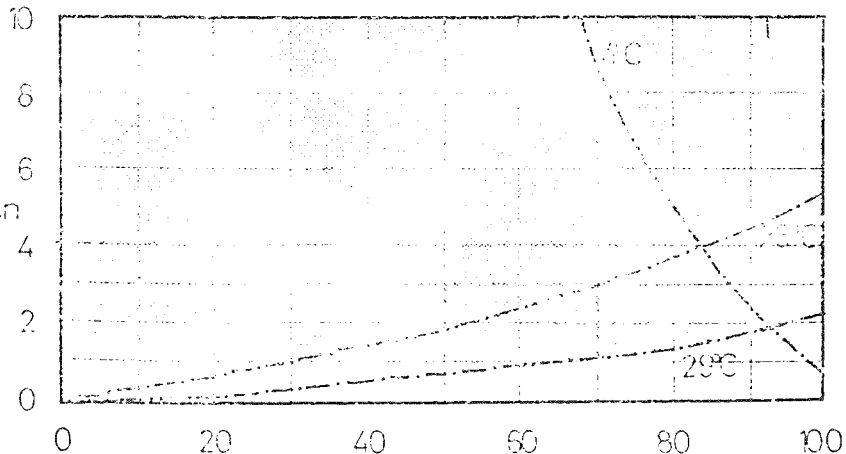
Single glazing,



Single glazing,
internal venetian
blind.



Double glazing,
mid-pane venetian
blind.



window size %

Figure 2.6. Sound reduction indices for partially open single and double glazing, after Ford and Kerry.

sound reduction index, dB.

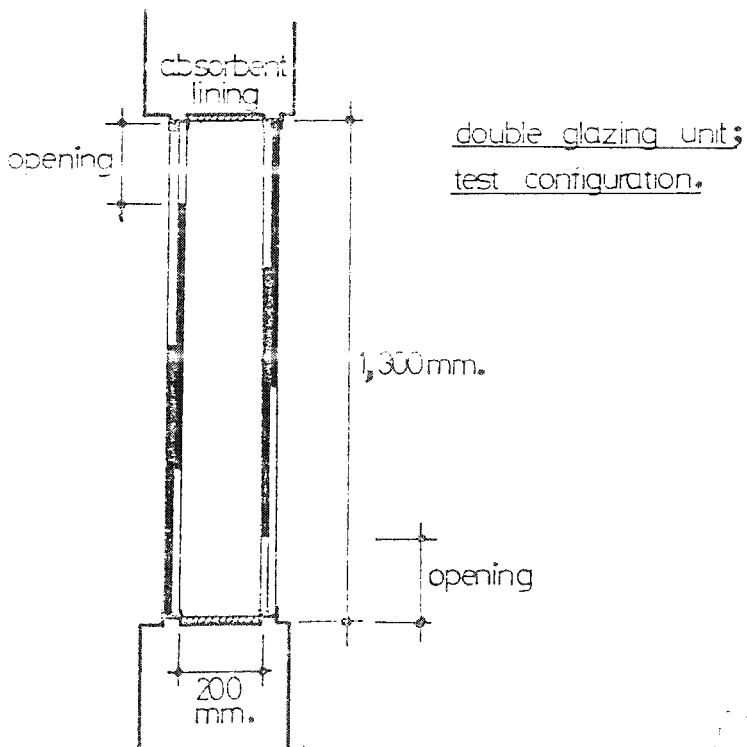
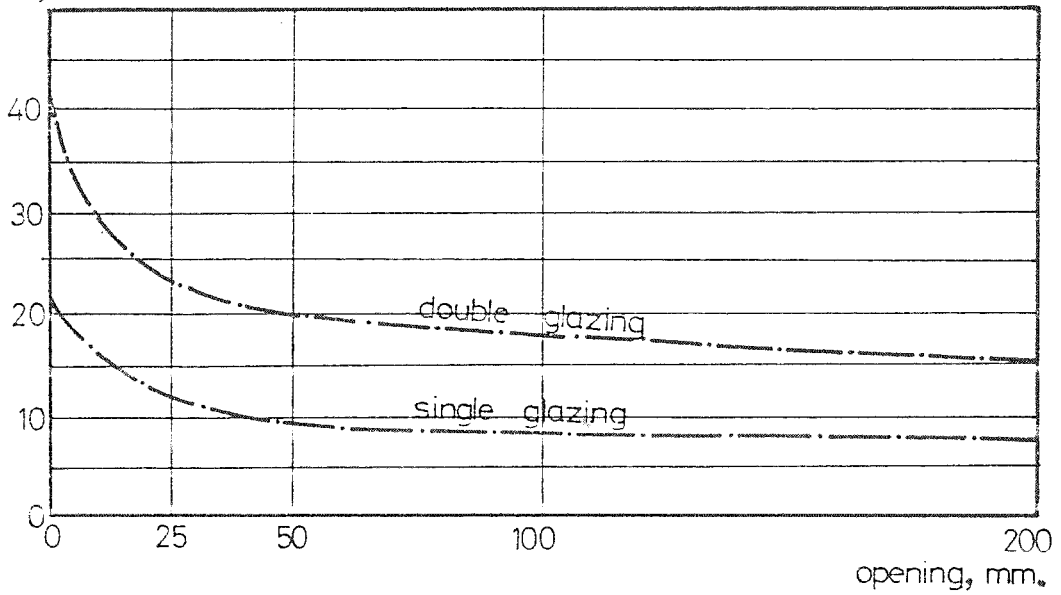


Figure 2.7. Spectrum of horizontal wind speed near the ground after, Van den Hoven

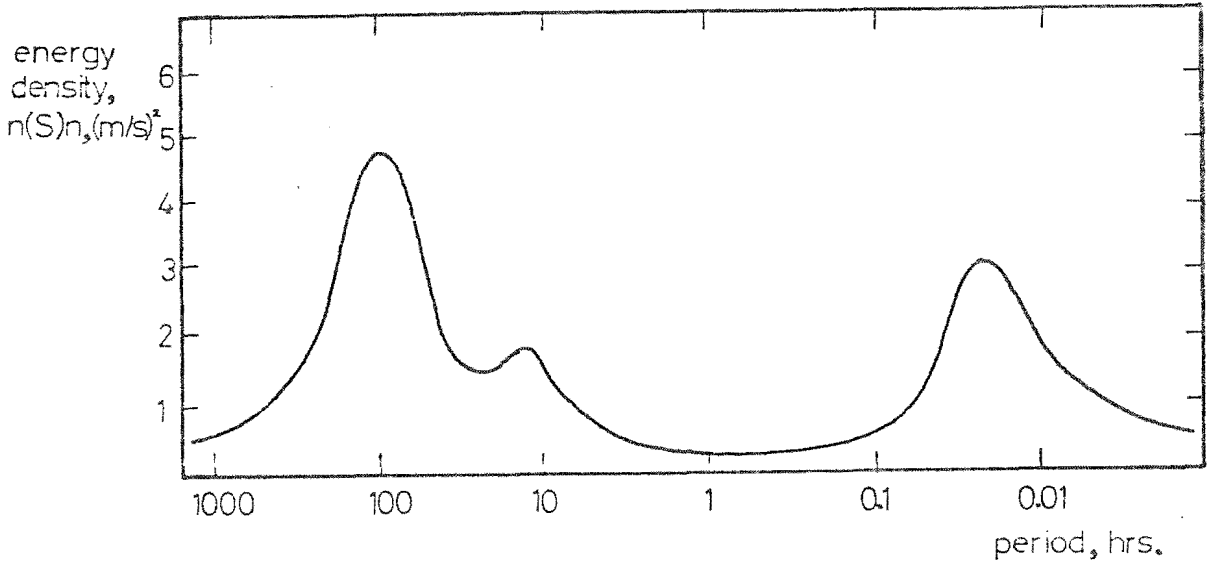


Figure 2.8. Mean wind velocity profiles for surfaces of different roughness, after Davenport.

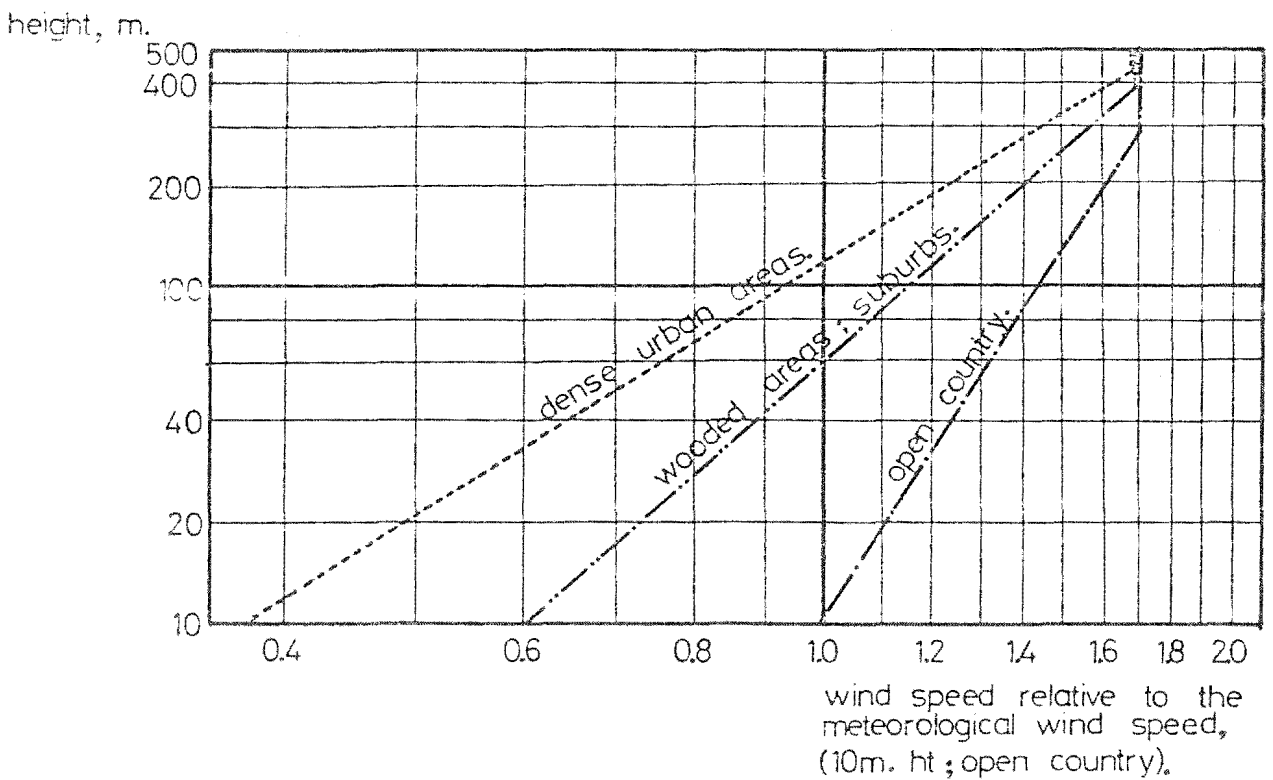
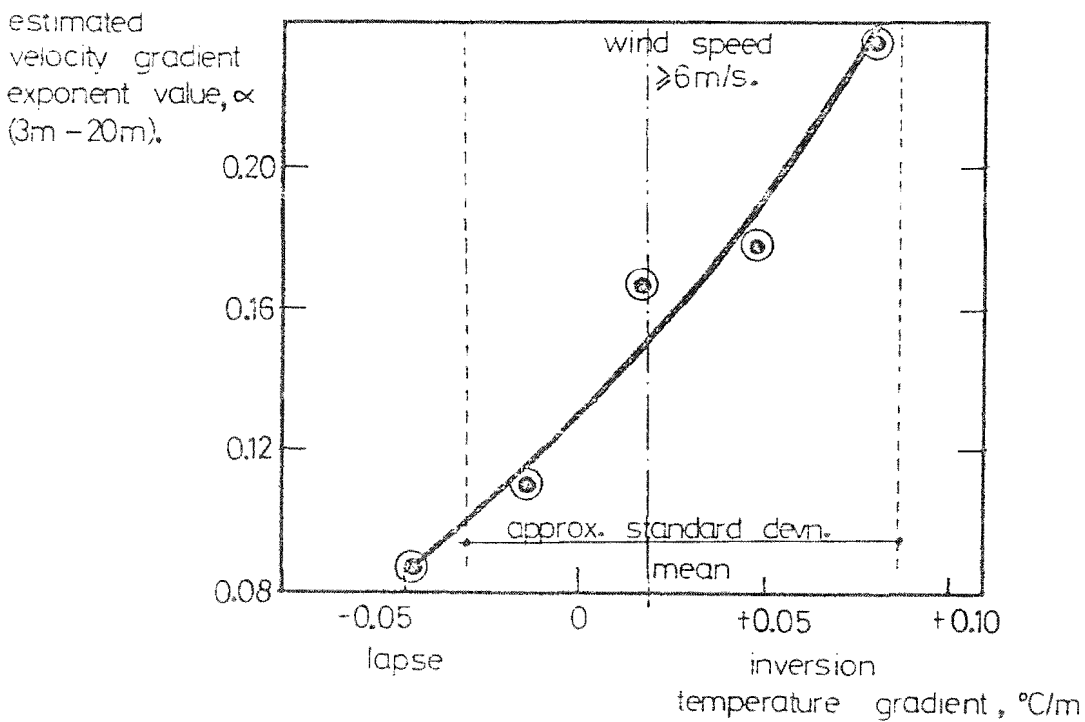
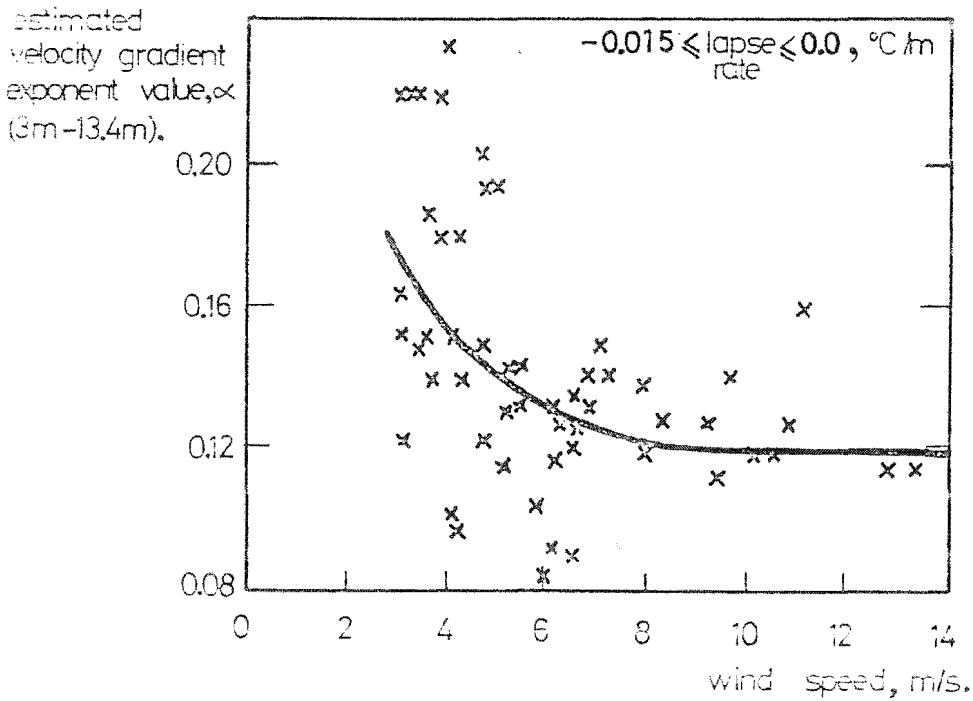


Figure 2.9. Variation of velocity gradient exponent, α , with wind speed and temperature gradient in open country in the first 20m., after Johnson.



3. A CRITICAL APPRAISAL OF PREVIOUS STUDIES OF NATURAL VENTILATION

3.1 Introduction

3.1.1 The study of the factors affecting natural ventilation of buildings and the resulting patterns of ventilation is relatively new; the first studies which put forward any quantitative guides to ventilation rates being carried out in the 1940's. Study of natural ventilation is complex because there are many inter-relating factors which affect patterns of ventilation. A list of the most important of these variables include wind speed, wind direction, velocity gradient, building shape, temperature differences and the air infiltration characteristics of all parts of the building.

3.1.2 Because of the complexity of these factors and in order to aid understanding, many of the studies which have been undertaken have made significant simplifications. This survey attempts to assess the contribution of existing studies of natural ventilation and in particular to evaluate the predictive techniques which have been evolved to date. From this assessment it has been possible to discover some of the major areas of uncertainty in current design techniques.

3.1.3 The existing work on natural ventilation falls into two main types. Most of the early studies used

observations from full scale buildings. Ventilation rates were measured, the characteristics of the various openings described and measurements of the climatic variables acting on the building recorded. These studies have been of great value in determining the factors affecting ventilation rates and in producing elementary rules describing their behaviour. There are two significant disadvantages with this type of study. Firstly, because natural ventilation depends on climatic variables over which the observer has no control, he must accept whatever combinations of conditions occur, in order to carry out his measurements. This fact makes the analysis of data from this type of study very difficult. Secondly, because of the number of variables which affect ventilation patterns, any type of systematic study is severely limited by the prohibitively large number of measurements which must be made.

3.1.4 The second type of study which has been done involves the use of analogue models of the ventilation system. Initially hydraulic and electrical analogues were used, and more recently digital computer programmes have been used to assess the patterns of ventilation. This type of study is able to control the external conditions accurately and give the experimenter much greater freedom to carry out systematic studies. However it is necessary to

establish the validity and limits of accuracy of the model, both in terms of the inherent accuracy of the analogue, and the values of the variables used in the models. Thus these studies must be made in conjunction with full scale studies. So far this does not seem to have been done.

3.2 Description of the full scale studies carried out to date

3.2.1 The earliest studies of natural ventilation were carried out in England, at the beginning of the century. After these little work was done until the work of Bedford in the 1940's. The results of measurements made on small housing units by Bedford et al (Bedford, 1943) show that for this type of building the air change rate with all openings firmly closed is of the order of 0.5 air changes per hour. Under normal conditions, and with a small ventilator open, an air change rate of 1.5 air changes per hour may be expected. Variation due to the angle of incidence of the wind on the ventilator is noted, typical values being given in Table 3.1. The dominant influence of a heated flue on the pattern of ventilation was also noted. No specific values for the characteristics of the openings or the wind speeds around the house were given.

3.2.2 Similar studies were carried out by Carne (Carne, 1945) using a tracer gas measurement technique. He used carbon dioxide as a tracer gas to measure the

TABLE 3.1 Air change rates noted by Bedford

Angle of incidence of wind relative to ventilator	Average air change rate, /hour
90°	3.0
45°	1.6
0°	1.2
ventilator on leeward face	1.2

ventilation rate in a small domestic building. The variation of ventilation rate with wind speed was found to be a complex relationship, but no explanation was offered. It was shown that, generally, the ventilation rate increased as the wind speed increased. The lack of a simple relationship may well be due to variation in wind pressures, as only the external wind speed and direction are used in the analysis, and no concept of pressure coefficient was used. The directionality of a wall ventilator was again noticed, as opposed to the chimney flue. Variation in flue area was contrived and it was shown that as flue area increased the average ventilation rate increased until a flue area of 0.009 - 0.012 m² was reached. As flue area increased beyond this area the change in ventilation rate became much less significant. This was interpreted as meaning that the flue area of 0.009 - 0.012 m² is roughly equivalent to the open area in the windows and doors of the building. For flue areas greater than this value the building fabric crackage area controls the ventilation

rate, whereas for flue areas lower than this the flue controls the building's ventilation rate. This study is of some significance as this was the first attempt to make a quantitative estimate of the air leakage characteristics of a building.

3.2.3 The most significant studies of natural ventilation on full scale buildings are a series of studies carried out by Dick, working for the Building Research Station (Dick, 1949), (Dick, 1951). The studies were carried out on a number of specially constructed experimental houses. The houses used were two storeys in height, semi-detached, and built in two lines. Standards and types of construction were designed to be typical of other new housing being built at that time. A second set of observations was made at a later time with the houses under normal occupation. From these studies a series of empirical equations were deduced which could be applicable to buildings of this type and standard of construction.

3.2.4 The importance of these observations lies largely in the accuracy of the observation of all the major factors affecting the ventilation rates. Wind speeds and directions and pressure coefficients were measured on the buildings. The pressure coefficient readings give values for the coefficients of drag of about 0.9. Measurements of the pressure drop across the windward face of the buildings give values of about

0.81 of the dynamic head, based on velocities of 2-10 m/s. The values of coefficients of drag compare well with results obtained in wind tunnel tests on model housing (Bailey, 1943). In the model tests the pressures acting on the windward and leeward walls were found to be in a different proportion, being nearer in value to each other. The large pressure drop across the windward face in the full scale observations is attributed to the larger area of the air outlets, and especially to the influence of the flues. Dick also suggested from his observations, that the pressure coefficients on the front and rear faces of the buildings varied with the angle of incidence of the wind in proportion to $\cos^2\theta$.

3.2.5 Measurements of the ventilation rates in the houses were also made. Measurements were made both of air change rates in individual rooms in the houses and of mean rates for the whole house. These measurements were made by introducing hydrogen tracer gas into the house and studying the rate of decay of the gas. The air change rate for the volume being considered was then deduced using an equation of the form:

$$- V_0 \frac{dc_t}{dt} = xc_t \quad \dots\dots (3.1)$$

where c_t is the concentration of tracer at time t ,
 x is the volume of air entering the room in time t ,
 V_0 is the volume of the room.

From these studies a series of empirical equations were presented showing the relationship between infiltration rate and wind speed and direction.

These were of the general form:

$$I = a + bW + cW \cos \theta + dW \sin \theta \quad \dots\dots (3.2)$$

where I represents infiltration rate,

a,b,c,d, are constants,

W represents wind speed,

θ represents angle of incidence of wind to the building face.

It was shown that the effect of wind direction was normally of secondary importance to wind speed and that a simpler and adequate relationship:

$$I = a + bW \quad \dots\dots (3.3)$$

was acceptable for representing the whole house ventilation rate.

3.2.6 Values of the constants which best fitted the observations were chosen. It was shown how ventilation design affected the values of these constants. The results were given for three living rooms having different methods of ventilation (Table 3.2). In the results for house 13, which has a living room with no flue, the effect of wind speed is the most marked. In house 33 the living room has an open fire and the effect of wind speed is less. In house 10, where there is a heated flue with underfloor ducted air supply, the

external wind speed is seen to have very little effect on the infiltration rate. Average ventilation rates for the whole house were also given for these three houses and may be seen in Table 3.3. The variation in these cases, where the houses are in general respects similar, are much less than the infiltration rates in the living rooms alone. As already mentioned, Dick showed that wind direction plays a relatively unimportant part in determining whole house air change rates. A typical set of results is shown for house number 33, (Figure 3.1).

3.2.7 The houses were also observed when under normal occupation (Dick, 1951). Typical ventilation rates were given, where the users opened windows as they wished, under normal conditions at two sites. The results are shown in Table 3.4. It can be seen that the ventilation rates are generally higher with higher wind speeds acting. Dick showed that because of the greater open area of window on the sheltered site the normal ventilation rate was higher than would be expected if strict proportionality to wind speed were assumed.

3.2.8. In a third paper (Dick, 1950), Dick showed theoretically how the ventilation rate in a house should be approximately proportional to the wind speed, or the square root of the internal/external temperature difference. He showed that the total ventilation rate is determined by whichever set of forces produced the

TABLE 3.2 Relationship between observed rates of air change and wind speed for living rooms with different ventilation systems, after Dick (Dick, 1949).

House 13	$I = 0.2 + 0.63 W$
House 33	$I = 1.6 + 0.29 W$
House 10	$I = 2.4 + 0.16 W$

I is the infiltration rate, air changes/hour.

W is the wind speed, m/s.

The living room in house 13 has no flue.

The living room in house 33 has a heated flue.

The living room in house 10 has a heated flue and ducted underfloor air supply.

TABLE 3.3 The relationship between observed rates of air change and external wind speed for whole houses after Dick, (Dick, 1949).

House 13	$I = 1.03 + 0.264 W$
House 33	$I = 1.29 + 0.198 W$
House 10	$I = 0.99 + 0.270 W$

I is the infiltration rate, air changes/hour.

W is the wind speed, m/s.

TABLE 3.4 The relationship between observed ventilation rates and wind speed at two different sites, after Dick (Dick, 1951).

	Site 1	Site 2
Design conditions	3.8 m/s. 7.8°C diff.	2.0 m/s. 8.9°C diff.
Av. infiltration rate, all windows closed	1.51	0.88
Increase in infiltration rate/open top windows	0.46	0.28
Increase in infiltration rate/open casement window	0.65	0.56

greater rate singly. In addition, the speed above which wind takes control may be found by equating the estimates of the air flow rate produced separately by wind and by temperature difference. The results of series of full scale measurements on an experimental house are given. These show that at wind speeds below the critical speed, ventilation rates are generally proportional to the square root of the temperature difference, while at wind speeds greater than this, the ventilation rate is approximately proportional to the wind speed. The results of the study may be seen in Figure 3.2.

3.2.9 A series of full scale experiments on small domestic buildings was also carried out in America. All these experiments used the rate of decay of a helium tracer gas to estimate ventilation rate, using a relationship of the form given in equation (3.1). The earliest work was done by Bahnfleth et al (Bahnfleth, 1957), who measured the variation of measurements of building infiltration rate with external conditions, on two domestic buildings. The results were corrected assuming a relationship between infiltration rate, wind speed and temperature difference of the form:

$$I = a + bW + c(dT) \quad \dots\dots (3.4)$$

where I represents infiltration rate, air changes/hr.

a, b, c are constants

W represents the external wind speed, m/s.

dT represents the internal/external temperature difference, °C.

Typical sets of results for the two sets of houses are given in Figure 3.3. It was found that for house 1, the average value of b (equation 3.4) was 0.029 air changes per hour for each m/s. increase in wind speed, while the average value for c was 0.006 air changes per hour/ $^{\circ}\text{C}$ increase in temperature difference. The corresponding values of b and c for house 2 are given as 0.027 air changes per hour for each m/s. increase and 0.009 air changes/hr./ $^{\circ}\text{C}$ temperature difference increase. The houses were described as having similar window crackage lengths, although insufficient information is given to permit any theoretical comparisons to be made. The higher infiltration rates, observed in house 2 at high wind speeds and temperature differences, were attributed mainly to the increased exposure of the house. The accuracy of the comparison must be doubted to some extent as wind speeds for house 1 are measured at a site not immediately adjacent to the house, and thus any micrometeorological effects in the vicinity of the house were not accurately recorded. Calculations, which overestimated the wind effects and ignored the stack effects give reasonable agreement with the observed ventilation rates. The agreement was not expected to be as good when high winds and small temperature differences were acting.

3.2.10 Similar studies were carried out by Jordan et al (Jordan, 1963), and Coblenz and Aachenbach

(Coblentz, 1963). Jordan showed that measured air change rates, corrected to 4.5 m/s. (10 m.p.h.) wind speed and 22°C (40°F) temperature difference, assuming an empirically derived relationship of the form of equation (3.4) could be expected to be in the range of 0.1 to 0.4 air changes/hr. for the buildings studied. A calculated rate, using estimated window leakage characteristics, was 0.23 air changes/hour. Coblentz and Aachenbach compared several different buildings; all small domestic buildings, of different age and construction. They found that higher infiltration rates tended to occur in two-storey buildings and also in old frame-built houses. Whether this was due to the frame construction or to deterioration of the building fabric was not determined. Values, corrected to 4.5 m/s. wind speed and 22°C temperature difference varied between 0.37 and 1.0 air changes/hr. Approximate estimates were "in reasonable agreement" assuming infiltration rates normal for tightfitting windows at one extreme and loosefitting at the other.

3.2.11 A study was also carried out by G. Tamura and A. Wilson (Tamura, 1963). This again gave results for two small domestic buildings in suburban areas. Tests were carried out under summer conditions with little or no temperature difference between the building interior and the outside air. The results showed that the infiltration rate was proportional to the wind speed.

Tests were also carried out under conditions where there were small wind speeds and large temperature differences acting. Under these conditions the infiltration rate was proportional to the square root of the difference in temperature. They also showed, from a series of tests with moderate wind speeds and temperature differences acting together, that the infiltration rate is less than that which would be expected assuming that the infiltration rates from the two sets of forces could be summed directly. At higher wind speeds where the infiltration rate due to wind alone would be significantly greater than that due to stack effect, the combined infiltration rate was observed to approach that which would be expected from wind alone.

3.3 Discussion of the results of the full scale studies

3.3.1 The full scale studies reviewed were carried out in a number of widely differing types of small domestic buildings. They are of value because they establish empirical relationships between the various factors affecting infiltration and ventilation, and give estimates of the wide range of infiltration rates likely to be present in these types of building under normal conditions.

3.3.2 Their value in terms of establishing predictive rules for natural ventilation and infiltration is limited by two significant factors.

Firstly, the range of buildings studied is entirely limited to one or two storey buildings. In these situations forces generated by stack effect are relatively small, and cases where stack effect is of greater importance, as in tall buildings, have only been studied in a few cases. The importance of air movement distribution internally is also relatively small in domestic buildings and is not studied in the papers. This factor is of much greater importance in larger buildings. Secondly, there is a lack of correlatable data from each study. The empirical equations derived in each paper are only applicable to the particular building studied. The techniques are not sufficiently refined to show accurately the importance of factors such as type of construction, building shape, degree of shelter of the building, the influence of other near-by buildings or the infiltration characteristics of the openings.

3.3.3 The studies do emphasise the wide range of infiltration rates likely to be met in practice. Ventilation rates in some buildings are greater than other nominally similar buildings by factors of 5 or 10. While all the studies conclude that the measured infiltration rates are approximately proportional to the external wind speed, the studies differ in their treatment of stack effect. Dick and Tamura carried out studies where they attempted to isolate the effects of

wind speed and temperature difference. They showed that where there is a relatively large temperature difference acting, with little or no external wind, the infiltration rate is proportional to the square root of the temperature difference. This is in contrast to Bahnfleth et al, and Jordan who assume a linear relationship between ventilation rate and temperature difference in their analyses. Dick and Tamura also show that under conditions where stack effect and wind are operating simultaneously the combined effect is less than would be supposed assuming the ventilation rates were directly additive.

3.3.4 Comparison of the various full scale studies is further complicated by the errors involved in the measurement techniques involved. The "rate of decay of tracer" technique for the measurement of ventilation rates assumes perfect mixing of the air in the study volume. This condition is very difficult to achieve in a whole house, divided by walls and floors. It is dependent upon the degree of agitation of the air internally and the type of tracer used. At the same time tracer gas will be lost by diffusion, and this will lead to an overestimate of the ventilation rate. This mechanism is mentioned as a possible source of error by Bahnfleth and Tamura, where it might be assumed to be of greater relevance because of the low air change rates involved. Accuracies will also be affected by the

method of sampling of the tracer gas used. The errors caused by these effects are more fully discussed in a paper by Hitchin and Wilson (Hitchin, 1967), but errors of up to $\pm 15\%$ are quoted as typical. As the magnitudes of the errors will be different in each case quantitative comparisons of the results become rather unreliable.

3.4 Description of analogue ventilation studies

3.4.1 The simplest analogue studies which have been noted are two analogue methods (Kurek, 1965), (Rajogopalan, 1963). They are both very simple, two dimensional techniques, more suited to demonstrating principles of ventilation rather than for producing accurate measurements. Neither paper mentions any Reynolds number calculations or any comparison with flow parameters in similar full scale situations with air. The methods are both essentially two dimensional in which no type of velocity gradient may be superimposed on the models. It is also impossible to model stack effects using these techniques. Consequently it is assumed that the models are used only for simple comparative studies and are of little use as accurate quantitative analogues.

3.4.2 In the first method Kurek used a model half immersed in water. He assumes that the depths of the water internally and externally adjacent to the walls of the model are proportional to the wind pressure generated.

No significant quantitative results are demonstrated. He noted that the time constant for pressure equalization due to changes in wind speed was very short, often less than one second. Rajagopalan and Rao used a flow visualisation technique. Photographs were taken of the water flow patterns through models and the flow rate was established from the proportional number of streamlines counted passing through the building to the number that would pass through an equivalent open space. The large open areas required, a minimum of 20% of the wall area, suggests that the technique is only really applicable to work in tropical climates.

3.4.3 Most of the analogue studies which have been carried out use electrical network analysis methods. All the digital analogue techniques use similar assumptions in the calculations, although with varying degrees of sophistication. Several papers (Gabriellson, 1968), (Tamura, 1969), (Tamura, 1970), (Karulek, 1970), (Rogelein, 1967), (Svetlov, 1966), (Bogoslovskii, 1967) describe the analogue techniques in general form or for one specific case. Harrison (Harrison, 1961) assessed what the likely infiltration rates which would occur over a range of typical building types would be. Jackman (Jackman, 1968), (Jackman, 1969), studied infiltration rates in office buildings under varying conditions and on the basis of his work, the infiltration section in the 1970 I.H.V.E. Guide has been written. This has

been based largely on nomograms from which estimations of infiltration rate can be made in design situations. Nelson, in the A.S.H.R.A.E. Publication on Energy Requirements for Heating and Cooling in Buildings (Nelson, 1971) presented a method suitable for completely computerised calculation of infiltration rates in buildings.

3.4.4 The earliest computational study was that by Harrison (Harrison, 1961). A simple, uniformly glazed slab block of either 50 ft. or 100 ft. in height, with solid end walls was taken to be the typical building form of office blocks. External pressures were calculated assuming a 3, 6 or 9 mph wind speed, depending on the degree of exposure of the building, and pressure coefficients of +0.5 and -0.5 for the building faces. A temperature difference of 35^oF was also assumed. For several types of building section (Fig. 3.4) in which the internal and stairwell resistances were expressed as multiples of the external wall resistances, the pressure drops across the external wall were calculated. An average and two extreme design pressure drops were extracted from all the cases studied. Typical average and extreme crack widths, crack infiltration characteristics and crack lengths per cubic foot of building were assumed. From these figures average and extreme infiltration rates were calculated (Table 3.5).

TABLE 3.5 Limits of design values of air change rates calculated from probable range of all possible variables for 15 m. high and 30 m. high buildings. after Harrison

	Building Ht.	Minimum	Mean	Maximum
Pressure drop across window wall mm.wg.	15	0.05	0.10	0.20
	30	0.08	0.15	0.35
Crack width-steel framed windows, mm.	15	0.75	1.00	1.25
	30	0.75	1.00	1.25
Infiltration rate per metre of crack m ³ /h/m.	15	0.16	0.44	1.00
	30	0.20	0.60	1.50
Crack length per unit volume in normal office buildings m/m ³ .	15	0.33	0.39	0.44
	30	0.33	0.39	0.44
Air change rate/hour	15	0.18	0.56	1.48
	30	0.24	0.77	2.16

The range of infiltration rates likely to be found was shown to range between 0.18 and 2.16 air changes per hour, which is somewhat lower than the then current I.H.V.E. recommended rates of 1.25 to 2.50 air changes per hour. Harrison suggested also that design air change rates due to stack effect alone on the lower storeys of tall buildings are, in many cases, of the same order as wind induced air change rates in the upper storeys.

3.4.5 Harrison's paper described a technique which estimates the orders of magnitude of pressure drops likely to occur in buildings, from which infiltration

rates may be inferred. The technique does not analyse the air movement patterns inside the building and provides only a simple estimate of the orders of ventilation rates which may be expected. The calculation is valid for a slab building only, under conditions of maximum possible infiltration. The internal resistances to air flow, which were defined as zero, 0.5, 1.0 or 1.5 times the external wall resistances, are at variance with the more normally assumed values for tall buildings (Tamura, 1969), (Jackman, 1969) which suggest values of the order of 0.5 times the outside wall resistance as being normal. These assumptions would lead to a heavier weighting for the buildings with low infiltration rates than is likely to occur in practice. The paper is most useful for its collection of data on typical crack widths in window-wall construction. Harrison recommends mean clearances of 0.04 inches (1 mm.) with upper and lower design limits of $\pm 25\%$. He suggested that typical values of window crackage length in modern construction vary between 0.7 ft/ft² (2.1 m/m²) of window to 1.6 ft/ft² (5.0 m/m²), the lower value being applicable to larger windows. Having studied typical wall/floor ratios he recommended typical figures for minimum and maximum crackage of 0.03 and 0.04 ft. of crack/cubic foot of building (0.3 - 0.4 m/m³) respectively.

3.4.6 Several papers have been noted which describe

the technique of calculation of ventilation rates in buildings, and demonstrate the technique with a simple example. A paper by Gabriellson and Porra (Gabriellson, 1968) considers a simplified situation where the example is a block of flats. The ventilation rate was related to the pressure difference acting across any opening by an equation of the form:

$$V = C.L.(\Delta P)^{1/n} \quad \dots (3.5)$$

where V is the volume flow rate, m³/hr.

C is the infiltration coefficient of the opening, m³/hr/m/mm.wg.

L is the length of the opening, m.

ΔP is the pressure difference across the opening, mm.wg.

n is an exponent, dimensionless.

The value of the exponent n was taken as 1.5 for all openings. This allowed open areas to be summed and thus reduced the complexity of the calculations involved. They assumed that all air flow resistance occurs at the external wall and that pressure differences through apartments were uniform.

3.4.7 Two papers by Tamura and Wilson (Tamura, 1969), (Tamura, 1970) demonstrate the use of a computational technique in predicting the effect of ventilated stacks on the spread of smoke during a fire. They are used to determine design parameters for optimum vertical shaft

dimensions, which are not of direct relevance here and so will not be discussed. They assumed a wind profile for smooth terrain and values of pressure coefficient of +0.8 for the windward face and -0.6 for all other faces. These values differ from the figures assumed by other workers, (coefficients of drag of 0.95, 1.0 and 1.1 are assumed by the Building Research Station (B.R.S., 1970), Harrison and Jackman in similar design situations). Values for typical component infiltration coefficients were taken from surveys of buildings, the values being for external walls, internal barriers and between floors. Tamura and Wilson showed that the flow of air directly between floors was insignificant in relation to the other patterns of flow, and also, as may be expected, that the characteristics of the external wall are most significant in determining the ventilation rate.

3.4.8 A paper by Karulek (Karulek, 1970) describes another analogue method again based on generally similar techniques. The governing equations for flow through building components were described and the ventilation rate calculated from the pressures outside the building. The assumptions are generally similar to other analogue methods. Infiltration through walls and floors was taken to be insignificant and therefore disregarded. Flow through windows and doors was described by an equation of the form of equation (3.5), where the value

of n for all openings was taken to be 1.5.

3.4.9 Rogelein (Rogelein, 1967) demonstrated a simplified method for calculating infiltration rates for a model building. The method is similar to that used by Harrison, and is used on a simple slab building with well separated floors, so that vertical patterns of flow are relatively unimportant. Rogelein argued that, knowing the pressure differences across the building from wind tunnel model studies, the infiltration rate may be calculated from an equation of the form:

$$V = A' \left(\frac{(B'/A')^{3/2}}{1 + (B'/A')^{3/2}} \right)^{2/3} (C_D \cdot P_V)^{2/3} \dots (3.6)$$

where A' represents the total leakage coefficient of the windward face.

B' represents the total leakage coefficient of the leeward face.

C_D is the pressure coefficient acting across the building.

P_V is the dynamic head at roof level.

The central part of the expression estimates the proportion of the total pressure drop across the windward face to that across the leeward face. Thus for a simple uniformly glazed building where $B' = A'$ the infiltration is worked out from a pressure which is half the mean coefficient between the two faces or zones of the faces of the building. A further simplification is made by substituting the equation:

$$V = A' \left(\frac{1.2 B'}{A' + B'} \right) \cdot (C_D \cdot P_V)^{\frac{2}{3}} \dots\dots (3.7)$$

This simplification was made on the assumption that, for the range of B'/A' from zero to 1.0, the total error is zero. At specific values of B'/A' some errors are introduced. For example, at $B'/A' = 1.0$, a common case, an error of about 5% will be introduced. The method can best be described as a simple approximation procedure which gives very general estimates of the total building infiltration rates likely to occur. It does not model situations where large vertical movements of air, due to stack effect or differential wind effects are involved. Another limitation is that the pressure coefficients were estimated using a wind tunnel model in uniform flow, that is with no modelled boundary layer. This will introduce further significant errors in the calculations particularly for buildings in urban areas.

3.4.10 A paper by Svetlov (Svetlov, 1966) describes, in general terms, the equations used in the calculation of infiltration rates. It deals mainly with the mathematical methods of solving the sets of simultaneous equations involved. The paper contains no significant quantitative information in terms of input data. In a paper by Bogoslovskii and Titov (Bogoslovskii, 1967), the assumptions made are similar to those made by other workers although the relation, between pressure difference and flow rate for window crackage, is

expressed in the form deduced by Dick and Thomas (Dick, 1953):

$$\Delta P = aV + bV^2 \quad \text{..... (3.8)}$$

where V is the volume flow rate

dP is the pressure difference

a, b are constants for each window

rather than the more normal exponential form. Several simplified examples are given in order to demonstrate the technique, but no detailed quantitative results are presented.

3.4.11 A series of analogue studies have been carried out by Jackman and den Ouden (Jackman, 1968), (Jackman, 1969). Den Ouden developed an electrical analogue for simulating ventilation patterns and rates, while Jackman developed a similar technique using a digital programme. Comparative studies, using the same assumptions and input data are reported to give a very good correlation of results. The studies were based on two simple multi-storey building shapes; a simple slab block uniformly glazed on two sides and a square tower, uniformly glazed on all four sides. In the studies a velocity gradient of a form typical of suburban flow, was assumed:

$$\frac{W_h}{W_{h'}} = \left(\frac{h}{h'} \right)^{\frac{1}{3}} \quad \text{..... (3.9)}$$

where W_h is the air velocity at height h, m

$W_{h'}$ is the velocity at a reference height h', m

Using this assumption and a similar assumption for flow over open ground Jackman and den Ouden obtained a correction factor for computing the wind speed at the site from knowledge of a remote meteorological wind speed. This correction was based on the work of Davenport (Davenport, 1965 b), who has shown that over typical open country the velocity gradient is of the form:

$$\frac{W_h}{W_g} = \left(\frac{h}{hg}\right)^{1/7} \quad \dots\dots (3.10)$$

where W_g is the geostrophic wind speed
 hg is the geostrophic wind height, typically 280 m. over open country.

Also over suburban areas the velocity gradient is of the form:

$$\frac{W_h}{W_g} = \left(\frac{h}{hg}\right)^{1/3} \quad \dots\dots (3.11)$$

where hg is the geostrophic wind height over suburban areas typically 500 m.

Thus for open country at a height of 6 m. (substituting in equation (3.10)):

$$W_{6m} = 0.58.W_g \quad \dots\dots (3.12)$$

Then at any height in a suburban area:

$$W_h = 1.73 W_{6m} \left(\frac{h}{500}\right)^{1/3} \quad \dots\dots (3.13)$$

where W_{6m} is the wind speed measured in open country at a height of 6m, the defined meteorological wind speed used by den Ouden and Jackman.

Pressure coefficients were obtained from wind tunnel model measurements. Values for the windward face of the slab block varied between +0.6 and +0.8 and values for the leeward face were constant at -0.4. Values for the square building plan were the same for the windward and leeward faces and values of -0.55 were taken for the sides of the building. These values are in reasonable agreement with other measured values.

3.4.12 Den Ouden and Jackman used an air flow equation of the same form as that used by Gabriellson and Porra (equation 3.5) but allowed each opening to have unique values of C and n . They showed how infiltration rates vary with window leakage factor, assuming wind speeds of 4.4 or 8.8 m/s and temperature differences of 20°C acting. In particular, typical values of infiltration rate were shown to be under 0.6 air changes/hr for a low building and under 1.3 air changes/hr for a tall building. These are compared to values for the same conditions from the I.H.V.E. Design Guide which are 1.5 to 1.75 air changes/hr respectively. It was shown that, under conditions where both wind and stack effect are acting together, the net infiltration rate for the whole building was approximately equivalent to that of the larger force acting alone (Figure 3.5).

The pattern of the internal flow rates was shown to be altered considerably by variation in the relative values of stack effect and wind speed acting.

3.4.13 On the basis of these studies the predictive technique used in the I.H.V.E. Guide, 1970 for infiltration rates in buildings has been devised (I.H.V.E., 1970). The method assumes that the infiltration rate may be calculated from the wind speed alone, as the stack effect, in maximum infiltration rate situations, will be of secondary importance to the effect caused by large wind speeds. For a building of known height, in a sheltered or exposed position a pressure factor is calculated. A coefficient of drag of 1.1 is assumed to be acting across the building. The pressure factor is equivalent to one half of this coefficient multiplied by the dynamic head of the wind at building roof level. The wind speed is then computed from an assumed meteorological design wind speed, and corrected to sheltered, urban or exposed sites. The nomogram which does this calculation is shown in Figure 3.6. The basic ventilation rate is then found by reading from the nomogram, against an assumed window wall leakage coefficient; the ventilation rate being given per metre of window crack. Corrections can be made for the internal resistance to air flow of the building; the correction factor being 1.0 where there is little or no internal resistance and dropping as the internal airtightness increases.

3.4.14 The algorithm for infiltration rate calculations, published by A.S.H.R.A.E., (Nelson, 1971) describes a recommended procedure for computing infiltration rate by digital computer. The equations and assumptions are similar to those used by Jackman, although of somewhat greater complexity. Allowances are made for infiltration through window cracks, wall surfaces and mechanical ventilation systems. The equations relating air flow to pressure difference are of the form used in equation (3.5), the value of exponent, n , being 1.66 for all window cracks. The method is of particular interest for its method of computing the pressures due to wind acting on the building, the results of which are summarised in Table 3.6. A pressure factor is found from the table and the pressure at any point on the building found by multiplying the factor by the assumed wind speed at that height. This assumption gives a pressure pattern which changes, as the velocity profile of the wind, with height. Most other analogue studies assume a constant pressure coefficient value over the building face, and though this approach may well give equally realistic values, especially for the windward face it does not correspond to the real situation. It is surprising that although the corrections for surrounding buildings, in the A.S.H.R.A.E. work, are quite complex, no corrections for the shape of the subject building are made. A comparison of pressure coefficients found by this and other methods for a building may be seen in Figure 3.7.

TABLE 3.6 Values of pressure correction factor for various building configurations after Nelson in the A.S.H.R.A.E. Infiltration Algorithm

Smaller buildings upstream of subject building

Space/ building width	Windward face $-45^{\circ} < \theta < 45^{\circ}$	Side face $45^{\circ} < \theta < 90^{\circ}$	Leeward face $90^{\circ} \leq \theta \leq 270^{\circ}$
0.5	$0.10 \cos \theta$	$-0.80 \cos \theta$	-0.30
1.0	$-0.10 \cos \theta$	$-0.50 \cos \theta$	-0.25
2.0	$0.10 \cos \theta$	$-0.40 \cos \theta$	-0.25
3.0	$0.10 \cos \theta$	$-0.40 \cos \theta$	-0.25
5.0	$0.25 \cos \theta$	$-0.60 \cos \theta$	-0.35
∞	$0.60 \cos \theta$	$-0.70 \cos \theta$	-0.35

Equal height or taller buildings upstream of subject building

Space/ building width	Windward face $-45^{\circ} < \theta < 45^{\circ}$	Side face $45^{\circ} < \theta < 90^{\circ}$	Leeward face $90^{\circ} \leq \theta \leq 270^{\circ}$
0.5	$-0.50 \cos \theta$	$-0.45 \cos \theta$	-0.25
1.0	$-0.50 \cos \theta$	$-0.30 \cos \theta$	-0.20
2.0	0.00	$-0.30 \cos \theta$	-0.20
3.0	$0.10 \cos \theta$	$-0.35 \cos \theta$	-0.20
5.0	$0.25 \cos \theta$	$-0.45 \cos \theta$	-0.25
∞	$0.60 \cos \theta$	$-0.70 \cos \theta$	-0.35

Taller building on leeward side of subject building

Space/ building width	Windward face $-45^{\circ} < \theta < 45^{\circ}$	Side face $45^{\circ} < \theta < 90^{\circ}$	Leeward face $90^{\circ} \leq \theta \leq 270^{\circ}$
0.5	$0.50 \cos \theta$	$0.45 \cos \theta$	0.45
1.0	$0.45 \cos \theta$	$0.30 \cos \theta$	0.30
2.0	$0.45 \cos \theta$	$0.10 \cos \theta$	0.10
3.0	$0.45 \cos \theta$	0.00	0.00
5.0	$0.50 \cos \theta$	$-0.10 \cos \theta$	-0.10
∞	$0.60 \cos \theta$	$-0.70 \cos \theta$	-0.35

θ is the angle between a plane normal to the building wall being considered and the direction of the wind.

No quantitative results of computed ventilation rates are given with the paper.

3.5 Discussion of the significance of the analogue studies

3.5.1 Analogue studies give more controlled analyses of the problems of natural ventilation when compared to full scale studies. The interrelation of the factors which control the processes of natural ventilation can be studied individually. Of the two types of analogue which have been studied, hydraulic and digital electronic, the digital electronic analogues are of much greater practical importance. The hydraulic analogues give only simple qualitative data of little use in predicting ventilation rate in new buildings. Several digital analogue studies of building infiltration have been carried out, in European countries and the United States. All the studies make similar basic assumptions about infiltration mechanisms. From these studies two types of predictive technique have been evolved. The first, as in the I.H.V.E. Guide, 1970, uses simplified nomograms with corrections for different types of building and climatic condition. The second, as in the A.S.H.R.A.E. Infiltration Algorithm, requires a complete computer study for each building under known climatic conditions.

3.5.2 None of the digital analogue studies quoted have been carried out on a comparative basis. In all the studies where quantitative results have been presented

the results are from calculations on real or hypothetical buildings in which no full scale or model scale studies have been attempted in order to verify the analogue results. This is a significant omission in a complex subject where few detailed full scale studies have been made to establish either the relevance of many of the factors affecting ventilation rate, or the accuracy of the input data.

3.5.3 The data assumed in different theoretical studies differs considerably between the studies. A summary of some of the data input assumptions may be seen in Figure 3.9. In particular different assumptions are made for values of pressure coefficient acting on the buildings studied. Gabriellson and Nelson assume a pressure coefficient increasing with height, while others assume a constant pressure over each face of the building. The former is probably a more realistic representation of real conditions, particularly for tall buildings. The values of the assumed coefficients of pressure acting across each wall of the building vary considerably. The lowest value of $(C_{pw} - C_{pl})$ for an unshielded building is given by Nelson as 0.95, while the highest assumption value is given by Tamura and Wilson as 1.4. Nelson also includes terms to allow for the shielding of the building which reduce still further the values of $(C_{pw} - C_{pl})$ under normal urban conditions.

3.5.4 Significant differences are also seen in the assumed infiltration characteristics of the external envelope of the building. Most studies assume a relationship between pressure difference and volume flow rate which is exponential; as in equation (3.5). Harrison, Svetlov and Bogoslovskii assume a relationship of the form given by Dick and Thomas, (Dick, 1953) as in equation (3.8). The values of the exponent n assumed varies between 1.5 and 2.0. This could lead to differences of the order of $\pm 15\%$ or more between the estimated ventilation rates for otherwise similar windows over working pressure ranges, (Figure 3.9). The range of infiltration coefficients for typical window types given in the papers, also vary over a considerable range; Harrison showing the highest values and the I.H.V.E. Guide the lowest. This divergence may be accounted for by variation in the quality of the window units. The range of values given by each of the authors suggests that the estimations given for generic window types are probably subject to quite large errors in any specific case.

3.5.5 The results given in the papers by Jackman and den Ouden show general agreement with the experimental results given by Dick and Tamura and Wilson. They show (Figure 3.5) that the total building ventilation rate may be approximated to the rate caused by stack effect or wind effect acting alone, whichever being larger.

They emphasise however that the balance of the internal flow patterns can be altered very significantly by the relative importance of the two effects.

3.5.6 All the digital analogue ventilation studies consider the effects of infiltration on the building only. No analyses of controlled natural ventilation have been attempted. The choice of suitable meteorological design data is not discussed in the papers with the exception of the I.H.V.E. Guide. Here a meteorological wind speed of 9 m/s is assumed to act in the design situation. This is roughly equivalent to a one percentile wind speed for a typical inland site in Britain. No allowance for geographical position or site topography is made. The wind speed is amended for urban or suburban situations. The effect of temperature difference is taken to be of secondary importance and is allowed for in simple corrections to the ventilation rate.

3.6 Conclusions

3.6.1 The general conclusions on the studies of natural ventilation are summarised below:

1. Full scale studies, although useful in establishing the principles of natural ventilation, have not been of sufficient accuracy to establish general predictive techniques.

2. Simple nomograms have been produced from digital analogue studies which are useful in estimating the gross infiltration rates for simple building forms under extreme meteorological conditions.
3. Accurate information on the internal flow patterns cannot be easily deduced from this technique.
4. Wholly computerised analogue studies can be used to predict infiltration rates under any meteorological conditions with greater detail.
5. Little guidance is given on the choice of suitable meteorological design data for specific sites.
6. There is considerable variance between different authors over the values of external pressure coefficients and window infiltration coefficient values.
7. None of the analogue techniques used to establish predictive methods have been compared with full scale or model scale studies to estimate their accuracy.

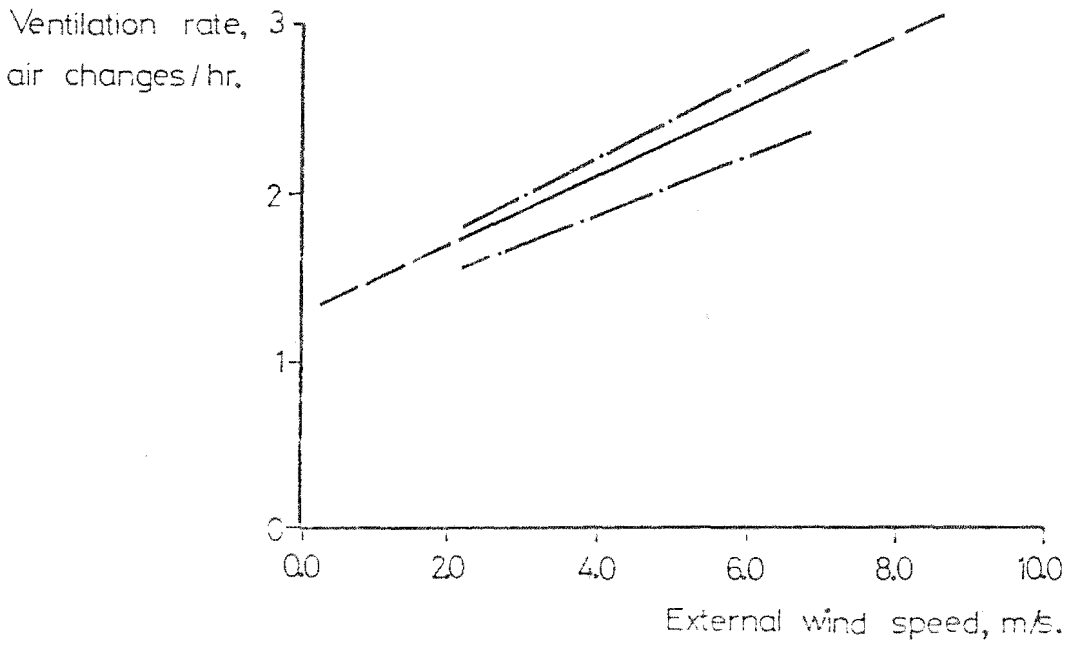
3.6.2 The main sources of inaccuracy in the analogue techniques are probably in the estimation of design wind speeds and estimation of the infiltration coefficients of the external wall. Extreme wind speeds for structural loading calculations for a particular site can be estimated from remote data with an accuracy of $\pm 50\%$ according to Waller et al (Waller, 1968). The accuracy of estimating less extreme data should be higher

but may still be $\pm 25\%$. The estimation of infiltration coefficients for external walls from generalised data for window types may be possible to an accuracy of $\pm 25\%$ or less. This could be improved by specific information from manufacturers. The effect of these inaccuracies on calculated ventilation rates is more significant in the case of wind data. A 1% error in wind speed may give, typically, a 1.2% error in computed ventilation rate, whereas a 1% error in infiltration coefficient will produce an error of less than 1% (see equation 3.5), because of the presence of internal partitions.

3.6.3 The techniques available are not suitable for assessing running costs or normal environmental performance standards for infiltration or controlled ventilation. In order to be able to assess this type of effect a more sophisticated treatment of the climatological input is required. In particular the use of bi-variate analyses of wind speed and temperature would be needed to assess the control and degree of variation of performance of infiltration and ventilation under normal working conditions. This type of procedure would require a computerised technique rather than simple nomograms, but would give much more useful information about the predicted performance standards of new buildings.

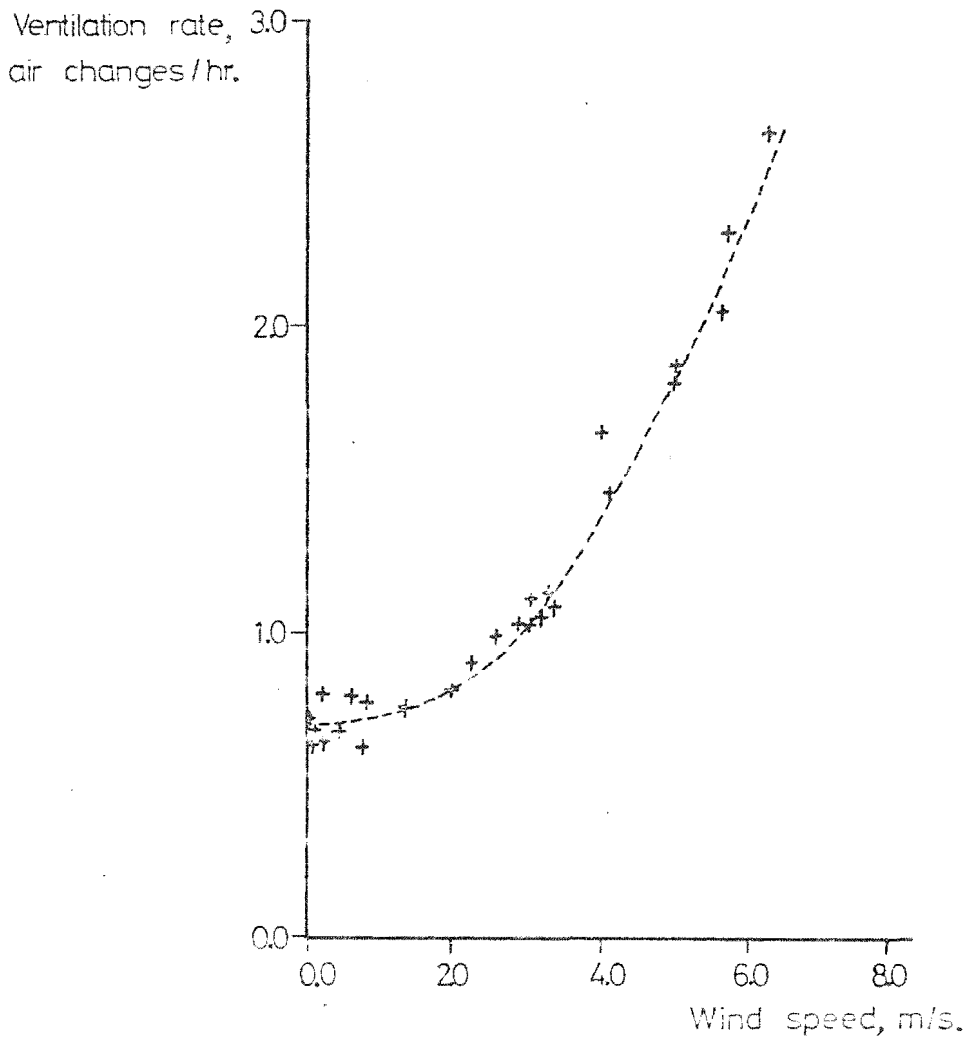
Figure 31. The effect of wind speed and direction on the
air change rate of a house, after Dick.

Results for house 33.



Mean air change rate for the season _____
 Limits of the effect of wind direction
 on air change rate - - - - -

Figure 32. The effect of wind speed on the air change rate in a house with a temperature difference of 5.56°C (10°F) acting, after Dick.



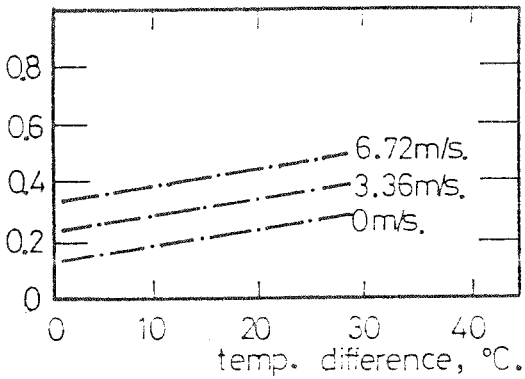
1.57 m/s. is the wind speed at which the ventilation rate due to the wind alone is theoretical equal to that due to stack effect alone.

Figure 3.3.

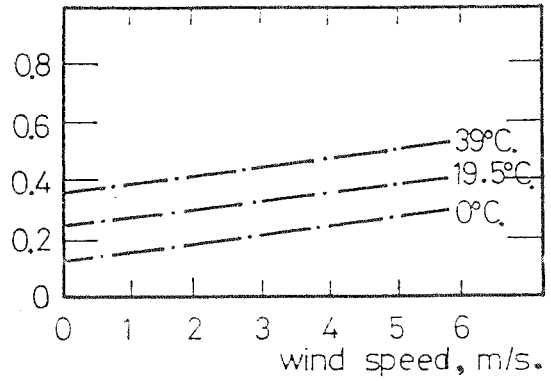
Relationship between observed ventilation rates
wind speeds and temperature differences for
two houses, after Bahnfleth et. al,

House 1.

air change
rate/hr

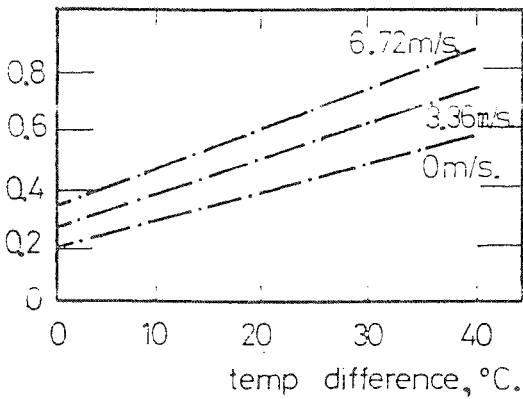


air change
rate/hr



House 2.

air change
rate/hr



air change
rate/hr

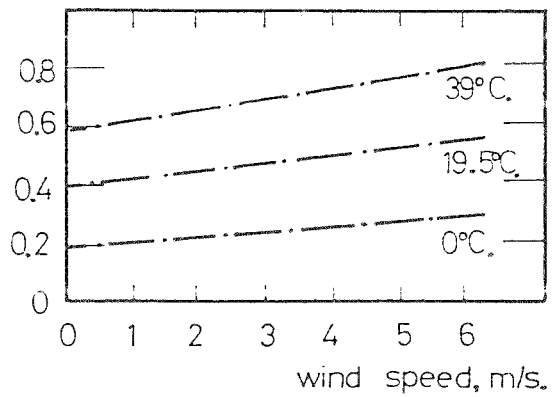
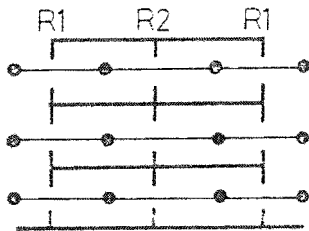


Figure 34.

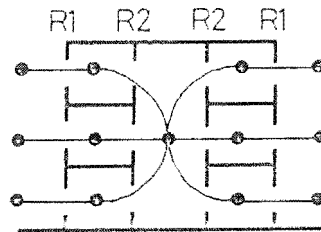
Schematic building forms assumed representative of typical building types, after Harrison

Case 1 Simple building, no connection between floors.



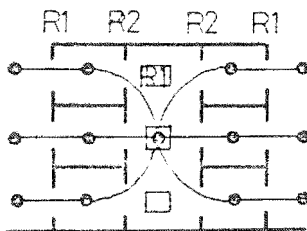
- 1A $R2 = 0$
- 1B $R2 = R1$
- 1C $R2 = 2 \cdot R1$
- 1D $R2 = 3 \cdot R1$

Case 2 Building with simple stairwell, no resistance to flow.



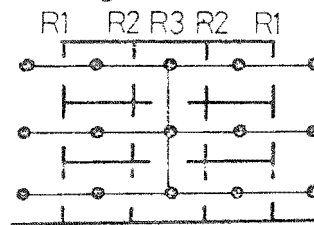
- 2A $R2 = R1$
- 2B $R2 = 2 \cdot R1$
- 2C $R2 = 3 \cdot R1$
- 2D $R2 = 4 \cdot R1$

Case 3 As case 2, windows in the stairwell.



- 3A $R2 = R1$
- 3B $R2 = 2 \cdot R1$
- 3C $R2 = 3 \cdot R1$
- 3D $R2 = 4 \cdot R1$

Case 4 Building with stairwell resisting flow at each floor level.



- 4A $R2 = R1 = 2 \cdot R3$
- 4B $R2 = R1 = 4 \cdot R3$
- 4C $R2 = 2 \cdot R1 = 4 \cdot R3$
- 4D $R2 = 3 \cdot R1 = 6 \cdot R3$
- 4E $R2 = 4 \cdot R1 = 8 \cdot R3$

Figure 3.5.

Theoretical ventilation rates in a ten storey building, after Jackman and den Ouden

- Effect of wind alone
- .-.-.-.- Effect of temperature difference alone
- Effect of combined forces

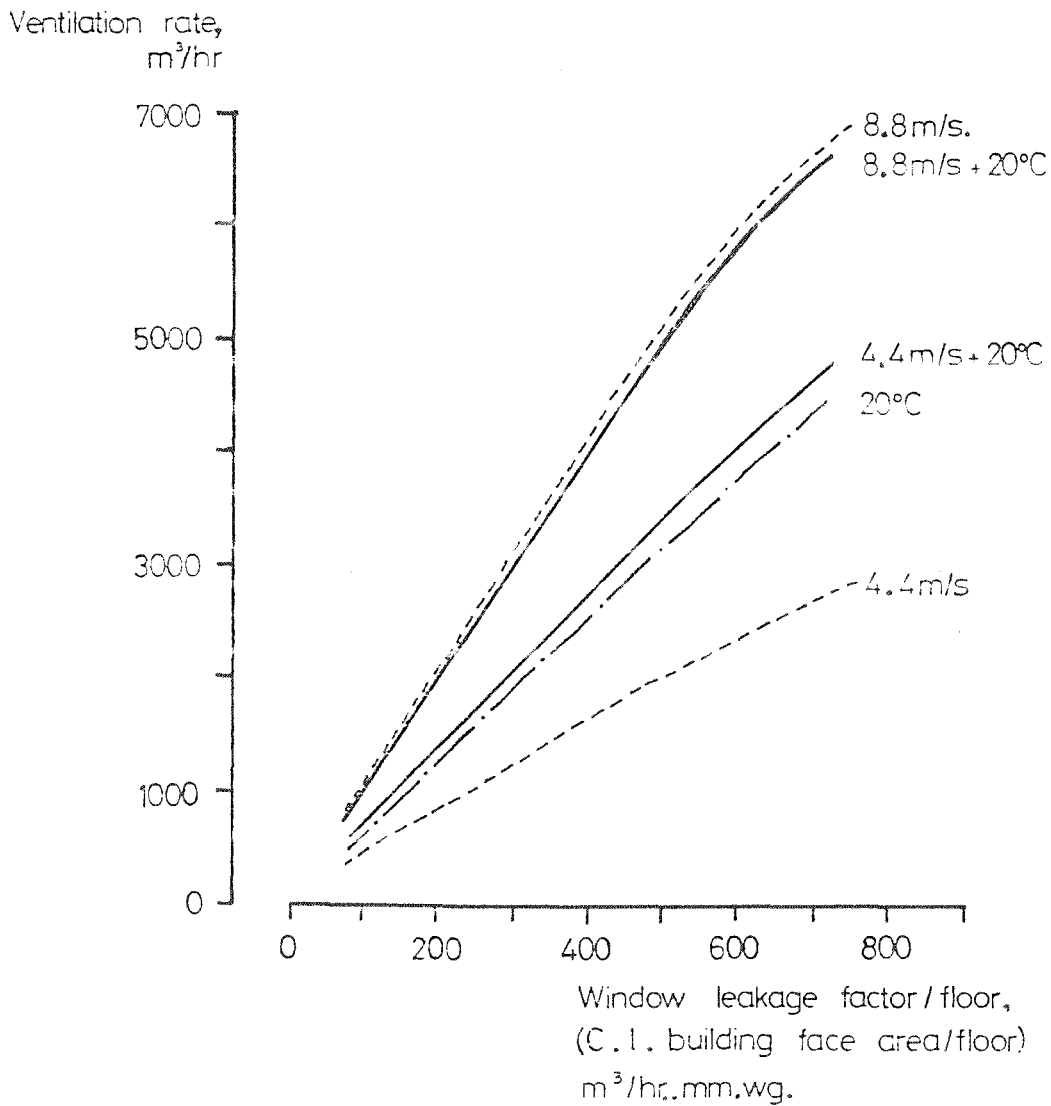


Figure 3.6.

Nomogram for calculating basic infiltration rate in buildings, from the I.H.V.E. Guide, 1970.

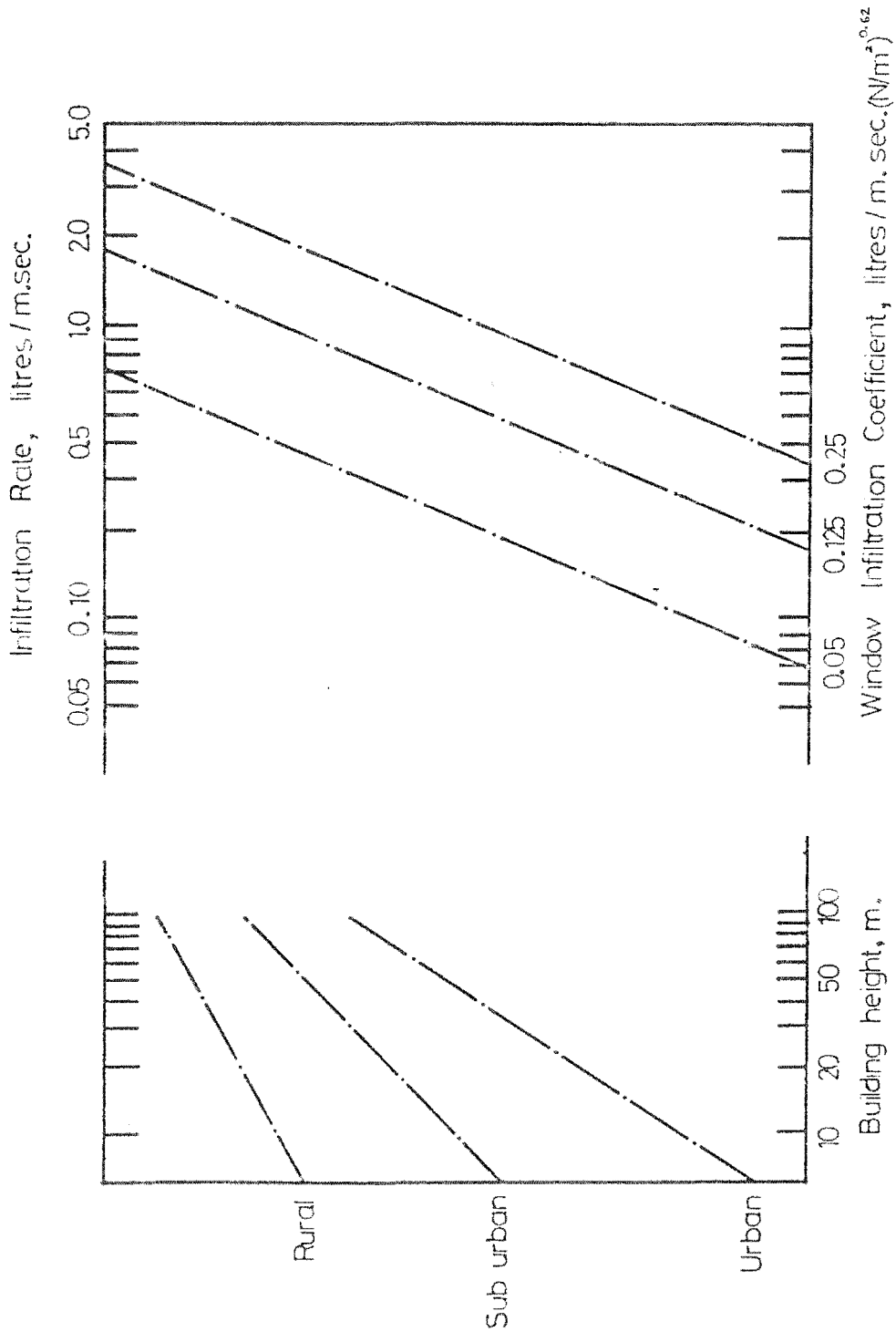
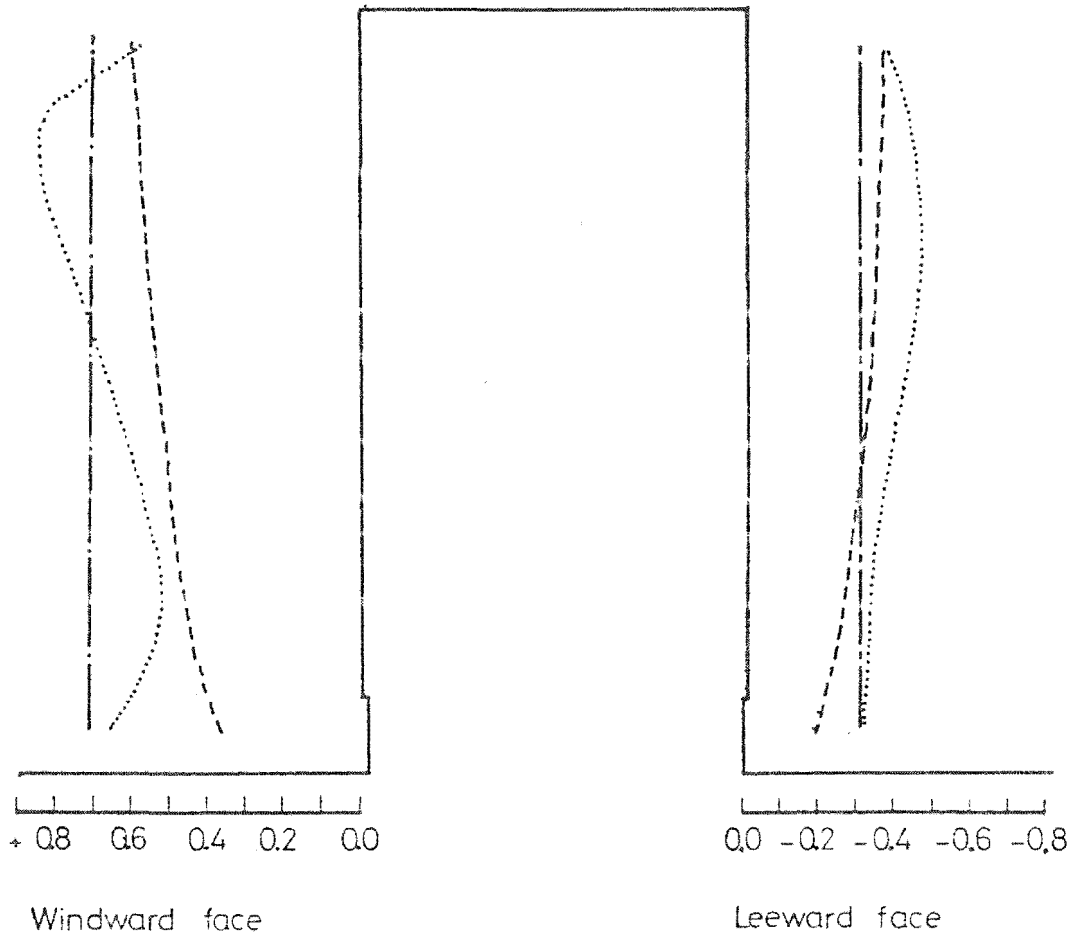


Figure 3.7.

A comparison of measurements of pressure coefficients on a model building with estimates from BRS Digest 119 and ASHRAE Infiltration Algorithm.



Jackman and den Ouden model studies
BRS Digest 119
ASHRAE Infiltration Algorithm

.....
—————
- - - - -

	Harrison	Gabriellson and Porra	Tamura and Wilson	Jackman and den Ouden	Rogelein	I.H.V.E. Guide, 1970	A.S.H.R.A.E. Algorithm
Building form applicable	Slab, uniform glazing	Rectangular	Square, uniform glazing	Slab, uniform glazing	—	Square, slab or rectangular, uniform glazing	Variable, unspecified
wind pressure input data	cpw +0.5 cpl -0.5	cpw +1.0 * cpl -0.3 cps -0.3	cpw +0.8 cpl -0.6 cps -0.6	cpw +0.7 cpl -0.4	no values given, model studies done	cpw + 0.55 cpl - 0.55	dependent on surroundings (table 6) *
wind directions studied	90° to main facades	45° or 90° to main facades	90° to main facades	90° to main facade	—	max. infiltration situation	as required (table 6)
type of flow equation used	$p = av + bv^2$	$v = k(p)^{1/n}$	$v = k\sqrt{p}$	$v = k(p)^{1/n}$	$v = k(p)^{1/n}$	$v = k(p)^{1/n}$	$v = k(p)^{1/n}$
value of exponent, n	—	1.5	2.0	1.6	1.5	1.6	1.66
range of window infiltration coefficients used	5.0 – 11.0 cmh/m/mm ^{0.6}	—	3.4 – 5.4 cmh/m/mm ^{0.5} ⊕	0.1 – 5.0 (typically 3.4) cmh/m/mm ^{0.6}	—	0.75 – 3.8 cmh/m/mm ^{0.6}	0.8 – 4.3 cmh/m/mm ^{0.6}
range of internal flow resistance coefficients used	0 – 4 x window wall coeff.	0	0.5 x window wall coeff.	0.2 x window wall coeff.	0.1 – 0.3 x window wall coeff.	0 – 5 x window wall coeff.	unspecified
notes:	cpw: mean pressure coeff windward face cpl: mean pressure coeff leeward face cps: mean pressure coeff side walls				* pressure coeff at height h expressed relative to wind speed at that ht. ⊕ expressed per unit area ext. wall.		

Figure 3.8.

A summary of the variables used in the digital analogue ventilation studies discussed previously.

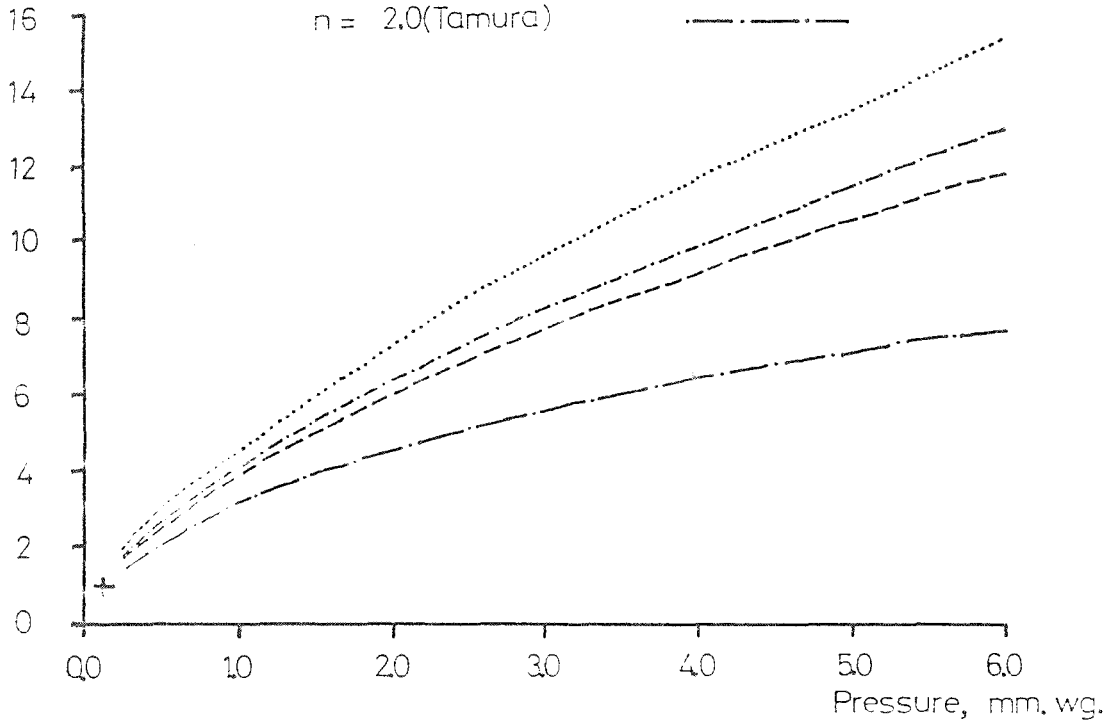
Figure 3.9.

The effect of variation of exponent, n , and coefficient reference pressure difference on air flow rates through windows over an assumed working range of 1–6 mm. wg. pressure difference.

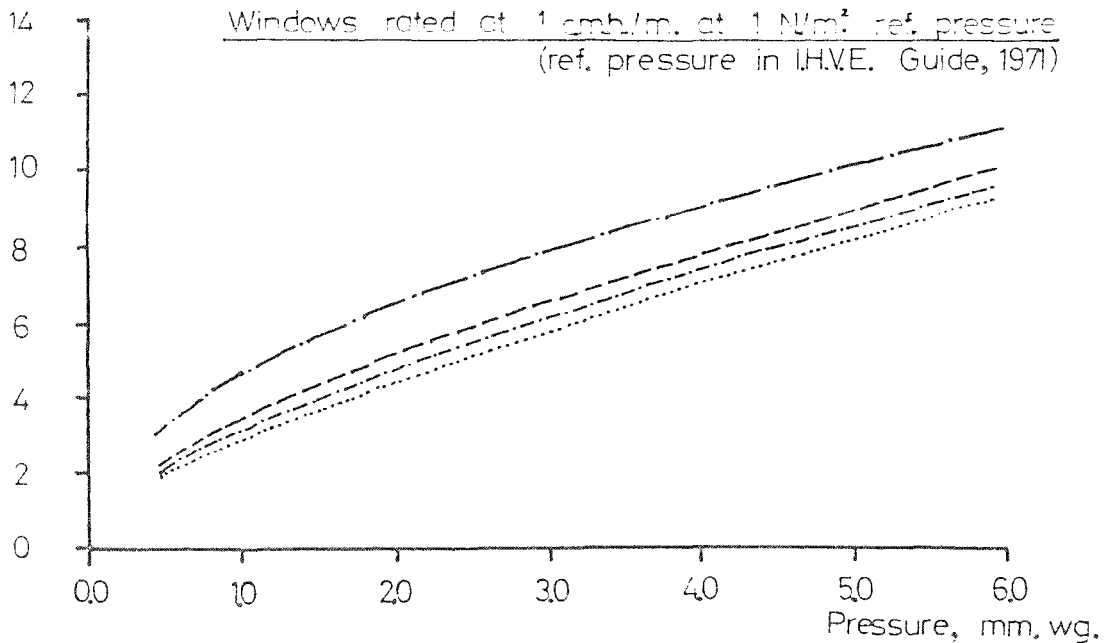
Flow equation : $V = C(dp)^{1/n}$

- $n = 1.5$ (Rogelein)
- $n = 1.6$ (Jackman)
- $n = 1.66$ (Nelson)
- $n = 2.0$ (Tamura)

Flow rate cm.h./m.



Windows rated at 1 cmh./m. at 1 N/m² ref. pressure
(ref. pressure in I.H.V.E. Guide, 1971)



Windows rated at 20 cm.h./m. at 20mm.wg. ref. pressure
(ref. pressure in B.S.I. Draft for development, No4, 1971)

4. AIR FLOW CHARACTERISTICS OF VENTILATION OPENINGS

4.1 Introduction

4.1.1 In the prediction of natural ventilation and infiltration rates in buildings the assessment of the air flow characteristics of the openings is one of the most important problems. The range of flow rates occurring through openings, varying from open windows to small constructional defects, is very large, and flows through any of these types of opening may be of significance in different buildings under different design conditions. The use of sophisticated analytical techniques are of little use if the available information on leakage characteristics is not of similar accuracy. Consequently for the assessment and development of predictive techniques both detailed air flow characteristics and the appropriate accuracy limits of these characteristics must be determined.

4.1.2 Most infiltration is assumed to occur through the gaps between doors and windows and their frames. The air-tightness of these components is difficult to predict. Air leakage is dependent on both the width of the gaps through which the air flows and their geometrical configuration, which is normally of a complex form. Infiltration may also occur through constructional defects in other building elements and, although this is often of secondary importance, it can be significant.

Both these sources of infiltration are dependent on the detailed design of the building's components, the quality of the materials of which these components are constructed and the care with which they are erected. Because of the complex interactive effect of these factors the theoretical prediction of leakage characteristics in practical design situations is very difficult.

4.1.3 Most air flow characteristics have been determined by experimental studies, and many of these have been carried out. Different research workers have suggested empirical expressions to describe the relationship between the air flows through these openings and the pressure differences acting across them. In the first section of the chapter several types of relationship are described and results obtained from them compared. From the empirical studies design infiltration rates have been suggested for different types of openings. Little information is available on the variability of these design rates due to different standards of construction or design, the effects of maintenance or long-term deterioration. In the second part of the chapter the available information is reviewed and the techniques used in current practice critically assessed.

4.2 Comparative analyses of expressions describing the infiltration characteristics of openings.

4.2.1 Mathematical expressions for the flow of air through openings of the type through which infiltration normally occurs are difficult to derive theoretically. Flow through large openings, such as that through some open windows, is relatively simple to describe theoretically, being similar to orifice flow. A coefficient of discharge of approximately 0.60 is normally assumed, from which can be obtained a flow equation of the form:

$$V = 8640.A.\sqrt{dP} \quad \dots\dots (4.1)$$

where V is the volumetric flow rate, m³/hr.

A is the open area of window, m².

dP is the pressure difference, mm.wg.

Similarly, flow in long thin tubes, where the flow is laminar, and the rate of flow is proportional to the pressure difference acting across the ends of the tube is also well understood. In the case of openings in buildings, through which infiltration typically occurs, the flow path is too long for flow to be modelled accurately by orifice flow and too short to assume laminar flow conditions. Because of these complications the expressions normally used have been developed empirically.

4.2.2 Three forms of expression which attempt to

describe the flow characteristics of these types of opening have been noted. The most commonly used expression, which has been used in most of the analogue studies reviewed previously, (Gabriellson, 1968), (Tamura, 1969), (Jackman, 1969), (Nelson, 1971) is one of the form:

$$V = C.L.(dP)^{1/n} \quad \dots\dots (3.5)$$

The flow rate is assumed to vary exponentially with the pressure difference acting across the opening. The value of the exponent used is between 0.5 and 1.0. The particular advantage of this type of expression, which probably accounts for its popularity, is the ease by which it can be manipulated mathematically. In comparison, Dick and Thomas (Dick, 1953), after a carefully planned series of experiments, suggested a relationship of the form:

$$dP = \frac{0.053}{y^2} (V + 0.22V^2) \quad \dots\dots (4.2)$$

where dP is the pressure difference, mm.wg.

V is the volumetric flow rate, m³/hr.

y is the opening gap width, mm.

In this expression, as flow rates increase, the type of flow changes from one in which the pressure difference and flow rate are related almost linearly to one in which the pressure difference is more closely related to the square of the flow rate. A third method of

expressing this relationship, (Lenkei, 1965), is to assume a relationship of the type:

$$V = L.y.CZ.\sqrt{\frac{2g.dP}{\rho}} \quad \dots\dots (4.3)$$

where L is the length of gap open to flow, m.

y is the opening gap width, mm.

CZ is a discharge coefficient.

g is the gravitational constant, m/s²

ρ is the density of air, kg /m³.

This is an equation typical of orifice flow, but uses empirically derived discharge coefficients which vary with orifice geometry and Reynolds number. This technique has been used in a suggested design method (Meckler, 1967).

4.2.3 The most widely used expression for determining the flow characteristics of window crackage is the exponential form. Many measurements of air leakage rate have been made over small ranges of pressure difference, and have been used to obtain design values of the leakage coefficient, C, (equation 3.5). The relationship between the leakage coefficient and the crack dimensions does not seem to have been investigated fully. Similarly the accuracy of the expression does not seem to have been studied over larger ranges of pressure difference. Values of the reciprocal of the flow exponent, n, are normally taken to be between 1.5 and 1.66. The variation of this

value with opening geometry again does not seem to have been investigated, although this value can be of importance in determining leakage rates from design air flow rates at reference pressure differences (Figure 3.9). A review of some assumed numerical values for these parameters is given in Figure 3.8.

4.2.4 In the experiments carried out by Dick and Thomas a number of short lengths of standard section timber and metal window were tested. These were arranged so that the gap width, y , could be accurately controlled. A range of gap widths between 0.125 mm. and 2.4 mm. were tested. Pressure differences between 12.5 mm.wg. and 0.125 mm.wg. were used. Dick and Thomas found that the flow rates were closely related to the width of the section of the air path which was narrowest, and to the length of this section. In an attempt to estimate the accuracy of the results, flow rates for complete windows of the same type were measured under the same conditions. Relating the flow rate values to the mean gap width values for the complete windows they found that the results showed an average error of less than 10% compared with the results found for the short lengths of window. This was explained by the effect of variation of the gap width around the window. Furthermore they suggested an expression to describe the relationship of the form given in equation 4.2. This gave an average error of $\pm 12\%$ when compared to the observed results for

the complete windows. A representative section of their test results are given in Figure 4.1.

4.2.5 In the technique suggested by Lenkei, an equation, representative of orifice flow, is used to calculate the air leakage rate:

$$V = L.y.CZ. \sqrt{\frac{2g.dP}{\rho}} \quad \dots\dots (4.3)$$

A large number of experimental values of the discharge coefficient, CZ, have been determined for the range of types of opening given in the paper, and these values are used in determining the flow rate. The discharge coefficients, which vary with Reynolds number, are shown in Figure 4.3. In cases of infiltration through cracks of uniform width, the Reynolds number based on a hydraulic diameter of 2y, was taken to be:

$$Re = \frac{2.W'.y.\rho.10^{-3}}{\mu} \quad \dots\dots (4.4)$$

where W' is flow velocity, m/s.

μ is dynamic viscosity, N.s./m².

Flow rates are found using an iterative technique: initially a discharge coefficient value is assumed and then an approximate flow rate found using equation 4.3. Using this flow rate value a Reynolds number can be calculated and a more accurate discharge coefficient found. By means of successive approximations an accurate value of leakage rate may be found. The method

has the advantage of giving acceptably accurate results over a large range of flow conditions, although it is tedious to use for many repeated calculations.

4.2.6 Neither Lenkei's nor Dick's expressions for determining air flow rates have a constant exponential relationship between volume flow rate and pressure difference as the pressure difference varies. This can be seen in Figure 4.3, where curves have been drawn, for a simple window crackage section, using both expressions. The two curves show good agreement; the air flow rate as shown by Dick's curve being approximately 10% higher than that taken from Lenkei's work. This agreement is within the order of accuracy given by Dick for his work, $\pm 12\%$, and a figure mentioned by Lenkei of $\pm 15\%$. It can be seen from the curves that they may be reasonably closely approximated by a simple exponential relationship, the approximation being more accurate over a limited range of pressure differences. In particular either curve may be represented by an exponential expression over a range of pressure differences of 50:1 with an error of less than 10%. Furthermore if the curve is carefully fitted at a maximum design pressure difference, the absolute error values, even when relative errors become large, do not cause large inaccuracies when compared to the maximum flow rates. This effect is demonstrated in Table 4.1. It may be concluded from these comparisons that the three types of expression are all similar, and

acceptably accurate in comparison to the accuracy of the available data on window crackage. Consequently the exponential form, being simplest to use in practice, can reasonably be used.

TABLE 4.1 Comparison between air leakage rates after Lenkei and an exponential relationship, equated at a design pressure difference of 5 mm.wg.

Pressure difference, mm.wg	Leakage rate, m ³ /hr.,		Error %	Error relative to max. leakage %
	after Lenkei	exponential form, n = 1.6		
5.0	8.3	8.3	0	0
2.0	6.2	6.0	-3	-2.5
0.5	3.9	3.9	0	0
0.2	2.0	2.2	+10	+2.5
0.05	0.65	0.90	+39	+3.0

4.2.7 The exponent value appropriate in this type of expression is dependent on the geometrical characteristics of the opening. The detailed effect of the crackage dimensions are not accurately known, and most workers make no allowance for variation due to this factor. The expressions developed by Dick and Thomas, and Lenkei imply that as the ratio of crackage width to flow length, y/l , decreases, and as the Reynolds number decreases, the

appropriate exponent value approaches unity. This phenomenon has been investigated further by Kreith and Eisenstadt (Kreith, 1957), in short capillary tubes. They show curves relating the y/l ratio to Reynolds number and exponent values for these openings, which are in reasonable agreement with the previously discussed work. To summarise this information for all types of opening is difficult because of the many factors involved. The problem may be simplified however, as in most window types the flow length, l , will be relatively constant in comparison with the other parameters involved. Air leakage curves were drawn for several different crack dimensions, (Figure 4.4), using Lenkei's method and assuming a flow length value of 5 mm., which is similar to the values found by Dick and Thomas in standard window types. The values of the exponent which best fits each curve for the pressure difference range 0.1 mm.wg. - 10.0 mm.wg. were found, and the results were compared with values obtained by analysis of Dick and Thomas' observations. The results, which show a distinct relationship between exponent value and leakage coefficient, are presented in Figure 4.5.

4.2.8 The flow exponent values have been related in Figure 4.5 to crackage infiltration coefficient rather than to the crack width, y , as this is a more commonly quoted figure. It may be seen that these results show reasonably consistent agreement. The results also agree

quite well with the figures given by Kreith and Eisenstadt. Other results may be expected to be subject to somewhat greater variability due to the range of possible flow lengths, and also changes in the detailing of other parts of the window crackage. Although these results cannot be said to be accurately representative of all types of crackage it is likely that they give an approximate guide to the characteristics of many types of window under normal conditions. The results suggest that significantly higher exponent values are appropriate at infiltration coefficients in the range $0.1 - 3.0 \text{ m}^3/\text{hr}/\text{m}$, measured at 1 mm.wg , than those normally assumed. This may be caused either by the continued assumption of exponent values appropriate to the less airtight types of window, or testing at relatively high pressure differences, typically $5 - 50 \text{ mm.wg.}$, which is well outside the normal working range. In either case the use of exponent values of approximately $0.6 - 0.66$ for high performance windows would lead to significant differences in performance when compared to values calculated from the exponent values indicated above. As an example the calculated infiltration rates for a window with a test air leakage rate of $12 \text{ m}^3/\text{hr}/\text{m}$. at 20 mm.wg. pressure difference would be $0.16 - 0.58 \text{ m}^3/\text{hr.}$ over a range of pressure differences of $0.1 - 0.5 \text{ mm.wg.}$, if an exponent value of 0.82 were assumed. Using a typical exponent value of 0.63 , the leakage rates under the same conditions would

be calculated as 0.44 - 1.20 m³/hr. Although the results given in Figure 4.5 are from a limited set of results a tentative relationship between exponent value and infiltration coefficient is suggested (Table 4.2) which may increase the accuracy of air leakage calculations.

TABLE 4.2 Suggested exponent values to be used when calculating infiltration for different types of window crackage.

Leakage coefficient range at 1 mm.wg., m ³ /hr/m.	Leakage coefficient range at 20 mm.wg., m ³ /hr/m.	Suggested Exponent values	Suggested Exponent reciprocal, n.
≥ 15	≥ 72	0.5	2.0
5 - 15	36 - 72	0.6	1.66
1.5 - 5	16 - 36	0.7	1.4
0.5 - 1.5	8 - 16	0.85	1.2
≤ 0.5	≤ 8	1.0	1.0

4.3 Design air leakage coefficient values.

4.3.1 The estimation of design leakage rates for different types of windows is complex. Performance varies with the design of the window, the material of which it is made, and the care with which it is fabricated. Information on which infiltration calculations may be based can be obtained either from general guides or specific manufacturers. The presentation of design rates

is given in several different ways by different references, although all the references present figures for generic window types. The I.H.V.E. Guide presents infiltration coefficients at a reference pressure difference of 1N/m^2 (0.10 mm.wg). Several American window manufacturers give figures, using the same system, but using 0.3 in.wg. or 1.2 in.wg. (7.6 or 30.5 mm.wg.) as the reference pressure difference (Sasaki, 1965), whilst in Belgium a reference pressure difference of 10 mm.wg. is used (Van Ackere, 1970). Extrapolation, assuming an exponential relationship, with an exponent value of 0.67 or 0.63, in order to calculate leakage rates at other pressure differences is recommended by these sources. The A.S.H.R.A.E. Guide presents leakage estimates at pressure differences of 2.5, 5.1, 7.6, 10.2, and 12.7 mm.wg. There is no guide for extrapolation of figures into the normal working range. The use of infiltration coefficients, rather than leakage rates presented for specific pressure differences, would seem to be a more generally useful system, as extrapolation to determine ventilation rates at other pressure differences can be more easily carried out. Presentation of data at different reference pressures then becomes a less significant problem, although ideally one standard pressure would be used.

4.3.2 Mean design leakage rates from these sources show reasonably close agreement, as may be seen in

Figure 4.6. However the range of leakage rates found in window types in any one of these categories has been found, in various studies (Sasaki, 1965), (Van Ackere, 1970), (Jackman, 1971), to be very much larger. In each of the studies a number of standard window units of varying standards of design and construction were tested at different pressures. The results cannot be accurately compared as the variation will depend upon the size of sample studied and the classification of window types. Jackman's figures however suggest that, generally, in any one of the standard classes of window unit specified in Figure 4.6, 33% might be expected to have coefficients either greater than double the design value or less than one half of this value. The results of these studies are summarised briefly in Table 4.3. The range of leakage rates in this type of classification is clearly too large for the accuracies of the coefficient values to be satisfactory for any detailed calculations.

4.3.3 Many manufacturers provide leakage rates for specific window types, measured under test conditions. Results taken from these sources should be of considerably greater accuracy as the variability due to differences in design and material is removed. Information on the accuracy of characteristics described with regard to specific window type is not generally available.

TABLE 4.3 Variation in leakage rates in general window classifications due to changes in design and standard of construction, m³/hr/m., for a 1 mm.wg. pressure difference, after Sasaki, Van Ackere and Jackman.

Window Type	Sasaki		Van Ackere		Jackman	
	minimum measured leakage	maximum measured leakage	minimum measured leakage	maximum measured leakage	16 %ile	84 %ile
pivoted, weather-stripped	0.14	1.0	0.0	3.8	0.18	1.2
sliding, weather-stripped	0.40	2.3			0.64*	
pivoted, not weather-stripped	0.60	3.2	0.25	8.0	1.6	6.0
sliding, not weather-stripped	1.40	5.4			2.4*	

* Values for all sliding windows tested

4.3.4 In order to provide a guide to manufacturers the British Standards Institute has proposed minimum performance requirements for air infiltration through windows, (B.S.I., 1971). For three grades of exposure - (sheltered, moderate and severe), the draft suggests that maximum air infiltration rates should not exceed 12 m³/hr/m. at test pressures of 10, 15 or 20 mm.wg. pressure difference respectively. These performance values are roughly equivalent to 2.4, 1.8 and 1.5 m³/hr/m.

at a pressure difference of 1 mm.wg. The present recommendations are of limited use to the designer. Requirements for air-tightness of individual windows vary with the type of building, the amount of glazing used and also with the type of ventilation used. In a naturally ventilated building a minimum background rate of ventilation, to control occupation products, is always required and consequently the required standards of air-tightness of windows may be limited to moderate values, and this ventilation provided by infiltration. In an air conditioned building this ventilation is supplied mechanically and any infiltration serves only to disturb the designated flow rates. The use of a standard method of testing with an extended range of standard performance grades, on which design criteria could be based would be of considerably greater assistance to the designer.

4.3.5 The final factor which affects the accuracy of data concerning infiltration in window units is the effect of long term deterioration. Deterioration may be caused by mechanical damage or through normal maintenance. The problem of deterioration through maintenance is likely to be of greater significance with materials which are not self-finished. Repainting high performance window units, for example, is likely to cause change in the crackage dimensions and deterioration of performance because of the less even paint surface. No information

is available concerning the effect of factors of this type on performance.

4.4 Conclusions

4.4.1 The conclusions concerning the techniques available for predicting the air flow characteristics of ventilation openings are summarised below:

1. The infiltration characteristics of openings of the type found in normal window crackage can be adequately described by an exponential relationship between air flow rate and pressure difference.
2. Exponent values normally assumed in current use are lower than the present studies indicate as appropriate.
3. The appropriate exponent values would seem to be related to infiltration coefficient values, becoming greater as infiltration coefficient values decrease.
4. The accuracy of infiltration coefficients, which are based on classification by general window type, and which are presented in this form in design guides is very low. This is because of the wide variety in standards of design and construction within each general window classification.
5. Test results or a grading system based on test results for specific window models are likely to be considerably more accurate, although no information is available on the likely levels of accuracy.

Figure 4.1. Infiltration through window gaps, after Dick and Thomas.

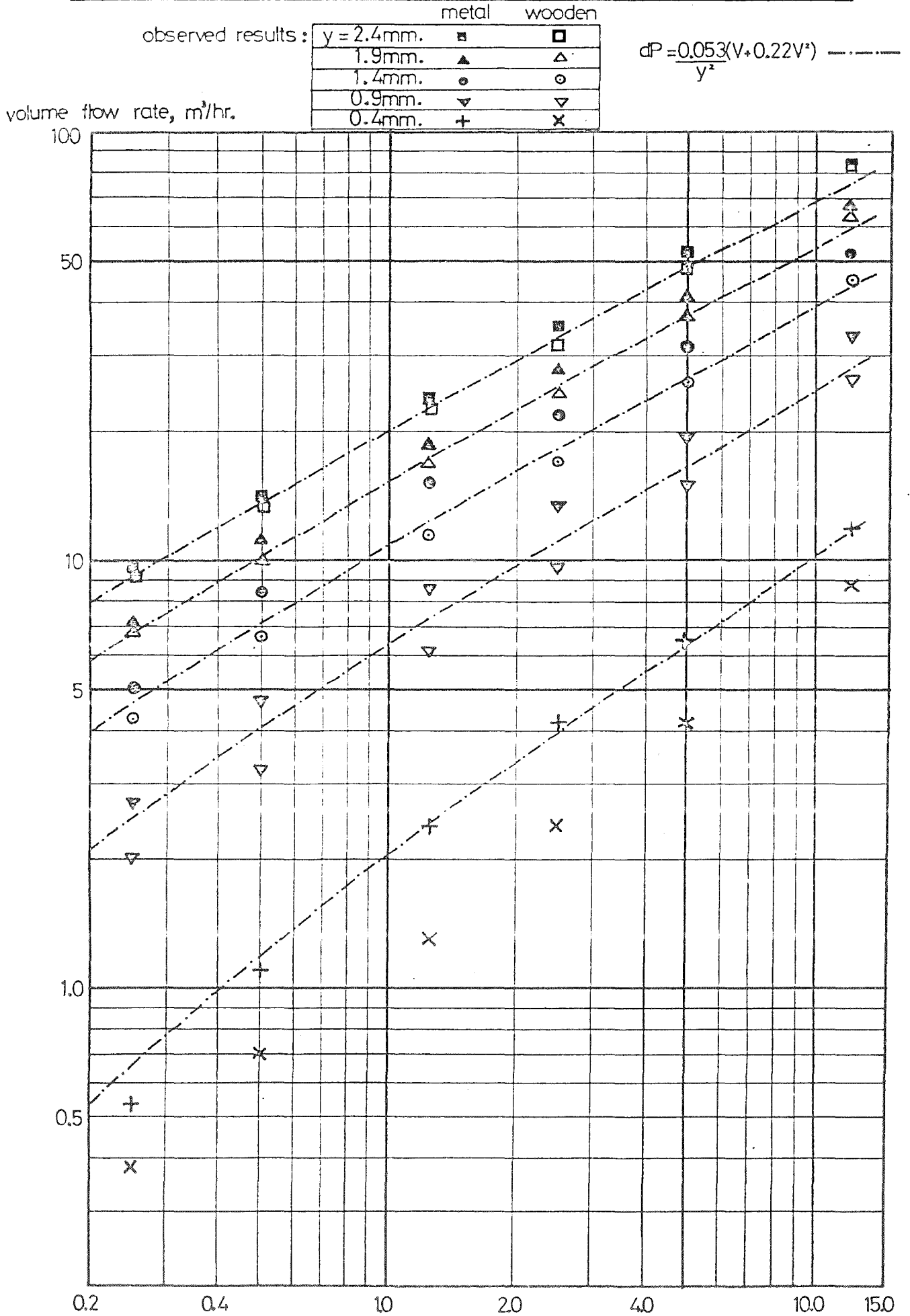
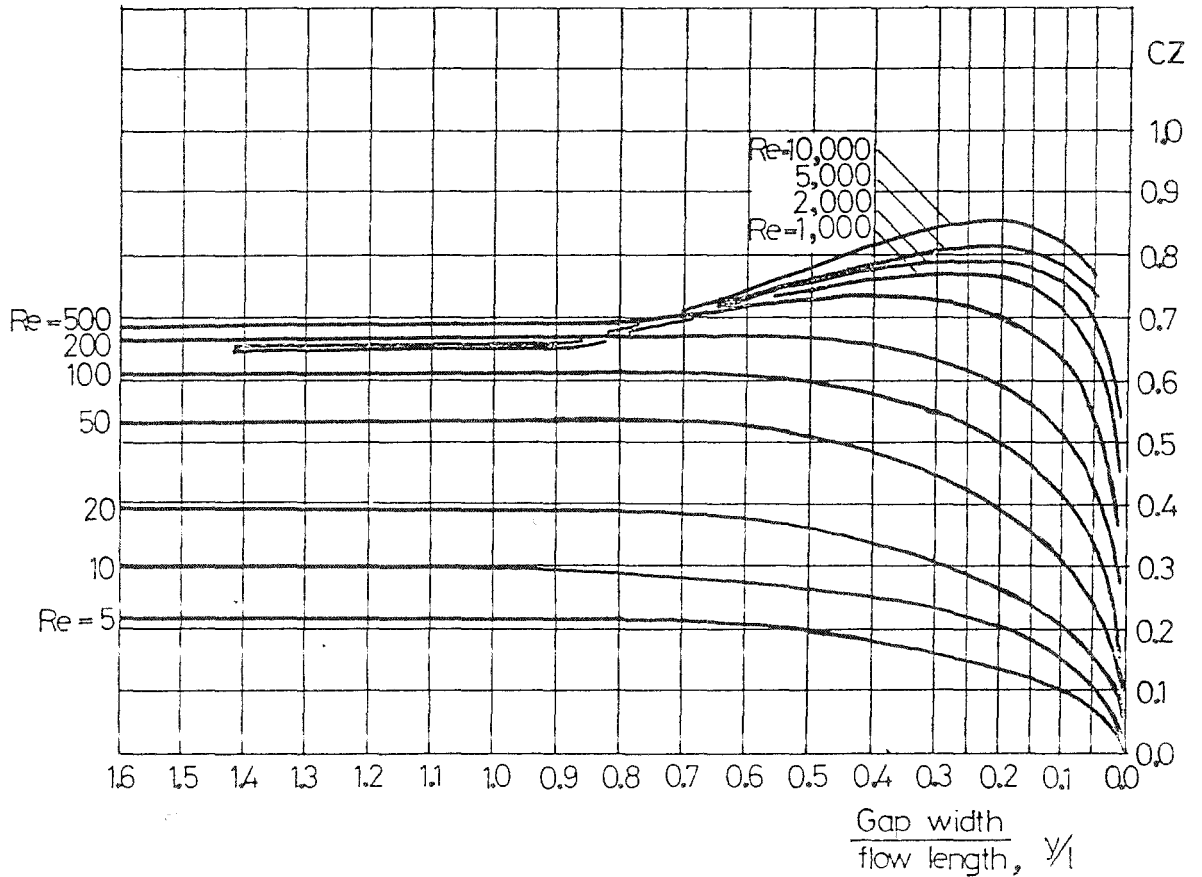


Figure 4.2. Orifice discharge coefficients for narrow slit openings at different Reynolds numbers, after Lenkei.



for narrow slit apertures :

$$V = L \cdot y \cdot CZ \cdot \sqrt{\frac{2g \cdot dP}{\rho}} \dots \dots \dots (4.3)$$

$$Re = \frac{2 \cdot y \cdot W \sqrt{\rho}}{\mu} \times 10^{-3} \dots \dots \dots (4.4)$$

Figure 4.3.

Variation of air flow rate with pressure difference for a simple opening, after Dick and Thomas, and Lenkei.

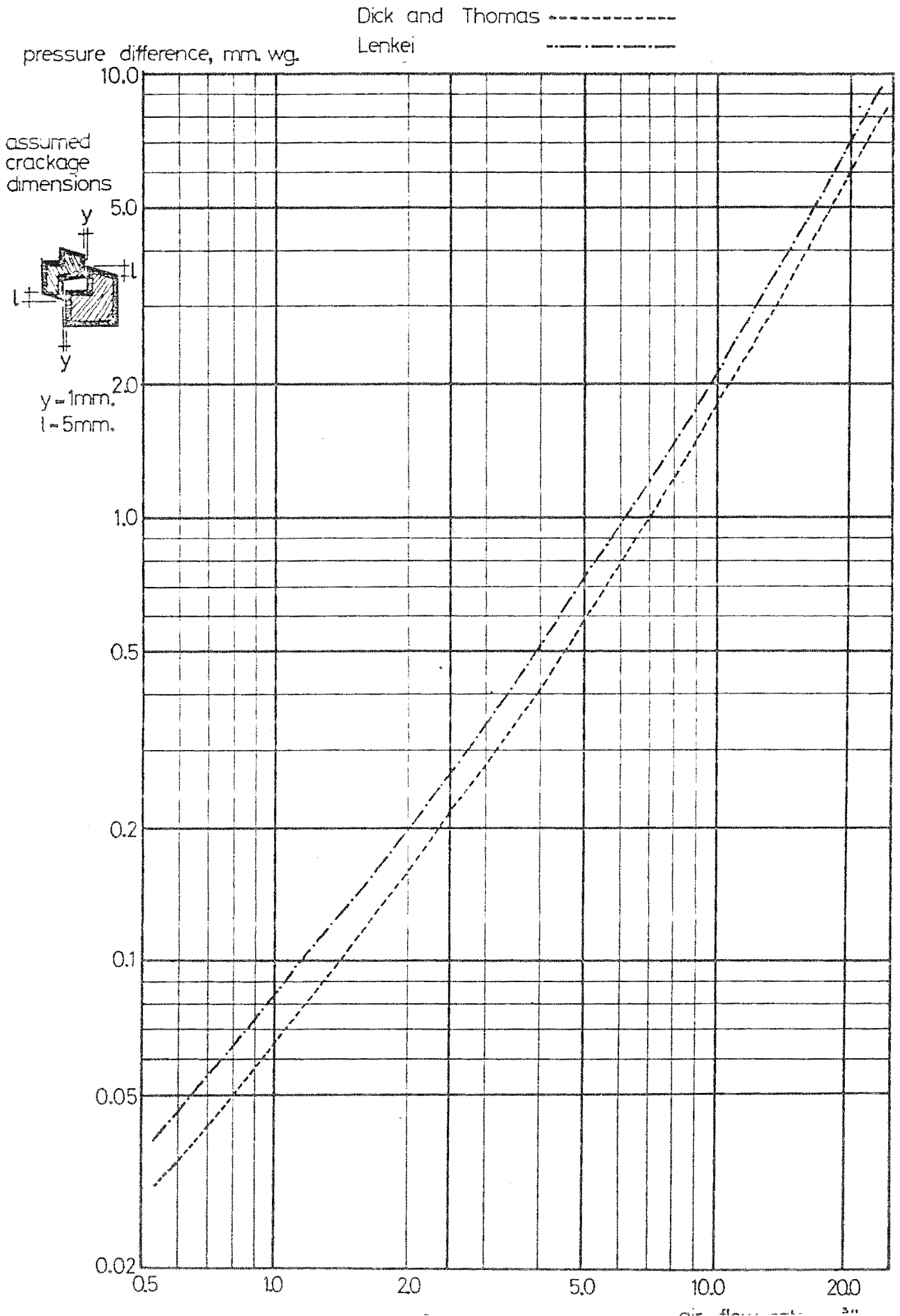


Figure 4.4. Infiltration through window gaps, after Lenkei.

volume flow rate, m³/hr/m.

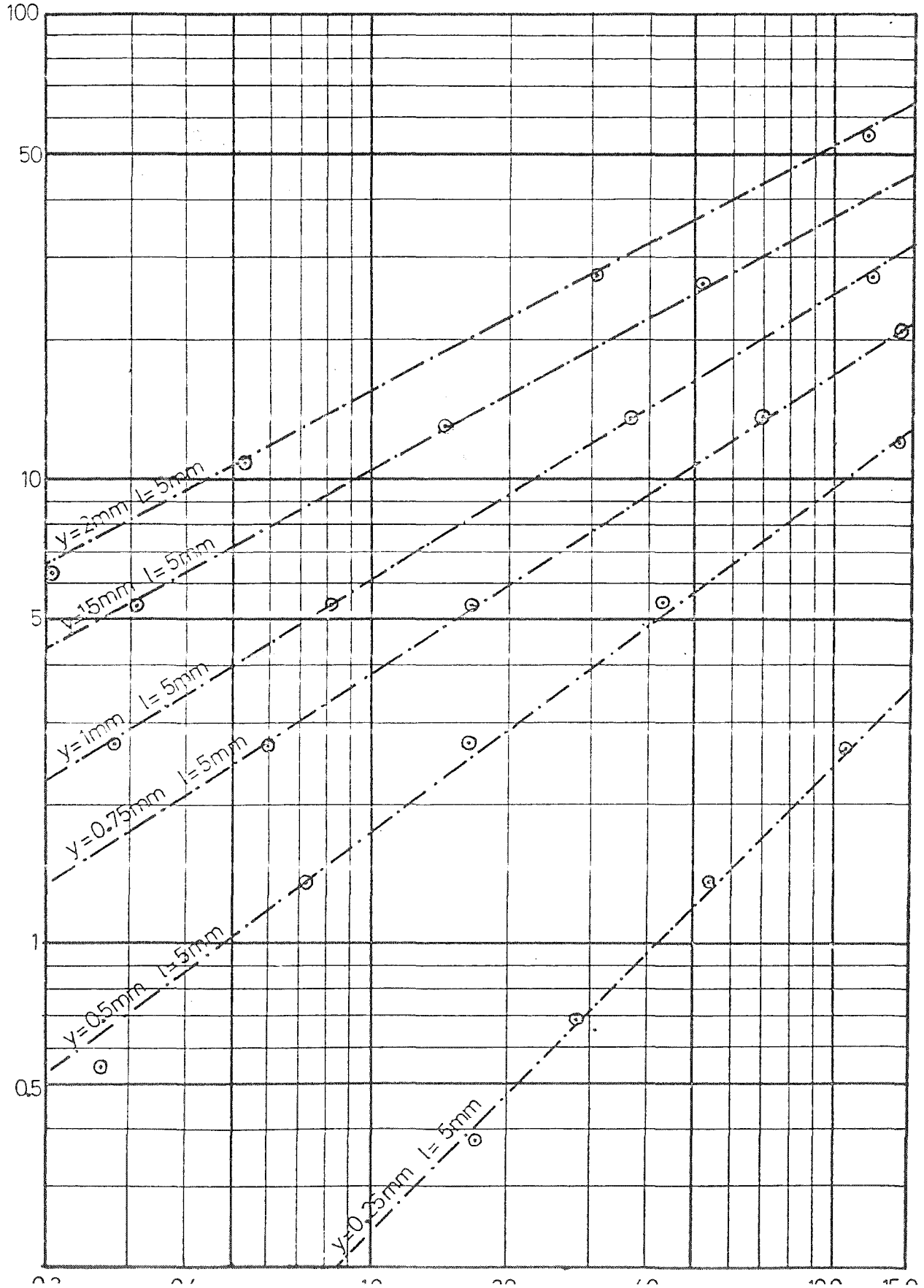


Figure 4.5.

Variation of infiltration coefficient, C , and flow exponent reciprocal, n , in the equation $V = CL(dP)^{1/n}$ after Lenkei, and Dick and Thomas.

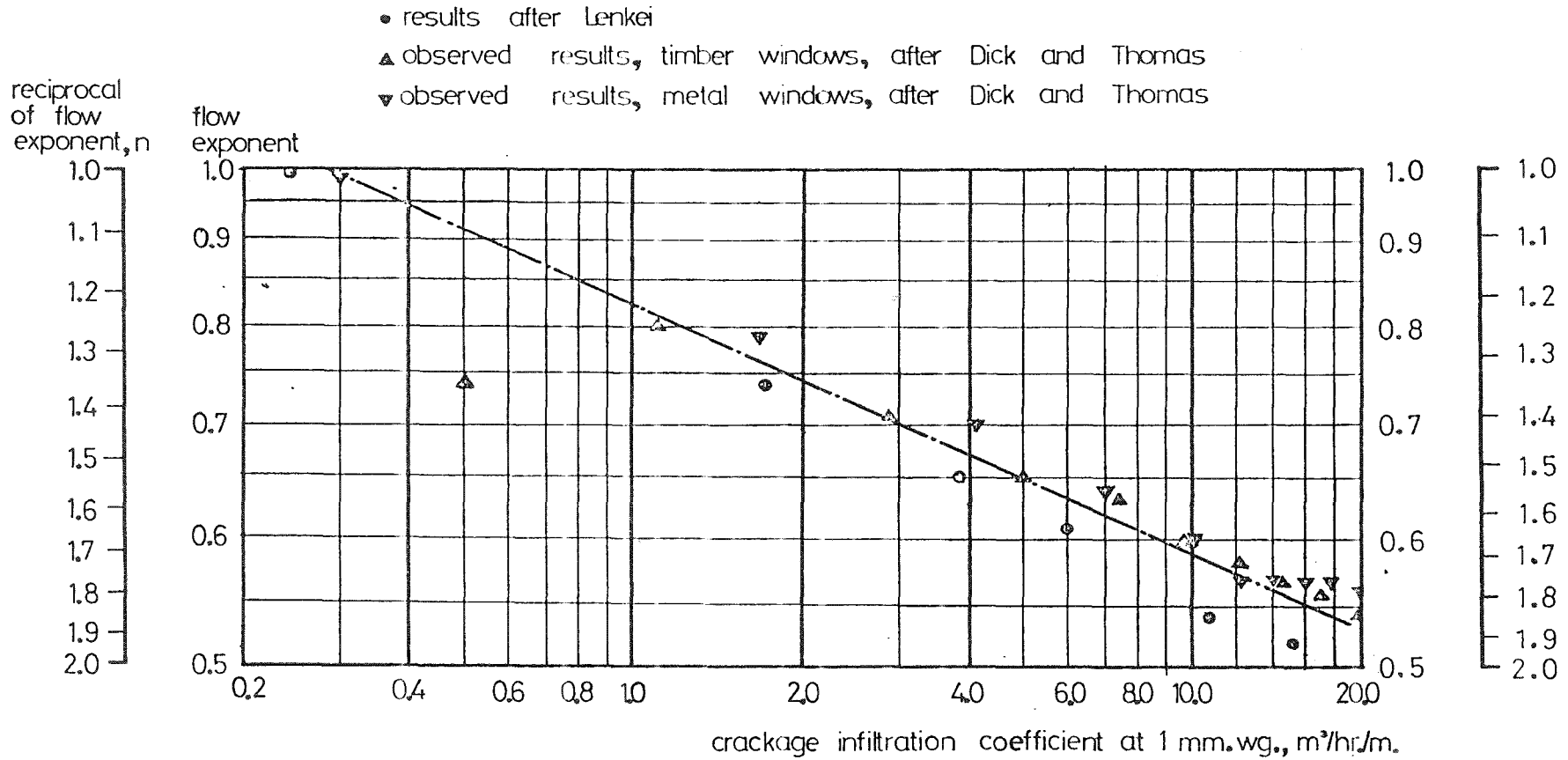
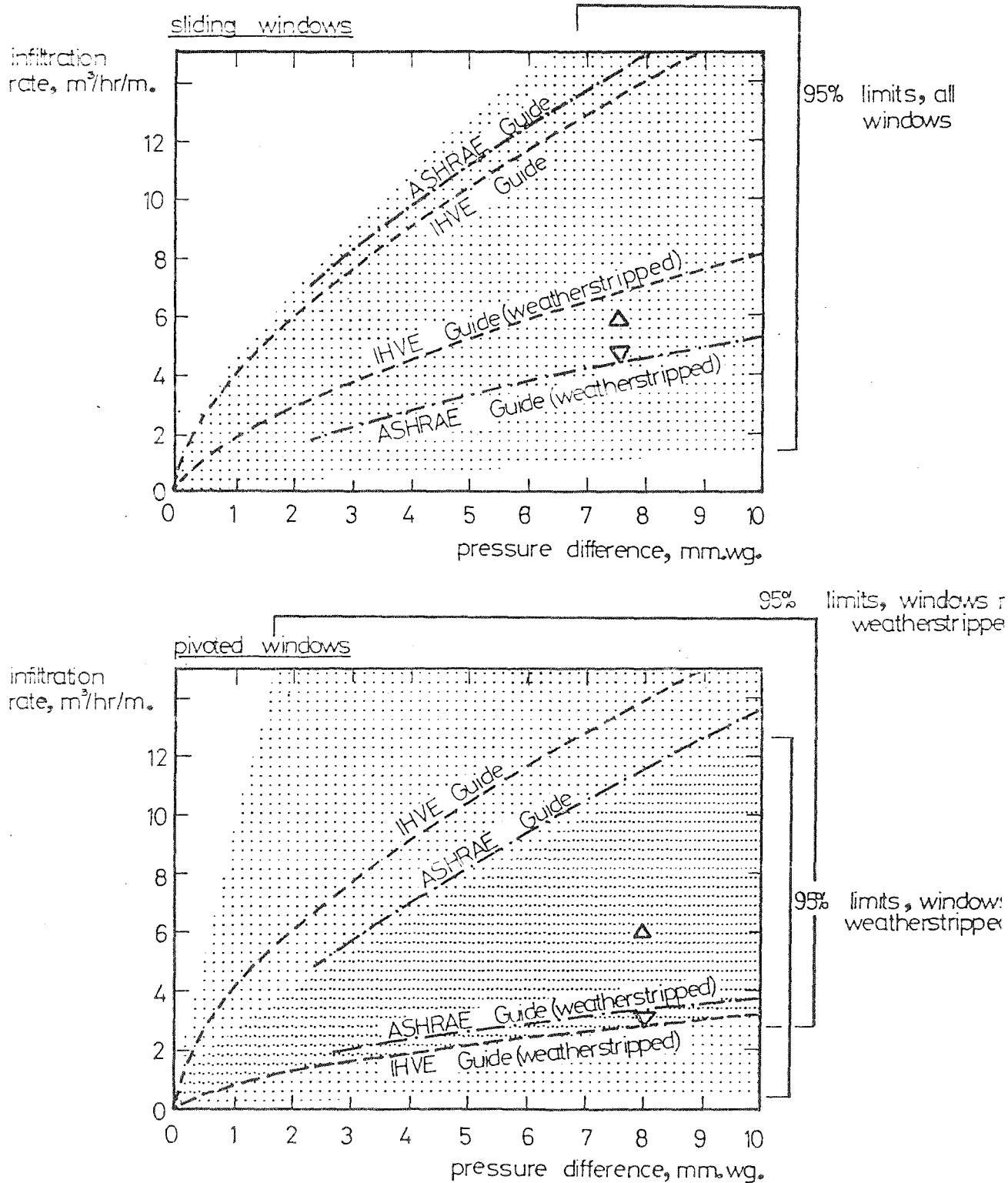


Figure 4.6. Infiltration rates for standard windows: design figures, and variability after Jackman.

U.S. Industry standards : steel windows \triangle
 aluminium windows ∇



5. DESCRIPTION OF THE DIGITAL ANALOGUE DEVELOPED TO PREDICT BUILDING VENTILATION RATES

5.1 Introduction

5.1.1 Digital analogue techniques are being used to produce design information on infiltration and natural ventilation in buildings. This is being done despite the lack of any comparative studies to establish the accuracy of the assumptions and data used in the analogue techniques. A major part of the work in the thesis was concerned with comparative studies between a digital analogue model and full scale and model scale studies. From these studies it was hoped to gain information on the inherent accuracy of the digital analogue method and the data requirements in order to improve design methods. Consequently a programme was written which calculates natural ventilation or infiltration rates in a simple building.

5.1.2 The programme used the same basic assumptions as used by other natural ventilation prediction programmes. These are:

1. that the building is considered as a series of compartments, each of which has a limited number of air flow paths into and out of it through which natural ventilation or infiltration may occur.
2. that each flow path has a characteristic flow resistance, representing a doorway, window, air duct

or open area, which may be expressed by an equation relating air flow through it to pressure difference acting across it.

3. that there is no resistance to air flow inside each compartment of the building.
4. that wind forces and stack effect produce external pressures outside each external opening in the building which are time-invariant over the period of time considered in the calculation.
5. that the internal air temperature in the building is uniform throughout the building.

5.2 Programme Specification

5.2.1 In the programme the maximum number of compartments which may be analysed was 211. These consisted of a maximum of 200 single rooms, up to 10 corridors, one for each floor of the building, and one common stairwell. The single rooms were assumed to be distributed as a maximum of 20 on each of up to 10 floors, each floor being able to have a unique number of rooms. The rooms could be of any required size as ventilation rates were expressed directly in m^3/hr from a knowledge of the room opening characteristics. Each single room was assumed to have two ventilation openings, one connecting it with the exterior of the building and one connecting it with the corridor on that floor. The stairwell compartment was assumed to be linked to each corridor and to have no other ventilation openings. The

stairwell compartment could be used to represent either one or several stairwells all opening onto the central corridor. Some representative building plans suitable for analysis by this type of programme are shown in Figure 5.2.

5.2.2 Each room in the building, and the openings in and out of that room, were identified by a floor number and room number. The lowest floor is taken to be floor 1. The rooms could be numbered in any order, thus allowing the user to choose a numbering system suited to the building plan. Each opening in the building was assumed to have air flow resistance characteristic values which were used in an equation of the form:

$$V = C.L.(dP)^{1/n} \quad \dots\dots (5.1)$$

The values of the total leakage coefficient, $C \times L$, and flow exponent, n , could be unique for each opening in the building.

5.2.3 The input information required by the programme consisted of the following values:

1. number of floors in the building,
2. floor to floor height, m.,
3. number of rooms on each floor (even number),
4. values of total leakage coefficient for exterior/
room opening and room/corridor opening for each room,
 $m^3/hr/mm.wg.^{0.6}$

5. values of flow exponent for exterior/room opening and room/corridor opening for each room,
6. values of total leakage coefficient and flow exponent for each corridor/stairwell opening,
7. wind pressure outside each opening expressed as a pressure coefficient with respect to free stream wind speed at building roof height,
8. assumed meteorological wind speed, m/s,
9. assumed mean internal/external temperature difference, °C.

One significant limitation of the programme is that corner rooms with windows opening onto two façades at two different external pressures are not accurately modelled. In these situations a representative external pressure should be taken. If this factor is likely to be important the flow from one window to the other could be considered separately and an estimation of the extra flow found.

5.2.4 The programme was designed to compute ventilation rate either for one specified set of design meteorological conditions or for an array of meteorological conditions covering the combinations of wind speed and temperature difference normally encountered. The array of meteorological values used consisted of wind speeds of 0.001, 1.0, 2.0, 4.0, 6.0 and 8.0 m/s and temperature differences of 0.0, 8.0, 16.0 and 24.0 °C. The design meteorological values may be

any values of wind speed or temperature difference which do not occur in the array. The meteorological wind speed input was an assumed wind speed from a remote site in open country at a height of 10 m., which was then converted to the site wind speed, assuming the site to be in an urban area. This form of input may easily be altered as was done in the comparative tests, to use the site wind speed as a direct input, or to produce site wind speeds characteristic of suburban or open sites.

5.2.5 The output information given by the programme consisted of the following values:

1. review of the input information used in the programme,
2. meteorological wind speed, m/s,
3. interior/exterior temperature difference, °C,
4. total infiltration rate for the building, m³/hr.
(total of all air flow rates entering the building through external openings),
5. average room ventilation rate, m³/hr.,
6. standard deviation of room ventilation rates, m³/hr.,
7. for each room:
 - pressure differences acting across the external and internal ventilation openings, expressed in mm.wg. and as pressure coefficient values,
 - flow rate and direction of flow, m³/hr.,
8. flow rate and direction of flow from the stairwell to the corridor at each floor level, m³/hr.,

9. pressures in the stairwell and each internal corridor, mm.wg.

The sign convention used for air flow rates and pressure differences in the programme was:

All flows towards the central corridor on that floor level, from any other part of the floor, are taken to be positive. All pressure differences which would act to cause positive flow rates are taken to be positive.

5.3 Programme Description

5.3.1 The programme was written in Fortran 1900 language for use on the Sheffield University I.C.L. 1907 computer. The programme works on the basis of making successive approximations of the ventilation rates occurring throughout the building until the estimated rates are within the required accuracy limits. The approximation techniques used in the programme are illustrated by the flow charts shown in Figure 5.1. These are discussed in more detail in the following section and related to the appropriate steps in the full programme. A print-out of the full programme is given in Appendix A1. In the following paragraphs figures in parentheses refer to line numbers of the programme shown in Appendix A1.

5.3.2 The analysis is carried out in three main consecutive steps in the programme. These are shown in

Figure 5.1. Initially the external pressures outside each of the external openings, caused by wind pressure alone, are found. Each floor is analysed separately, considering it to be isolated from the rest of the building. The pattern of ventilation for the floor is found, and also the absolute pressure on the corridor of each floor. A flow diagram of this section may be seen in Figure 5.1(a). The detailed operations are noted below:

1. Each floor is considered in turn, (74, 152).
2. The convergency rate figure is set to one, (75).
3. Initial internal pressures are set up (76 - 85):
the corridor pressure is set to the average of all the external pressures acting outside that floor, the room pressures are set to half the difference between the corridor pressure and the appropriate external pressure.
4. The accuracy limits are set up, (86 - 87):
the current values of two pressure differences are set to LIM1, LIM2; at the end of the cycle the current values are compared with LIM1, LIM2. If the pressure difference values have changed by more than 1/1000 of their value during the cycle LIM1 and LIM2 are set to the new current values and the cycle repeated.
5. The ventilation rates are calculated through all openings on the floor and are balanced, (88 - 104):
for each room in turn the flow rates in and out are equated, each being set at the average of the two flow rates,
for the corridor, the net flow is found and the room/corridor flow rates altered proportionally so

that the net flow is made zero,
the balance of air flow through each room is
checked and if necessary adjusted,
the balance of air flow into the corridor is
checked and if necessary adjusted.

6. The pressure differences are re-calculated and
balanced, (105 - 134):
they are correlated with the values of the external
pressures and altered so that they are in agreement
with these values.
7. The number of cycles carried out is checked. If
this is over 50 the analysis is stopped, the number
of cycles and current values being written out,
(135-6, 141-2).
8. The relevant pressure differences are checked
against LIM1, LIM2 and if not sufficiently accurate
the approximation cycle is repeated, (137 - 140).
9. The variable values used to calculate the combined
ventilation rates are set up, (143 - 151).

5.3.3 In the second section of the analysis the stack
effect, assumed to be acting alone, is considered. A
neutral zone height is found such that the net flow from
all corridors to the stairwell is zero. The corridors
are assumed to be at zero pressure relative to each other
from forces other than stack effect. The stack pressures
found by this analysis are added to all relevant wind
induced pressures found in the initial analysis step.
Figure 5.1(b) shows a flow diagram for this section and
the detailed steps are again noted below:

1. Assume an initial neutral zone height of half of the building height, and calculate the pressures due to stack effect, (157 - 160).
2. Calculate the net flow into the corridor from each stairwell (161-5).
3. If the net flow into the stairwell is zero add the relevant stack pressures to each level of the building assuming the current value of neutral zone height (166, 189 - 195).
4. If the net flow into the stairwell is positive, decrease the neutral zone height progressively, in steps of $1/500$ building height, until the net flow becomes zero or negative, (166 - 177, 189 - 195)
if the net flow becomes zero assume the current neutral zone height value,
if the net flow becomes negative assume a value half way between the current value and the value used in the previous cycle,
add the relevant stack pressures to each level of the building.
5. If the net flow into the stairwell is negative increase the neutral zone height progressively, in steps of $1/500$ building height, until the net flow becomes zero or positive, (166, 178 - 195):
if the net flow becomes zero assume the current neutral zone height value,
if the net flow becomes positive assume a value half way between the current value and the value used in the previous cycle,
add the relevant stack pressures to each level of the building.

5.3.4 The combined ventilation rates, assuming both wind and stack effect to be acting simultaneously, are calculated in the third section of the programme. Each floor is analysed again, this time with the presence of the stairwell, at the appropriate pressure, taken into account. Flow rates are balanced until the net flow into each central corridor from the rooms on the floor and the stairwell is again zero. These results are taken to represent the final estimated ventilation pattern for the building. Once again a flow diagram is given, (see in Figure 5.1(c)) and the detailed steps noted below:

1. Each floor is considered in turn (200, 256).
2. The pressure difference between the relevant corridor and the stairwell is calculated (201, 202).
3. The increment value is set, (203):
the ventilation pattern is found by a series of approximations, altering the corridor pressure by increments; the incremental values are made progressively smaller and the accuracy limits are assumed to be met when the incremental values become equal to preset limiting values.
4. The stairwell to corridor pressure difference is decreased by a factor of one increment, (204-5):
as the flow pattern for each floor was previously balanced, the introduction of the stairwell at a different pressure will cause the corridor pressure to be altered, the corridor pressure becoming nearer in value to the stairwell pressure.

5. All pressure differences on the floor are re-calculated, (206 - 219):
this procedure is carried out by a series of approximations; the pressures cannot be simply altered in proportion due to the different possible flow exponent values of the openings.
6. The flow rates are calculated for these new pressure differences, the flow for each room balanced, and the pressure differences re-calculated from the balanced flows (220 - 239).
7. The net flow into the central corridor is calculated, (240 - 250):
if the net flow is positive and the stairwell to corridor pressure difference is positive or if the net flow is negative and the stairwell to corridor pressure difference is negative then the corridor pressure has not been altered sufficiently to balance the total flow on the floor; the stairwell to corridor pressure difference is reduced further, if these conditions are not met then the corridor pressure has been compensated at least enough and the accuracy check is made.
8. The value of the increment is checked, (251 - 254):
if this is larger than the preset limiting value then the value of the increment is reduced by a factor of ten, the corridor pressure reset to its previous value and the calculation repeated from step 4,
if the incremental value is sufficiently small the analysis is stopped.

5.3.5 Summary ventilation rate values are calculated from the final calculated detailed ventilation rates



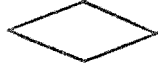
(257 - 274), and the results are printed (275 - 306). The values of temperature difference and wind speed assumed in the input are cycled in turn, and in that order, if this type of analysis is required (308 - 327). Each time the temperature difference is changed the second and third steps are repeated. Only when the wind speed is changed is the first step repeated in addition.

5.3.6 One further approximation is made in the programme which has not been discussed. The stairwell pressure in the final analysis is set to the mean wind-induced corridor pressure and the flow rates into and out of the stairwell are not balanced by the programme. However the stack pressures are calculated from the estimated neutral zone height so that the stack induced ventilation through the staircase would be balanced (paragraph 3.5). As these ventilation forces are likely to produce the major part of the vertical air movement it was decided that the added accuracy which might be achieved in balancing the stairwell air flow system would not justify the increase in computing time required.

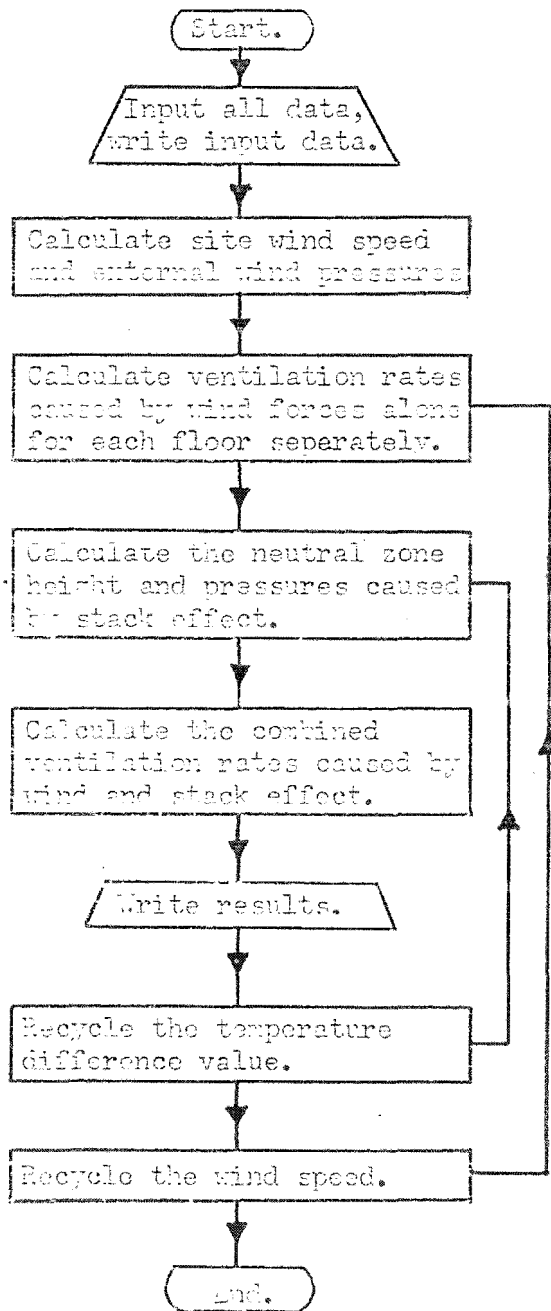
Figure 5.1.

Flow chart for building ventilation prediction program, BT5VENT4.

Symbols used in flow diagram.

-  Any processing operation except a decision.
-  Input or output.
-  Decision.

Flow diagram, summary chart.



See Figure 5.1(a) for detailed flow chart for this section.

See Figure 5.1(b) for detailed flow chart for this section.

See Figure 5.1(c) for detailed flow chart for this section.

Figure 5.1(a).

Calculation of ventilation rates due to wind alone, floors considered in isolation.

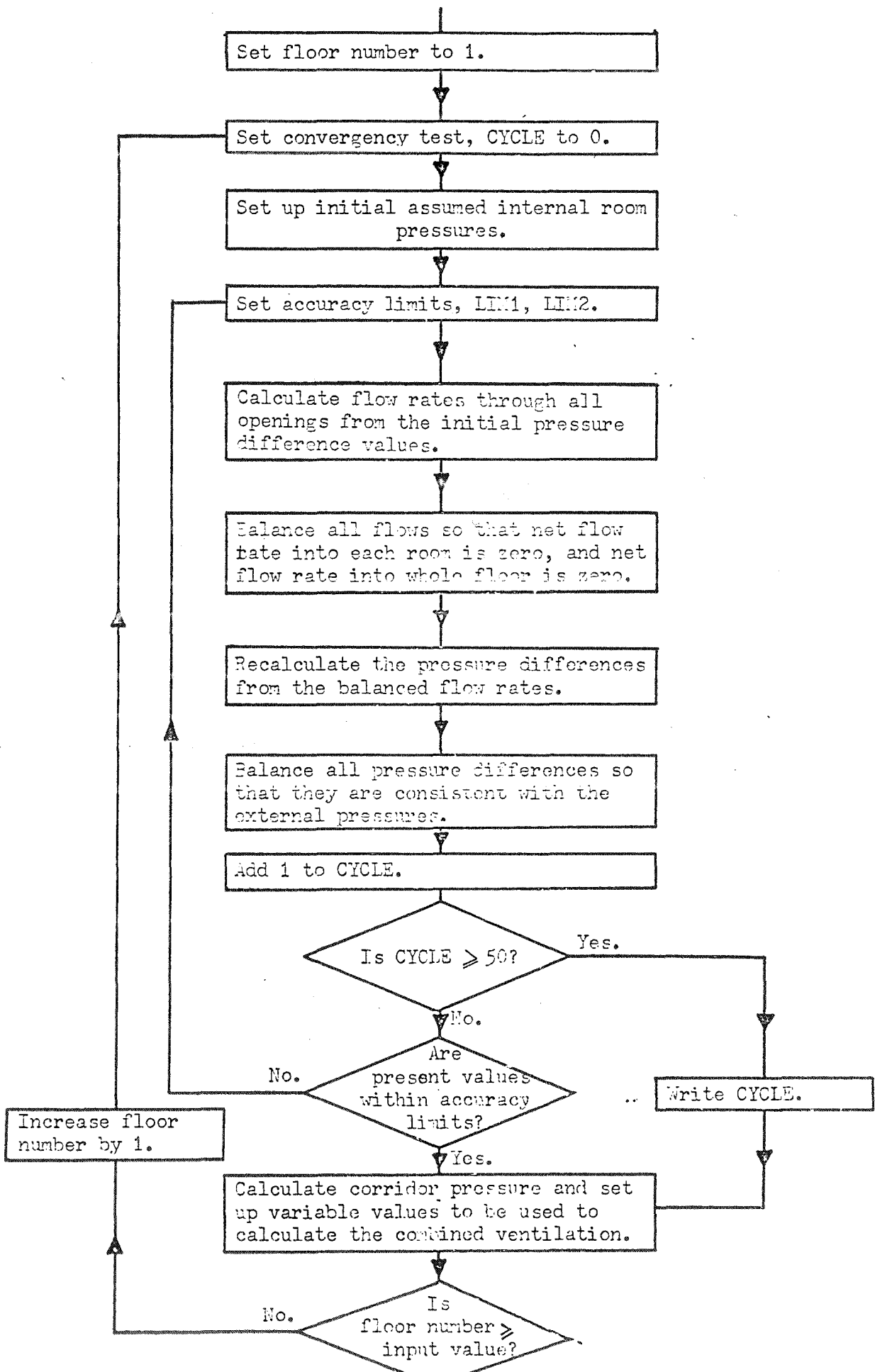


Figure 5.1(b). Calculation of neutral zone height.

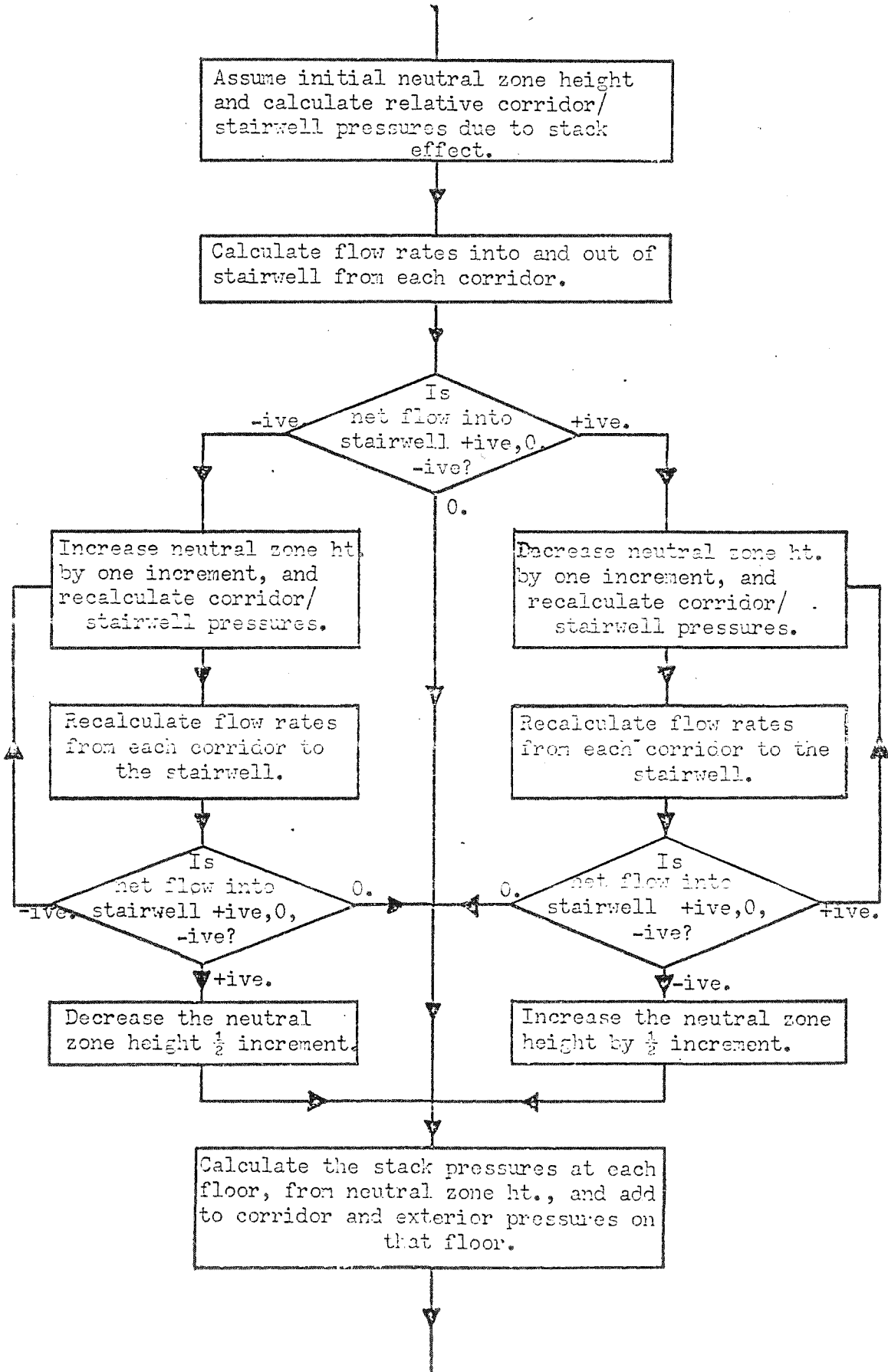


Figure 5.1(c).

Calculation of combined ventilation rates.

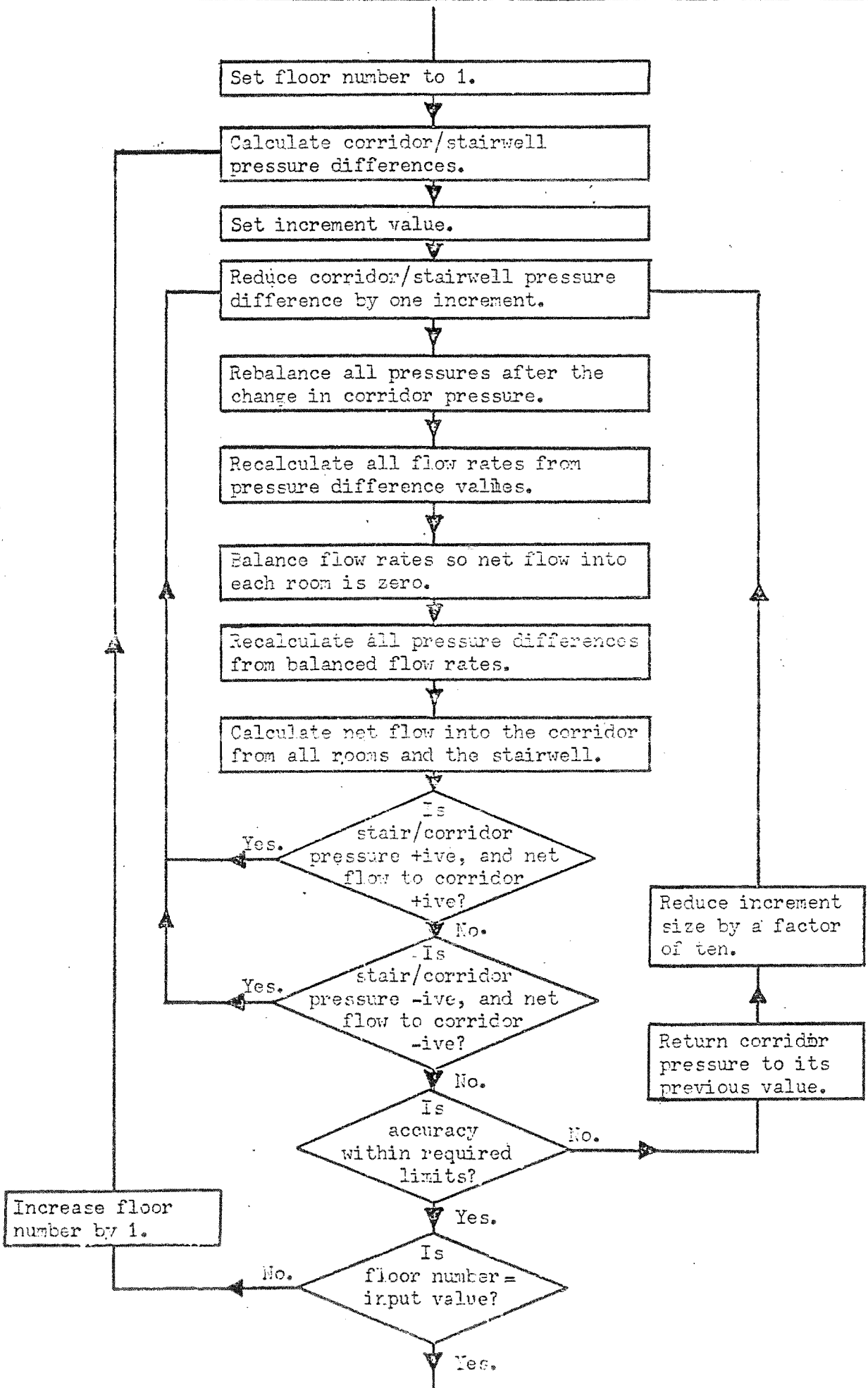
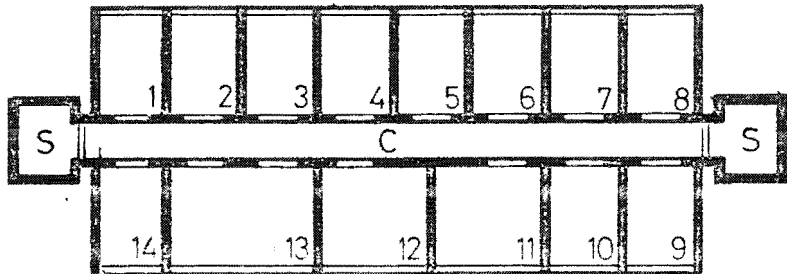


Figure 5.2.

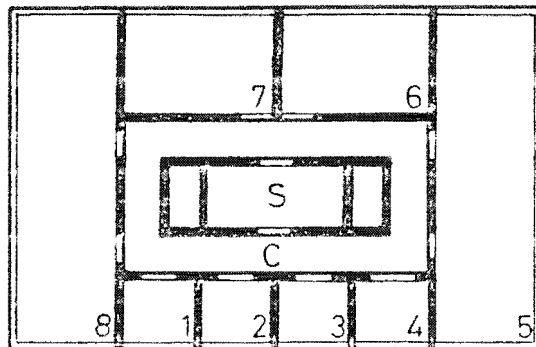
Typical plan forms suitable for analysis by
BT5VENT4

S Stairwell
C Corridor

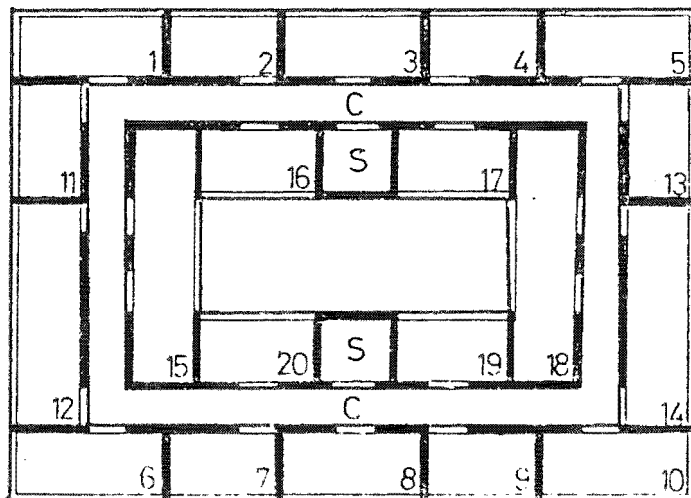
Slab block:



Uniformly glazed building:



Courtyard building:



6. RESULTS OF COMPARATIVE FULL SCALE VENTILATION STUDIES

6.1 Introduction

6.1.1 An important part in the development of any analogue system is the testing of the model to determine the limits of its accuracy. This may be done by comparing analogue results with full scale observations. The relatively small number of full scale studies carried out to date serve as an indication of their difficulty. However it is because of the paucity of these results that the importance of testing the analogue technique becomes greater if it is to be used as the basis for a design technique. Consequently, in order to attempt to assess the performance of the analogue a comparative study was made between results obtained from the analogue and a series of full scale observed results.

6.1.2 Tamura and Wilson carried out a series of full scale tests on a small building, (Tamura, 1965) the results of which have been used here in the comparison with the analogue technique. It is significant to note that very few of the papers giving full scale results give sufficient information for any valid comparative calculations to be carried out. In particular sufficient data about the external climate of the building is often lacking.

6.1.3 The results from this comparison are necessarily limited. The building studied is a small

single-storey domestic dwelling with basement. In the paper the effect on ventilation rate of wind speed and direction, stack effect and wind and stack effect acting together are studied. It has only been possible to compare results for the situations with no stack effect taking place. Stack effect taking place on one floor through sash windows is not modelled by the programme, as it is designed mainly to study multi-storey buildings. These comparisons attempt to give some indications of the accuracy of the analogue technique.

6.2 Description of the full scale study:

6.2.1 A full description of the test house, house number 1, is given in Tamura and Wilson's paper. A plan of the building is given in Figure 6.1. It is a single storey, timber framed building, with basement. Internal wall surfaces are plasterboard. The plan area is 77.1 m^2 and the net volume, including basement, and allowing 10% for furnishings is given as 336 m^3 . Figures for window crackage are given as an equivalent length to that of average fit, double-hung, wood sash, weatherstripped windows, the figures being based on data from the A.S.H.R.A.E. Guide and Data Book. These figures are given in Table 6.1.

6.2.2 Ventilation rates were determined from measurements with a katharometer of the rate of change of concentration of helium gas discharged in the house.

All internal doors were open during the periods of measurement. A circulating blower was also operated continuously during each test. It was assumed that a fairly uniform concentration of helium was achieved under test conditions. Wind speeds were recorded by a cup anemometer mounted next to the house and at a height of 7.6 m. The house was situated on the edge of a housing area, with its south wall facing a wooded region.

6.2.3 The results of the full scale leakage tests are given in Table 6.2 and are also shown in Figure 6.2. The air change rates given are net rates including the basement area. The line of best fit, computed assuming a linear relationship between wind speed and air change rate, is drawn. The increase in air change rate for each metre per second increase in wind speed is 0.037. No significant effect of wind direction can be noted from the records. An apparent ventilation rate of 0.037 air changes per hour was obtained with no wind speed and only small temperature differences.

6.3 Description of the analogue calculations

6.3.1 In order to carry out the comparative calculations it was necessary to make a further set of assumptions. The height of the building was taken to be 4 m. This allowed sufficient height for one storey and sufficient basement above ground level to let in windows. The recorded average wind speed was corrected

TABLE 6.1 Equivalent window crackage lengths in test house No. 1 (Tamura and Wilson)

Equivalent length of crackage, ft.				
Elevation	N	S	E	W
First Floor	38.7	0.0	126.0	155.9
Basement			32.6	
	<u>38.7</u>	<u>0.0</u>	<u>158.6</u>	<u>155.9</u>

The assumed leakage coefficient for this standard equivalent crackage is given as 60 cuft./hr/ft/0.3 in.w.g.

TABLE 6.2 Infiltration test results, house No. 1 (Tamura and Wilson)

Test No.	Date	Temp. difference, °C.	Average Wind Velocity, m/s	Wind Direction	Infil-tration Rate/hr.
9	1.8.61	1.7	1.36	N	0.07
10	2.8.61	-2.5	1.88	E	0.10
11	3.8.61	-1.1	2.69	NW	0.16
12	4.8.61	-1.1	0.45	E	0.07
13	10.8.61	-3.3	3.18	SW	0.17
14	14.8.61	1.1	1.53	W	0.09
15	16.8.61	3.3	3.62	N	0.17
16	17.8.61	-1.1	1.22	W	0.08
17	18.8.61	-1.7	1.62	SW	0.11
18	21.8.61	3.3	3.22	E	0.14
19	22.8.61	1.7	0.45	S	0.06
20	23.8.61	1.7	2.59	E	0.13

to four metres height using a power law relationship, with an exponent of 0.3. This seems a typical exponent for a suburban situation, as discussed by Harris (Harris, 1970). Values of crackage length were assigned to each window. These had to be estimated as relative amounts of the crackage on each elevation from the verbal description of the windows. Finally values of pressure coefficient had to be assumed. These were based on the figures given in Building Research Station Digest 119 and the assumed figures may be seen in Figure 6.3. Also in the calculations the effect of the basement windows was not included due to uncertainty about the relevant pressure coefficients. Consequently the house volume was reduced by a factor equivalent to the reduction in window area, to 300 m³, to compensate for this.

6.3.2 The standard leakage coefficients given in the paper are assumed to be 60 cu.ft/hr/ft at a pressure difference of 0.3 inches w.g. This leakage coefficient was assumed in the calculations. The equation relating volume flow rate through a crack to the pressure difference across the crack is represented as:

$$V = C.L. (dP)^{1/n} \quad \dots (6.1)$$

where V is the volume flow rate m³/hr

L is the crack length, m

dP is the pressure difference, mm.w.g.

n is an exponent.

Typical values of the exponent, n , for windows of the type described have been abstracted from the work of Dick and Thomas (Dick, 1953). The assumed value is 1.6.

Then as the assumed value of C is

$$C = 60 \text{ cu.ft./hr./ft. at } 0.3 \text{ in.w.g.}$$

This is equivalent to

$$\begin{aligned} & 5.61 \text{ m}^3/\text{hr./m. at } 7.6 \text{ mm.w.g.} \\ & = 5.61 (1/7.6)^{1/1.6} \text{ m}^3/\text{hr./m. at } 1 \text{ mm.w.g.} \\ & = 2.02 \text{ m}^3/\text{hr./m./mm.w.g.}^{0.6} \quad \dots\dots (6.2) \end{aligned}$$

Consequently the assumed figures of leakage coefficients may be seen in Figure 6.1. The assumed values of leakage coefficients for all internal doors were taken to be 10,000 $\text{m}^3/\text{hr./mm.w.g.}^{0.6}$. This represents a typical figure for an open doorway. In fact the resistance to air flow of the doorways is so small as to have virtually no control on the average air change rate.

6.3.3 Using these figures calculations were carried out under each set of average external conditions noted in the paper, where the mean wind was from a primary cardinal direction. Calculations were not carried out to simulate the three conditions where the mean wind direction was from a secondary direction due to lack of certainty of the appropriate pressure coefficient values. In this way nine of the twelve sets of test conditions were simulated.

6.3.4 The results of the calculations are given in Table 6.3, and in Figure 6.4. A line of best fit was

found in the same way as for the full scale results, that is assuming a linear relationship between wind speed and air change rate. The increase in air change rate for each metre per second increase in wind speed is 0.033. No significant spread of results due to wind direction can be seen. An apparent ventilation rate of -0.008 air changes per hour was found from the line of best fit with no wind speed or temperature difference.

6.3.5 A further analysis of the computed and full scale observations was made by computing lines of best fit assuming that the infiltration rate varied in proportion to the wind speed to the power 1.25. This was the exponent assumed in the analogue tests. From these analyses the line of best fit for the observed results was found to be:

$$I = 0.023 W^{1.25} + 0.050 \quad \dots\dots (6.3)$$

and the line of best fit for the computed results was found to be:

$$I = 0.023 W^{1.25} + 0.002 \quad \dots\dots (6.4)$$

These lines of best fit are shown in Figure 6.5. For each of these four lines of best fit the root mean square deviations from the lines were calculated. The R.M.S. deviations assuming a linear relationship are ± 0.010 for the observed results and ± 0.009 for the computed results. The R.M.S. deviations assuming an exponent of 1.25 are ± 0.007 for the observed results and ± 0.011 for

TABLE 6.3 Computed infiltration figures, house No. 1.

Simulation of Test No.	Average wind speed, m/s.	Wind Direction	Calculated Infiltration Rate/hr.
9	1.36	N	0.028
10	1.88	E	0.058
12	0.45	E	0.009
14	1.53	W	0.047
15	3.62	N	0.096
16	1.22	W	0.035
18	3.22	E	0.114
19	0.45	S	0.005
20	2.59	E	0.087

TABLE 6.4 Summary of results given in paper

Lines of best fit

Linear relationship, full scale observations from Tamura
and Wilson

$$I = 0.037 W + 0.037 \quad \text{R.M.S. error } \pm 0.010$$

Linear relationship, computed results

$$I = 0.033 W - 0.008 \quad \text{R.M.S. error } \pm 0.009$$

Exponential relationship, full scale observations from
Tamura and Wilson

$$I = 0.023 W^{1.25} + 0.050 \quad \text{R.M.S. error } \pm 0.007$$

Exponential relationship, computed results

$$I = 0.023 W^{1.25} + 0.002 \quad \text{R.M.S. error } \pm 0.011$$

I is infiltration rate, air changes/hr.

W is wind speed, m/s.

the computed results. A summary of the results obtained is given in Table 6.4.

6.4 Discussion of results

6.4.1 The results of the full scale tests show generally a higher ventilation rate for any given wind speed than the computed results. The rates of increase of ventilation rate for standard increase of wind speed are very similar. They are 0.037 air changes/metre per second for the full scale results and 0.033 air changes/metre per second for the model situation. The difference in apparent ventilation rates between the two sets of results at zero wind speed is 0.045 air changes per hour. This means that over the range of wind speeds used the relative error between the two sets of results is virtually constant.

6.4.2 In order to assess the significance of these results it is necessary to consider the errors involved in obtaining them. In particular, for both sets of results, there is an apparent ventilation rate occurring at zero wind speed. In the case of the computed results the reason for this may be explained fairly simply. The assumed opening characteristics used in the calculations, as noted earlier, are of the form:

$$V = C.L. (dP)^{1/1.6} \quad \dots (6.5)$$

$$\text{or } V \propto (dP)^{0.62}$$

Now as the pressure differences produced across the building are proportional to the square of the wind speed, W

$$\begin{aligned} \text{then } dP &\propto (W)^2 \\ \text{or } \quad v &\propto (W)^{1.25} \end{aligned} \quad \dots\dots (6.6)$$

Initially the results from the computer study were analysed in the same way as the full scale results, in order to form a valid comparison. The line of best fit was computed assuming a linear relationship between wind speed and volume flow rate. As this is not the actual case (Equation 6.6) the line of best fit will depend on the values of wind speed chosen for analysis. The line may also have some apparent ventilation rate at zero wind speed.

6.4.3 In order to illustrate this effect both sets of results were analysed assuming that the relationship between wind speed and volume flow rate was as given in equation 6.6. The rates of increase of the ventilation rates for a standard increase of wind speed are again very similar. The difference in apparent ventilation rates between the two sets of results, 0.048 air changes per hour, is also very similar. However the computed results show a reduction in the apparent ventilation rate at zero wind speed to less than 0.002 air changes per hour (Figure 6.5). Thus the error is reduced to one fifth of the previous error. The apparent ventilation rate at zero wind speed of the full scale results is increased to

0.050 air changes. This is probably a more accurate estimate of the zero error than the previous 0.037 air changes per hour.

6.4.4 This apparent ventilation rate at zero wind speed shown in the full scale results is relatively large. The major factors causing errors in the observed ventilation rates given by Tamura and Wilson are the diffusion of the tracer gas through the building fabric, and the fact that the stack and wind effects could not be entirely independently investigated; that is there was some ventilation due to small changes in external temperature during the tests. There are other factors which could lead to significant errors in the observations. Non-uniform distribution of the helium gas, because of imperfect mixing, would produce erroneous readings. The accuracies of the readings from the katharometers, at the low flow rates observed, is likely to be lower than at more usual ventilation rates. The omission of any estimation of the adventitious ventilation occurring will lead to the computed ventilation rates being too low. The assumptions made in the data used in the calculation, noted in section 6.3, will also act as possible sources of error in the computed ventilation rates.

6.4.5 Of the factors which may affect the accuracy of the full scale observations two could produce effects leading to systematic overestimates of the ventilation rate due to wind alone. These are diffusion and the

simultaneous action of small stack effects. Loss of helium through the building will lead to a faster rate of decay and an apparent error in the infiltration rate. The theoretical estimation of diffusion rate is complex. A simplified analysis, in which diffusion is assumed to take place through the window crackage only, suggests an apparent error in the ventilation rate in the order of +0.01 air changes/hour, (Appendix A2). This calculation underestimates the magnitude of this effect as it does not take into account diffusion through the solid surfaces. Model tests (Malinowski, 1971) show that diffusion of a nitrogen tracer is only affected to a small extent by external air velocity. As helium, which has a higher diffusion rate, is used as the tracer in Tamura's experiments the effect of external wind speed will probably be less. The error in the full scale ventilation rate due to this effect is taken to be positive, relatively constant with wind speed and having a value greater than 0.01 air changes/hour. Field measurements by Howard (Howard, 1966) of ventilation rates calculated from the rate of decay of a hydrogen tracer, show a similar constant positive error with wind speed due to diffusion of the gas.

6.4.6 The second factor which may affect the accuracy of the full scale results is the possibility of non-uniform mixing of the tracer gas. This would lead to unrepresentative sampling of the tracer gas and a possible overestimate of the ventilation rate. The use of the

internal air mixing system during the tests was designed to minimise this factor. Because of the high air movement rates internally, due to the fans, the quality of the mixing, and thus the errors in the apparent ventilation rate are unlikely to be affected greatly by the infiltration rate, and any error is likely to be relatively constant with wind speed. The loss in accuracy of the katharometers at the very low air change rates observed is likely to be significant; the observing period being quite long to establish a significant amount of loss of tracer gas. Although this will affect individual readings, it should not necessarily produce any systematic error in the ventilation rates.

6.4.7 The small temperature differences acting during the tests will lead to overestimates of the ventilation rate caused by wind acting alone. The magnitude of this effect is extremely difficult to isolate in the full scale observations. It may be seen from the relationship between wind speeds and temperature differences causing the same ventilation rates (Tamura, 1965), given in Tamura and Wilson's paper that all the tests, except tests 12 and 19, took place with temperature differences significantly less than those which would cause an effect equal to that caused by the wind. The ventilation rates which would be caused by these temperature effects acting alone can be estimated generally as 50-60% of those caused by the wind alone.

The combined effect of wind and temperature difference, as observed, may then be expected to be approximately 10% greater than may have been expected from the wind alone. The errors would be greater in tests 12 and 19 where the temperature differences are relatively larger. The errors then may be of the order of 0.01 to 0.02 air changes/hour.

6.4.8 The last possible source of error to be considered is ventilation through other cracks in the building fabric. Non-consideration of this effect will lead to computed ventilation rates which are lower than those actually occurring. Figures of leakage coefficients for plastered wood frame construction obtained from the A.S.H.R.A.E. Handbook of Fundamentals are of the order of $0.025 \text{ m}^3/\text{hr.}/\text{m}^2/\text{mm.wg}^{0.6}$. The equivalent coefficient for all the wall surfaces in the test building will be of the order of $10 \text{ m}^3/\text{hr.}/\text{mm.wg}^{0.6}$. Inclusion of this factor in the calculation will lead to an increase of the computed ventilation rates by approximately 5%.

6.4.9 It can be seen that the estimation of the errors in the observed ventilation rates is extremely general. Loss of tracer gas by diffusion and higher ventilation rates due to the stack effect acting simultaneously are probably the more important mechanisms causing error. Non-uniform mixing of the tracer gas and the adventitious ventilation will also produce errors which would help to explain the discrepancy between the

full scale results and the computed results.

6.4.10 The results of the two sets of tests were also compared in terms of the degree of spread of points from the line of best fit. Assuming a linear relationship between wind speed and ventilation rate the R.M.S. deviation in the full scale observations is 0.010 air changes. In the computed results the R.M.S. deviation is 0.009 air changes. Assuming an exponential relationship the R.M.S. deviation in the full scale results is 0.007 while in the computed results the error is 0.011 air changes per hour. Here there is reasonably good agreement between the observed and computed sets of results.

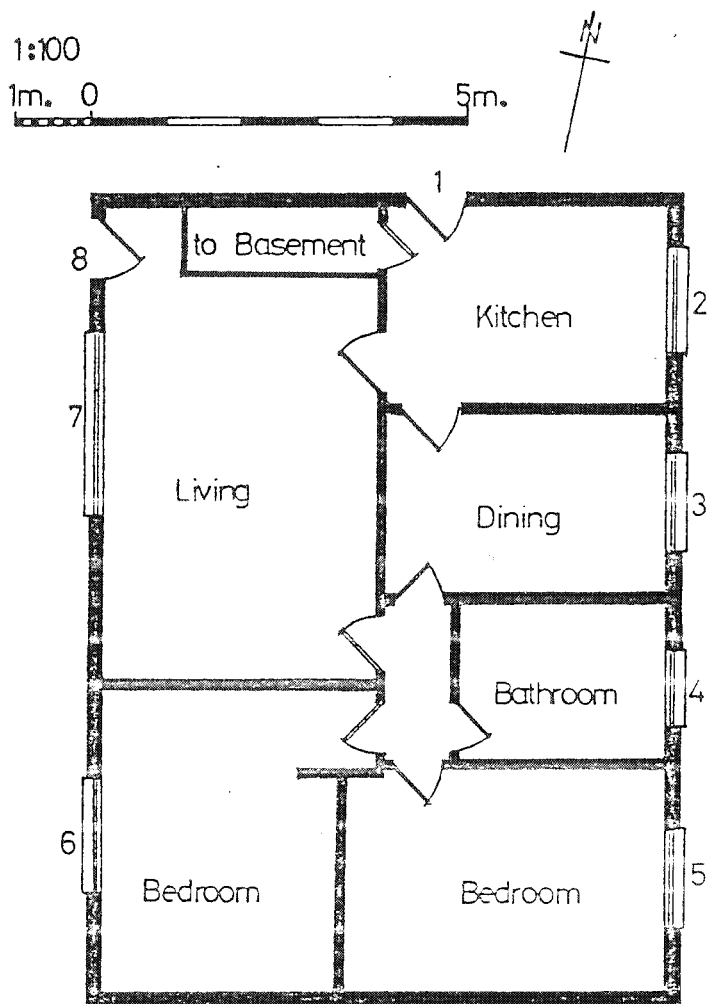
6.5 Conclusions

6.5.1 Comparisons of the variation of full scale infiltration rates with wind speed were made between full scale observations on a small domestic dwelling and calculations using a digital model. The calculated results are in good agreement with the full scale results in terms of the rate of change of infiltration rate with wind speed. Analysis assuming an exponential, rather than a linear, relationship between ventilation rate and wind speed gives a better explanation of the zero error. The computed results agree with the full scale results in showing that the total infiltration rate is more sensitive to wind speed than to wind direction. The full scale results show consistently higher ventilation rates

than the computed results. This difference is caused by several factors leading to overestimates of the full scale ventilation rate; diffusion effects and the temperature differences acting being probably the more significant ones. Any estimate of the magnitude of the error is extremely difficult but it may be of the same order of magnitude as the difference between the observed and the computed results.

6.5.2 Although the agreement between the observed and computed rates of increase of ventilation rate with wind speed are good, it must be emphasised that this is probably largely fortuitous. The assumptions made in the data used for the calculation and the possible errors in the full scale observations are of such magnitude that only general conclusions may be drawn. The study emphasises that the likely accuracy of the full scale results are not high enough to enable results from this type of study to be used to establish the accuracy of the assumptions used in analogue techniques. Further, closely controlled comparative tests need to be carried out before the limits of accuracy of the current computational techniques can be established in practice.

Figure 6.1, Plan of house no.1, after Tamura and Wilson.



Assumed leakage coefficients.

Opening	Elevation	Crackage Length, m.	Coefficient, $m^3/hr. mm. wg^{0.6}$
Door, 1	N	11.8	23.7
Window, 2	E	10.6	21.3
Window, 3	E	10.6	21.3
Window, 4	E	6.1	12.3
Window, 5	E	10.6	21.3
Window, 6	W	10.6	21.3
Window, 7	W	24.3	49.8
Door, 8	W	11.8	23.7

Figure 6.2.

Comparison of observed ventilation rate with wind speed after Tamura and Wilson.

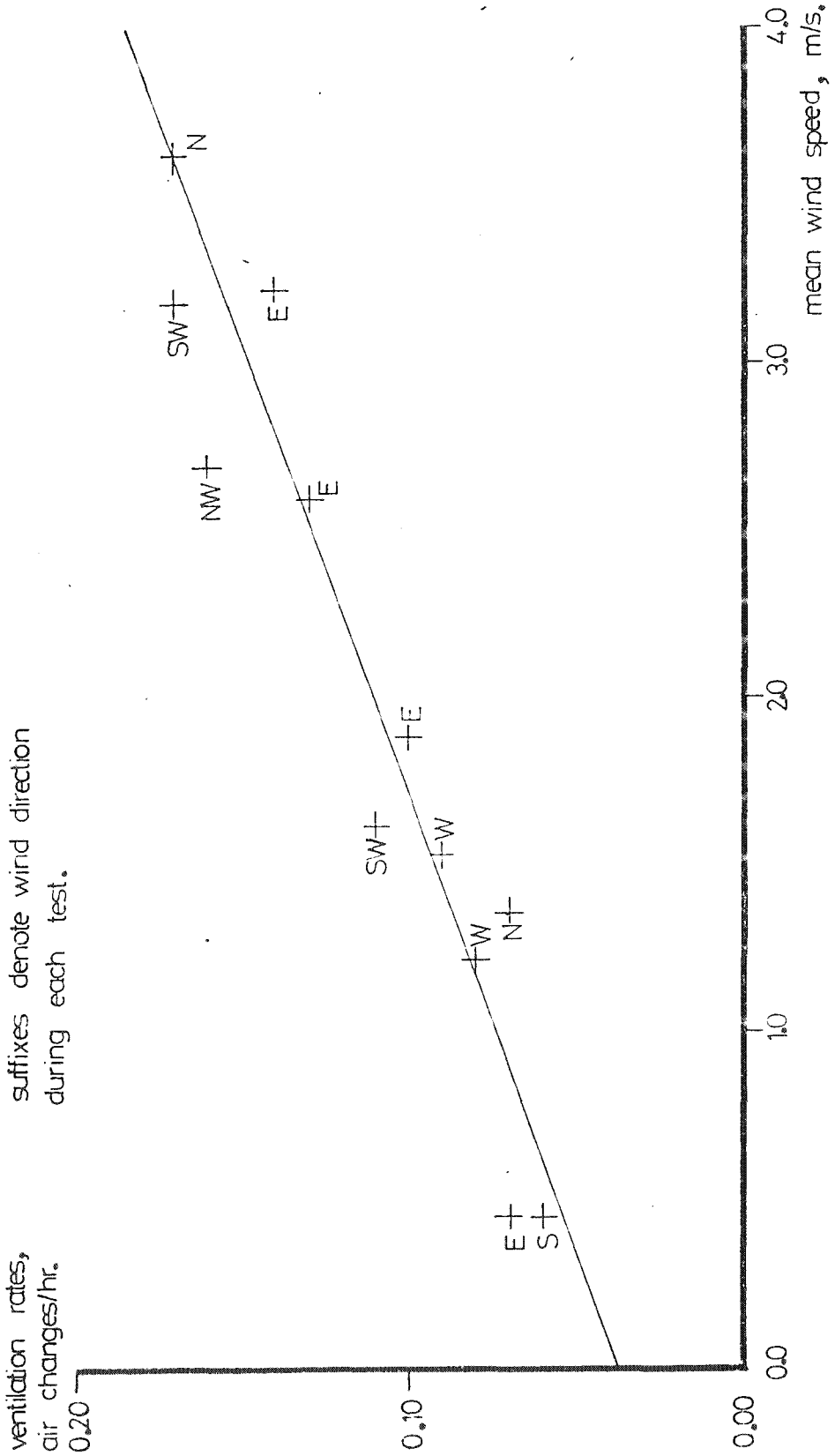
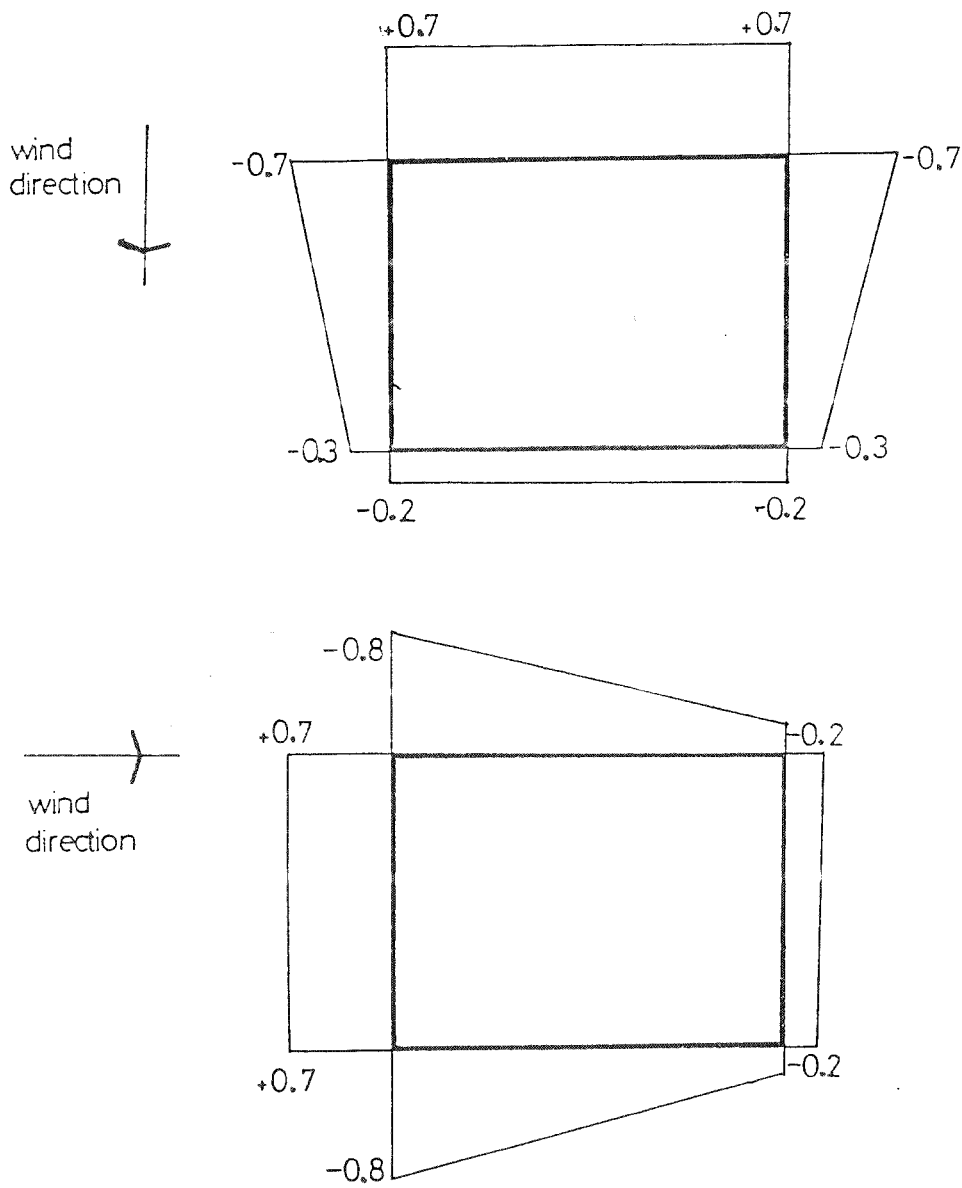


Figure 6.3. Assumed pressure coefficients based on B.R.S. Digest 119.



ventilation rate,
air changes/hr,
0.20

suffixes denote wind direction
during each test.
only tests with wind from the
primary cardinal directions are
included in these results.

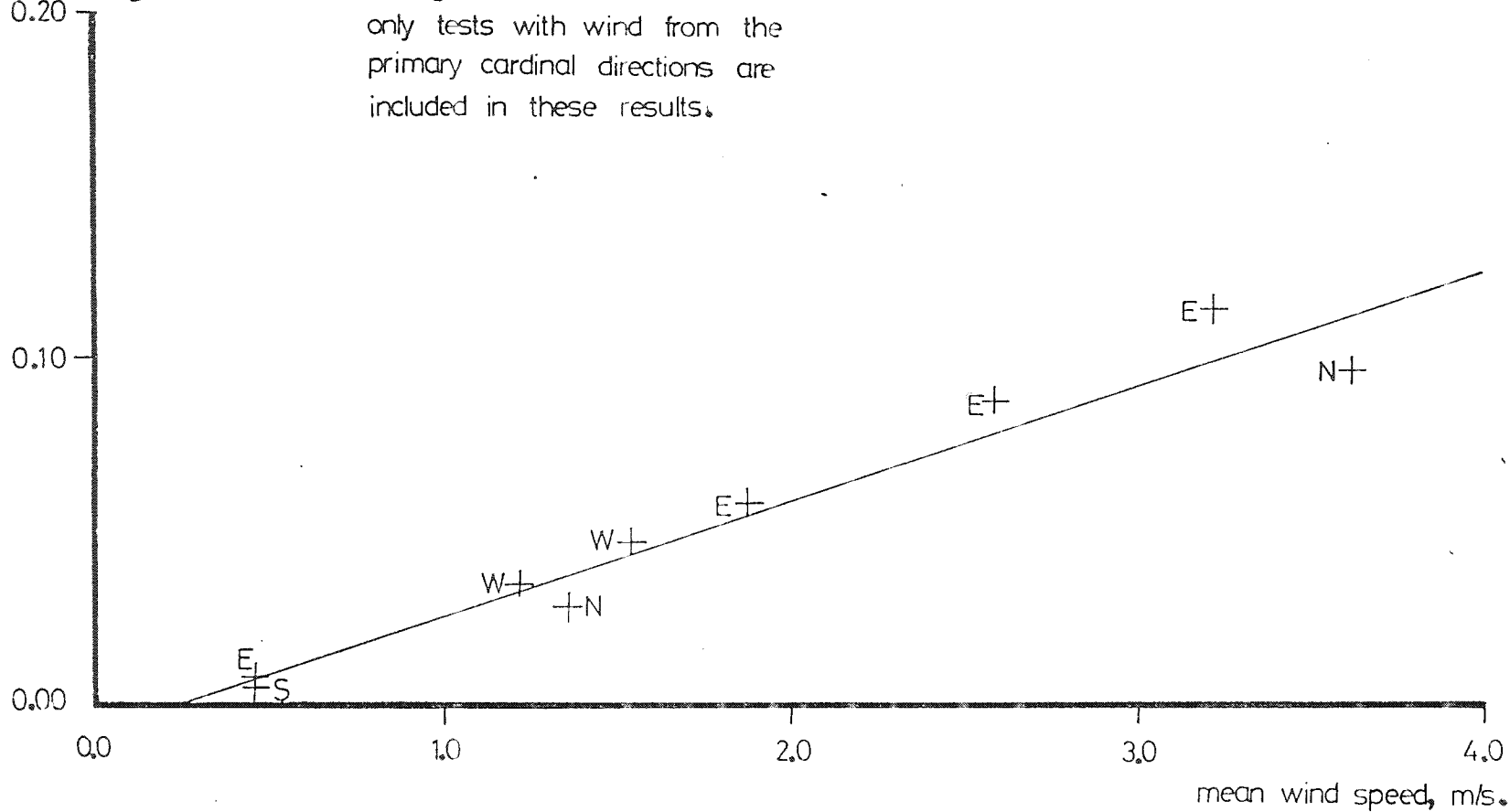
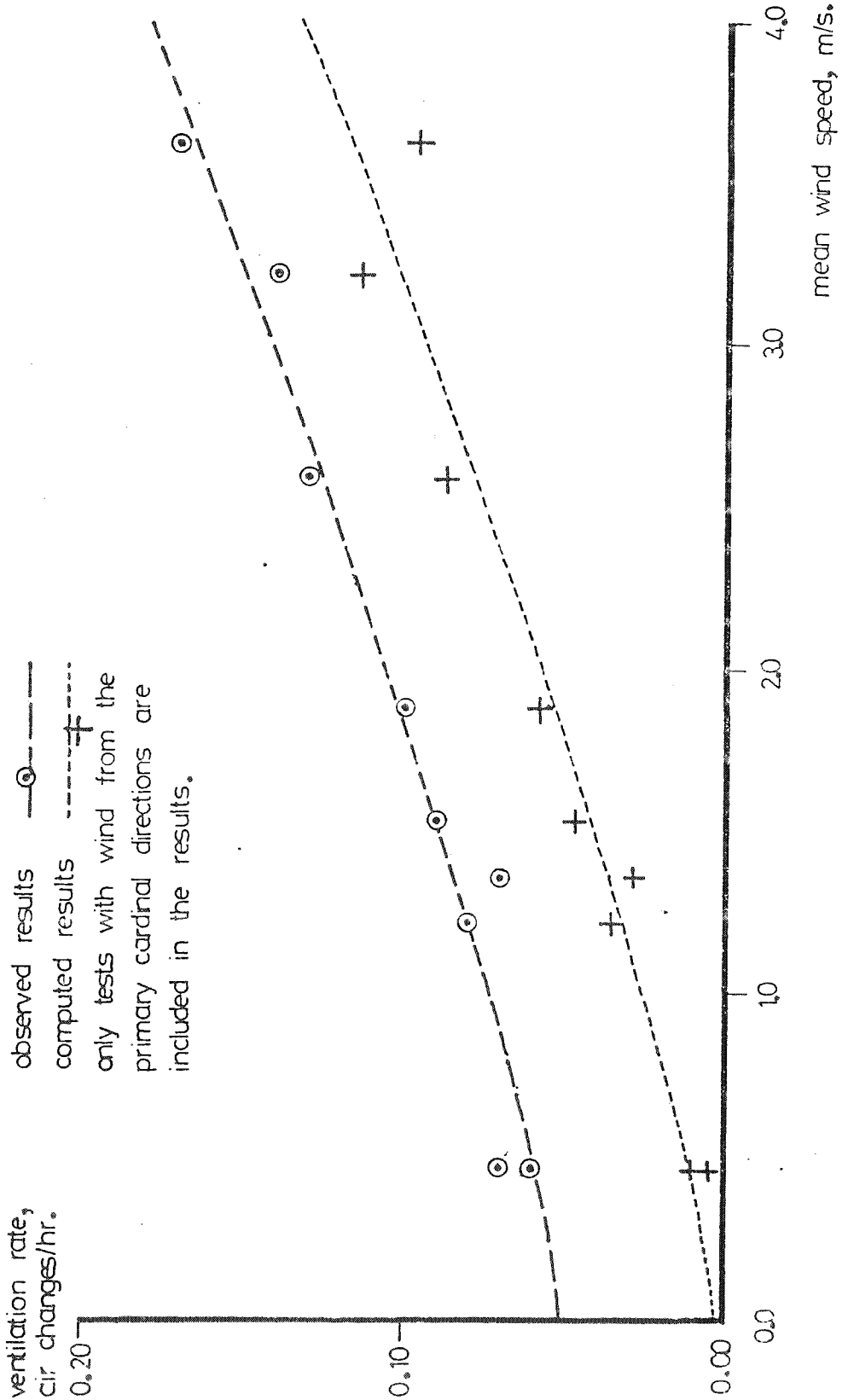


Figure 6.4.

Comparison of computed ventilation rate with wind speed.

Figure 6.5.

Comparisons of lines of best fit for observed and computed results assuming an exponential relationship between wind speed and ventilation rate.



7. MODEL VENTILATION STUDIES - EXPERIMENTAL APPARATUS AND TECHNIQUES.

7.1 Introduction

7.1.1 In order to attempt a more detailed study of the prediction of natural ventilation rates a series of model ventilation studies were carried out. These studies were made on a comparative basis; wind tunnel model results were compared with results from digital analogue studies. In this way two major aspects of the problem of natural ventilation were studied. These were:

- a) to make detailed studies of the natural ventilation of a known object under controlled conditions, and
- b) to assess the accuracy of the digital analogue predictive technique by comparing the observed and computed results.

7.1.2 The number of factors which have some effect on the amount and pattern of ventilation or infiltration is too large to enable a comprehensive study to be made. It was therefore decided to limit the study by using one standard building form. Variation in the shape of a building is influential in the pattern of ventilation mainly because a change in shape affects the pressure patterns at the ventilation openings of the building. As this effect could be studied alternatively by varying the number and distribution of these openings and the

aerodynamic properties of the wind stream around the building it was thought that one standard building form would be sufficient to show these effects. The models have been built so that a variable number of calibrated orifices can be used to represent the openings for ventilation in the building. Pressure tappings have been introduced into one face so that the external pressure coefficients can be measured and the pressure coefficients at the positions of the ventilation openings estimated by interpolation.

7.1.3 The wind tunnel in which the tests have been carried out is an open-circuit tunnel with a closed working section. The lateral dimensions of the working section are 600 mm. x 600 mm., and its length, including the distance upstream of the model mounting position available for modification of the boundary layer, is 2.0 m. A section through the wind tunnel may be seen in Figure 7.1. Tunnel working speeds are in the range 0-25 m/s.

7.2 Model theory

7.2.1 Model studies of naturally induced air flow patterns have been carried out previously by several authors, (Smith, 1951), (Givoni, 1962). These studies have dealt, generally, with situations of the type likely to be met in tropical and sub-tropical countries where very high ventilation rates through large window openings

are typical. No studies have been noted where ventilation and infiltration rates are modelled through open areas of the order of one per cent of the facade area, which is more typical of the situations encountered in cool temperate climates.

7.2.2 In aerodynamic modelling the more significant parameters which must be considered in order to ensure similarity in the air flow patterns around the model and the full scale case are geometric similarity, the Reynolds numbers of the two flows and the blockage ratio in the model study. Reynolds number is defined by the equation:

$$Re = \frac{W'.d.\rho}{\mu} \quad \dots\dots (7.1)$$

where W' is air velocity, m/s.

d is a scale dimension, m.

ρ is fluid density, kg /m³.

μ is dynamic viscosity, N.s/m².

The Reynolds number for model and full scale flows should be equal to ensure exact similarity between the air flow patterns in the two situations. In model work around buildings it is normally very difficult to produce the same Reynolds numbers as would occur in full scale situations. However, as objects with sharp edged corners and plane surfaces tend to produce the same flow patterns over a fairly wide range of Reynolds numbers,

this condition is normally relaxed.

7.2.3 Smith (Smith, 1951) made a number of wind tunnel investigations in which he tried to determine the extent to which Reynolds number modelling may be relaxed. In his studies he used the reattachment positions of the separated flow in the lee of his models as a criterion for flow similarity. He studied several different building shapes using varying air velocities and model shapes. The reattachment positions remained relatively constant, but past certain limits the results became very variable. In particular he used a variable E to express these limits:

$$E = \frac{2A \cdot W^2}{q} \dots\dots (7.2)$$

where A is frontal area, m².

q is perimeter past which air flows, m.

In his model tests he found that the lower limit of E, below which the flow pattern did not remain stable, was approximately 0.25 m²/s. for all the model shapes tested. He compared some of the results with full scale observations on a building for which the value of E was approximately 16 m²/s. and found results consistent with model tests on a scale model. Smith's work does not refer to the flow conditions of the tests or the limiting aspect ratios of the models which may alter flow conditions considerably and the relevant values of E. However the work must be used to give some order of

magnitude to the extent to which Reynolds numbers can be relaxed, as little other work has been done in this field.

7.2.4 Smith also compared air flow patterns in the models with the patterns in a full scale experimental building. The results show that provided the details of the model are accurately reproduced the air flow patterns can be faithfully reproduced. Givoni (Givoni, 1962) in a series of model experiments showed that air speeds measured inside a model building bear an almost constant relationship with the external wind speed. Unfortunately he gives no comparative full scale results with which to estimate the accuracy of the results. No other studies have been noted which give modelling criteria for wind induced building ventilation.

7.2.5 When considering modelling fluid flow through small orifices, and relating these values with values in full scale cases, it would seem advantageous that the Reynolds number of the flow through the model orifices should be of the same order as that through the full scale openings. The Reynolds number is defined as in equation 7.1:

$$Re = \frac{W \cdot d \cdot \rho}{\mu} \dots\dots (7.1)$$

A suitable scale dimension which may be used with openings of differing geometry is the hydraulic radius (Lenkei, 1965):

$$Rh = \frac{\text{cross sectional area of opening}}{\text{length of perimeter of opening}} \dots (7.3)$$

However the scale length normally used in defining Reynolds number is the equivalent diameter of the opening, which is equivalent to four times the hydraulic radius. For a long thin crack, typical of the type of orifice shape through which infiltration or controlled ventilation will occur:

$$Rh = \frac{y \cdot L}{2(y + L)}$$

where L is the crack length,
y is the crack width,
and as in this situation $L \gg y$

$$Rh \approx \frac{y}{2} \dots (7.4)$$

Thus for a long narrow opening the Reynolds number of the flow through the opening may be represented as:

$$Re \approx \frac{2 \cdot W' \cdot y \cdot \rho}{\mu} \times 10^{-3} \dots (7.5)$$

where y is the crack width in mm.

7.2.6 The order of magnitude of maximum full scale Reynolds numbers for typical infiltration openings under normal conditions may be estimated from equation (7.5). Assuming a maximum infiltration coefficient of $10 \text{ m}^3/\text{hr}/\text{m}/\text{mm.wg.}^{0.6}$ (Figure 3.8) and a maximum pressure difference of 5 mm.wg then the maximum infiltration rate ,

V, will be approximately 26 m³/hr/m. length of opening. But for one metre of length of opening the flow velocity, W', may be seen to be:

$$W' = \frac{0.28 V}{y}$$

and substituting in equation (7.5):

$$\begin{aligned} \text{Re} &\approx \frac{0.56.V.\rho}{\mu} \times 10^{-3} \\ &\approx 1000. \end{aligned}$$

Thus the working range of Reynold's numbers for flow through full scale infiltration openings may be taken as 0 - 1000.

7.2.7 A model form was chosen which satisfied the requirements of Smith's work on external flow similarity and had openings giving model flow Reynolds numbers of the same order as full scale. Plan dimensions of the model were 120 mm. x 120 mm. and the height was 90 mm. A range of velocities between 12.5 m/s and 25 m/s were used in the tests for which the corresponding values of the parameter E were 0.9 - 1.8 m²/s. The ventilation openings in the models were sets of 1.0 mm. and 2.5 mm. diameter holes. For these openings the hydraulic radius may be calculated as:

$$\begin{aligned} \text{Rh} &= \frac{\pi r^2}{2\pi r} \\ &= r/2 \end{aligned} \quad \dots\dots (7.7)$$

Then the flow Reynold's numbers for these openings may be found as:

$$\begin{aligned} \text{Re} &= \frac{2 \cdot W \cdot r \cdot \rho}{\mu} \times 10^{-3} \\ &= \frac{0.56 \cdot V \cdot \rho}{\pi \cdot r \cdot \mu} \dots\dots (7.8) \end{aligned}$$

The maximum values of volume flow rate at a pressure of 15 mm.wg are approximately 0.19 m³/hr. and 0.03 m³/hr. for the 2.5 mm. diameter and 1.0 mm. diameter holes respectively. Thus for the 2.5 mm. diameter holes:

$$\begin{aligned} \text{Re max.} &= \frac{0.56 \times 0.19 \times 1.2}{\pi \times 1.25 \times 1.8 \times 10^{-5}} \\ &\approx 1800. \end{aligned}$$

And for the 1.0 mm. diameter holes:

$$\begin{aligned} \text{Re max.} &= \frac{0.56 \times 0.03 \times 1.2}{\pi \times 0.5 \times 1.8 \times 10^{-5}} \\ &\approx 700. \end{aligned}$$

Thus the working range of Reynold's numbers through the model openings may be taken as 0 - 1800 and 0 - 700 for the 2.5 mm. diameter and 1.0 mm. diameter holes respectively. The blockage ratio of the model was approximately 3%: no blockage corrections were made in the experiments therefore.

7.2.8 It was also decided to attempt to design the model with the same order of porosity as is normally found in buildings with all windows nominally closed or

some open for ventilation. A figure for typical building permeability for office buildings with all windows closed is given in B.R.S. Digest 119 (B.R.S., 1970) as 0.01 to 0.05 per cent of the face area. Opening some windows for ventilation may result in permeabilities rising to maximum values of the order of 5 per cent of the face area. The models were tested with varying numbers of ventilation openings, the minimum number representing a porosity of approximately 0.05 per cent of the model face area, and the maximum a figure of 0.5 per cent of the face area.

7.3 Ventilation rate measurement techniques

7.3.1 Several techniques have been used in studies of natural ventilation and infiltration for assessing ventilation rates. The methods available and their limitations have been described by Hitchin and Wilson (Hitchin, 1967). In most full scale studies various methods using a tracer gas have been used to indicate the mean ventilation rate in a building (see Section 3.2). In some studies measurements of air velocities have been made in order to help gain some knowledge of flow rates and patterns. These have generally been done by photographing moving flow indicators or using anemometers of various types. Model studies have also been carried out in which flow patterns have been observed by photographing moving indicators, and estimates of ventilation rates made by measuring flow

velocities at finite points using hot-wire anemometers (Smith, 1951), (Givoni, 1962), (Wannenber, 1957).

7.3.2 The full scale techniques which have been noted are not generally suitable for use in small scale model experiments. The use of a tracer gas, measuring either the stable continuous concentration or the rate of decay of the tracer in a small model is difficult. In particular there are difficulties in finding a representative sampling position and in assessing the quality of mixing in the model, which would affect results. The volume of the connecting leads and analysis chamber of the gas concentration analyser is large in relation to the small volume of the model and to compensate accurately for this effect is also difficult. Finally the rate of tracer gas release required in the model would be very small and the accuracy with which this could be controlled is not likely to be high. For these reasons it was decided not to attempt to use a tracer gas ventilation rate measuring technique in the model studies.

7.3.3 The technique used in some previous model studies, by Givoni and others, of measuring flow velocities at discrete points in a model is also unsuitable in the present studies. Givoni measured flow velocities, using hot wire anemometers in a grid of positions in a large (650 mm. x 650 mm. x 500 mm.) model. He used the mean velocity reading as an indication of the

ventilation rate in the model. Furthermore the significance of the flow readings were corroborated using flow visualisation studies. These studies were carried out with models in which the porosities were of the order of 25 per cent of the building face areas. In the present studies, where the porosities are of the order of one per cent the internal flow patterns are liable to be less predictable, and less easily seen in flow visualisation studies. At the same time flow velocities are likely to be less uniform throughout the model and will be much lower; mean velocities will be 0.1 m/s or less for 10 m/s external speeds and the range of porosities being studied, which is near the limit of accuracy of normal velocity measuring techniques.

7.3.4 As the previous measurement techniques were not suitable for monitoring the model flow it was decided to attempt to develop alternative measuring techniques. Two types of model were used, one which measured the ventilation rate directly and one in which the internal pressures inside the model were measured. From these models information about the accuracy of the digital analogue technique could be inferred.

7.3.5 In the first set of model studies the internal pressures inside the model were studied. The digital analogue technique relies essentially on balancing the internal pressures in the building, from knowledge of the external pressures and the opening characteristics,

so that the net air flow into the building is equal to that leaving it. By measuring the external pressures and using calibrated openings in the model it is possible to calculate what the internal pressures should be under differing sets of conditions. By measuring the internal pressures in the model and comparing the results it is possible to get some information on the accuracy of the computer method. Consequently it was decided to attempt to use a model which is air tight apart from the ventilation openings and in which the internal pressures may be measured.

7.3.6 A second set of model studies was carried out using the same model shape and orifice positions, in which flow measurements were made directly. It was decided to attempt to use an orifice plate mounted in a rigid diaphragm placed across the model to measure the flow rate. In this way estimates can be made of the mean volumetric flow rate through the model. The effect of the orifice plate system on the model will be very small if the pressure drop through the orifice system can be kept small in relation to the pressure drop across the model. A pressure drop across the orifice of one per cent of the pressure drop across the model will lead to a reduction of flow through the model of approximately 0.5 per cent. The system has the advantage of being simple to use and gives an accurate reading of the actual flow rate through the model rather than a deduced flow rate from velocity measurements at discrete points. The

main disadvantage of this type of model is that ventilation openings may only be located in two opposite walls.

7.4 Description of Internal Pressure Measurement Models

7.4.1 The models used for these measurements were hollow perspex cuboids. Their dimensions were 120 mm. x 120 mm. x 90 mm. high. The interior of each model was divided by two floors at heights of 30 mm. and 60 mm. The floors and roof of the model were constructed from 6 mm. perspex sheet, the walls from 3 mm. perspex sheet. All joints in the models were carefully sealed, as the model was being built, using perspex cement, in order to make them air tight at working pressures. The models were mounted on circular perspex bases, 12 mm. in thickness and 200 mm. in diameter which could be positioned in one wall of the wind tunnel working section, flush with the surface of the wall. A section through a model is shown in Figure 7.2.

7.4.2 Openings through which the model may be ventilated were made at a number of positions on each face of the model. The positions formed a square grid at centres of 30 mm. The positions of these openings may be seen in Figure 7.3. One additional opening position was located in the centre of each of the two intermediate floors in the model in order to simulate vertical flow between floors. Two ventilation opening

types were used in the model tests, holes of 2.5 mm. diameter and holes of 1.0 mm. diameter. These opening sizes were chosen to reproduce the flow characteristics of open windows and typical building infiltration passages respectively. In the models using 2.5 mm. diameter holes one opening was located at each grid position. In the models using 1.0 mm. diameter holes four openings in a square pattern, and at 2 mm. centres, were located at the grid position.

7.4.3 On one face of each model twelve external pressure tapings were made. These tapping positions also formed a square grid at 30 mm. centres, the measuring positions being established midway between the ventilation openings, as seen in Figure 7.3. The pressure tapings were made from lengths of 1.5 mm. internal diameter stainless steel tubing mounted flush with the external face of the model, and taken out through the base of the model. Two pressure tapings, made from the same type of tubing, were mounted at each internal level of the model. They were mounted at the same level as the openings on their floor, at opposite sides of the model, 5 mm. from the inside face of the model and at a horizontal distance of 10 mm. from the centre-line of the openings. In the model incorporating the 1.0 mm. diameter openings tapings were located near the centre of each floor of the model, in order to check that the pressure measurements obtained were representative of the mean internal pressure in the model. Each internal pressure

tapping was blanked off when not in use with a nylon cap, to ensure that no leakage occurred into the model from outside the wind tunnel.

7.4.4 The ventilation openings used in the model tests were calibrated in a small air duct under conditions of constant flow. Pressure difference across the plate was measured using an inclined tube manometer, and flow rate was measured using a 'Gapmeter' flowmeter. The calibrations were carried out over a range of pressure differences between 2.0 mm.wg. pressure difference and 25.0 mm.wg. pressure difference, which is representative of the range of working pressures in the model tests. A full account of the calibration and the treatment of the results is given in Appendix A3. The calibration curves obtained for the two orifice sizes were:

For the 2.5 mm. diameter holes, in 3 mm. thick sheet

$$V = 0.0494. (\Delta P)^{1/1.69} \dots\dots (7.9)$$

and for the 1.0 mm. diameter holes, in 3 mm. thick sheet

$$V = 0.00597 (\Delta P)^{1/1.68} \dots\dots (7.10)$$

The calibration is in good agreement with results calculated from Lenkei's paper (Lenkei, 1965). The 95% confidence limits for both calibrations have values of the order of $\pm 4\%$ of the coefficient.

7.4.5 During the calibration tests various methods of blocking the ventilation openings to air flow were attempted. It was found that two layers of selotape

adhesive tape fixed over the holes, and rubbed down well gave no observable changes in flow rate from the flow rate through the same number of open holes in an otherwise solid perspex sheet. Consequently this method was used for blanking off openings in order to change the layout of the ventilation openings.

7.5 Description of the Orifice Plate Model

7.5.1 The orifice plate chosen as being most suitable for the model ventilation rate measurements was taken from B.S. 1042 (B.S., 1964). It was a conical-entrance orifice plate, based on the design given in part 10 of the British Standard. It is particularly suitable for measuring flow rates in viscous fluids as the coefficient of discharge remains relatively constant over a range of Reynolds numbers between 250 and 200,000.

7.5.2 The orifice plate was constructed in a diaphragm of 6 mm. perspex sheet which was placed across the ventilation model. Short settling lengths of pipeline, the upstream section with a bell mouth entry, were attached to each face of the orifice plate. The orifice was positioned concentrically with the pipelines. The orifice plate was built to comply with the specifications given in B.S. 1042, Part I in all possible details. A section through the orifice plate model is shown in Figure 7.4 and a detail section through the orifice plate shown in Figure 7.5.

7.5.3 The orifice diameter was 18.5 mm. The orifice plate thickness was 2.0 mm., the length of the parallel bore being 0.4 mm., and the axial length of the conical entrance 1.6 mm. The upstream and downstream pipe sections had nominal diameters of 58.5 mm. The pressure tapings were located in the walls of the pipes, immediately adjacent to the faces of the orifice plate and flush with the pipe surfaces. The upstream pipeline extended a distance of 64 mm. from the orifice plate, which is approximately equivalent to one diameter of the pipe. The downstream pipe extended from the orifice plate for a distance of 20 mm., which is approximately equivalent to 0.3 pipe diameters. The design of the orifice plate satisfied the specification of the standard orifice plate in all respects with the exception of the lengths of the upstream and downstream settling pipe lengths. Because these pipe lengths did not meet the specification laid down, and because the orifice plate was used for a non-standard flow measuring situation the plate was independently calibrated over the working range and the results compared with the standard calibration.

7.5.4 The standard calibration for an orifice of this type is given by the equation:

$$V = 0.01252.CZ. \epsilon .F.(D_o)^2. (dP/\rho)^{0.5} \dots (7.11)$$

where CZ is the orifice discharge coefficient,

ϵ is the orifice expansibility factor,

F is the velocity of approach factor,
 Do is the orifice plate diameter, mm.,
 D is the orifice plate pipeline diameter, mm.

and the Reynolds number of the flow is given by the equation:

$$Re = 0.354.V.\rho/\mu.Do \quad \dots\dots (7.12)$$

The velocity of approach factor, F, is found from the relationship:

$$F = 1/\sqrt{(1 - (Do/D)^4)} \quad \dots\dots (7.13)$$

For the orifice geometry specified F = 1.005 and found from nomograms in B.S. 1042 is 1.000 for working flow rates. The coefficient of discharge for the orifice plate is stated as 0.734 for Reynold's numbers in the range 250 - 5000. Using these values the standard calibration equation for the orifice plate becomes:

$$\bar{v} = 2.885 \sqrt{dF} \quad \dots\dots (7.14)$$

and the expression for Reynold's number becomes:

$$Re = 1276V \quad \dots\dots (7.15)$$

Thus over the working range of 0.2 to 3.0 m³/hr., the range of Reynolds numbers will be approximately 250 to 4000.

7.5.5 Calibration of the orifice plate was carried out over the working range of flow rates with the orifice in

position in the ventilation rate model. The layout of the calibration equipment is shown in Figure 7.6. Air flow rates were measured by means of a "Gapmeter" air flow rate meter. Pressure differences were measured by connecting the pressure tapings to a micromanometer. The electrical output of the micromanometer was connected to a "Solartron" data logger, which was used to operate an electric typewriter in order to obtain automatic printout of the output voltage.

7.5.6 The system was connected as in Figure 7.6. A suction pump was used to provide the necessary flow rate, the flow being accurately controlled by a valve on the tube connecting it to the flow meter. A series of readings were then taken. In each case a recording of the zero flow micromanometer output voltage was made, a sequence of five readings being taken at one second intervals. The flow was then started and measured by the flow meter. Simultaneously a recording of ten readings of the micromanometer output voltage were made. A further record of five zero flow output voltages was then made. The mean difference between the flow and zero flow voltages was converted to a pressure difference and plotted against the flow rate.

7.5.7 The calibration curve for the orifice plate with no impedance is shown in Figure 7.7. The calibration equation was found to be:

$$V = 2.890 \sqrt{dP} \quad \dots (7.16)$$

The 95% confidence limits being ± 0.07 dP, equivalent to an error of $\pm 2.5\%$ of the flow rate. This calibration compares closely with the theoretical calibration (Equation 7.14).

7.5.8 The calibration was repeated with the front plate in place, then with the rear plate of the ventilation model in place, to check the effect of these obstructions on the calibration. Figure 7.8 shows the calibration with the front plate in position. The calibration in this case differed from the previous one by up to 30% over some parts of the working range. Several alterations to the model were tried in order to remove this discrepancy which was thought to be due to distortion of the flow by the small openings in the model front plate. The introduction of a spreader plate, which was placed across the front of the upstream pipe in the model (Figure 7.4) gave a calibration of similar form to that for the orifice plate alone. The spreader plate was positioned 3 mm. in front of the upstream pipe. There was a 4 mm. gap at each side of the plate between itself and the model wall. This ensured that whatever the configuration of the model front plate all air reaches the orifice plate from the same directions. The calibration of the orifice plate with model front plate and spreader plate in position is also shown in Figure 7.8. Figure 7.9 shows the calibration with the model rear plate in position. The calibration agrees reasonably with that for the orifice plate alone and consequently

the model back plate was taken to have no influence on the orifice plate calibration over the working range.

7.5.9 A combined calibration using the points obtained for the orifice plate with spreader plate, orifice plate with spreader plate and model front plate and orifice plate with spreader plate and model back plate was made. This gave a combined calibration equation of the form:

$$V = 2.865 \sqrt{\Delta P} \quad \dots (7.17)$$

The 95% confidence limits were calculated at ± 0.126 dP which corresponds to approximately $\pm 4.5\%$ of the flow constant. This calibration was used in the model experiments with an assumed accuracy of $\pm 5\%$. The full calibration measurements are presented in Tables 7.1 to 7.4.

7.5.10 The model front and back plates, in which the ventilation openings were all located, were screwed to the model side walls, the joints then being taped. The ventilation openings were of the same type as those used in the internal pressure measurement models. They were placed on a rectangular grid of 30 mm. high by 15 mm.

7.6 Experimental technique

7.6.1 The model experiments were carried out under two contrasting sets of flow conditions. In the initial set of experiments the model was mounted in the wind tunnel with a relatively smooth, wooden, surface upstream.

TABLE 7.1 Calibration of orifice plate

Mean zero flow voltage, mV	Mean flow voltage, mV	Voltage difference, mV	Pressure difference, mm.wg.	Flow meter volume flow rate m ³ /hr.
+ 102.25	+ 16.90	85.35	0.884	2.70
+ 102.45	+ 29.50	72.95	0.756	2.49
+ 102.20	+ 43.00	59.80	0.621	2.27
+ 102.00	+ 55.30	46.70	0.484	2.02
+ 101.90	+ 64.90	37.00	0.383	1.82
+ 101.55	+ 71.50	30.05	0.311	1.64
+ 102.80	+ 77.50	25.30	0.263	1.52
+ 101.25	+ 78.70	22.55	0.233	1.40
+ 101.80	+ 88.70	13.10	0.136	1.07
+ 15.34	+ 7.00	8.34	0.0864	0.864
+ 15.51	+ 10.81	4.70	0.0487	0.636
+ 15.61	+ 12.27	3.34	0.0347	0.522
+ 15.69	+ 14.26	1.44	0.0149	0.354

Furness micromanometer calibration 96.5 mV \equiv 1.00 mm.wg.

TABLE 7.2 Calibration of orifice plate with model front
wall in place

Mean zero flow voltage mV	Mean flow voltage, mV	Voltage difference, mV	Pressure difference, mm.wg.	Flow meter volume flow rate m ³ /hr.
+ 0.05	- 30.30	30.35	0.314	1.58
+ 0.20	- 23.30	23.50	0.244	1.38
+ 0.35	- 17.55	17.55	0.181	1.19
- 0.10	- 14.50	14.40	0.149	1.08
- 0.15	- 7.90	7.75	0.0800	0.768
- 0.26	- 6.42	6.16	0.0638	0.642
- 0.32	- 4.89	4.57	0.0473	0.522
- 0.37	- 3.08	2.71	0.0281	0.360
- 0.42	- 1.51	1.09	0.0113	0.228

Furness micromanometer calibration 96.5 mV \equiv 1.00 mm.wg.

TABLE 7.3 Calibration of orifice plate with model front plate and spreader plate in place.

Mean zero flow voltage, mV	Mean flow voltage, mV	Voltage difference, mV	Pressure difference, mm.wg.	Flow meter volume flow rate m ³ /hr.
+ 19.75	- 14.70	34.45	0.357	1.75
+ 20.30	- 5.34	25.64	0.276	1.51
+ 20.85	+ 2.80	18.05	0.187	1.27
+ 101.50	+ 120.35	18.85	0.196	1.29
+ 83.50	+ 100.00	16.50	0.171	1.20
+ 107.40	+ 120.40	13.00	0.135	1.05
+ 21.45	+ 11.30	10.15	0.105	0.924
+ 2.52	+ 9.68	7.16	0.0742	0.786
+ 4.03	+ 9.00	4.97	0.0515	0.636
+ 4.83	+ 8.08	3.25	0.0337	0.510
- 2.21	- 0.67	1.54	0.0160	0.360
+ 6.06	+ 6.76	0.70	0.0072	0.228

Furness micromanometer calibration 96.5 mV \equiv 1.00 mm.wg.

TABLE 7.4 Calibration of orifice plate with model rear plate in place.

Mean zero flow voltage, mV	Mean flow voltage, mV	Voltage difference, mV	Pressure difference, mm.wg.	Flow meter volume flow rate m ³ /hr.
+ 14.20	+ 2.50	11.70	0.121	1.03
+ 33.45	+ 22.85	10.58	0.110	0.966
+ 33.25	+ 26.15	7.10	0.0738	0.780
+ 12.55	+ 7.96	4.59	0.0475	0.636
+ 11.51	+ 8.36	3.15	0.0337	0.498
+ 9.89	+ 8.25	1.64	0.0170	0.360
+ 8.75	+ 6.54	2.21	0.0229	0.426
+ 2.97	+ 2.20	0.77	0.080	0.234

Furness micromanometer calibration 96.5 mV \equiv 1.00 mm.wg. —

This was designed to produce a boundary layer similar to the type occurring over open country. In the second set of experiments a length of considerable ground roughness was introduced upstream of the model. This surface roughness was introduced to produce boundary layer conditions similar to those which might occur in urban areas. This turbulent boundary layer was developed using randomly spaced solid blocks, which extended upstream of the model for a distance of approximately 1.800 m. The blocks had plan dimensions of 75 mm. x 25 mm., and heights of 25 mm., 50 mm. or 75 mm. The surface roughness did not extend right up to the model, but stopped at a distance of approximately 350 mm. from it, so that the effects of the nearest individual blocks would not have an overriding influence on the flow pattern around the model. The mounting position of this surface roughness is shown in Figure 7.1 and the roughness is shown, in position, in front of the model in Figure 7.10.

7.6.2 Measurements of the velocity gradients were made at the model mounting position for both sets of flow conditions, using a traversing pitot-static tube. Turbulence intensity measurements were also made at the same position using a traversing hot wire anemometer. The results of these measurements are shown in Figure 7.11. The velocity gradient measurements are in reasonable agreement with power-law gradients, the best values of the exponents being 0.14 for the simulated non-

urban flow, and 0.45 for the urban flow. These values are of similar magnitude to those generally assumed for these types of flow (Davenport, 1967), although the turbulence intensity values are rather lower than typical full scale values.

7.6.3 During all sets of tests the air velocities were measured using a pitot-tube mounted on the centre-line of the tunnel, with the model in position. In an initial set of measurements the reading from this pitot-tube was correlated to the reading from the pitot-tube placed at the model roof height but with the model removed. This was done for both sets of flow conditions. From these measurements a correction factor was found, for each set of flow conditions, by which the centre-line velocity pressure was multiplied to give the model roof level velocity pressure. This corrected velocity pressure was then used in calculating all pressure coefficient values in the test results. Prior to each new set of readings this correction factor was checked by measuring a representative set of external pressures on the model and comparing the coefficients with the initial set of pressure coefficients found for the model.

7.6.4 The internal pressure measurement models were used initially to determine the external pressure coefficients on the faces of the building. Pressure measurements were taken, at each of the 12 measuring points shown in Figure 7.3, relative to the tunnel static

pressure at the pitot-tube position. Measurements were made at angles of incidence from 0° to 345° in 15° intervals, for both sets of flow conditions. Pressure coefficients for these points were calculated and pressure coefficients at the ventilation opening positions obtained by interpolation. The external pressure coefficient distributions observed are given in Appendix A4.

7.6.5 The internal pressure measurement models were then used to measure the internal pressures inside the model under various conditions, and the results compared with calculated internal pressures. The tests were repeated at a later time using the orifice plate model to measure the actual ventilation rates and the results again compared with the calculated ventilation rates. By using the two models in conjunction and obtaining information on both the pressure difference distributions in the models and the flow rates a much more comprehensive knowledge of the pattern of ventilation was obtained.

7.6.6 Measurements of internal pressure in the model were made using the following procedure. The model was set up with the model front face set at the required angle to the flow, θ . The tunnel was set to the required speed, using a pitot-tube mounted on the tunnel centre-line, and an inclined tube manometer, to measure the dynamic head of the flow. The differences in pressure between the model interior, measured at the internal pressure tappings

on each floor level of the model, and the tunnel static pressure were measured using the inclined tube manometer. The model was turned to angles of $(\theta + 180^\circ)$, $(360 - \theta)^\circ$ and $(180 - \theta)^\circ$ and at each angle the measurements were repeated. Finally the dynamic head of the air flow was again measured.

7.6.7 In all sets of measurements taken the ventilation opening areas on opposite sides of the model were nominally equal. Any difference in opening area on the sets of opposite faces would produce errors in the observed internal pressures. By turning the model through 180° and averaging the results any error of this type was negated. Similarly the models were turned to $(360 - \theta)^\circ$ and $(180 - \theta)^\circ$ in order that any effects due to the air flow direction being not parallel to the tunnel centre-line might be allowed for. The internal pressure measurements, for each floor, were averaged and expressed as an internal pressure coefficient. For each set of measurements, the internal pressures were computed using the relevant air flow characteristics for the openings, and the relevant interpolated external pressure coefficients. The observed and computed pressure coefficient values were compared.

7.6.8 The experimental set-up for measurement of model ventilation rates was as shown in Figures 7.12 and 7.13. The pressure tappings from the orifice plate model were connected to one set of terminals of a "Furness"

micromanometer. A second set of terminals were short-circuited with a short length of tubing, so that they remained at zero pressure difference relative to each other. The electrical output of the manometer was connected to a "Solartron" data logger which, in turn, operated an electric typewriter. The system was calibrated using an internal calibration system in the micromanometer and measuring the electrical output at the calibration values.

7.6.9 Measurements of ventilation rates through the models were then made using the following procedure. The tunnel was set to the required speed and the dynamic head of the air flow measured, using an inclined tube manometer, at the pitot-tube mounted on the tunnel centre-line. The output voltage from the micromanometer was measured at zero pressure difference using the short-circuit. The terminals from the orifice plate were then switched in and a set of twenty voltage readings, measured at half second intervals, from the output were recorded by the typewriter. The short-circuit was then switched in again and the output voltage for zero pressure difference again found. Finally the dynamic head of the air flow was again observed. The results of each set of measurements were repeated at an angle of $(360 - \theta)^{\circ}$ to the flow in order to compensate for the effects of flow not parallel to the tunnel centre-line.

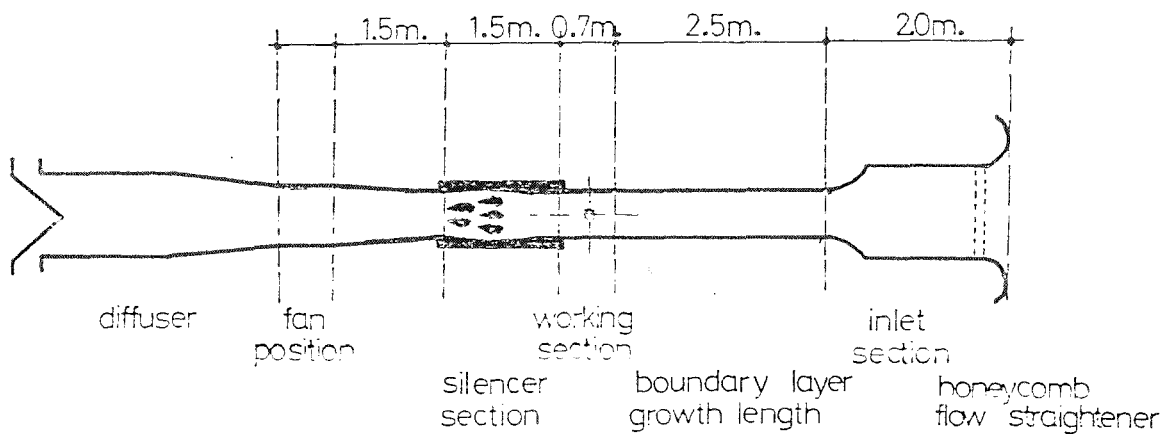
7.6.10 For each set of measurements the mean zero pressure difference voltage was found and this value was subtracted from the orifice plate voltages. These voltage differences were then converted to pressure differences and volume flow rates. The mean volume flow rate through the model was found. This procedure was followed in order to eliminate any errors, due to fluctuations in flow rate, which would be caused by using a mean pressure difference to calculate the mean flow rate (A.S.M.E., 1959). The mean dynamic head of the flow was corrected by multiplying by the appropriate factor to calculate the wind speed at model roof level. The ventilation rate was then calculated as a rate corrected to 20 m/s wind speed using the relationship:

$$\begin{aligned}
 v &\propto (\Delta P)^{1/n} \\
 \Delta P &\propto (W)^2 \\
 v &\propto (W)^{2/n} \\
 \text{or } V_{20} &= V_W \cdot \left(\frac{20}{W}\right)^{2/n} \quad \dots\dots (7.18)
 \end{aligned}$$

For each set of measurements the volume flow rates were computed using the relevant air flow characteristics and interpolated external pressure coefficients and an assumed wind speed of 20 m/s. The observed and computed ventilation rates were compared. A typical set of results for the models are given, in full, in Appendix A5.

Figure 7.1. Wind tunnel details.

Plan, 1:100.



Detail showing working section with simulated ground roughness in place.

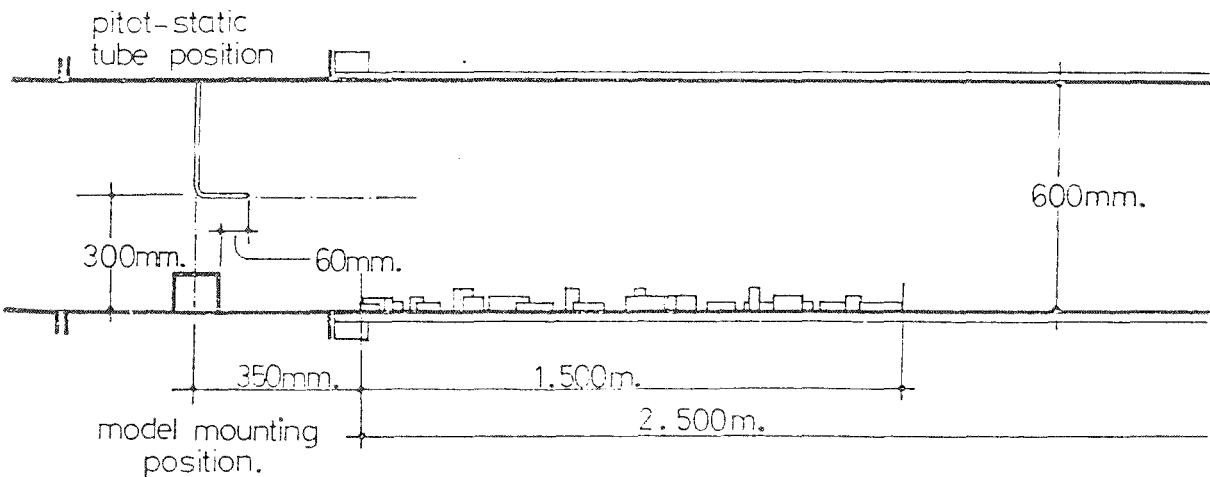


Figure 7.2. Section through internal pressure measurement model ; 2.5mm diameter openings.

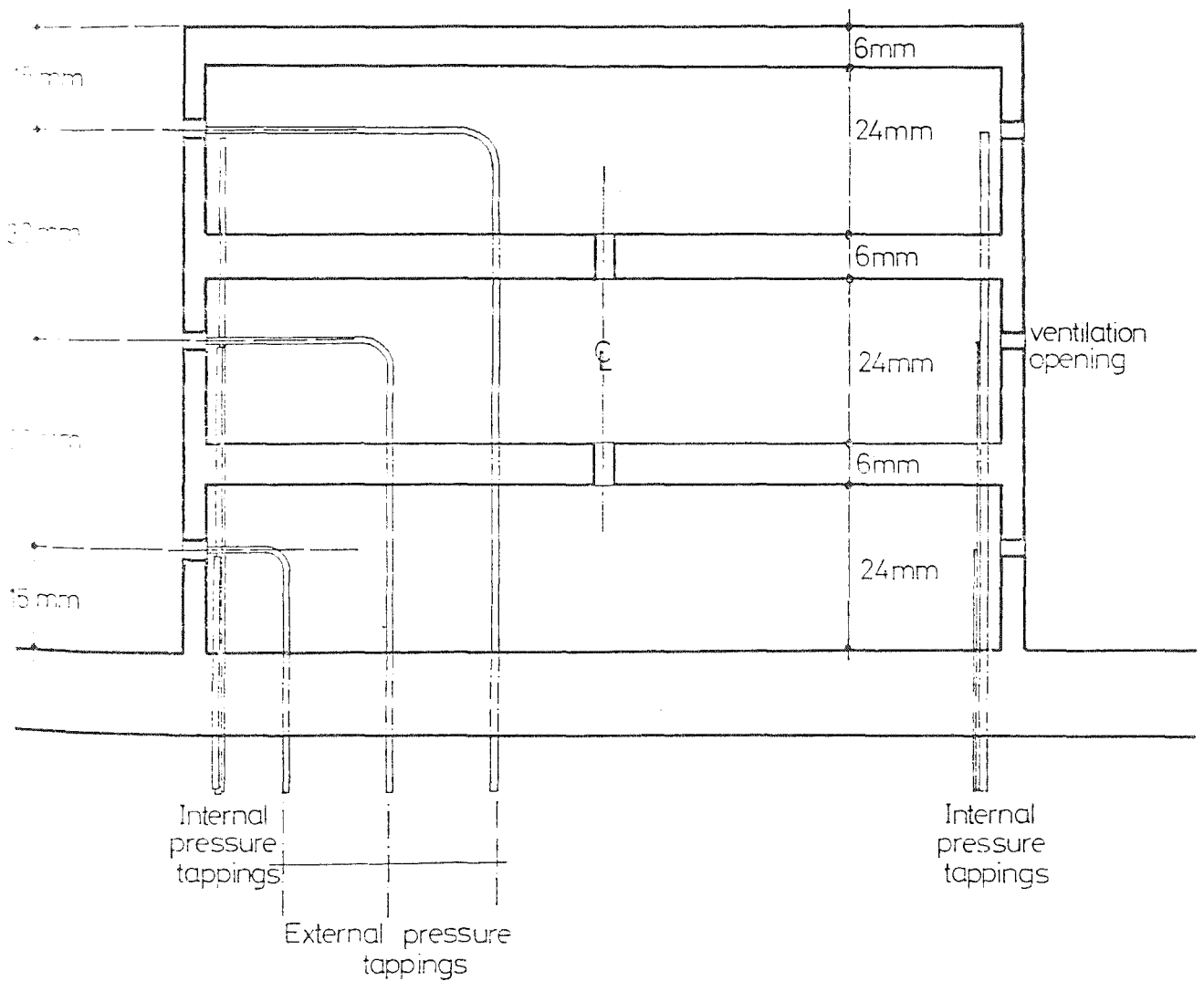
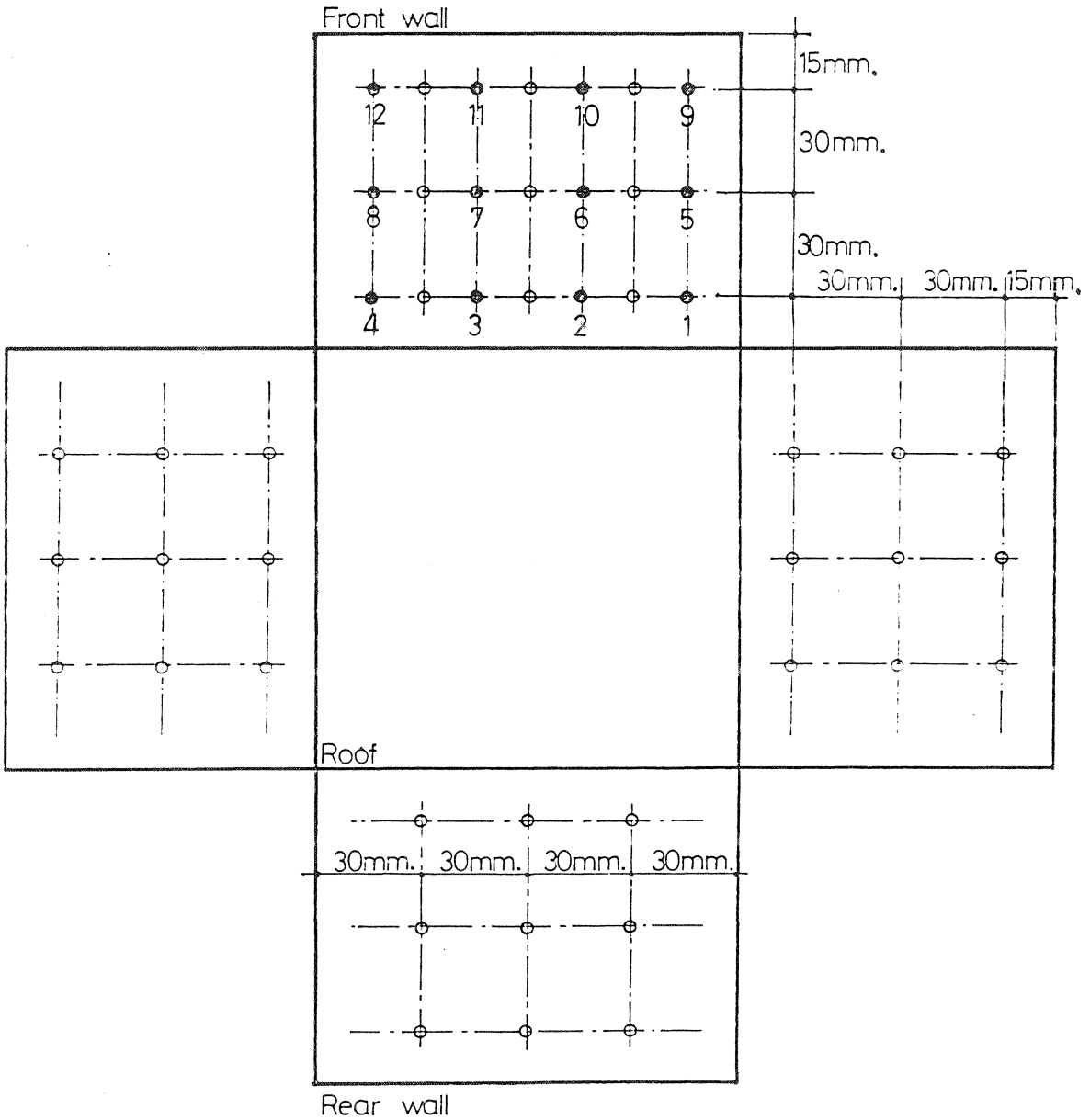


Figure. 7.3. Exploded view of internal pressure measurement model, showing external pressure measuring positions and ventilation opening grid.

- External pressure measuring position
- Ventilation opening grid position



(viewed from above)

Figure 7.4. Section through orifice plate model.

- a orifice plate
- b pressure tapping
- c flow spreader plate
- d model front plate
- e model back plate
- f guide pipeline

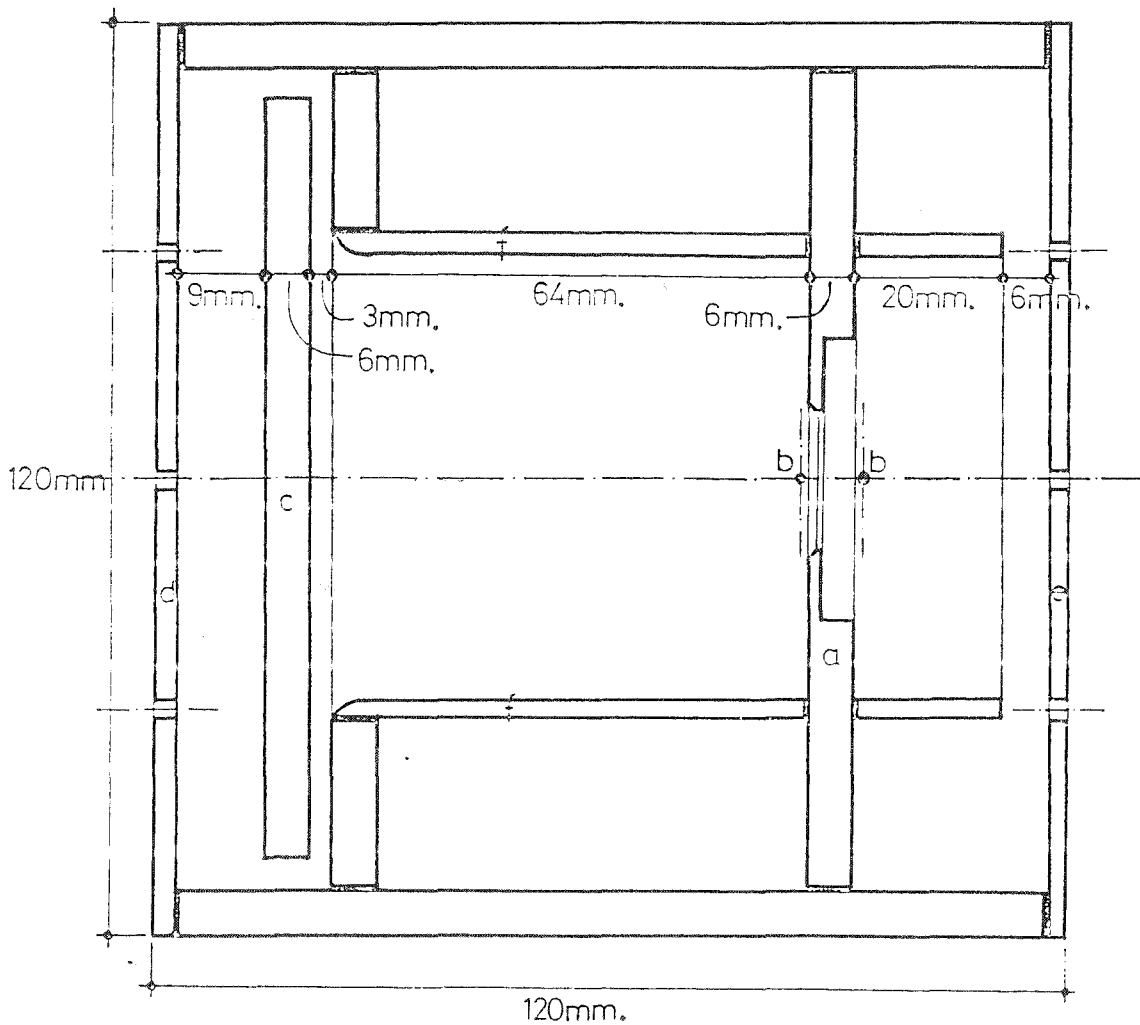


Figure 7.5.

Detail section through orifice plate.

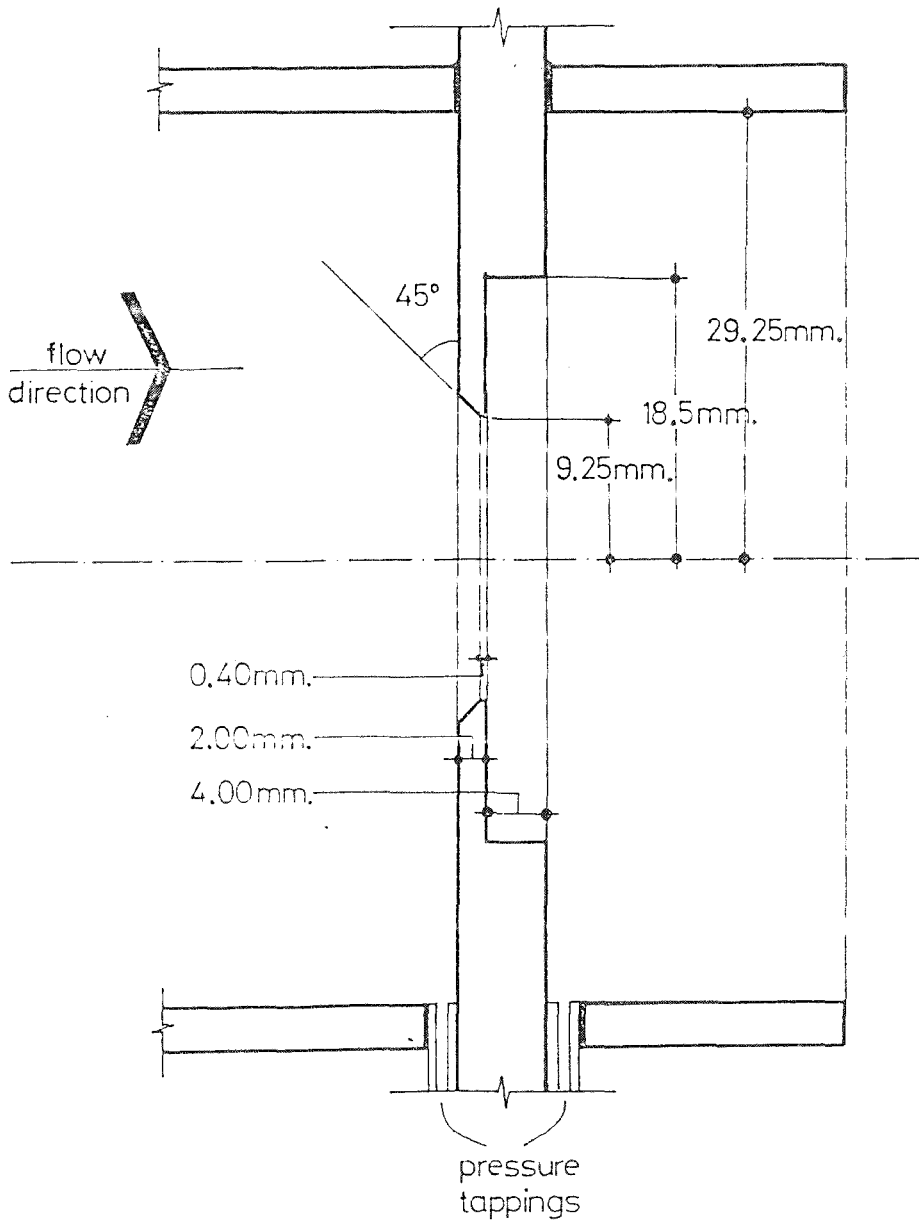
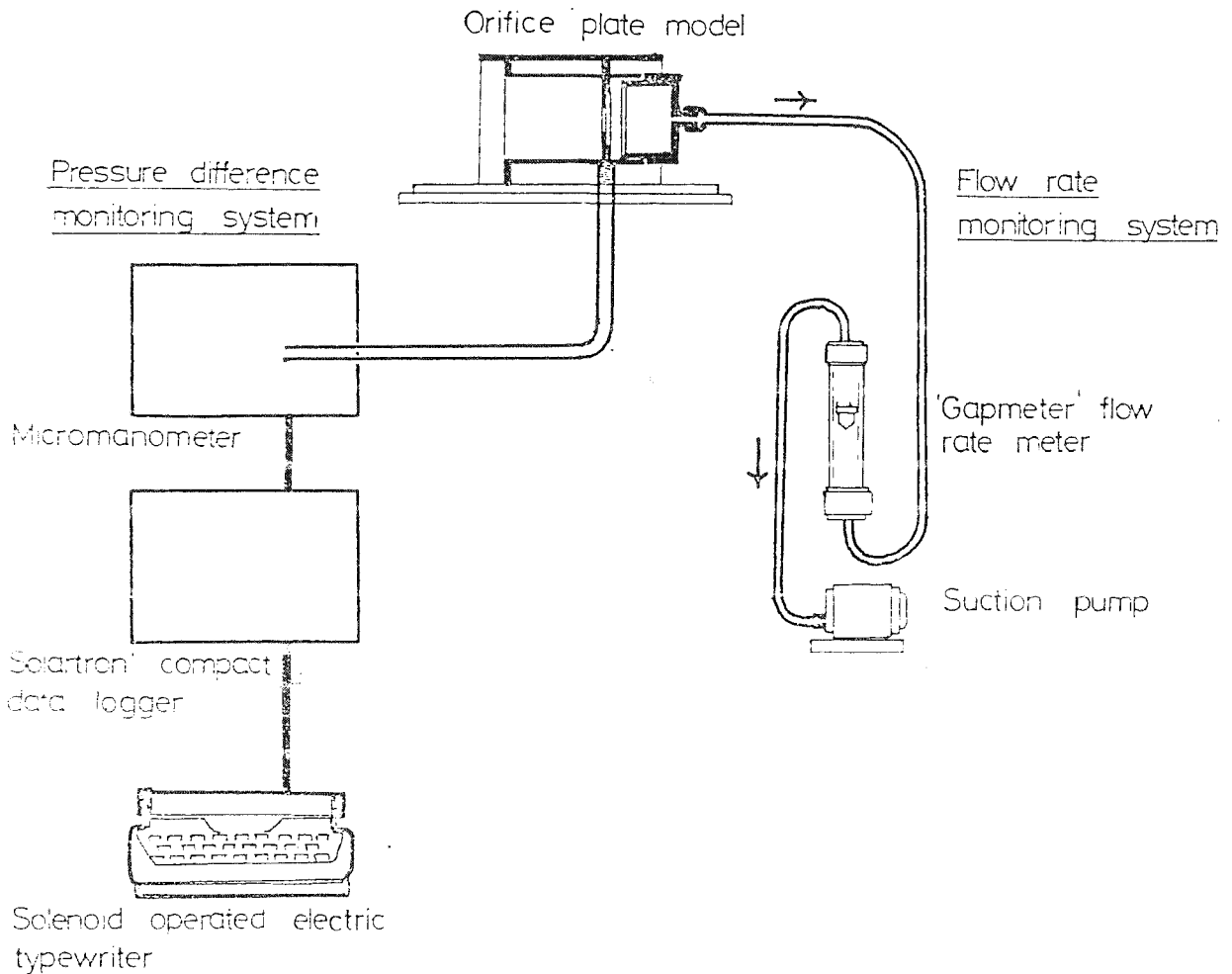
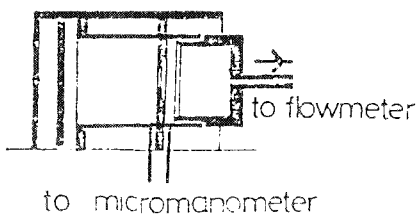


Figure 7.6. Schematic layout of orifice plate calibration equipment.



Arrangement for testing orifice plate with model front plate and spreader plate.



Arrangement for testing orifice plate with model back plate.

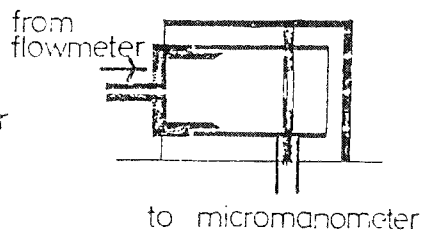


Figure 7.7. Calibration of standard orifice plate.

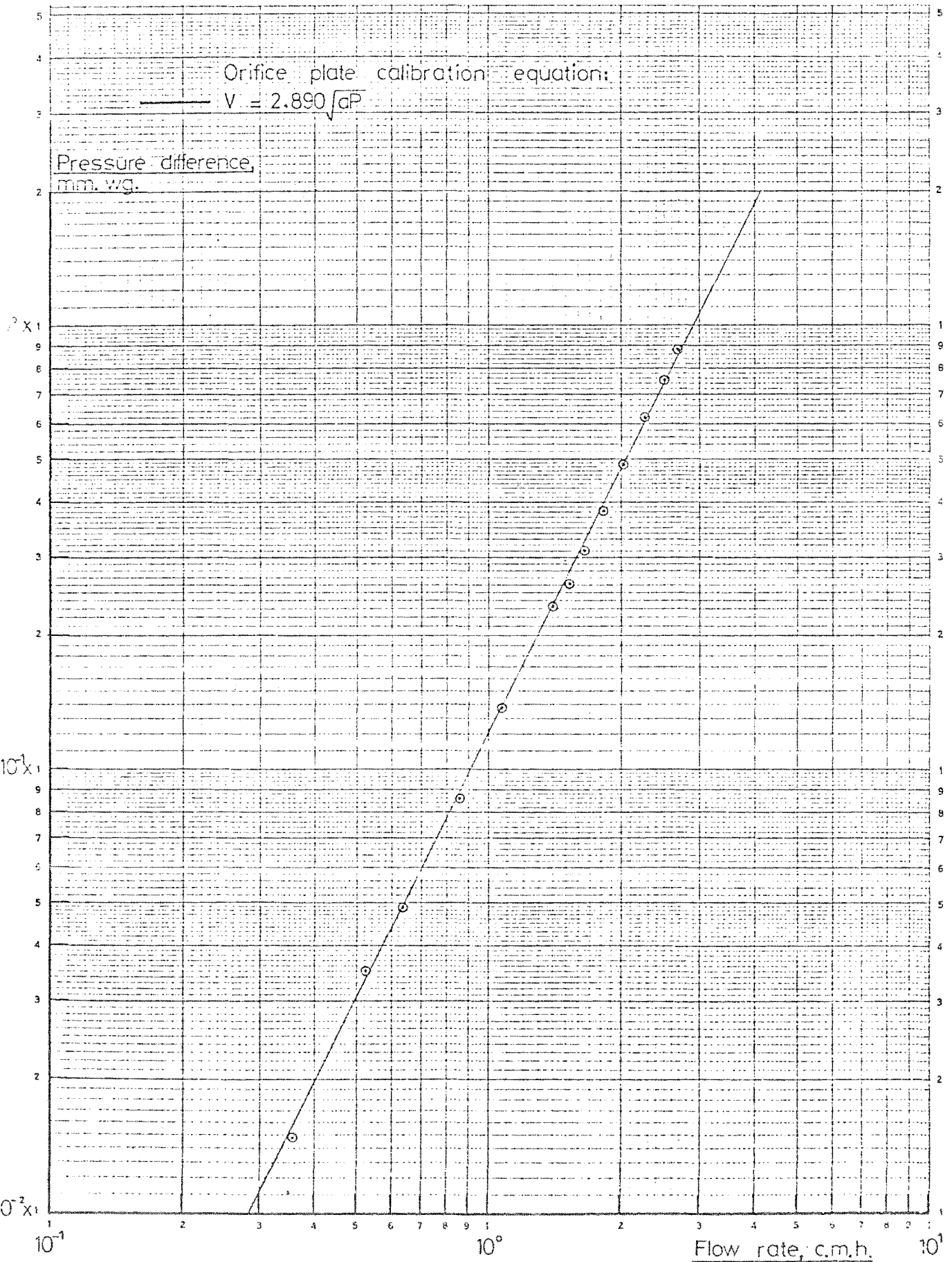


Figure 7.8.

Calibration of orifice plate model, showing the effect of the model front plate.

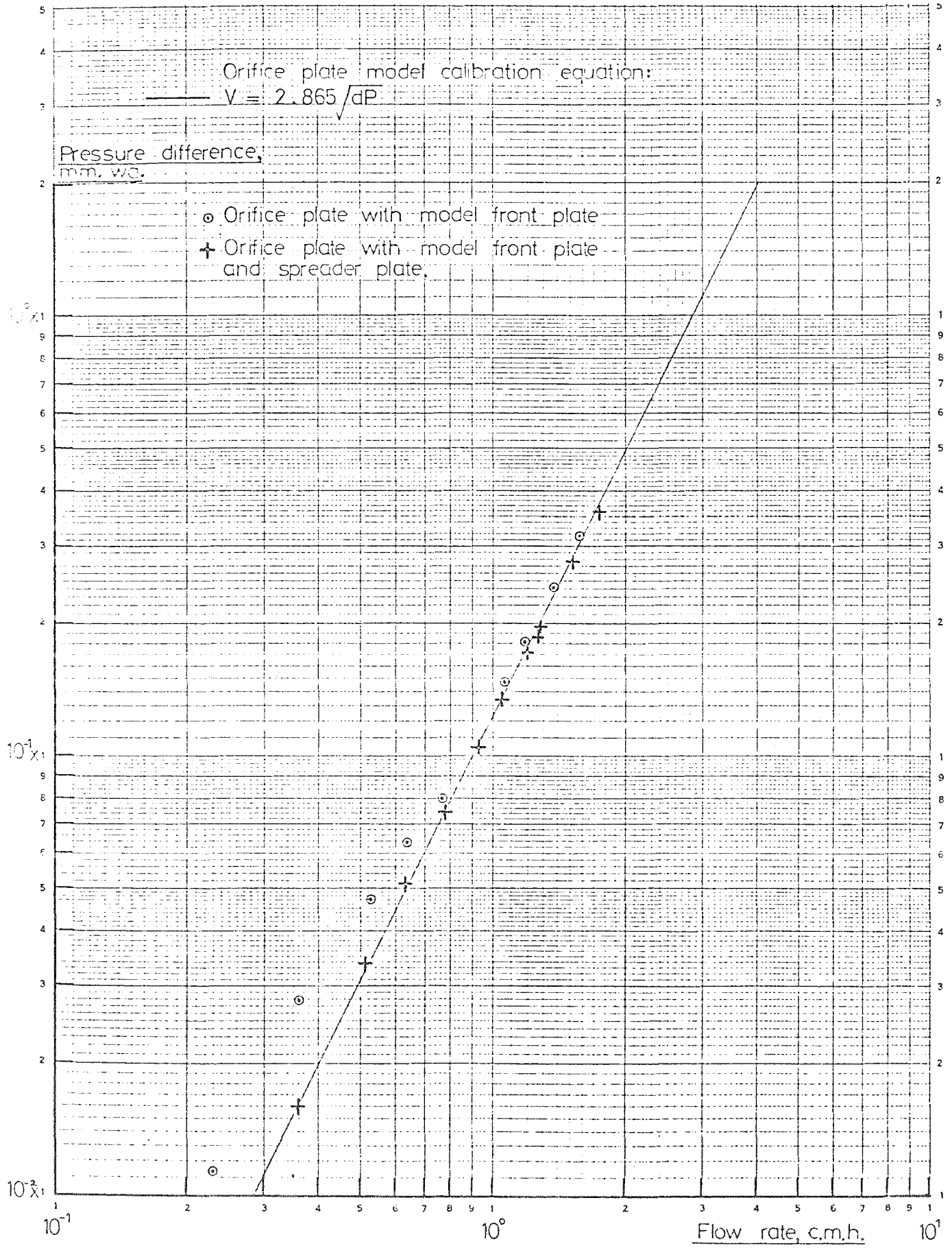


Figure 7.9. Calibration of orifice plate model, with model back plate in position.

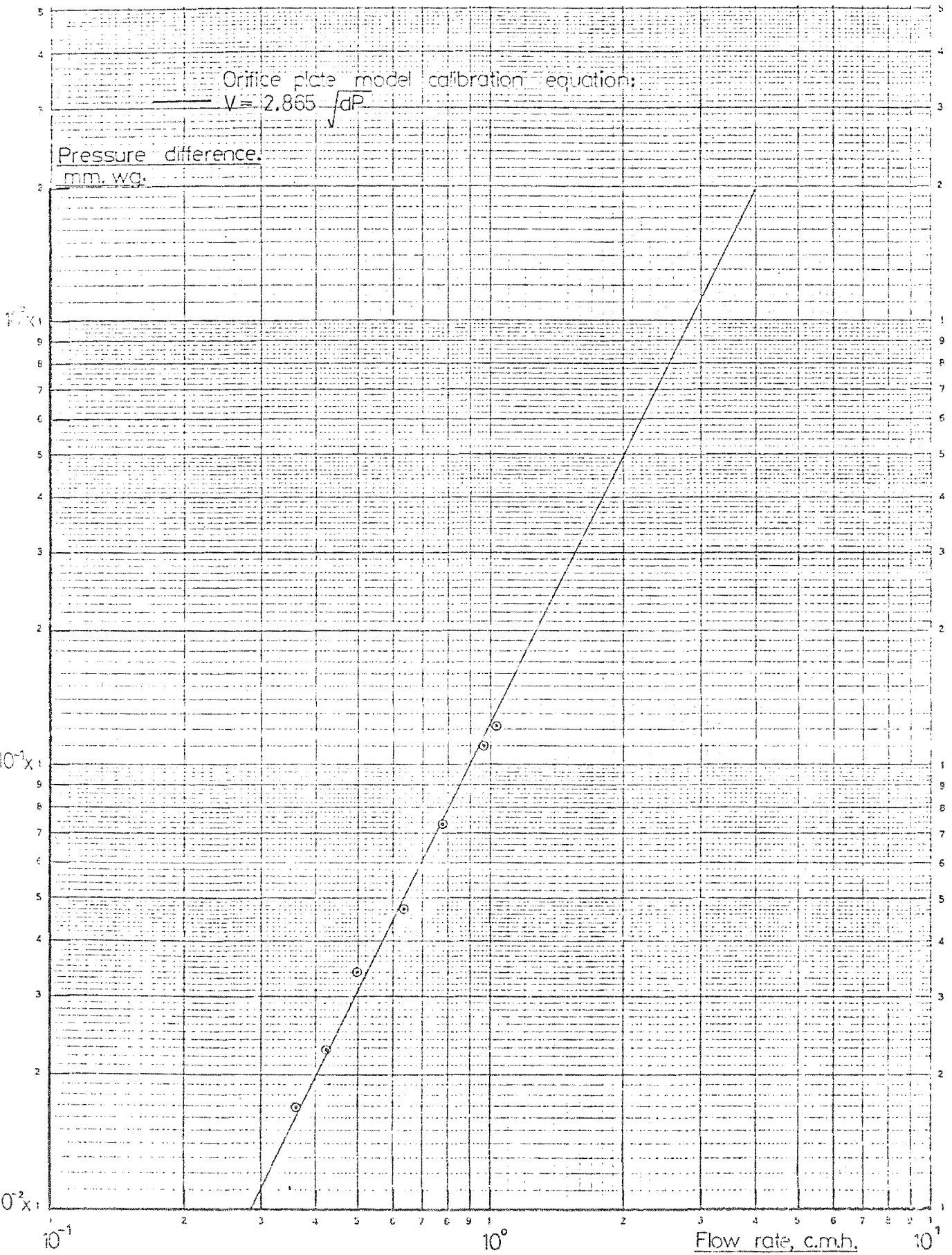


Figure 7.10. Orifice plate model mounted in the wind tunnel with the surface roughness in position.

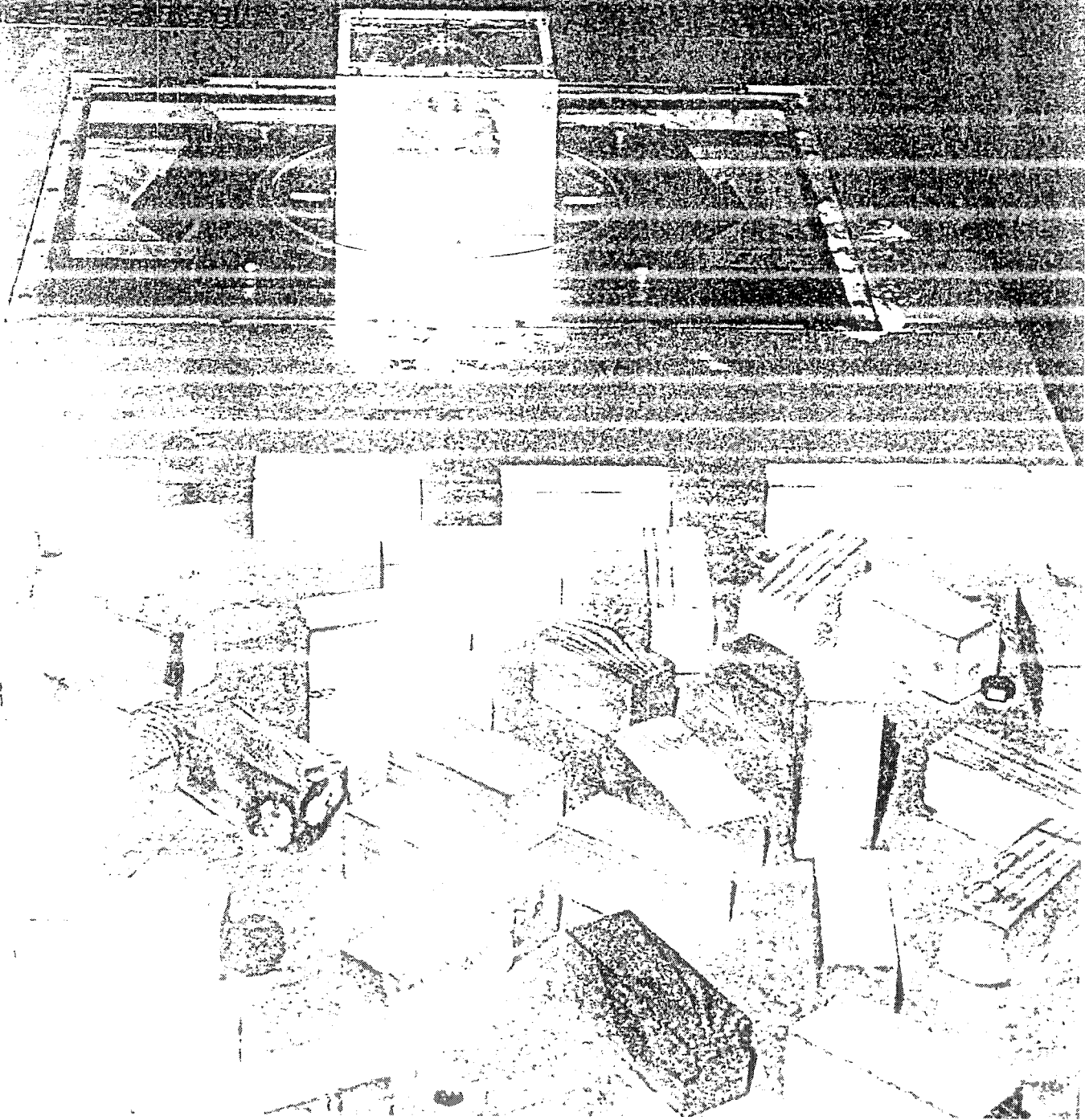


Figure 7.11.

Variation of velocity and turbulence intensity with height in model tests.

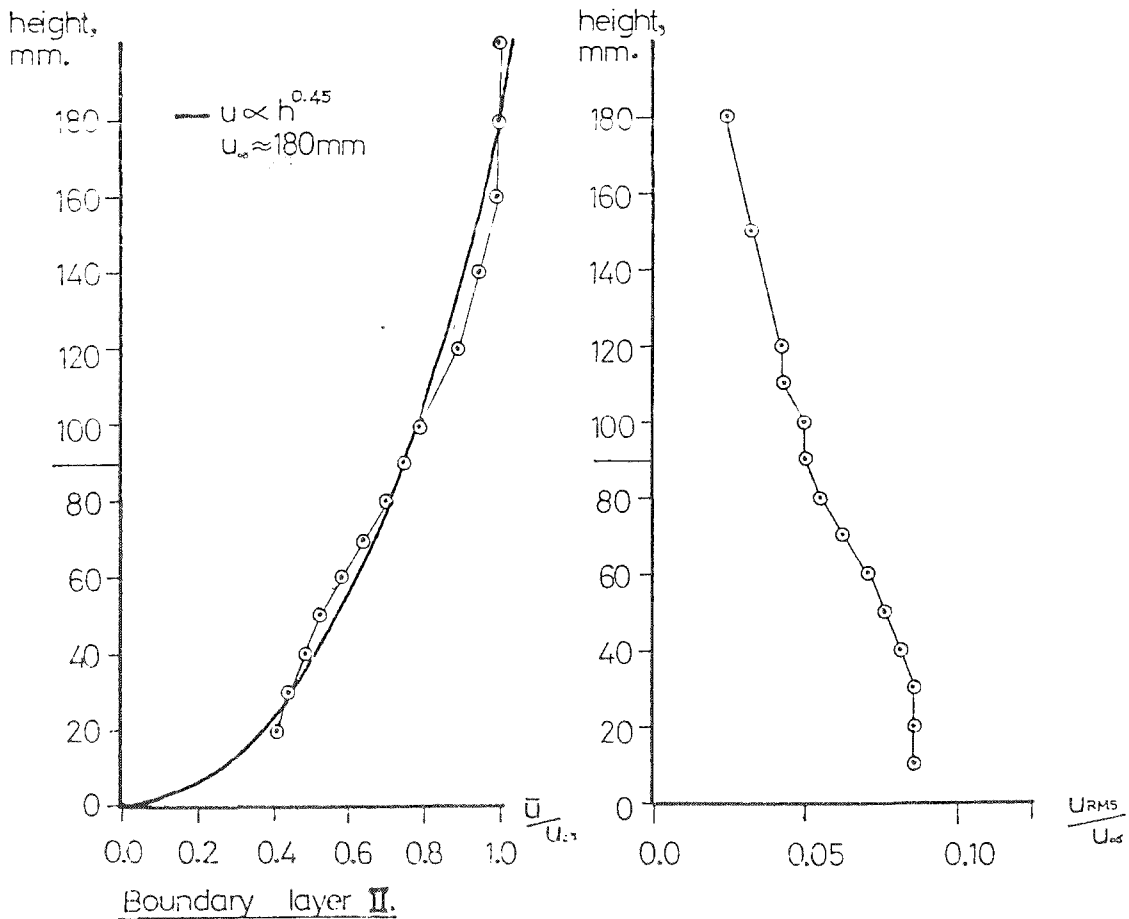
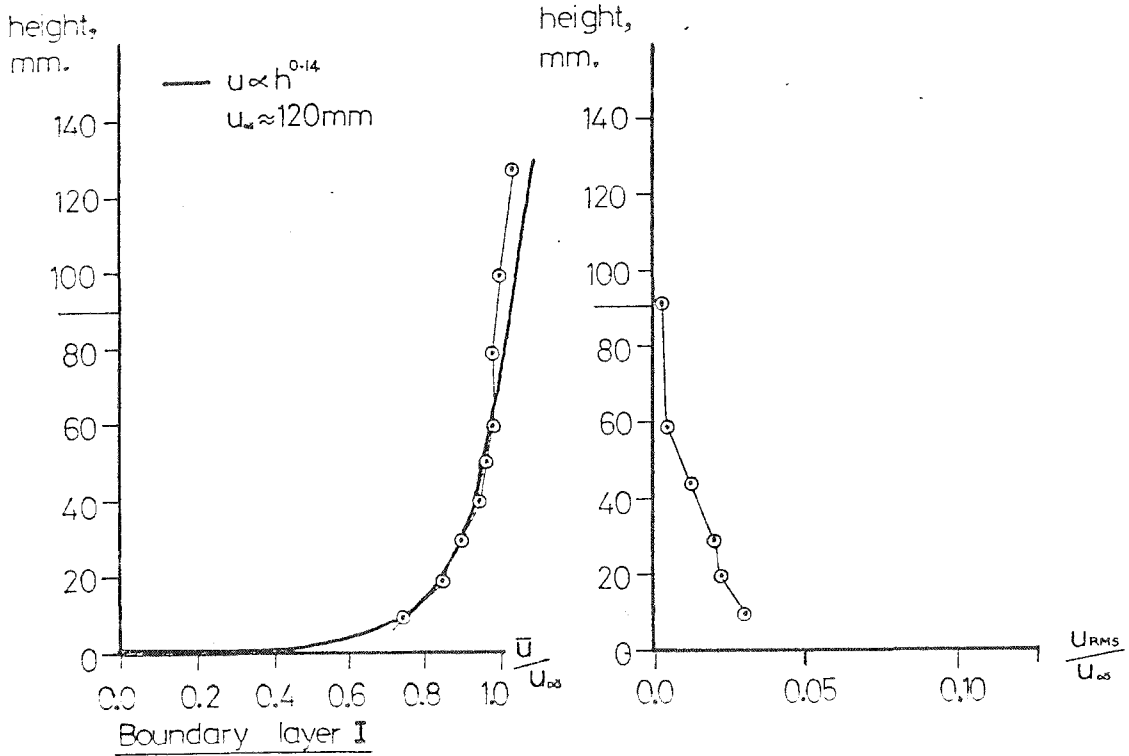
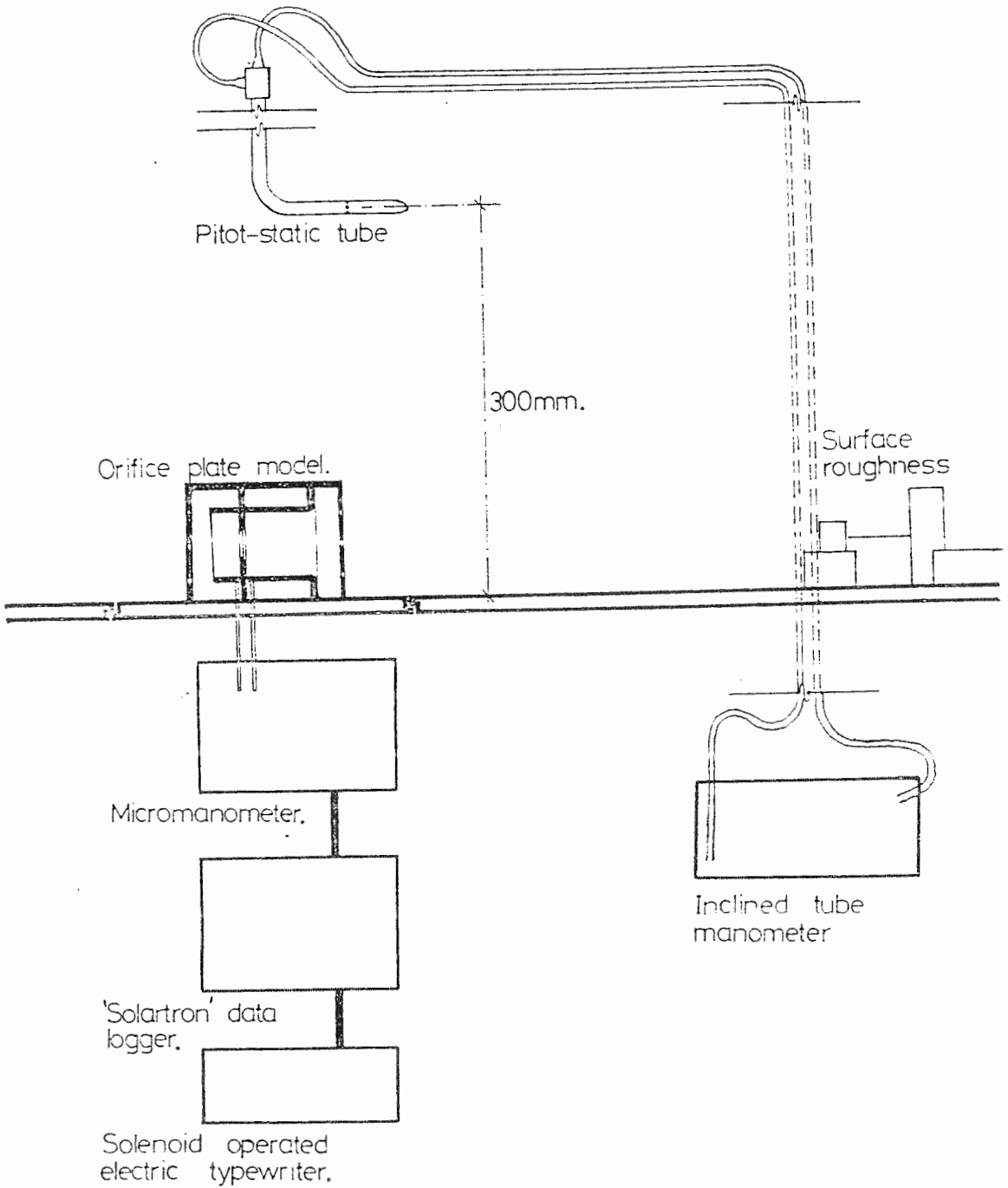


Figure 7.12.

Experimental apparatus used with the orifice plate model.



Figure 7.13. Schematic layout of model ventilation rate measurement apparatus.



8. MODEL VENTILATION STUDIES - RESULTS AND DISCUSSION

8.1 Introduction

8.1.1 Model ventilation studies were carried out to study the ventilation of an accurately defined set of models under closely controlled conditions, and to compare the results of the model studies with calculations using the digital analogue. The models, which have been described in the previous chapter, were used to measure either the internal pressures in the model, with respect to a reference pressure, or the mean air flow rate through the model. For each set of model observations the ventilation rate and internal pressures were calculated, using the observed external pressures, recorded in Appendix A4, in conjunction with the digital analogue described in Chapter 5.

8.1.2 In the initial experiments the internal pressure measurement model was used to investigate the effect of varying ventilation opening positions. Three opening distribution patterns were used: one with openings distributed uniformly over the four walls of the model, the second having a distribution pattern with two major faces (each having nine openings) and two secondary faces (each with three openings) and finally a model form with openings in two opposite faces only. More detailed studies were then made using the model with the simplest opening configuration, that is with openings in two opposite faces only. In this series of studies the air

velocity, number of openings per face, opening sizes and boundary layer flow characteristics were systematically altered, and the internal pressures measured. This second set of experiments was then repeated, using the orifice plate model, and ventilation rates measured. The results of the experiments were compared with the computed figures, from which an estimate of the accuracy of the analogue technique was made.

8.1.3 Experimental studies were also undertaken to investigate the effect of simplifications in the input data on the accuracy of calculated ventilation rates. Two forms of data simplification were considered in this part of the work:

- a) The use of mean external pressure coefficient values for each face of the building, instead of individual values for each opening. This was investigated by repeating the comparative calculations and considering the additional errors introduced.
- b) The effect on internal ventilation rates of small scale surface features of the model, which are neglected in tables listing standard pressure coefficient values. This was done by repeating one series of model measurements with a number of small surface features attached to the major faces of the model; the range of the resulting ventilation rates being taken as an indication of the inaccuracies inherent in

disregarding this aspect of design.

8.2 External pressure coefficient measurements

8.2.1 External pressure coefficient values, which were required in order to carry out the calculations for the comparative studies, were calculated from initial sets of measurements of the external pressures acting on the models in the two different boundary layers described previously (paragraph 7.6.2). These pressure coefficient values are recorded in Appendix A4. The variation of the mean pressure coefficient value, with angle of incidence of the airflow, for both boundary layers, is shown in Figure 8.1. The variation of the mean pressure coefficient with angle of incidence follows a similar pattern in both cases, although the values measured in boundary layer II are proportionally smaller than those measured in boundary layer I. This effect can be explained by the reduction in mean air velocity over the model's height, due to the different velocity profiles in the boundary layers. Similar results have been obtained by Baines in model tests carried out in different boundary layers (Baines, 1965).

8.2.2 The mean pressure coefficient values are in reasonably good agreement with accepted design values assumed for this shape of building, as shown in Table 8.1. In Table 8.1 the model values are compared with corresponding values taken from B.R.S. Digest 119 (B.R.S., 1970). The values measured in boundary layer I show very

good agreement with the design figures, whereas the shelter caused by the less steep velocity gradient of boundary layer II makes the values measured in that boundary layer lower than the design figures.

TABLE 8.1 Comparison of observed pressure coefficient values with design figures given in B.R.S. Digest 119 for the model form used.

Angle of incidence of airflow	B.R.S. Digest 119	Observed mean coefficient values	
		Boundary layer I	Boundary layer II
0°	0.7	0.76	0.52
90°	-0.6	-0.65	-0.34
180°	-0.25	-0.23	-0.14
270°	-0.6	-0.65	-0.38

8.2.3 The pressure coefficient values observed in both boundary layers at angles of incidence of θ° and $(360 - \theta)^\circ$ showed small systematic differences. These differences were interpreted as being caused by swirl in the working section resulting in the air flow over the model not being parallel to the tunnel centreline. Consequently the pressure coefficient values used in the comparative studies were calculated by averaging the appropriate values for each opening position at angles of incidence of θ° and $(360 - \theta)^\circ$. This correction, which was repeated when measuring ventilation rates and internal pressures in the models, compensated for the effects of the swirl.

8.2.4 The pressure coefficient values acting at the ventilation opening positions were estimated from the values measured at the pressure tapping locations. The openings were always located either in identical positions, on other model faces, to the pressure tappings or halfway between two pressure tapping positions and on the same level. In the first case assumed values were taken to be equal to the observed values, while in the second case the values were calculated by linear interpolation from the values measured at the two adjacent tapping positions.

8.3 Comparative model ventilation studies - experimental results

8.3.1 In the initial studies carried out the effect of opening positions on the internal pressures in a porous model was studied. Internal pressures were measured and calculated for the model using different patterns of ventilation openings. Three opening patterns were used, representing a uniformly glazed building, an intermediate type and a building glazed on two opposite faces only (Figure 6.2). The measurements were made in boundary layer I, using 2.5 mm. diameter openings to create the porosity.

8.3.2 The variation of observed and computed values of the internal pressures with angle of incidence of the airflow for the three configurations are shown in Figures 8.3, 8.4 and 8.5. The internal pressures were measured

separately at each level of the model, and are presented separately in the figures. The variation of internal pressures between floors of the model, in any set of conditions, was relatively small, being normally less than 0.05 of the dynamic head of the flow. The variation in computed and observed values on the separate levels could not be compared accurately as the relevant internal resistances in the model could not be simulated exactly in the programme, which assumed the presence of an internal stairwell. Consequently comparisons were made between the mean observed internal pressures and corresponding mean computed internal pressures.

8.3.3 Variations of mean internal pressure occurred with changes in distribution of the porosity in the three cases. In all three cases there were significant differences between the observed and computed mean internal pressures at certain angles of incidence. In the simplest case, opening configuration C (Figure 8.5), the observed pressure was significantly lower than the computed pressure at angles of incidence from 0° to 60° . The differences between the observed and computed values became much smaller at angles of incidence of 75° and 90° . These angles corresponded to those at which the mean pressure on the windward face of the model had become negative. The differences between the observed and computed pressures were interpreted as being due to changes in the operating efficiency of some or all of the openings on either the windward or leeward faces of

the model. At an angle of incidence of 75° the flow conditions adjacent to the windward porous face might be expected to have been significantly changed because of separation of the flow from that face. Consequently it was suggested that the discrepancies between the observed and computed pressures might have been caused by reductions in the efficiency of the openings in the windward face of the model; and that these reductions were relatively large at angles of incidence between 0° and 60° and were smaller when the upstream porous face of the model entered the separated flow region.

8.3.4 This hypothesis could be used to explain with reasonable accuracy the results obtained with the other opening configurations tested, (configurations A and B, Figure 8.2). For both remaining opening configurations a similarly large discrepancy would be expected at angles of incidence of 30° , 45° or 60° , where both the windward faces of the model are exposed to positive pressure. Smaller differences would be expected at angles of incidence of 0° , 15° , 75° or 90° , when one face only would be exposed to these conditions, as this single face would be relatively less influential in determining the internal pressure in the model. Furthermore the above hypothesis would suggest that the discrepancy between the observed and computed results would be greater when the more porous faces in configuration B (Figure 8.4) were facing the direction of flow (0° and 15°) than when the less porous faces of the same configuration faced the

main flow (75° and 90°). These trends were observed (Figures 8.3 and 8.4).

8.3.5 These discrepancies were sufficiently large to suggest that quite large differences between the actual and theoretical modes of operation of the model occurred. A series of more detailed studies were carried out in an attempt to determine the behaviour of the model more accurately. In these studies the model was used with the simplest opening configuration; with equal numbers of openings on two opposite faces of the model. The measurements of mean internal pressure in the model were repeated at different velocities for the same opening size and boundary layer conditions, and the results are presented in Figure 8.6. The observed mean internal pressures followed similar patterns to those presented in Figure 8.5 and no systematic differences were observed due to the change in air velocity. The effect of variation in porosity of the model faces on the mean internal pressures was also investigated by repeating the measurements with three and one opening(s) per face. The observed and computed results are shown in Figures 8.8 and 8.10. These results showed similar trends to the previously observed values at higher porosities, although the results could not be compared directly as both the computed and the observed internal pressures change at different porosities.

8.3.6 Comparative analyses of the results were

carried out by calculating and plotting for each set of results the ratio of mean pressure drop across the windward openings to mean pressure drop across the leeward openings. This expression may be used as an indication of the relative efficiency of operation of the openings in the windward and leeward faces of the model, as is noted below:

flow into model,

$$V_1 = m.C.e_w(C\bar{p}_w - C\bar{p}_i)^{1/n} .P_v \quad \dots\dots (8.1)$$

and flow out of model,

$$V_2 = m.C.e_l(C\bar{p}_i - C\bar{p}_l)^{1/n} .P_v \quad \dots\dots (8.2)$$

where V is the volume flow rate, $m^3/hr.$

m is the number of openings/model face

C is the calibrated opening flow coefficient,
 $m^3/hr/mm.wg.$

e_w is the mean efficiency of operation of the openings in the windward face

e_l is the mean efficiency of operation of the openings in the leeward face

$C\bar{p}_w$ is the mean external pressure coefficient acting outside the openings in the windward face of the model

$C\bar{p}_i$ is the mean model internal pressure coefficient

$C\bar{p}_l$ is the mean external pressure coefficient acting outside the openings in the

leeward face of the model

P_v is the dynamic head of the air flow at
the reference position, mm.wg.

and as the net flow into the model is zero:

$$\begin{aligned} & m.C.e_w.(C\bar{p}_w - C\bar{p}_i)^{1/n}.P_v \\ & = m.C.e_l.(C\bar{p}_i - C\bar{p}_l)^{1/n}.P_v \end{aligned}$$

$$\text{or } \frac{e_w}{e_l} = \left(\frac{C\bar{p}_i - C\bar{p}_l}{C\bar{p}_w - C\bar{p}_i} \right)^{1/n} \quad \dots\dots (8.3)$$

8.3.7 The results showing the effect of change in wind speed or porosity on the relative operating efficiencies of the openings, analysed by this method, are shown in Figure 8.18. The pressure difference ratios calculated from the observed internal pressures followed similar patterns for the five sets of results at angles of incidence between 0° and 60° , the mean value of the ratio being approximately 1.43 at 0° and reaching a maximum value of approximately 1.80 at 45° and 60° . The value of the pressure difference ratio for the computed results varied between 1.01 and 1.03 over this range of angles of incidence. At an angle of incidence of 75° the results showed a considerably wider degree of variation. The pressure difference ratios observed for the model with nine openings per face stayed at high values while the values observed in the models with reduced porosity decreased in value. This difference

was thought to have been caused because, at this angle of incidence, three of the nine openings in the windward face of the model with full porosity acted as air outlets, so that the number of inlets and outlets became unequal and consequently the pressure difference ratio was distorted. This pattern of behaviour was confirmed by flow visualisation. If allowance is made for this change in behaviour in the most porous model, the real relative orifice operating efficiency at this angle can be shown to increase significantly, as happened in the other cases.

8.3.8 The observations of the variation of mean internal pressure with angle of incidence were also repeated in boundary layer II, using the same opening configurations and sizes. The results of these studies are shown in Figures 8.7, 8.9 and 8.11. In these cases the variation of both computed and observed internal pressures with angle of incidence was much smaller due to sheltering effect of the velocity profile. The discrepancies between the observed results and the computed results followed similar patterns to those seen in the results obtained in boundary layer I. Comparative analyses were carried out in a similar manner and the variation of pressure difference ratio and relative opening operating efficiency with angle of incidence are presented in Figure 8.18. No systematic differences in pressure difference ratio could be identified due to variation in wind speed or model porosity. The results followed a similar pattern to those observed in boundary

layer I, the pressure difference ratio increasing in value from approximately 1.45 at 0° to a maximum of approximately 1.76 at 45° and reducing in value to about 1.38 at 75° .

8.3.9 The observations were finally repeated in both boundary layers and using the same opening configurations with a second model in which 1.0 mm. diameter openings were used to form the ventilating openings. The variation of observed and computed internal pressures with angle of incidence for these tests is shown in Figures 8.12 - 8.17, and the variation of the pressure difference ratios, calculated from these results, is presented in Figure 8.19. The observed and computed internal pressures showed similar discrepancies to those observed in earlier tests, although the magnitude of the differences was much less. This effect may be seen clearly in the values of the pressure difference ratios which ranged between 1.14 and 1.58 for the results measured in boundary layer I and 1.12 and 1.39 for the results measured in boundary layer II.

8.3.10 In the second part of the comparative studies the orifice plate model was used to measure ventilation rates under similar conditions to those which had been used in the previous studies. Measurements and comparative calculations were carried out using 9 or 15 2.5 mm. diameter openings per face and 36 or 60 1.0 mm. diameter openings per face on the opposite faces of the

model. Measurements were made in the two boundary layers used in the previous section of the study. The observed and computed ventilation rates are presented in Figures 8.20, 8.21, 8.22 and 8.23. For each set of conditions ventilation rates were measured at several wind speeds, and the observed rates corrected to a 20 m/s. wind speed. The mean observed ventilation rate, corrected to 20 m/s. wind speed was calculated and compared to the computed rate. These results are summarised in Tables 8.2 and 8.3.

8.3.11 The observed ventilation rates measured in boundary layer I, using the model with 2.5 mm. diameter openings to produce the ventilation, showed significant differences from the corresponding computed ventilation rates. At all angles of incidence the observed ventilation rates were lower than the computed rates. The observed ventilation rates, measured at different wind speeds, represented a constant ratio of the corresponding computed ventilation rates. The mean observed ventilation rates, corrected to a 20 m/s. wind speed, at an angle of incidence of 0° were 2.66 and 1.60 $\text{m}^3/\text{hr.}$ for 15 and 9 openings per face respectively. These corresponded to computed ventilation rates of 2.86 and 1.70 $\text{m}^3/\text{hr.}$, and represented 94% and 93% of the computed rates. The observed ventilation rates showed increasing differences from the computed ventilation rates as the angle of incidence increased, reaching a maximum value at 60° , where the observed rates represented approximately

TABLE 8.2 Computed and mean observed ventilation rates
for a 20 m/s. wind speed, 2.5 mm. diameter
openings.

Boundary layer I

Angle of Incidence	Computed Ventilation Rate, m ³ /hr.	Observed Ventilation Rate, m ³ /hr.	Standard Deviation of Observed Rates, m ³ /hr.
15 openings/face			
0°	2.86	2.66	0.04
15°	2.92	2.66	0.05
30°	2.78	2.38	0.06
45°	2.61	2.15	0.09
60°	2.31	1.88	0.04
75°	1.51	1.38	0.03
9 openings/face			
0°	1.70	1.60	0.02
15°	1.74	1.62	0.02
30°	1.66	1.50	0.02
45°	1.56	1.37	0.05
60°	1.38	1.19	0.02
75°	0.80	0.70	0.07

Boundary layer II

Angle of Incidence	Computed Ventilation Rate, m ³ /hr.	Observed Ventilation Rate, m ³ /hr.	Standard Deviation of Observed Rates, m ³ /hr.
15 openings/face			
0°	2.31	1.98	0.03
15°	2.31	1.96	0.05
30°	2.23	1.77	0.08
45°	2.19	1.63	0.09
60°	2.14	1.55	0.05
9 openings/face			
0°	1.37	1.19	0.03
15°	1.37	1.17	0.03
30°	1.33	1.08	0.06
45°	1.31	0.97	0.07
60°	1.28	0.94	0.03

TABLE 8.3 Computed and mean observed ventilation rates
for a 20 m/s. wind speed, 1.0 mm. diameter
openings.

Boundary layer I

Angle of Incidence	Computed Ventilation Rate, m ³ /hr.	Observed Ventilation Rate, m ³ /hr.	Standard Deviation of Observed Rates, m ³ /hr.
60 openings/face			
0°	1.68	1.64	0.03
15°	1.68	1.65	0.02
30°	1.59	1.58	0.06
45°	1.48	1.45	0.06
60°	1.29	1.26	0.05
36 openings/face			
0°	0.98	0.96	0.03
15°	1.00	0.99	0.04
30°	0.95	0.94	0.02
45°	0.88	0.85	0.04
60°	0.77	0.75	0.02

Boundary layer II

Angle of Incidence	Computed Ventilation Rate, m ³ /hr.	Observed Ventilation Rate, m ³ /hr.	Standard Deviation of Observed Rates, m ³ /hr.
60 openings/face			
0°	1.29	1.23	0.04
15°	1.29	1.23	0.03
30°	1.24	1.13	0.04
45°	1.22	1.09	0.06
60°	1.18	1.05	0.04
36 openings/face			
0°	0.76	0.70	0.03
15°	0.77	0.68	0.04
30°	0.74	0.63	0.04
45°	0.72	0.63	0.06
60°	0.70	0.59	0.03

84% of the computed rates. The discrepancy decreased at an angle of incidence of 75° , where the observed rate represented about 89% of the computed rate. Mean observed ventilation rates, expressed as proportions of the computed flow rates, are summarised for all sets of model conditions in Figures 8.24 and 8.25.

8.3.12 The observed ventilation rates measured in boundary layer II, using the model with 2.5 mm. diameter openings, show similar behaviour to those measured in boundary layer I. The observed ventilation rates were again lower in all cases than the corresponding computed rates. The discrepancies were in all cases relatively larger than those measured in boundary layer I, but followed a similar pattern with variation of the angle of incidence. The mean observed ventilation rate at 0° angle of incidence was equivalent to 86% of the computed rate, and the discrepancy increased to a maximum value at an angle of incidence of 60° , where the observed rate represented 74% of the computed rate. No measurements were taken at 75° because of very large variations in the pressure difference readings across the orifice plate which suggested that the results could be unreliable.

8.3.13 The observations were also repeated in the two boundary layers using 1.0 mm. diameter openings. The observed ventilation rates in both sets of conditions were lower than the computed rates, but the discrepancies

between the respective values were in these cases considerably smaller. The observed ventilation rates measured in boundary layer I showed little variation with angle of incidence, being equivalent to 98% of the computed rate at 0° and 97% of the computed rate at 45° , the largest observed discrepancy. The results of the measurements taken in boundary layer II showed a greater variation with angle of incidence, although the variations were not as great as those measured with the 2.5 mm. diameter ventilation openings. In this case the observed ventilation rate at 0° was equivalent to approximately 93% of the computed ventilation rate and that measured at 60° was approximately equivalent to 88% of the computed ventilation rate.

8.3.14 The mean observed ventilation rates are presented non-dimensionally in Figure 8.26 in an attempt to reduce the data obtained. The largest variation in ventilation rate was due to the change in boundary layer flow. Ventilation rates measured in boundary layer II varied between 70% and 81% of the corresponding measurements made in boundary layer I. The ventilation rates measured in the models with 2.5 mm. openings were in all cases lower than those measured with 1.0 mm. openings. The ventilation rates measured using the larger openings varied between 88% and 94% of the corresponding rates measured through the smaller ones. Small variations in ventilation rate were noted with changes in porosity, however the magnitudes of these differences were within

the limits of the experimental accuracy. The results presented in Figure 8.26 suggests that for a better reduction of results, other non-dimensional parameters need to be included. A consideration of additional parameters is made in the following section.

8.4 Discussion of results of the comparative study

8.4.1 Both the ventilation rates and the internal pressures measured in the model tests showed significant differences from the computed results. The measured internal pressures were in most cases lower than the computed values, indicating that a larger proportion of the total pressure difference acting across the model acted across the windward wall of the model than acted across the leeward face of the model. The measured ventilation rates were lower than the corresponding computed ventilation rates. The results from the two sets of observations appeared to be related to each other, as the magnitudes of both discrepancies followed similar patterns with variation of angle of incidence of the airflow and ventilation opening size.

8.4.2 In order to assess the significance of the results it is necessary to consider the errors involved in obtaining them. The observed mean internal pressures were subject to errors due to fluctuations in the readings on the manometer scale, which was read by eye. However for each set of conditions the recorded pressure represented an average of twelve observed pressures.

It is estimated that the recorded pressure could be measured to an accuracy of the order of ± 0.25 mm.wg. This order of accuracy of measurement would result in pressure coefficients being accurate to between ± 0.01 and ± 0.015 , which would result in the pressure difference ratios being accurate to between ± 0.10 and ± 0.15 . Errors could also be caused by leakage; any leakage might be expected to be shown up as variation in internal pressure with changes in porosity or orientation of the model. No significant variation was observed with changes in these parameters. Ventilation rates were measured, according to the calibration to an accuracy of $\pm 5\%$. Errors could also be caused by extra leakage through the model. Any errors of this type would again be expected to be shown up by variation of the non-dimensional ventilation rate with change in porosity as the effective porosity would not increase at the same rate as the nominal porosity. No trends of this type were apparent in the results. The discrepancies between the observed and computed values in both cases were systematically larger than these accuracy limits, and consequently could not be attributed to experimental error.

8.4.3 By combining the data describing the pressure difference distributions on the windward and leeward model faces and the model ventilation rates, estimates of the operating efficiencies of the openings in these faces of the model were made. These estimated values are presented

in Table 8.4. The analysis suggested that the openings in the leeward face of the model operated near to their calibrated efficiencies in all the model tests, whereas the openings in the windward face operated at significantly lower efficiencies than the calibrated values. Three possible causes were considered in attempting to explain this behaviour:

- a) Variation of external pressure distributions over the model faces due to the presence of pressure "sinks" adjacent to the openings.
- b) Reductions in orifice efficiency due to fluctuations in the pressures acting across the openings.
- c) Reductions in orifice efficiency caused by lateral flow over the model surfaces.

8.4.4 The presence of pressure "sinks" adjacent to openings acting as air inlets has been described by Lawson (Lawson, 1968). The effect of air inlets in a plane surface is to cause variation in pressure over the surface, pressures becoming locally much lower than the mean pressure at very small distances from the openings. Due to this effect the pressure differences acting across openings will normally be lower than would be indicated from the mean pressure measured over the surface. This phenomenon was not considered to be a significant source of error, because the openings used were calibrated with reference to pressure differences measured at relatively large distances from the openings, and this procedure

was repeated in the model measurements.

TABLE 8.4 Mean estimated operating efficiencies of windward and leeward face openings, from pressure difference ratios and ventilation rates measured in model tests.

Angle of incidence	Orifice efficiency as a proportion of calibrated value				
	0°	15°	30°	45°	60°
2.5 mm. diameter openings, boundary layer I					
windward face	0.86	0.84	0.82	0.74	0.73
leeward face	1.04	1.02	1.01	1.02	1.01
2.5 mm. diameter openings, boundary layer II					
windward face	0.79	0.78	0.73	0.65	0.66
leeward face	0.96	0.95	0.93	0.88	0.87
1.0 mm. diameter openings, boundary layer I					
windward face	0.92	0.92	0.92	0.87	0.88
leeward face	1.06	1.06	1.07	1.08	1.09
1.0 mm. diameter openings, boundary layer II					
windward face	0.86	0.82	0.80	0.81	0.81
leeward face	0.99	0.96	0.95	0.94	0.94

8.4.5 The effect of fluctuations in mean pressure difference on the efficiency of operation of openings is difficult to assess accurately and is normally ignored when calculating natural ventilation, as external pressures are assumed to be static. Significant pressure fluctuations did occur in the model studies, due to variations in the speed and direction of the airflow and

to eddy shedding from the model. In order to establish the significance of these fluctuations a simple analysis was carried out. Assuming that sinusoidal variations in pressure took place across the openings, integrated flow rates through the openings were computed. No allowances were made for inertial effects, the frequency distribution, or waveform of the pressure fluctuations, and consequently this analysis could only be considered as a very crude estimate of the order of magnitude of these effects. The results of the analyses, presented in Figure 8.27, suggested that the opening efficiencies reduced considerably as the pressure fluctuations increased in value. Measurements of the R.M.S. pressures acting on the model were also made, using a "Scanivalve" pressure transducer. Values of the R.M.S. pressures measured are shown in Figure 8.28. From these measurements estimates of the reduction in operating efficiency of the openings due to this effect were made, and these, together with the other corrections made, are summarised in Table 6.7.

8.4.6 The reductions in efficiency of both the 1.0 mm. and the 2.5 mm. diameter openings due to the pressure fluctuations measured in boundary layer I were estimated to be very small. At most angles of incidence it was estimated that the efficiency of the openings would have been between 0.98 and 1.00 of their calibrated efficiencies. The largest reductions in efficiency would have been at angles of incidence between 75° and 105° , and at these angles the openings would have been operating

at efficiencies of approximately 0.95 of the calibrated value. The reductions in efficiency due to the pressure fluctuations measured in boundary layer II were larger. The estimated operating efficiencies of the openings in the windward face varied between 0.91 at 0° and 0.96 at 60° . Smaller reductions in efficiency were calculated for the openings in the leeward face; estimated values being between 0.98 and 1.00 of the calibrated value. Thus it seems unlikely that the pressure fluctuations are the main cause of the discrepancies between the observed and computed results.

8.4.7 The third possible explanation of the experimental results which was considered was the alteration of the opening performance due to air streams flowing laterally across the openings. The effect of lateral air movement on the performance of the openings used in the model tests was determined experimentally by repeating the calibration measurements for the openings with an air stream, of known velocity, flowing past the calibration plate. The calibration apparatus (Appendix A3) was set up at the open end of a small air duct, with the test plate aligned with one wall of the duct. The flow velocity was measured using a pitot-tube mounted adjacent to the openings and at a distance of 3 mm. from the plate. Calibration measurements were made with no lateral flow and then in several flows of different velocity. The results are presented in Tables 8.5 and 8.6. The efficiencies of operation of the openings, when

TABLE 8.5 Calibration measurements for 2.5 mm. diameter openings with different external lateral flow velocities.

Lateral flow velocity, m/s.	Dynamic head, Pv, mm.wg.	Pressure difference dP, mm.wg.	dP/Pv	Effective orifice efficiency (dP _o /dP) ^{0.53}
Volumetric flow rate, 0.210 m ³ /hr.				
0.0	0.0	15.2	∞	1.00
8.0	4.0	19.9	5.0	0.87
12.7	9.9	21.7	2.2	0.83
17.2	18.0	23.5	1.3	0.80
Volumetric flow rate, 0.175 m ³ /hr.				
0.0	0.0	10.2	∞	1.00
8.0	4.0	13.9	3.5	0.85
12.7	9.9	15.4	1.5	0.81
17.2	18.0	17.1	1.0	0.76
Volumetric flow rate, 0.136 m ³ /hr.				
0.0	0.0	6.0	∞	1.00
8.0	4.0	8.6	2.2	0.83
12.7	9.9	9.8	1.0	0.77
17.2	18.0	11.0	0.6	0.73
Volumetric flow rate, 0.100 m ³ /hr.				
0.0	0.0	3.1	∞	1.00
8.0	4.0	4.5	1.1	0.81
12.7	9.9	5.5	0.6	0.74
17.2	18.0	6.5	0.4	0.68

TABLE 8.6 Calibration measurements for 1.0 mm. diameter openings with different external lateral flow velocities.

Lateral flow velocity, m/s.	Dynamic head, Pv, mm.wg.	Pressure difference dP, mm.wg.	dP/Pv	Effective orifice efficiency $(dP_o/dP)^{0.60}$
Volumetric flow rate, 0.028 m ³ /hr.				
0.0	0.0	12.6	∞	1.00
4.0	1.0	12.85	12.8	0.99
7.2	3.2	12.8	4.0	0.99
11.9	8.6	13.4	1.6	0.97
16.0	15.5	13.5	0.9	0.96
Volumetric flow rate, 0.023 m ³ /hr.				
0.0	0.0	9.15	∞	1.00
4.0	1.0	9.25	9.4	0.99
7.2	3.2	9.5	2.9	0.98
11.9	8.6	9.8	1.1	0.96
16.0	15.5	10.1	0.7	0.94
Volumetric flow rate, 0.017 m ³ /hr.				
0.0	0.0	5.3	∞	1.00
4.0	1.0	5.4	5.5	0.99
7.2	3.2	5.5	1.7	0.98
11.9	8.6	5.8	0.7	0.95
16.0	15.5	6.1	0.4	0.91
Volumetric flow rate, 0.011 m ³ /hr.				
0.0	0.0	2.5	∞	1.00
4.0	1.0	2.6	2.6	0.98
7.2	3.2	2.6	0.8	0.98
11.9	8.6	2.9	0.4	0.91
16.0	15.5	3.2	0.2	0.86

acting as air inlets, were significantly lower than the calibrated values, and decreased as the lateral flow velocity increased. It was found that the efficiency could be related to the ratio of the pressure difference acting across the opening to the dynamic head of the lateral flow, as shown in Figure 8.29. The measurements were repeated with the openings acting as outlets. Under these conditions the efficiencies did not appear to be significantly affected by the lateral flow.

8.4.8 Estimates of the influence of this effect on the observed results were made by measuring the lateral flow velocities around the model and calculating the reduction in efficiency of the openings in the windward model faces. Measurements of the air velocities were made using a hot wire anemometer with the probe mounted adjacent to one face of the model. The anemometer probe was mounted in three positions, at equal intervals along the face, at a height of 45 mm., and a distance of 3 mm. from the model surface. At each angle of incidence a mean velocity was found, and the results presented as proportions of the free stream roof height air velocities (Figure 8.30). The velocities found, although not necessarily accurately representative of the flow conditions over the whole face, gave approximate values of the lateral flow velocities. The reductions in estimated efficiency due to this cause followed much more closely the pattern seen in the observed results. The 2.5 mm. diameter openings were affected to a much greater

extent than the 1.0 mm. diameter openings. It is thought that this effect occurred because the air supply for the 1 mm. holes is drawn from the air much nearer to the model surface, where the flow rate is lower due to a boundary layer effect caused by the model surface. The reductions were also larger for the observations made in boundary layer II, due to the higher lateral flow velocities relative to the pressure differences acting across the model. The size of the correction also increased as the angle of incidence increased, the maximum value being, for both boundary layers, at an angle of 60° . The correction was lower at the angle of 75° due to the reduction in flow velocity across the surface. Consequently it can be seen that the values of the corrections estimated for this effect agree reasonably well with the discrepancies between the observed and computed results. It is likely that these flow conditions are the major factor causing the discrepancies.

8.4.9 Corrections were made to allow for the combined effects of the lateral flow and pressure fluctuations on the efficiency of operation of the model openings, and using these values approximate estimates of corrected ventilation rates and internal pressures were made. These are presented in Table 8.7. The corrected ventilation rates agreed well with the observed values, the average error between corresponding values for all sets of results being approximately 3%. The corrections to the ventilation rates calculated for the 1.0 mm. diameter

TABLE 8.7 Summarised corrected ventilation rates and pressure difference ratios allowing for the effects of pressure fluctuations and lateral flows over the model surfaces.

Corrected ventilation rates

Boundary layer I	0°	15°	30°	45°	60°	75°
1.0 mm. diameter openings	0.99	0.99	0.98	0.97	0.95	0.96
2.5 mm. diameter openings	0.94	0.94	0.91	0.86	0.82	0.86
Boundary layer II						
1.0 mm. diameter openings	0.93	0.93	0.94	0.93	0.93	
2.5 mm. diameter openings	0.86	0.85	0.84	0.80	0.80	

Corrected pressure difference ratios

Boundary layer I						
1.0 mm. diameter openings	1.02	1.02	1.05	1.10	1.18	1.07
2.5 mm. diameter openings	1.25	1.25	1.42	1.68	1.96	1.53
Boundary layer II						
1.0 mm. diameter openings	1.20	1.18	1.20	1.18	1.18	
2.5 mm. diameter openings	1.58	1.54	1.72	1.88	1.92	

openings in boundary layer I were the smallest in value; the mean ventilation rate being 0.97 for angles of incidence between 0° and 60°, while the observed value was 0.98. The largest corrections were calculated for

the 2.5 mm. diameter openings in boundary layer II; the mean value of corrected ventilation rate being 0.83 of the computed ventilation rate, while the observed value was 0.81. The pressure difference ratios showed less good agreement. Values calculated for the 2.5 mm. openings agreed quite well with the observed values, but the values calculated for the 1.0 mm. diameter openings were lower than the observed values. In all cases however the corrections indicated that larger pressure drops would be expected to occur across the windward face, due to reduced efficiency of operation of those openings, as was observed in the model experiments. Consequently the combined effect of these two factors was taken to be a reasonable explanation for the discrepancies noted between the observed and computed results.

8.5 Additional experimental results

8.5.1 In addition to the comparative model results two further small studies were carried out. In the first the ventilation rate calculations were repeated, for all the model studies carried out, using mean pressure coefficient values for the model face instead of individual values for each opening. The total ventilation rates calculated under these conditions showed close agreement with the previously calculated rates. The agreement between the two sets of ventilation rates was within 2 - 3% for all sets of results. It was concluded from this study that mean pressure coefficient

values could be used to calculate total ventilation rates with no significant loss of accuracy, as the differences were well within the accuracy limits of other data used in natural ventilation calculations.

8.5.2 The influence of small scale surface features on ventilation rates was also investigated in order to estimate the inaccuracies caused by neglecting these features when choosing appropriate pressure coefficient values. Ventilation rate measurements were repeated using the orifice plate model with 15 x 2.5 mm. diameter openings per face in two opposite faces. Three separate types of surface feature were applied to the porous faces of the model and in each case ventilation rate measurements were made at angles of incidence of 0° , 30° and 60° . The configurations consisted of patterns of 3 mm. x 3 mm. perspex strips representing beams, columns and a grid of beams and columns outside the building envelope. The strips representing beams were mounted at heights of 30, 60 and 90 mm., and those representing columns spaced uniformly at 12 mm. intervals. Small variations in ventilation rate were observed when compared to the measurements made with a smooth model surface. The variations were all within $\pm 7\%$ of the previously observed ventilation rates and again are within the limits of accuracy available of other data used and within the limits of accuracy of operation of the programme.

8.6 Conclusions

8.6.1 The results of the comparative studies of natural ventilation of a series of simple models showed that ventilation rates and pressure distributions throughout the model could not be accurately predicted using conventional natural ventilation theory. Calculated ventilation rates were higher than the observed rates; the differences between observed and predicted ventilation rates increased in more turbulent flow conditions and in the tests carried out with the larger ventilation openings. The pressure difference distributions also showed significant variation from the computed distributions. Pressure differences were larger across the windward model faces than across leeward faces. In some conditions, using the model with two identical porous faces, the pressure drop across the windward face reached $\frac{2}{3}$ of the total pressure drop across the model.

8.6.2 The discrepancies between the observed ventilation rates and pressure distributions and the corresponding computed values were caused by reductions in the efficiency of the ventilation openings when compared to their calibrated efficiencies under conditions of steady pressure difference. The openings in the windward faces of the models were affected to a much greater extent than the openings in the leeward faces. The reductions in efficiency are thought to have been caused by fluctuations in the pressure difference acting

across the openings and by lateral flow along the surfaces of the model faces. Approximate corrections allowing for these effects showed good agreement with the observed ventilation rates.

8.6.3 The computed ventilation rates showed discrepancies from the observed rates of 0% - 20%. It is possible that in full scale buildings discrepancies of this order of magnitude will also occur as the relative lateral flow velocities and pressure fluctuations will probably be of a similar order of magnitude to those experienced in the model work. Full scale measurements of the distribution of wind loads on buildings have shown that relatively high wind loads are carried on the windward faces of the buildings (Newberry, 1968), and this behaviour was also noted in the model studies. The limits of accuracy of available data for predicting design wind speeds, window infiltration coefficients and pressure coefficient values is such that the digital analogue could be used to produce an acceptably accurate estimate of total ventilation rates. Simplification of information requirements by using mean pressure coefficient values for the building faces, ignoring the effect of small scale surface features, did not lead to significant additional errors.

Figure 8.1. Observed model pressure coefficients at different angles of incidence.

boundary layer I — — — — —
boundary layer II - - - - -

Mean pressure coefficient, C_p .

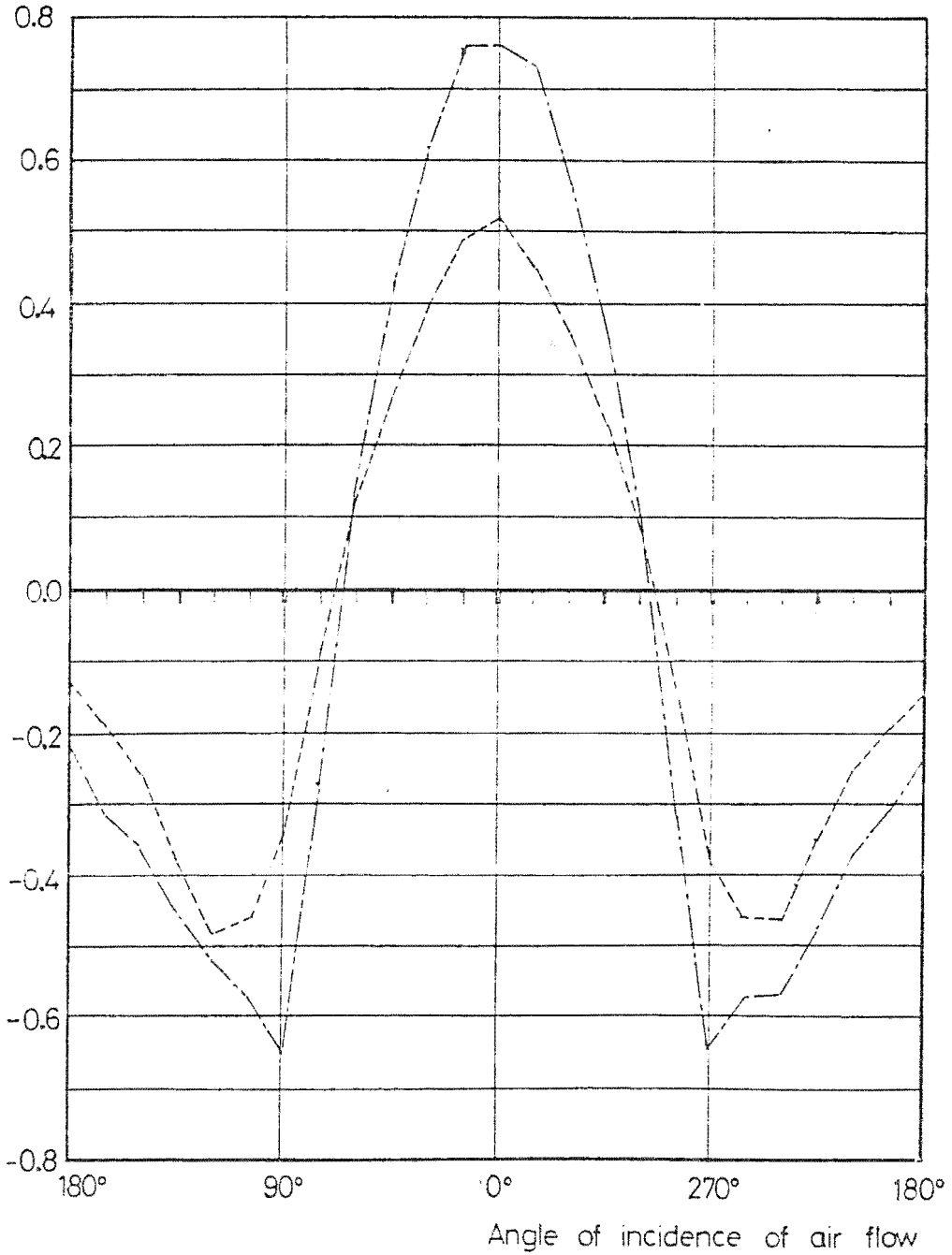
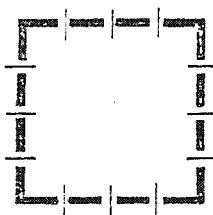


Figure 8.2. Opening positions used to evaluate variation of internal pressure with opening configuration; figures 8.3, 8.4, 8.5.

Plan views:

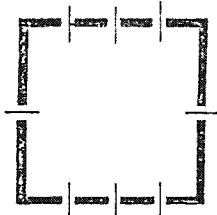
configuration A,
uniformly glazed:

9 openings/wall



configuration B,
intermediate:

9 or 3 openings
/wall



configuration C,
two walls glazed:

9 openings/glazed wall

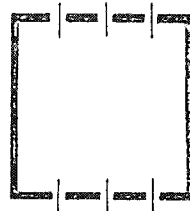


Figure 8.3. Observed and computed internal pressures, opening configuration A, boundary layer I, variation with angle of incidence.

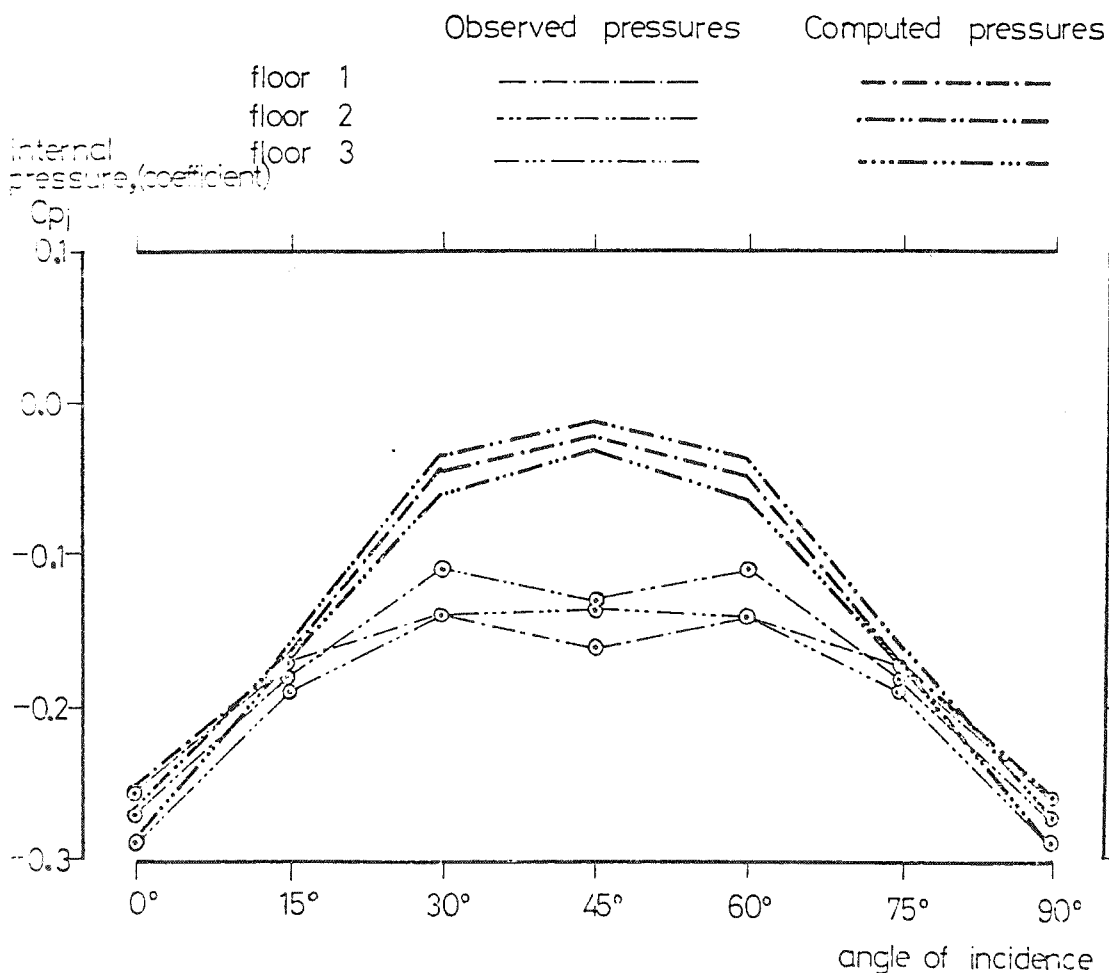


Figure 8.4. Observed and computed internal pressures, opening configuration B, boundary layer I, variation with angle of incidence.

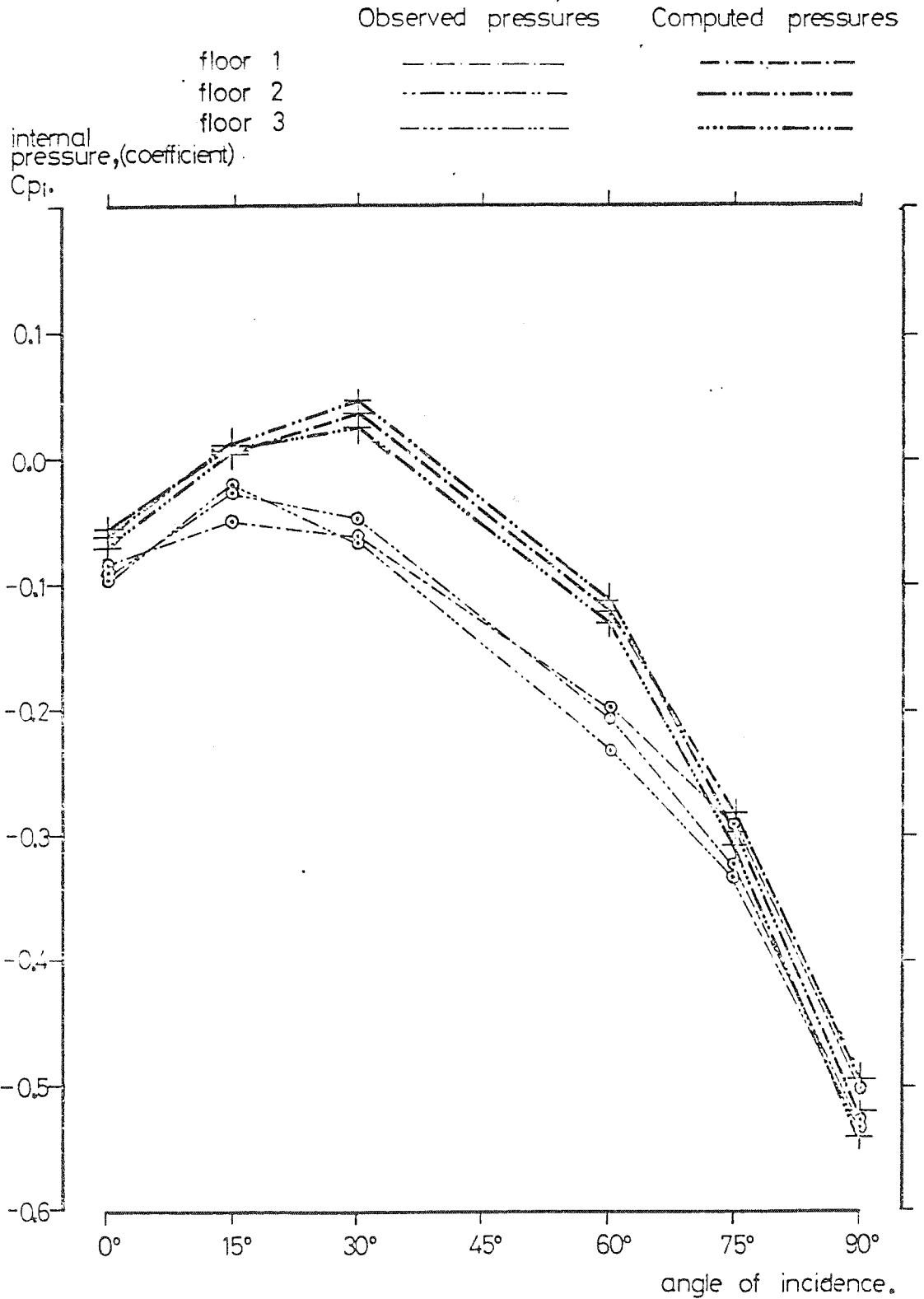


Figure 8.5. Observed and computed internal pressures, opening configuration C, boundary layer I, variation with angle of incidence.

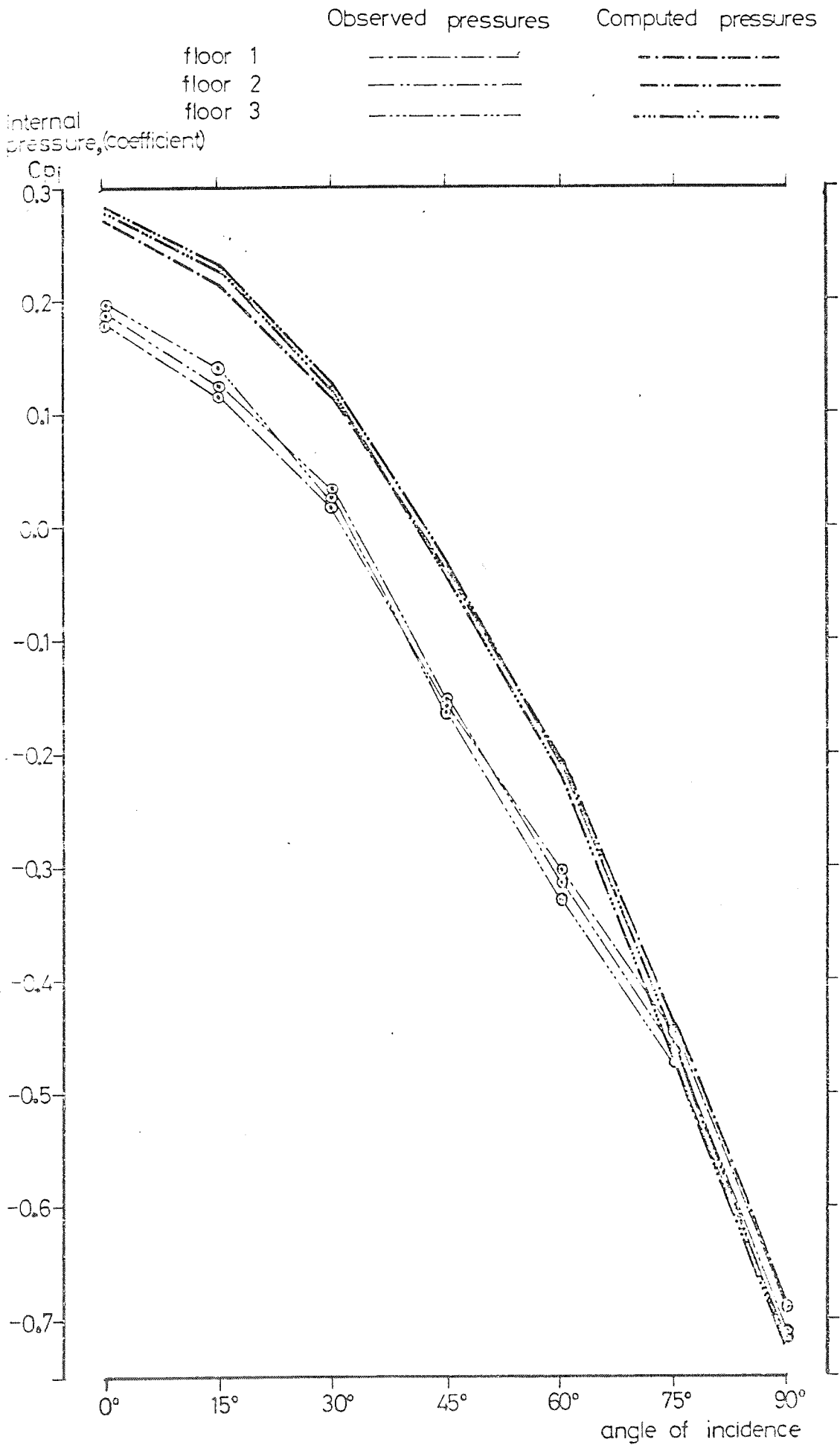


Figure 8.6. Variation of observed and computed mean internal pressures with angle of incidence of airflow, opening configuration C, 9x2.5mm openings/face, boundary layer I.

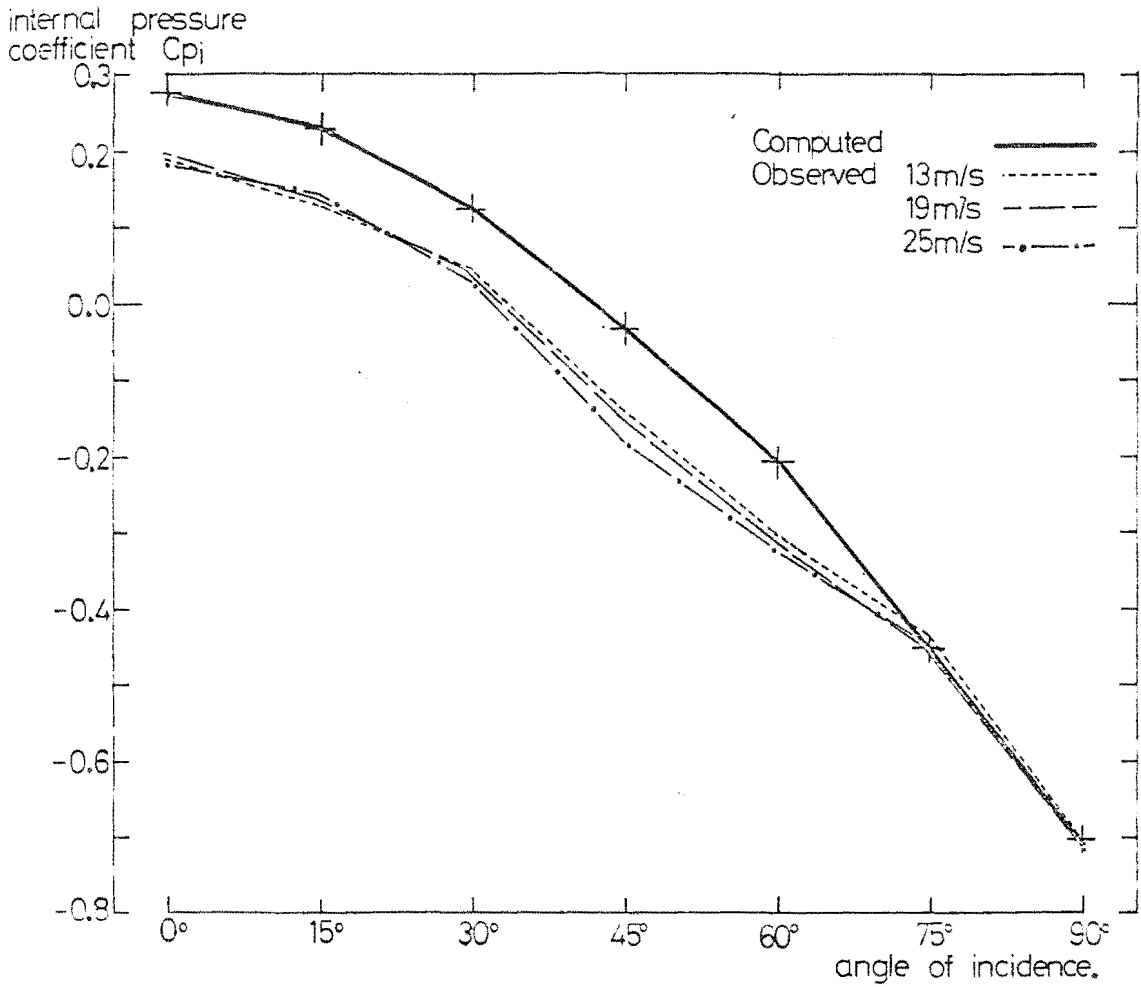


Figure 8.7. Variation of observed and computed mean internal pressures with angle of incidence of airflow, opening configuration C, 9x2.5mm openings/face, boundary layer II.

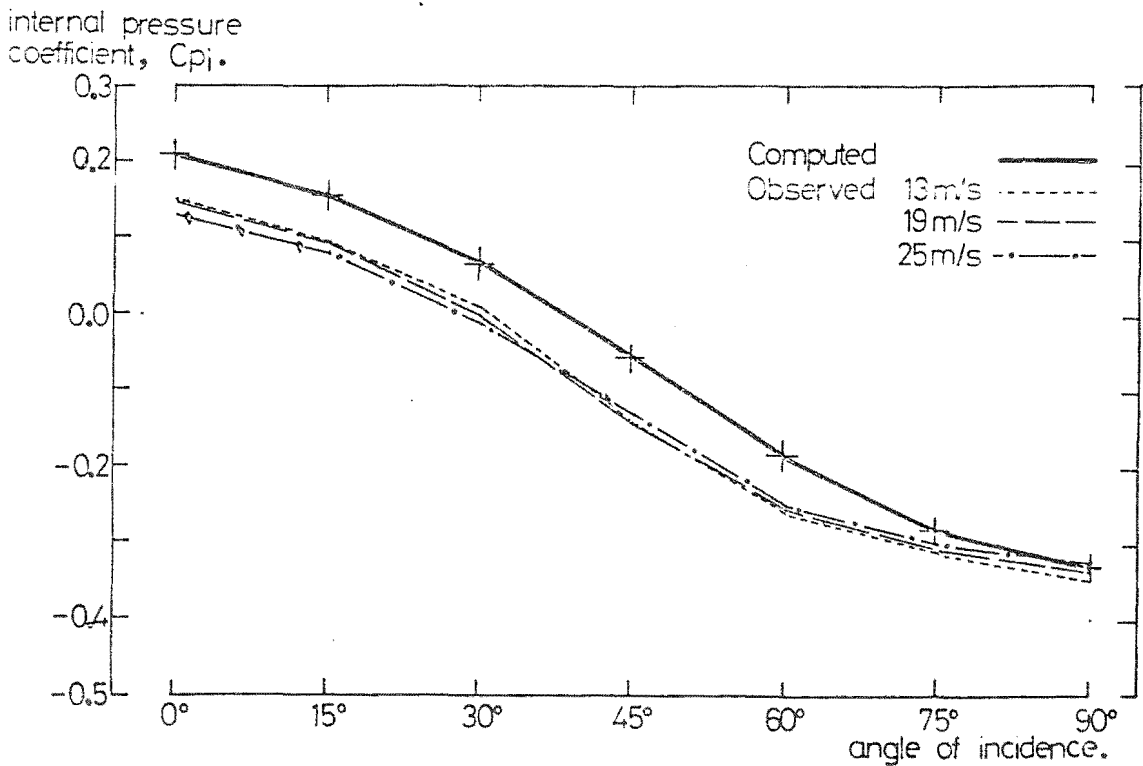


Figure 8.8.

Variation of observed and computed mean internal pressures with angle of incidence of airflow, opening configuration C, 3x2.5mm. openings/face, boundary layer I.

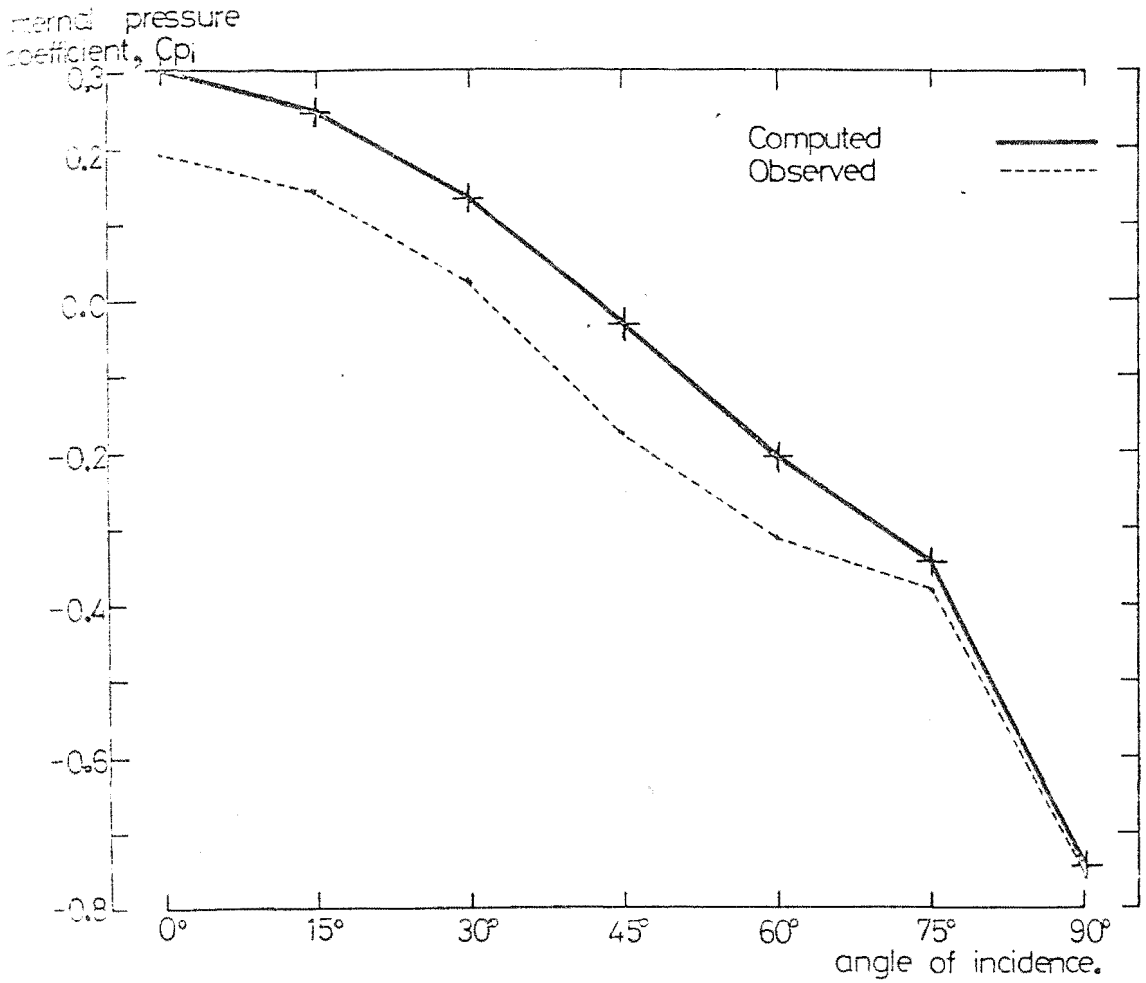


Figure 8.9.

Variation of observed and computed mean internal pressures with angle of incidence of airflow, opening configuration C, 3x2.5mm. openings/face, boundary layer II.

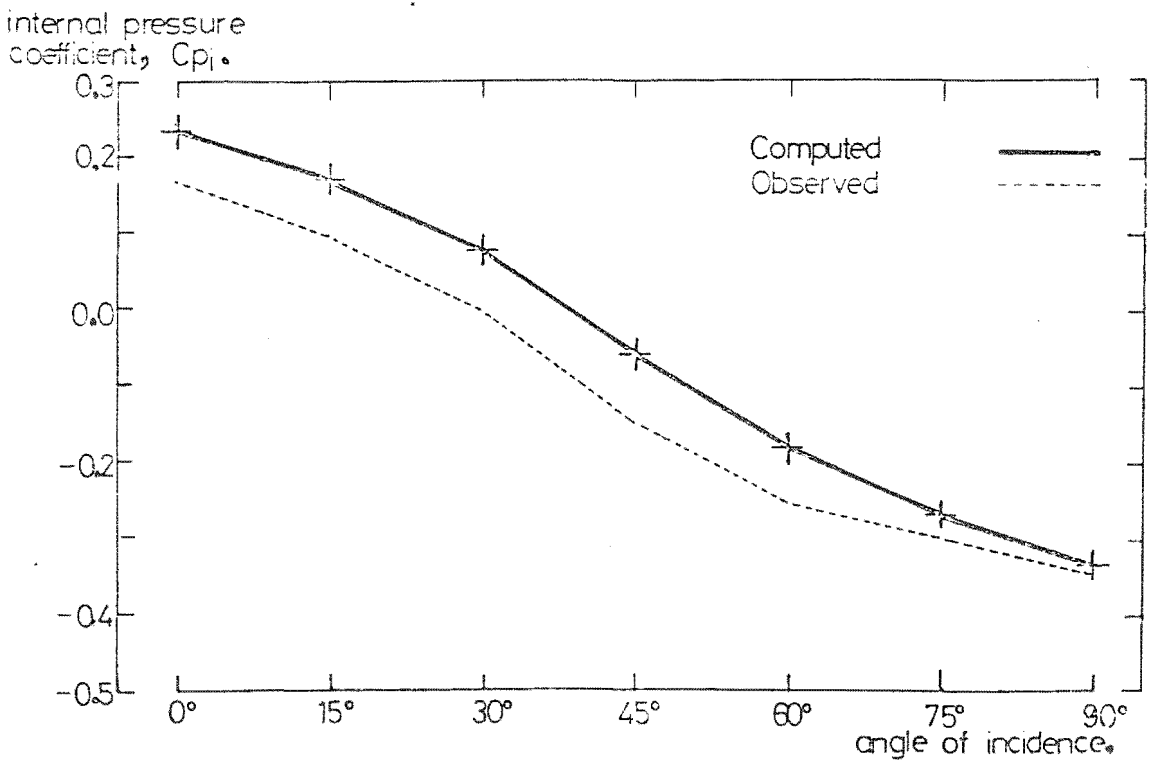


Figure 8.10. Variation of observed and computed mean internal pressures with angle of incidence of airflow; opening configuration C, 1×2.5 mm. openings/face, boundary layer I.

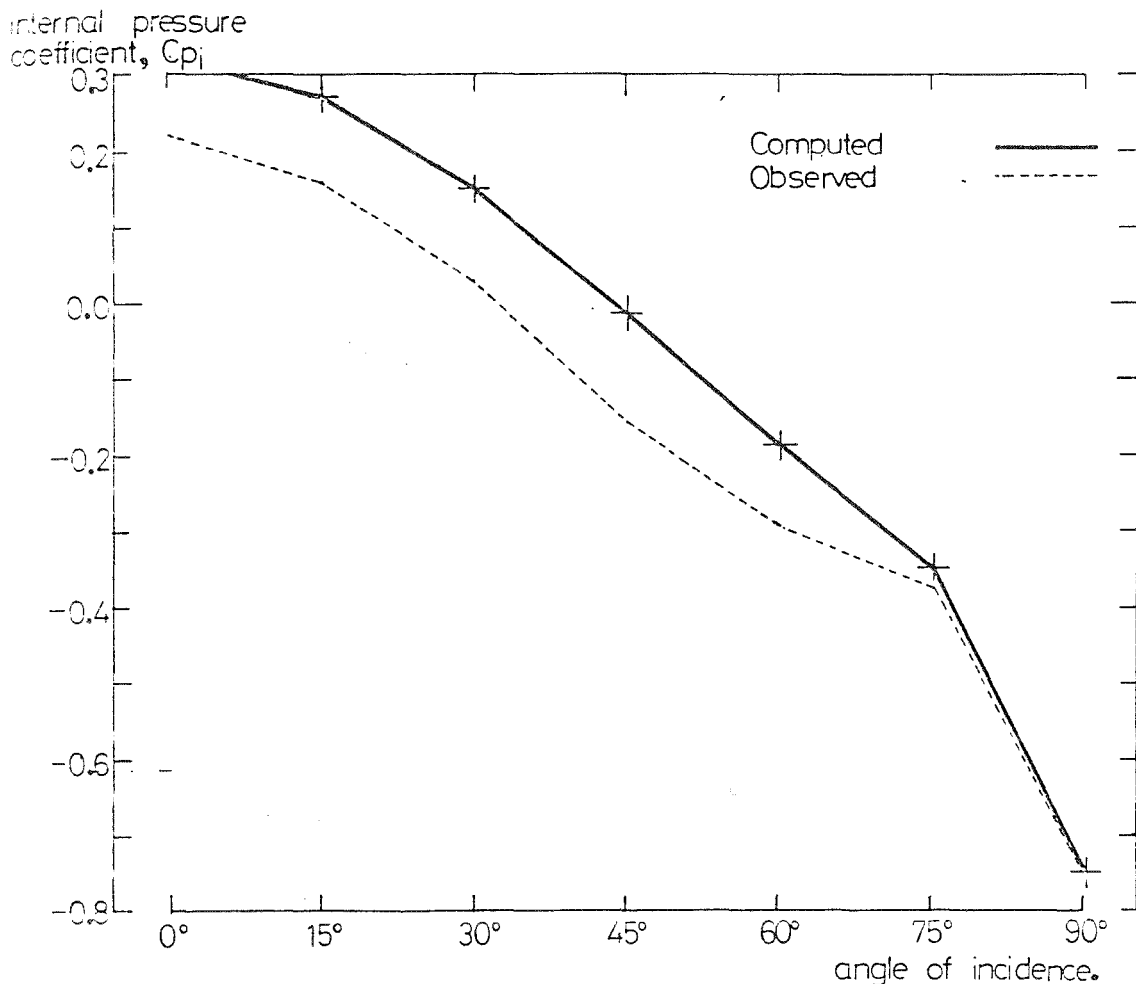


Figure 8.11. Variation of observed and computed mean internal pressures with angle of incidence of airflow; opening configuration C, 1×2.5 mm. opening/face, boundary layer II.

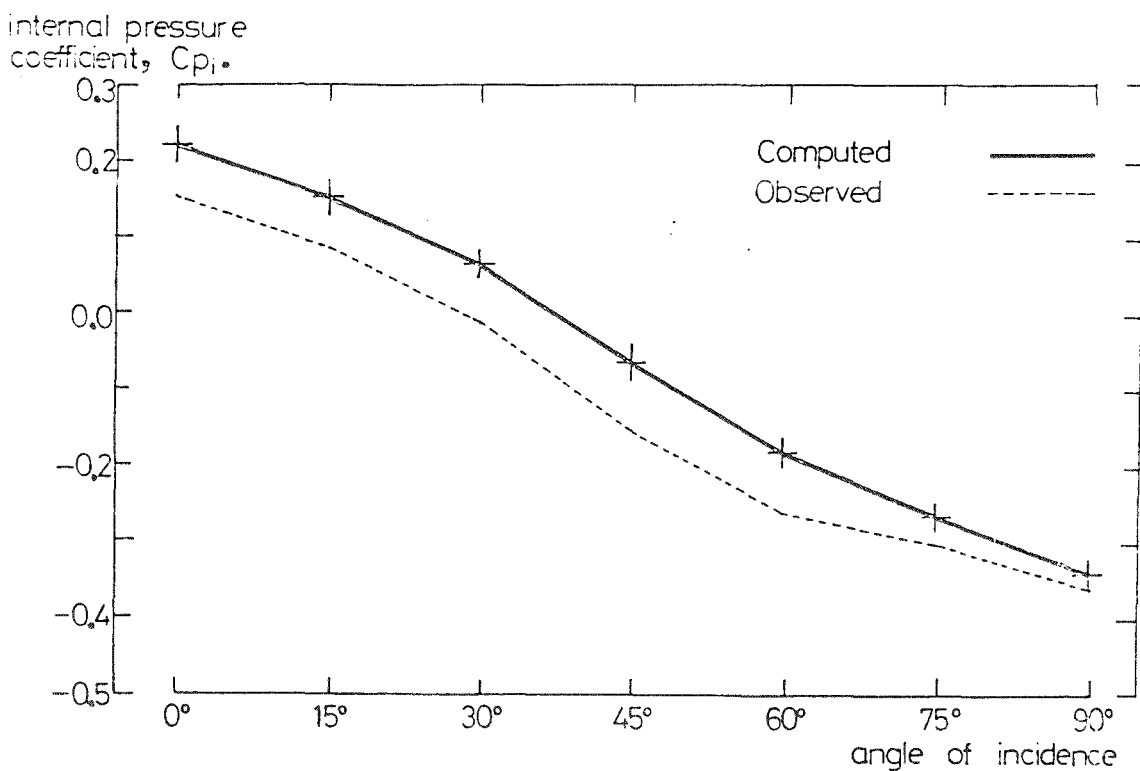


Figure 8.12. Variation of observed and computed mean internal pressures with angle of incidence of airflow, opening configuration C, 36×1.0mm. openings/face, boundary layer I.

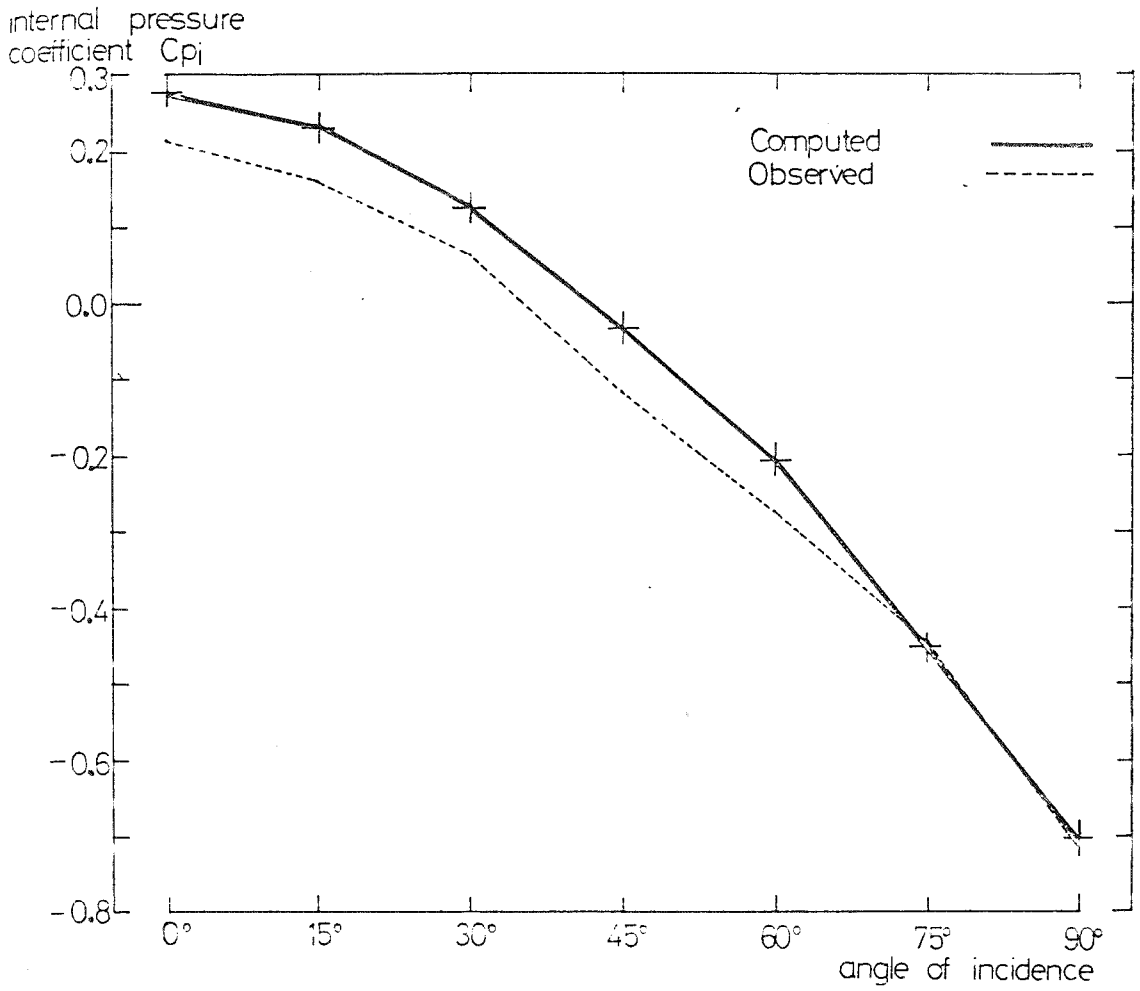


Figure 8.13. Variation of observed and computed mean internal pressures with angle of incidence of airflow, opening configuration C, 36×1.0mm. openings/face, boundary layer II.

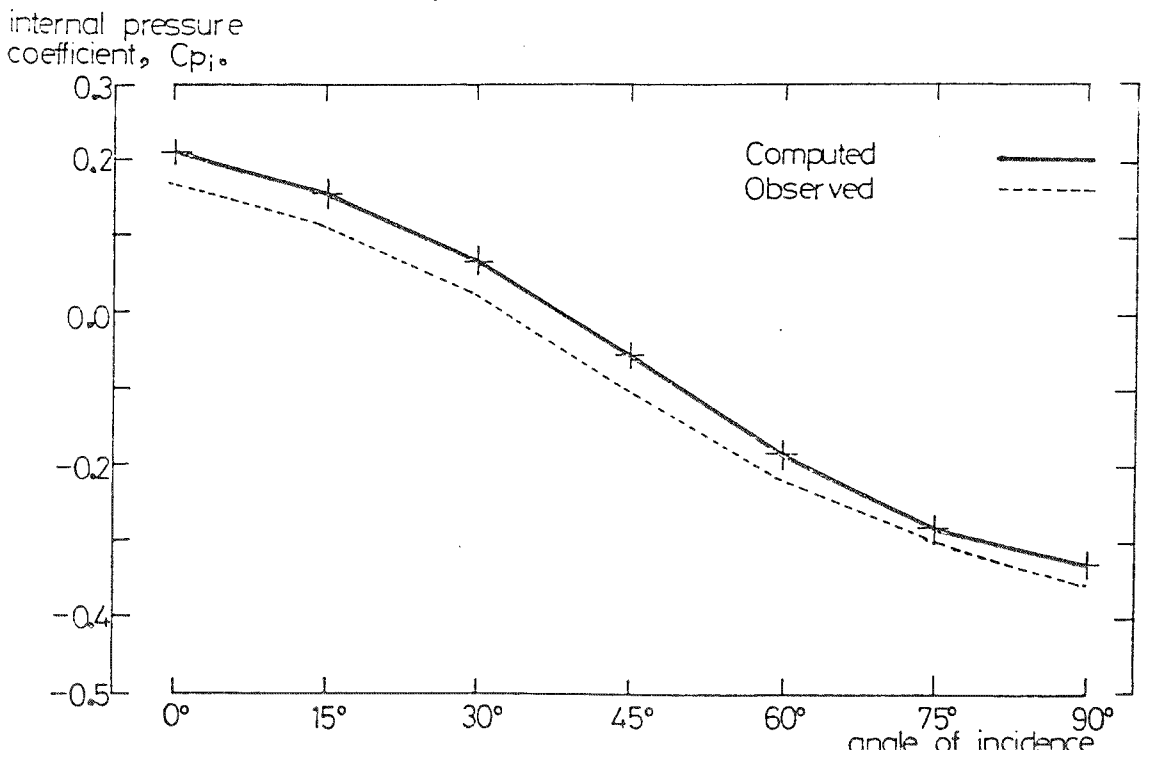


Figure 8.14. Variation of observed and computed mean internal pressures with angle of incidence of airflow, opening configuration C, 12x1.0mm. openings/face, boundary layer I.

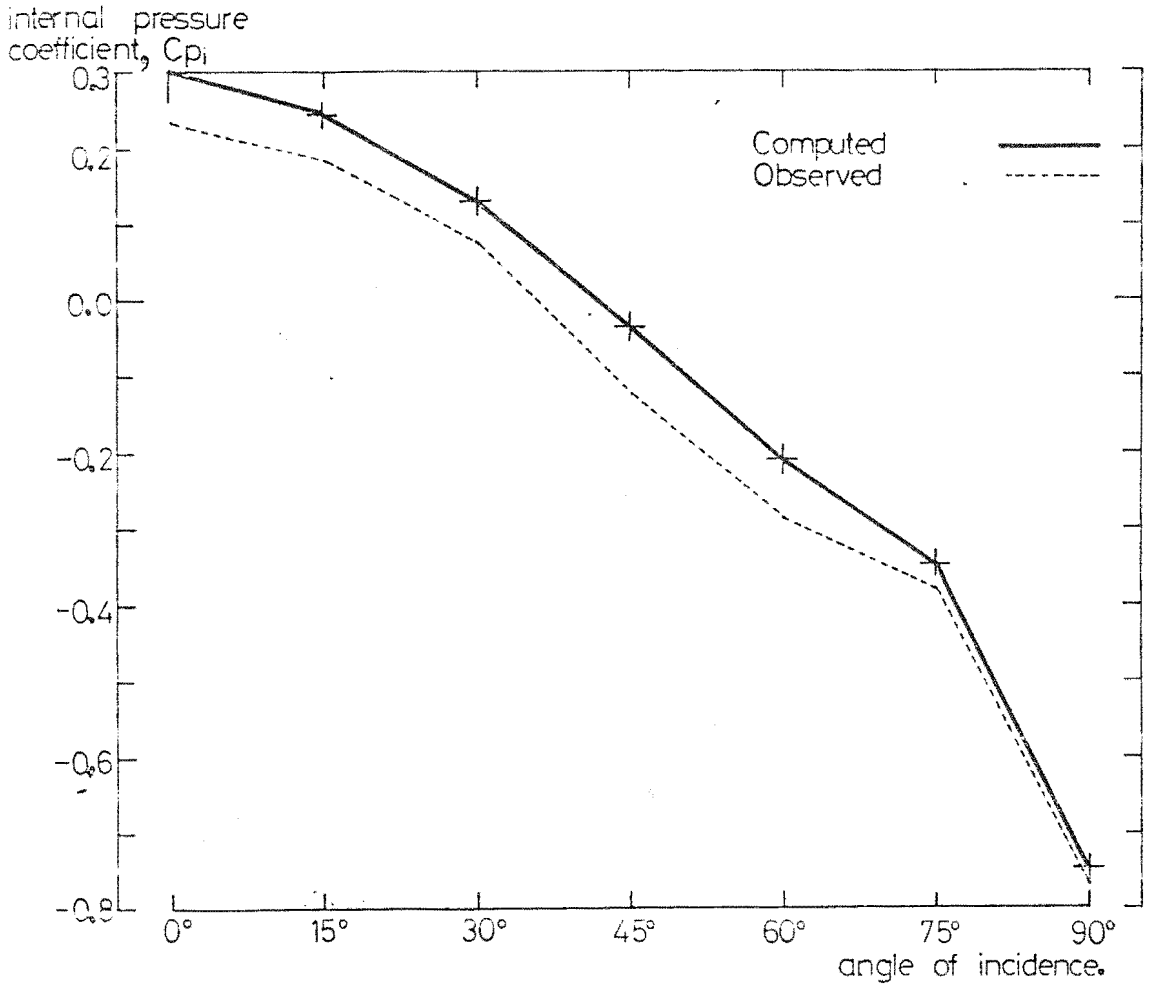


Figure 8.15. Variation of observed and computed mean internal pressures with angle of incidence of airflow, opening configuration C, 12x1.0mm. openings/face, boundary layer II.

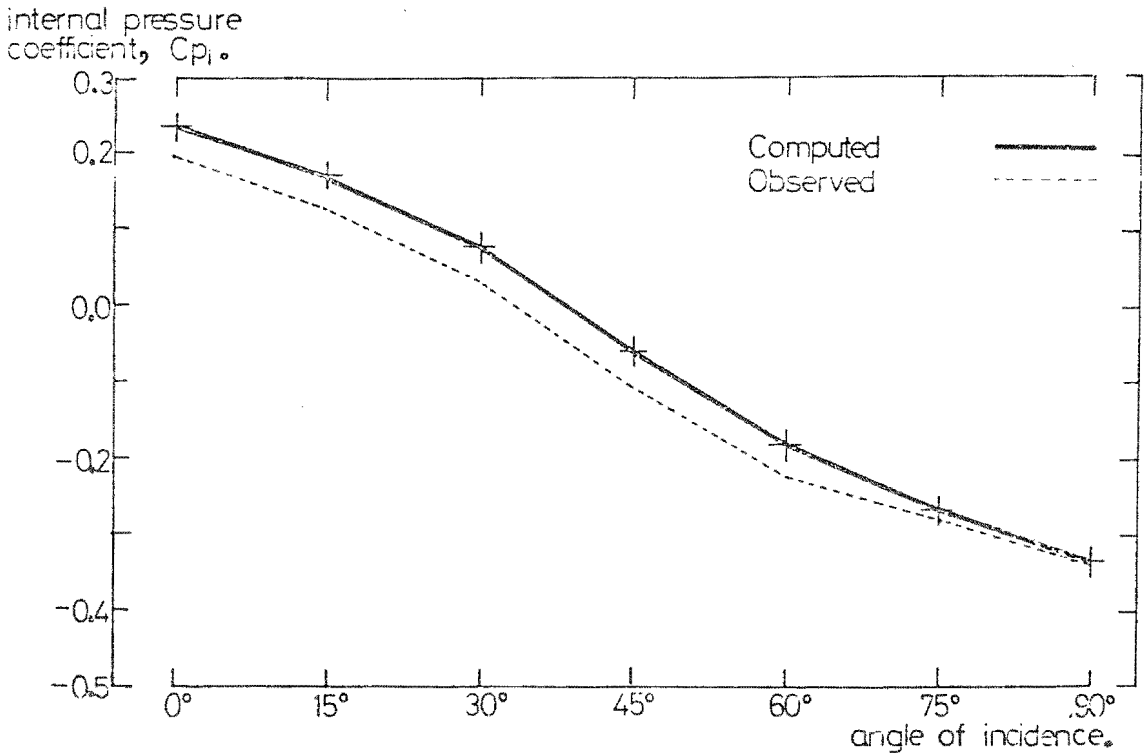


Figure 8.16. Variation of observed and computed mean internal pressures with angle of incidence of airflow; opening configuration C, 4×1.0 mm, openings/face, boundary layer I.

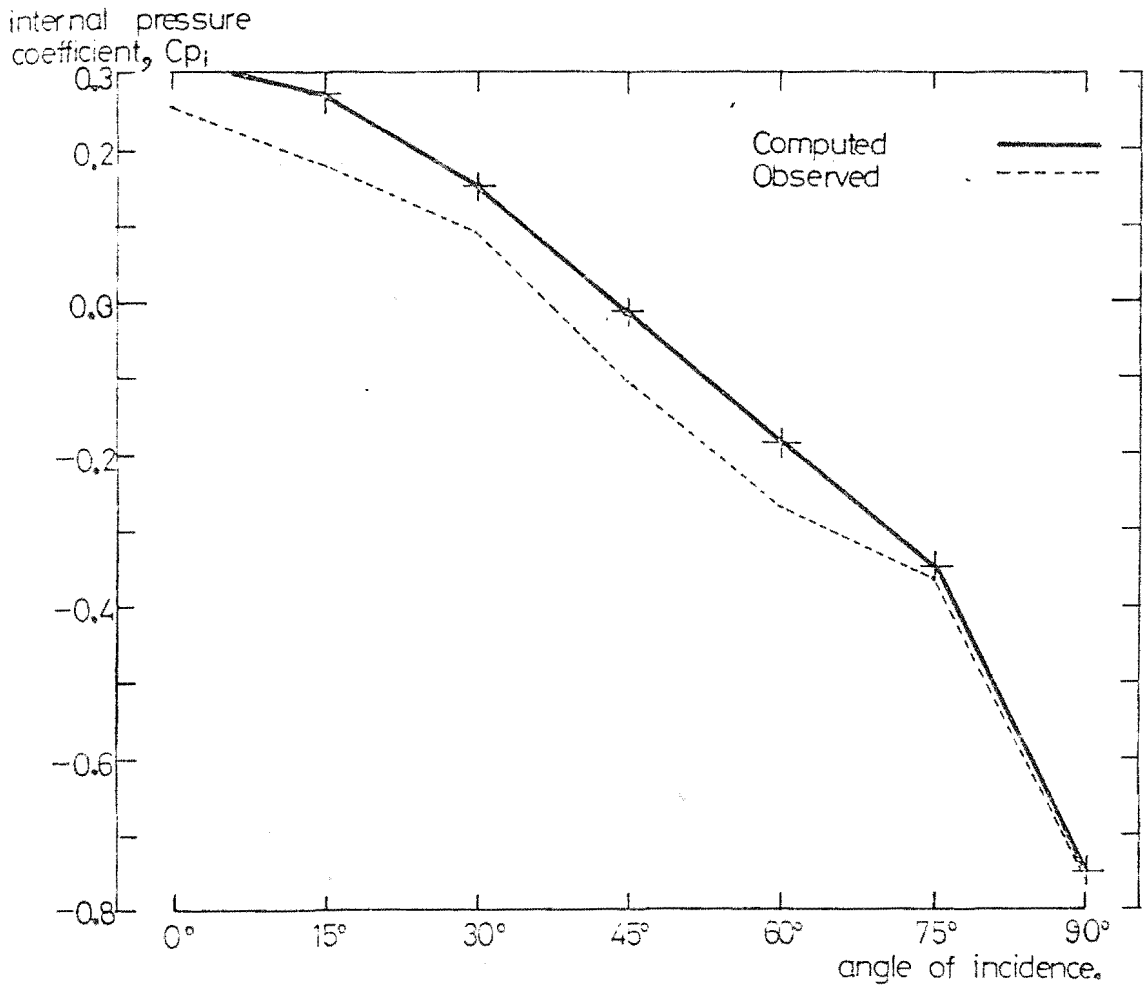


Figure 8.17. Variation of observed and computed mean internal pressures with angle of incidence of airflow; opening configuration C, 4×1.0 mm, openings/face, boundary layer II.

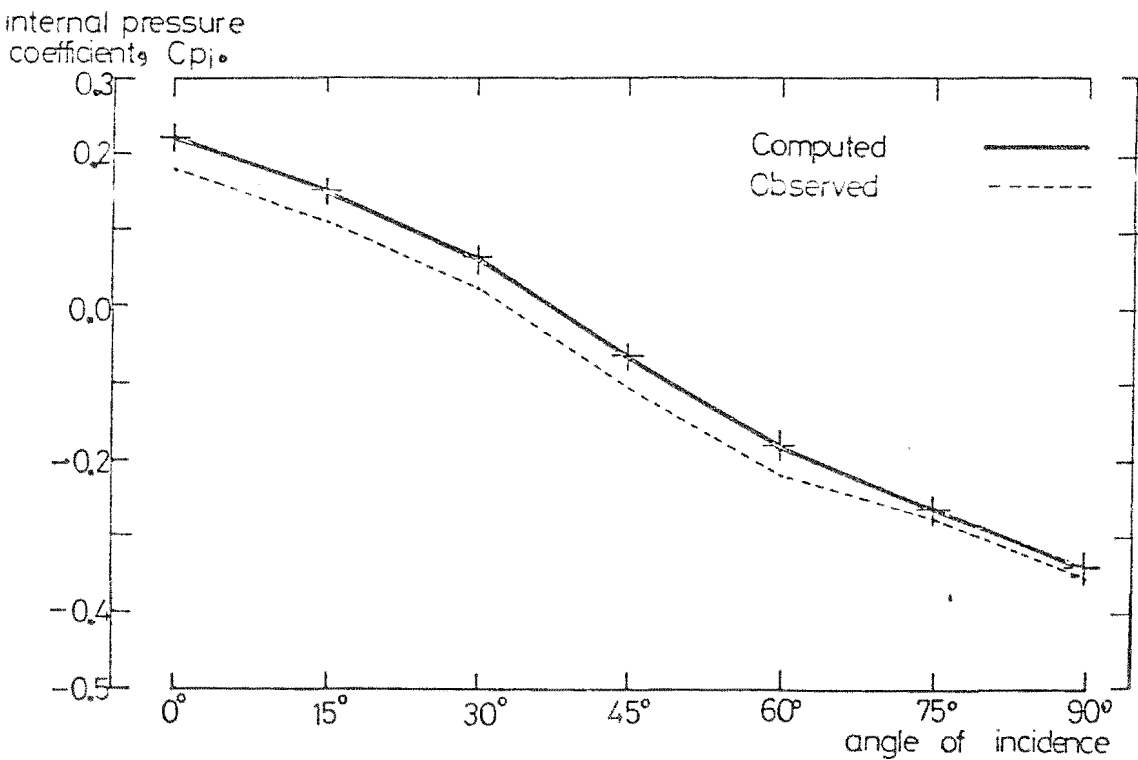


Figure 8.18. Variation of pressure difference ratio, $(C_{p_w} - C_{p_i}) / (C_{p_i} - C_{p_l})$ and relative orifice operating efficiency, (e_w/e_l) , windward face openings: leeward face openings, with angle of incidence, 25mm openings.

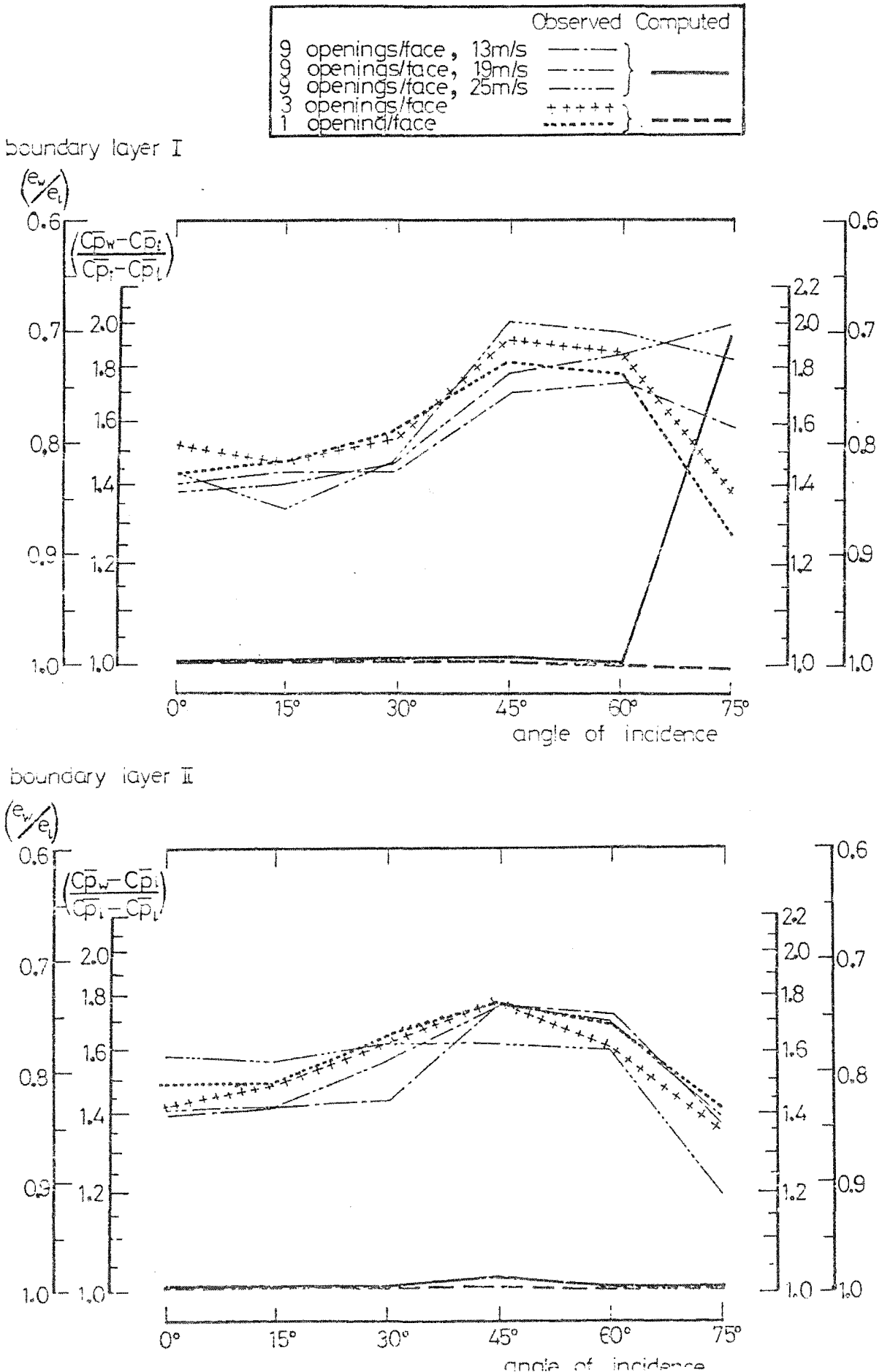


Figure 8.19.

Variation of pressure difference ratio, $(\overline{Cp}_w - \overline{Cp}_i) / (\overline{Cp}_i - \overline{Cp}_l)$ and relative orifice operating efficiency, (e_w/e_i) , windward face openings, leeward face openings, with angle of incidence, 1.0mm openings.

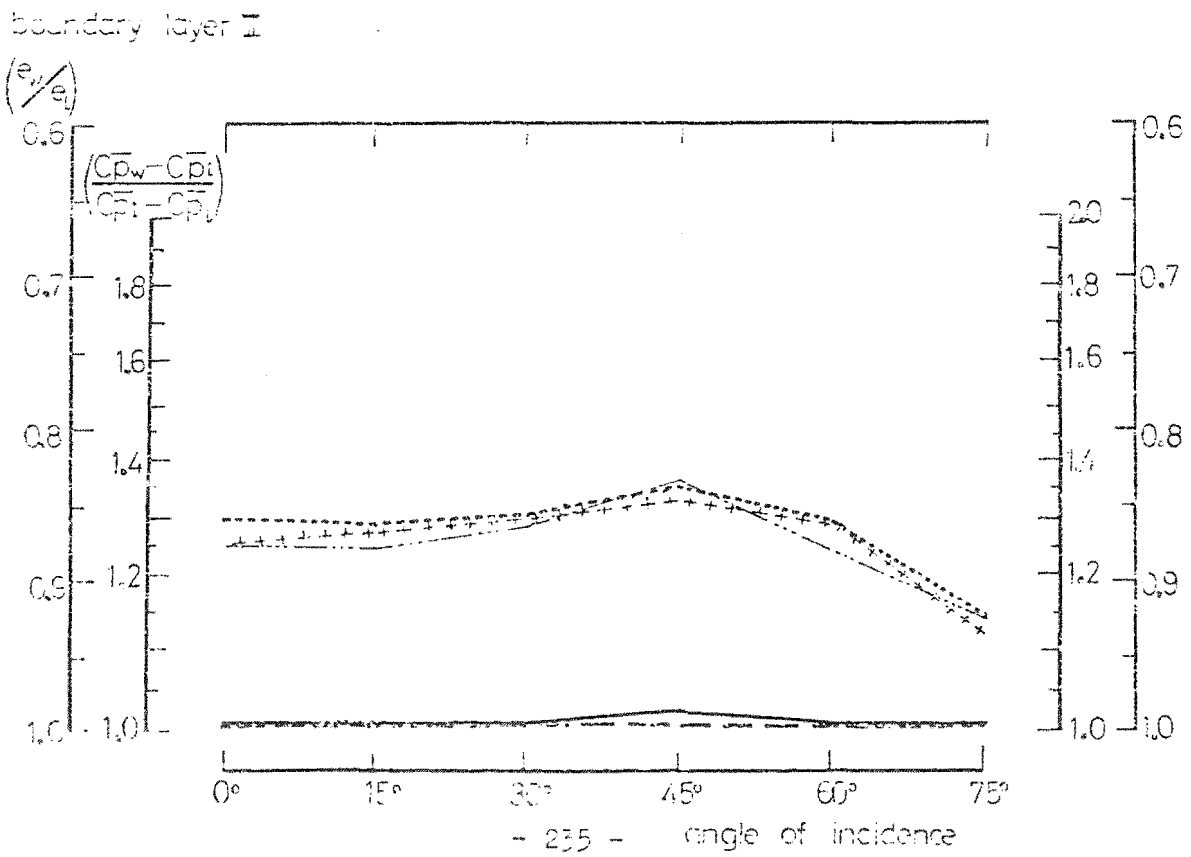
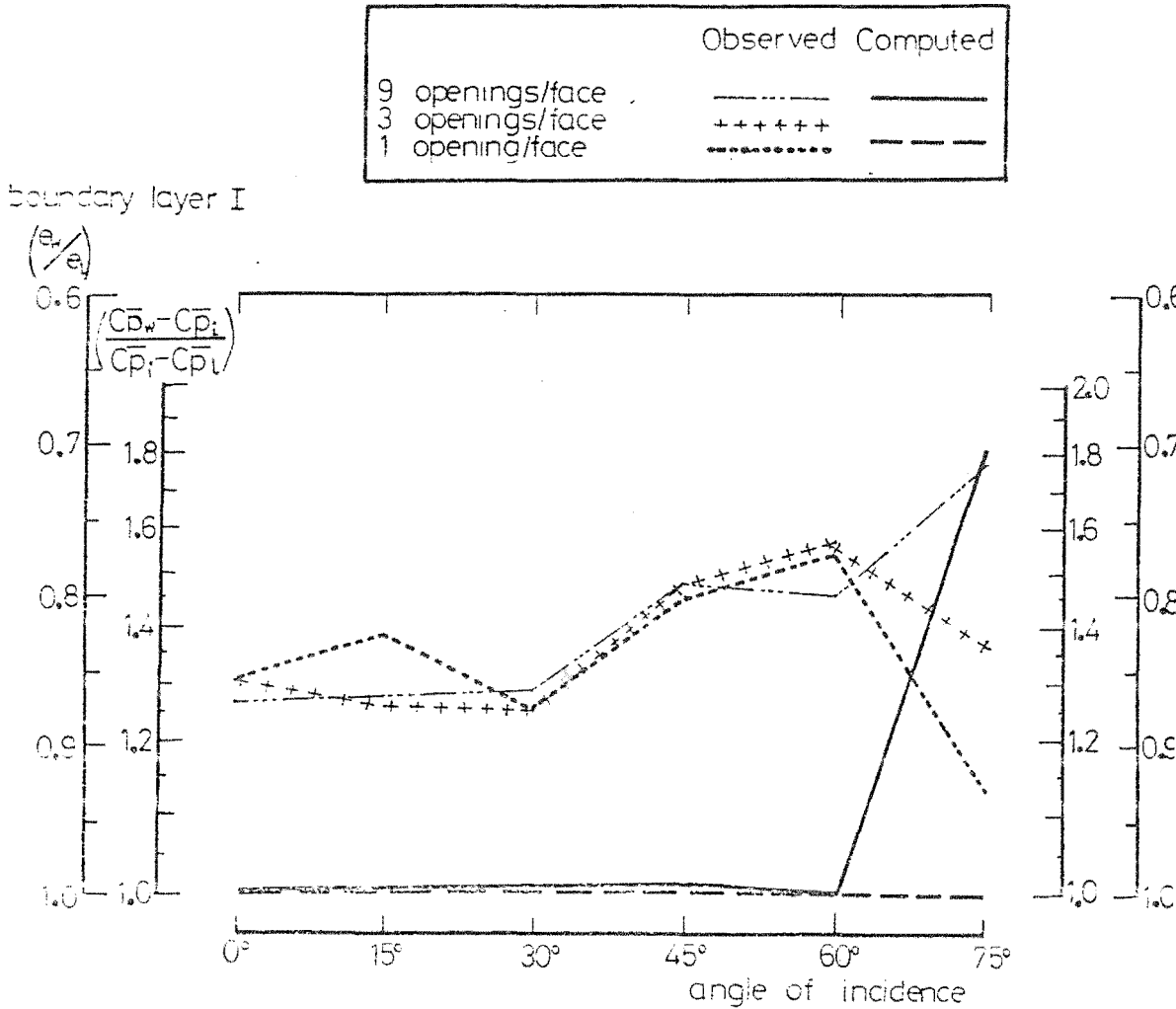
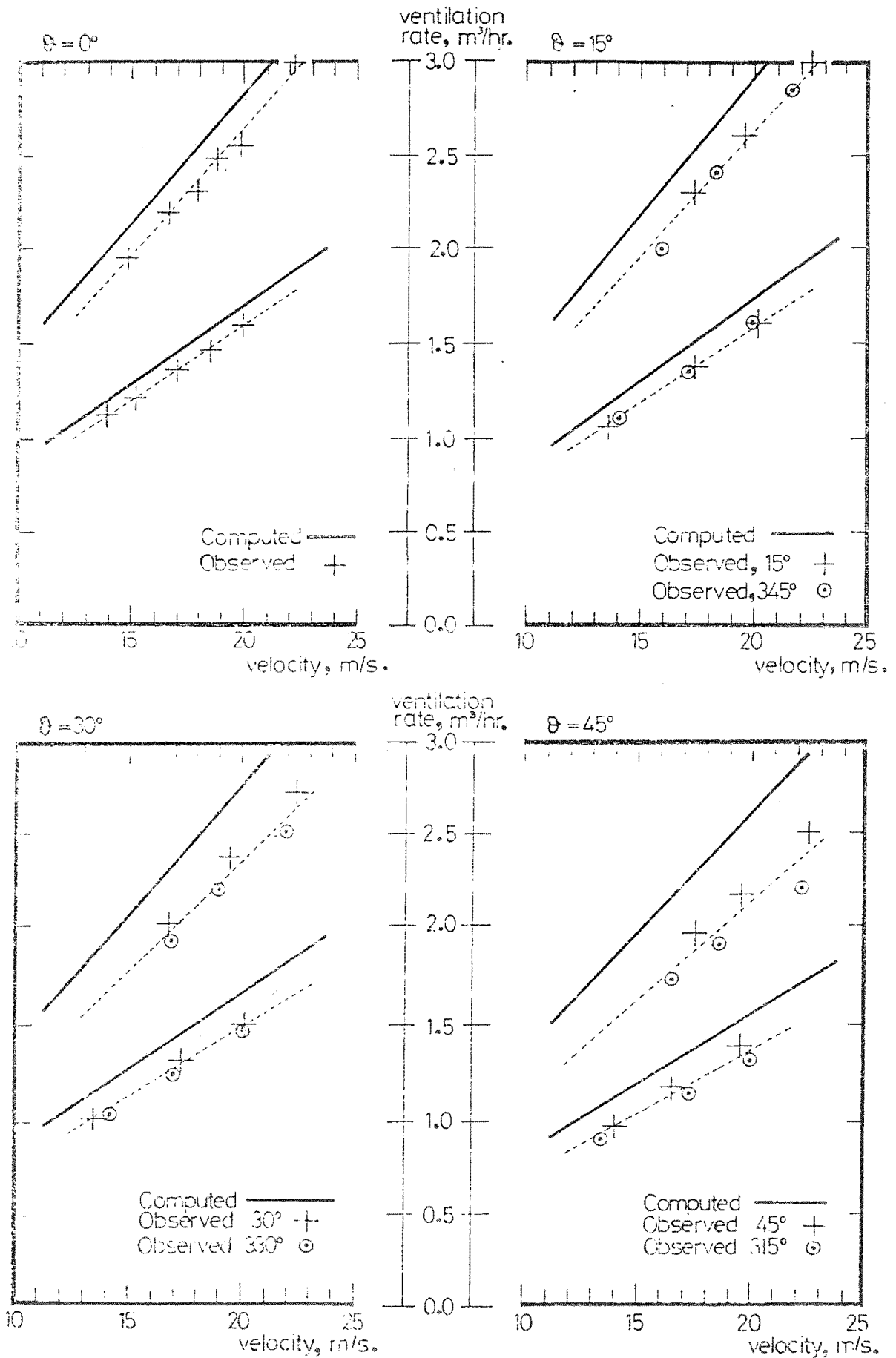


Figure 8.20.

Variation of observed and computed ventilation rates with air velocity, opening configuration C, 9 and 15 x 2.5mm, openings/face, boundary layer I.



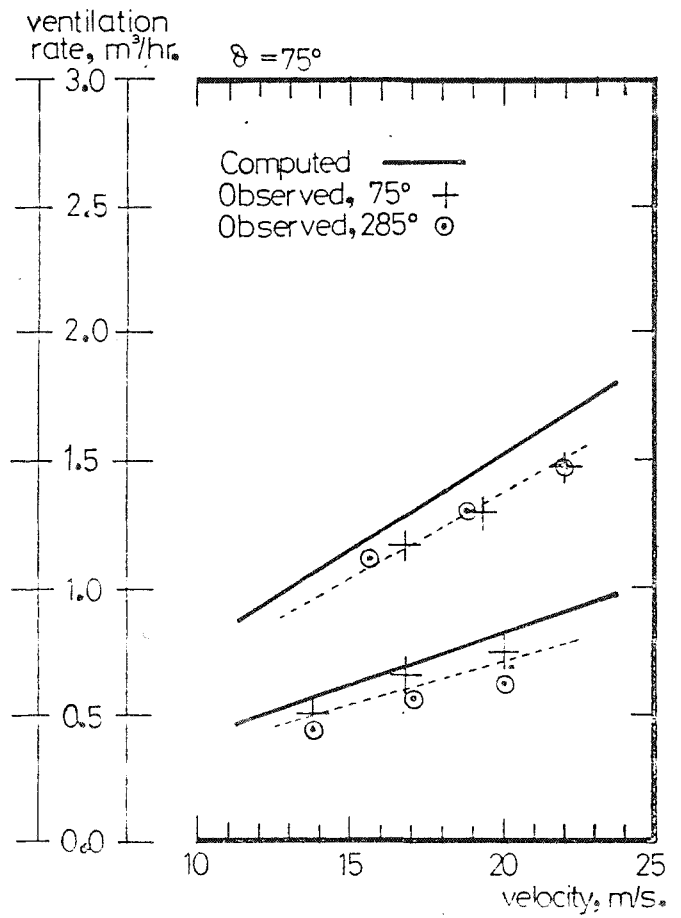
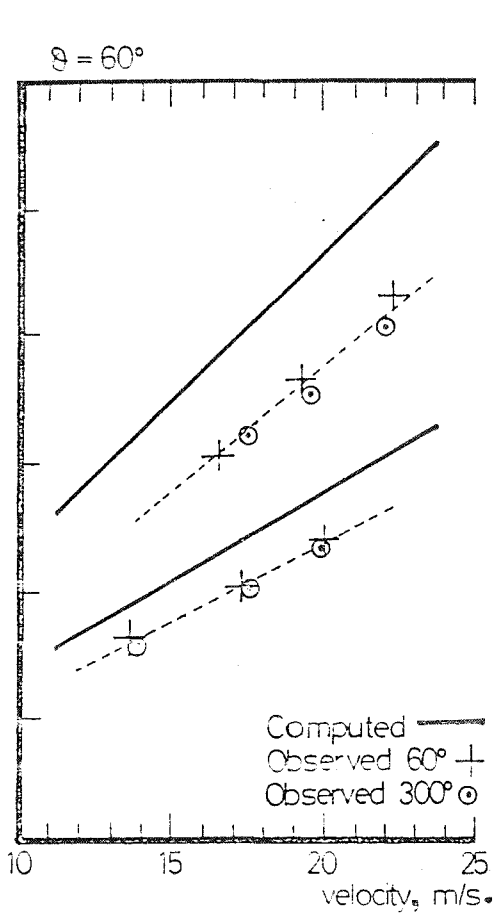
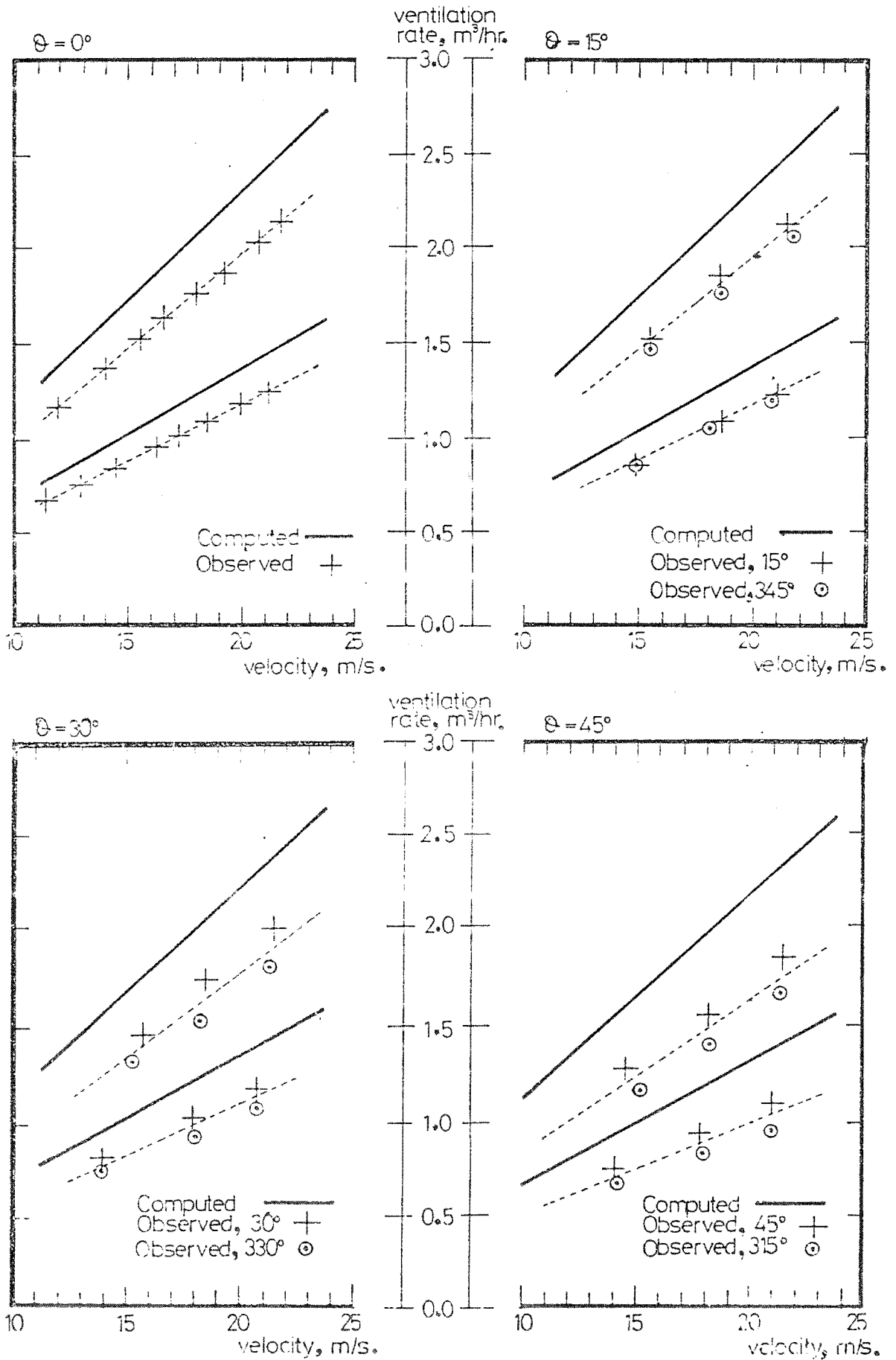


Figure 8.21.

Variation of observed and computed ventilation rates with air velocity, opening configuration C, 9 and 15 x 2.5mm, openings/face, boundary layer II.



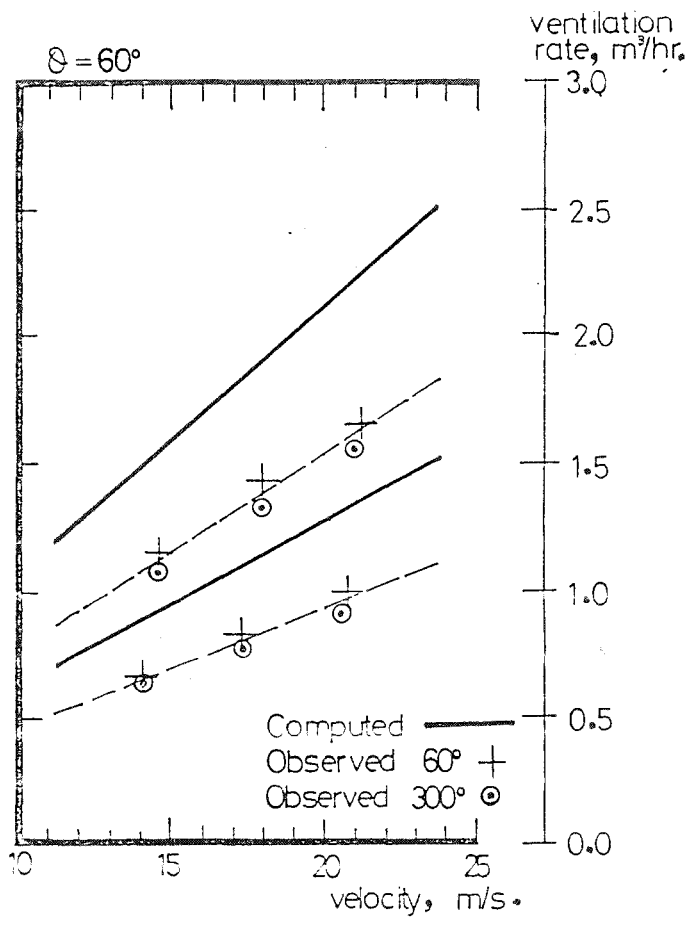


Figure 8.22.

Variation of observed and computed ventilation rates with air velocity, opening configuration C, 36 and 60 × 1.0 mm. openings/face, boundary layer I.

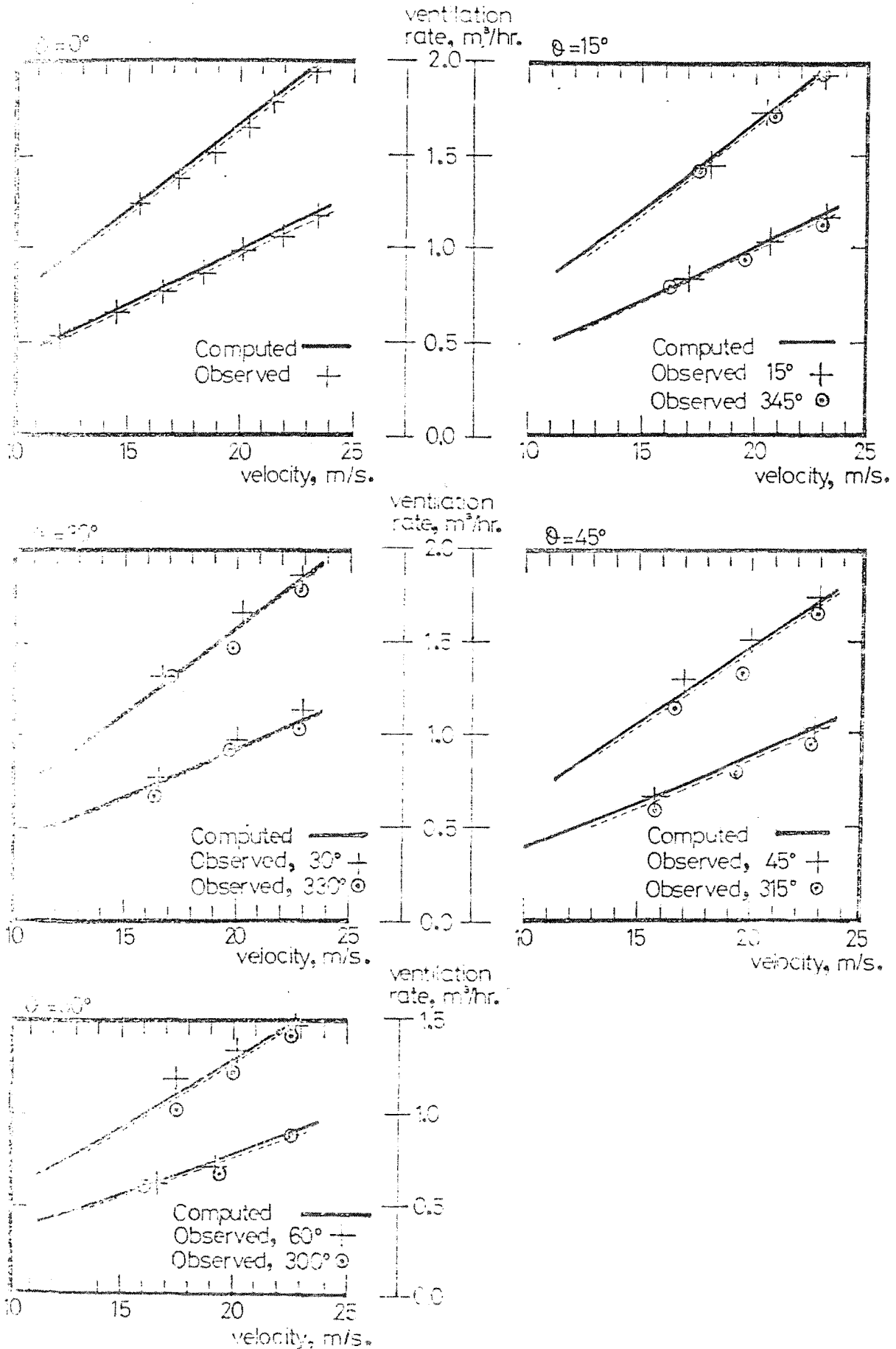


Figure 8.23.

Variation of observed and computed ventilation rates with air velocity, opening configuration C, 36 and 60 × 1.0 mm. openings/face, boundary layer II.

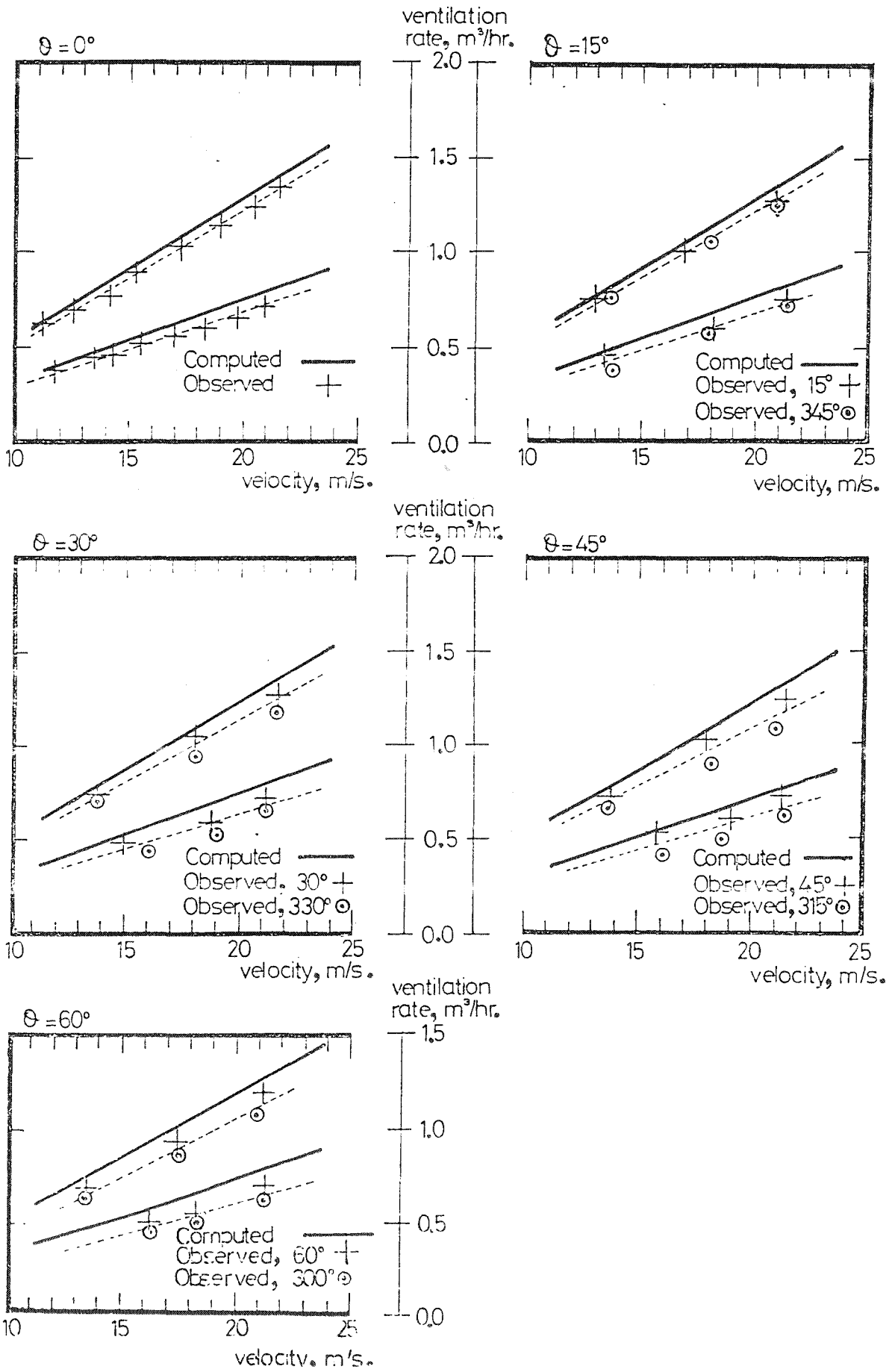


Figure 8.24. Variation of relative ventilation rate with angle of incidence, 2.5mm. openings.

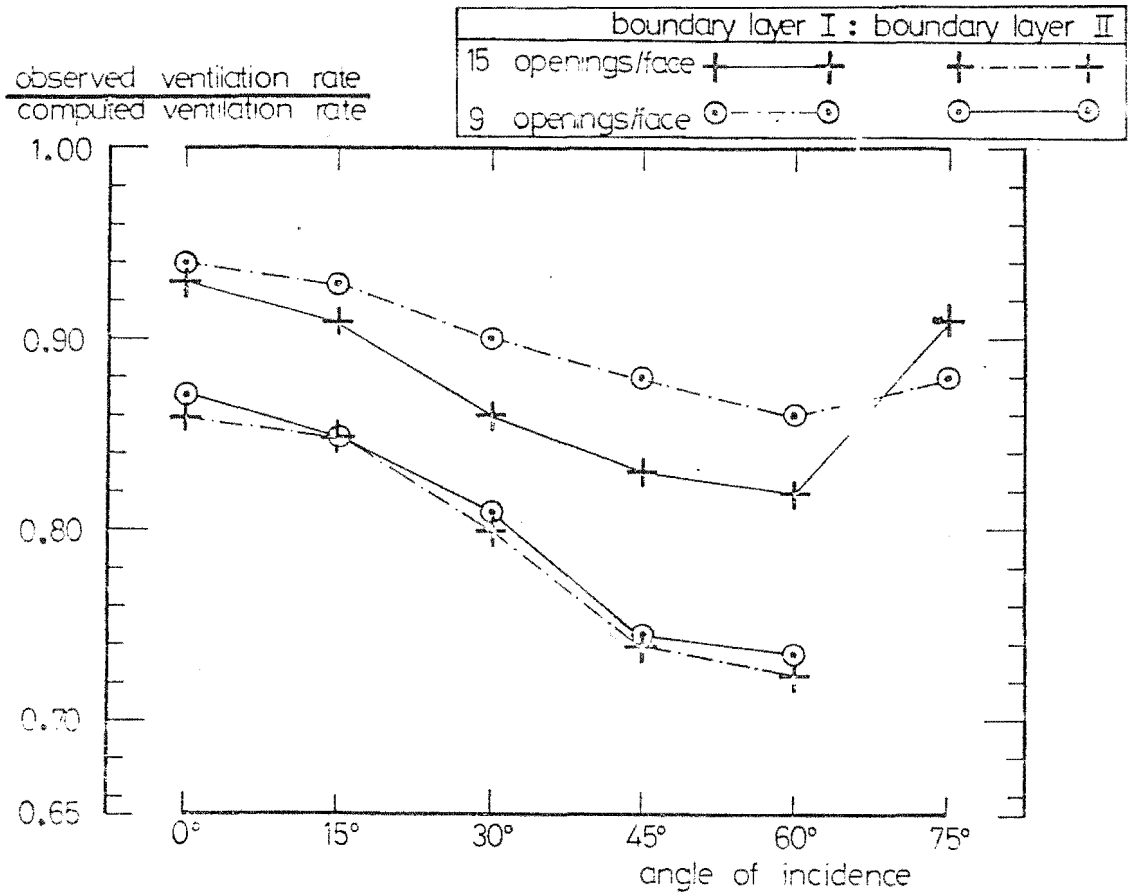


Figure 8.25. Variation of relative ventilation rate with angle of incidence, 10mm. openings.

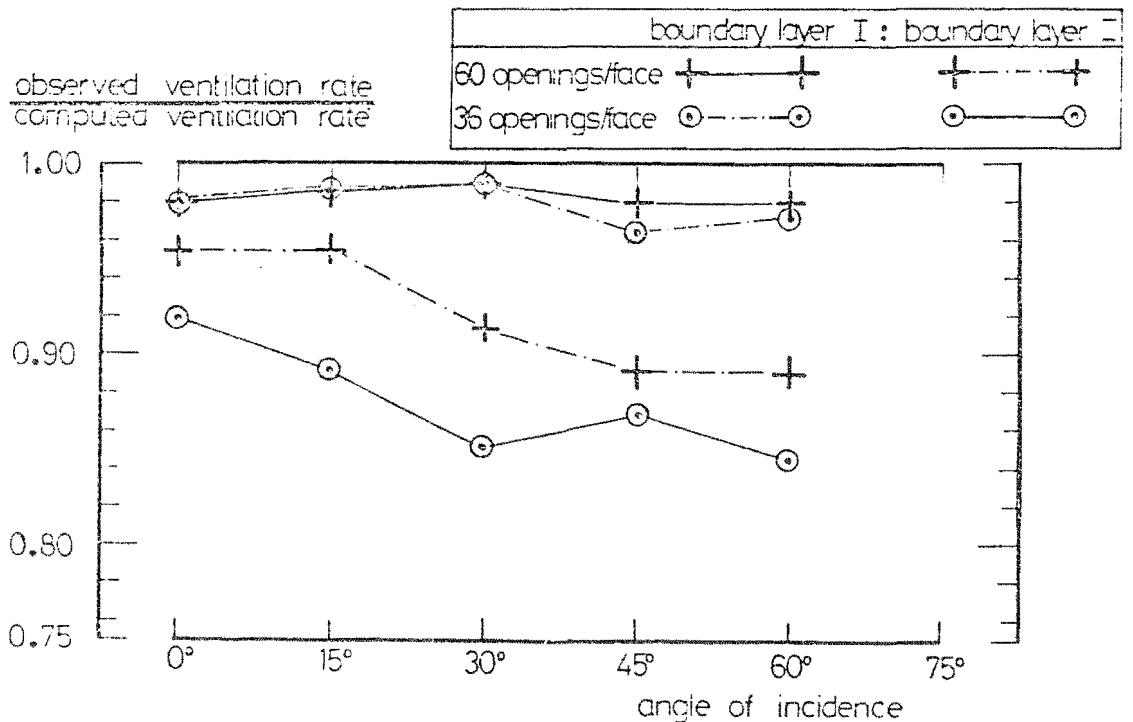


Figure 8.26. Variation of non-dimensional ventilation rate, $\frac{V}{(m \cdot C \cdot (Pv/2)^{1/n})}$, with angle of incidence.

where V is observed ventilation rate, $m^3/hr.$
 C is opening leakage coefficient, $m^3/hr/mm.wg^{1/n}$
 m is number of openings/face
 Pv is dynamic head of flow, $mm.wg.$
 $1/n$ is an exponent

- | | | | |
|----|----------------------|---|---|
| 15 | 2.5mm. openings/face | + | + |
| 9 | 2.5mm. openings/face | ⊙ | ⊙ |
| 60 | 1.0mm. openings/face | + | + |
| 36 | 1.0mm. openings/face | ⊙ | ⊙ |

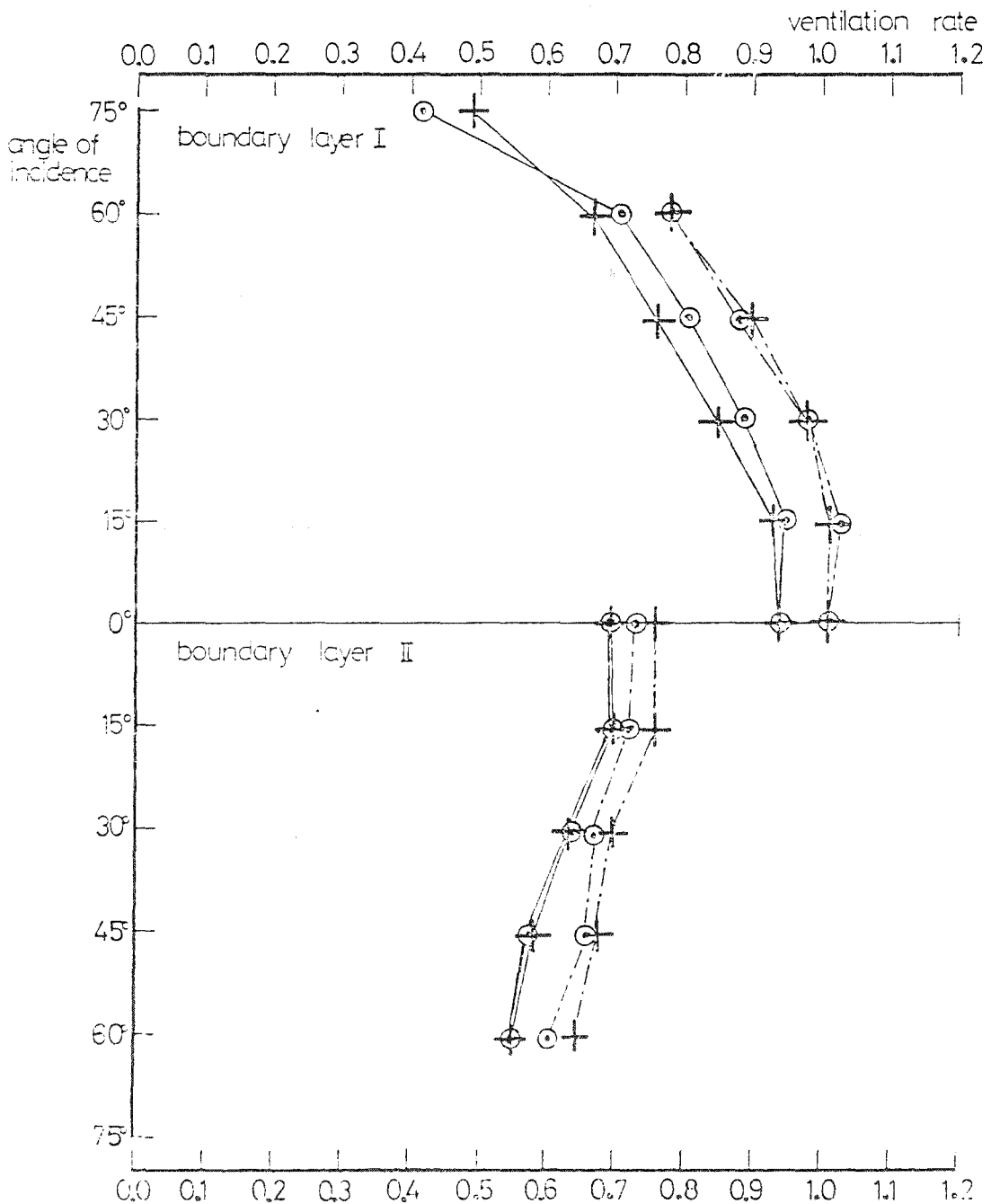


Figure 8.27. Variation of computed orifice operating efficiency with magnitude of pressure fluctuations.

orifice efficiency, relative to performance at zero pressure variation

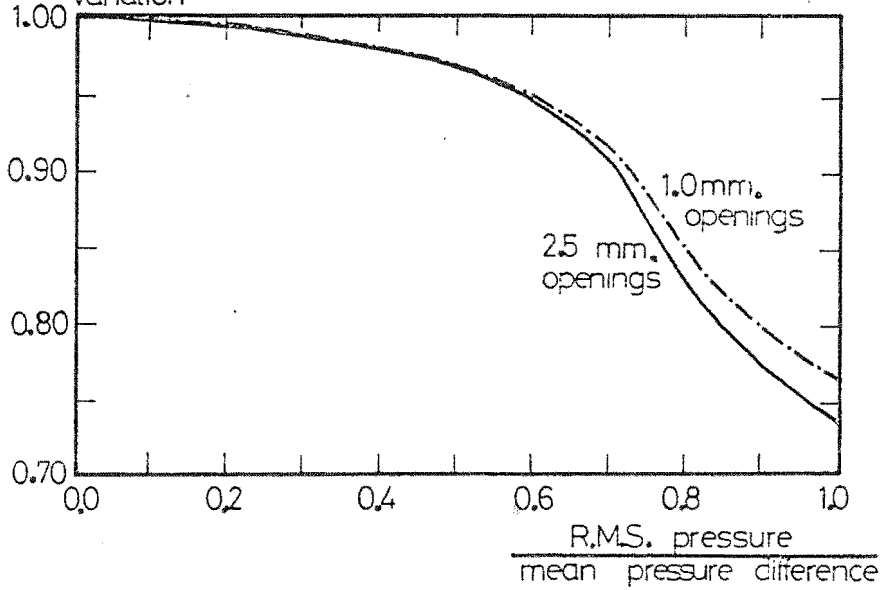


Figure 8.28. Variation of mean R.M.S. pressure coefficient with angle of incidence.

R.M.S. pressure coefficient, $C_{p_{RMS}}$

boundary layer I - - - - -
boundary layer II ————

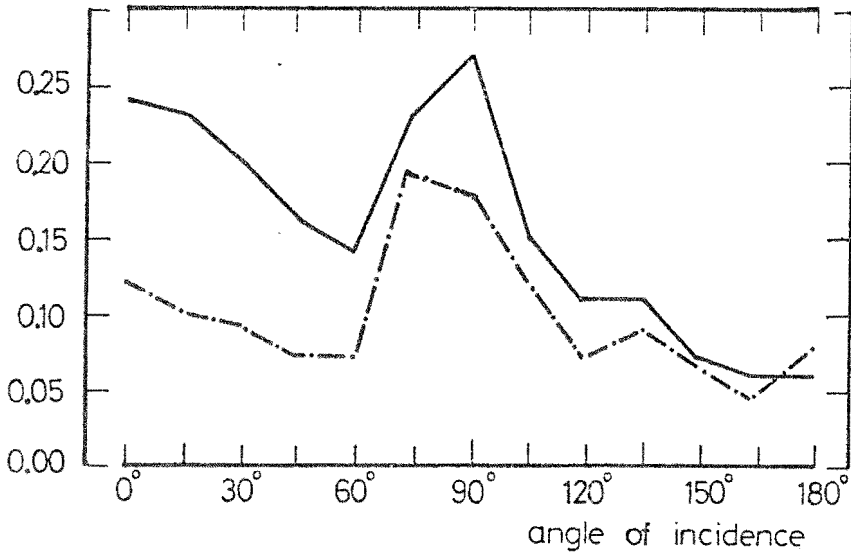


Figure 8.29. Variation of orifice operating efficiency with lateral flow velocity.

orifice efficiency, relative to performance with no lateral flow

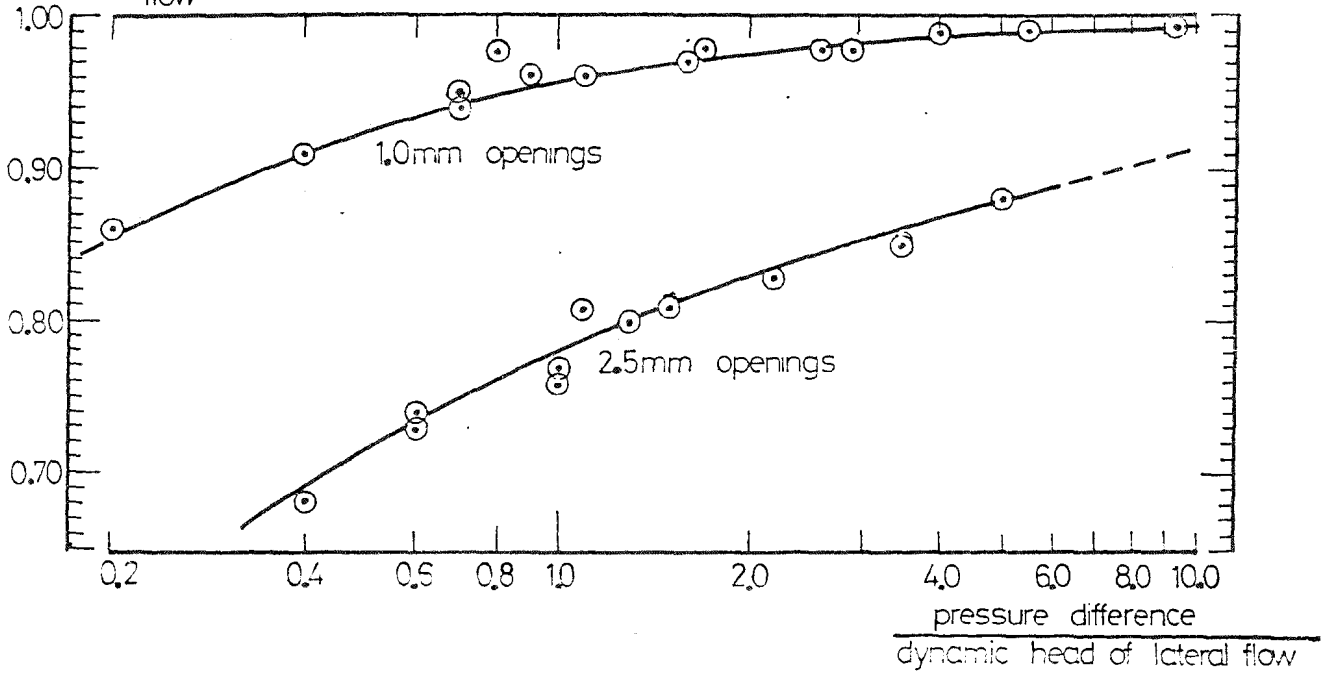
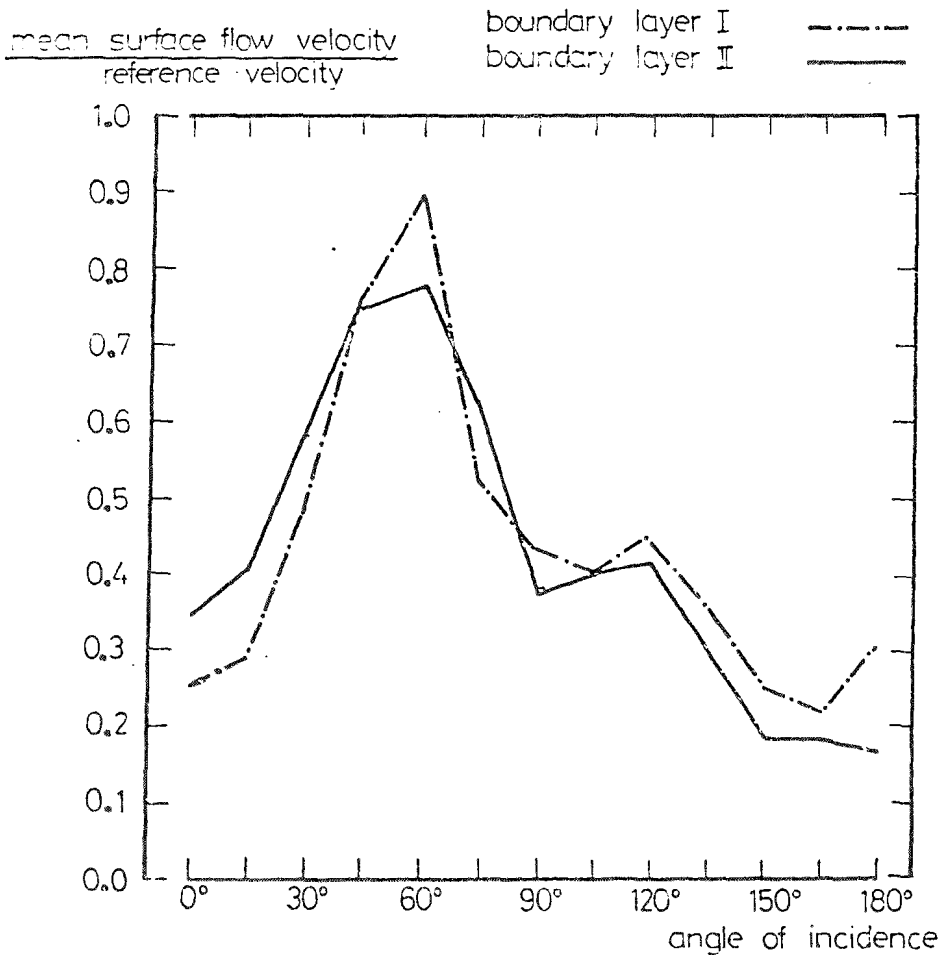


Figure 8.30. Variation of mean lateral flow velocities, expressed relative to the free stream roof height velocity, with angle of incidence.



9. A DISCUSSION ON DESIGN METHODOLOGIES

9.1 Introduction

9.1.1 The model studies discussed previously have demonstrated that ventilation rates and pressure difference distributions cannot be predicted absolutely accurately if the simplifying assumptions made in natural ventilation theory are used. However ventilation rates predicted using this type of analogue, at least in situations of wind induced cross ventilation, are within acceptable accuracy limits when considered in relation to the accuracy of other input variables. Natural ventilation is caused by naturally occurring motive forces, and consequently, ventilation rates are variable and dependent upon the meteorological conditions occurring at the building. Three major meteorological factors are normally assumed to affect natural ventilation; wind speed (which may be further subdivided into mean speed, turbulence intensity and wind speed profile), external temperature and wind direction. In order to develop suitable methodologies for predicting design ventilation rates careful consideration of the appropriate design meteorological conditions must be made.

9.1.2 The choice of appropriate meteorological design conditions varies with the situations the designer wishes to investigate. Generally three situations will be of greatest interest to the designer when considering the design of natural ventilation in buildings. These are:

1. the maximum rate of heat loss from the building under winter design conditions. A considerable proportion of the total heat loss of a building takes place because of losses due to infiltration or ventilation.
 - Consequently an estimate of the infiltration rate when the heat loss from the building is a maximum must be made in order to size heating plant and distribution networks.
2. the average rate of heat loss from the building throughout the heating season. An assessment of the average infiltration rates must be made to estimate running costs for the building.
3. the degree of environmental control available in proposed designs in summer conditions. At an early stage in the design process a decision must be made on the environmental control methods to be used. The feasibility of using natural ventilation for controlling internal conditions will affect the need for mechanical ventilation and may limit the permissible degree of glazing or permissible building depth. In this context the designer must be able to evaluate the amount of ventilation possible under design conditions so that an approximate estimate of the likely quality of environmental control can be made.

9.1.3 The design methodologies currently available have been discussed critically in section 2.4. In this chapter some of the factors affecting the development of

such methodologies are considered briefly in relation to the methods currently available and possible alterations or additions to the methods suggested.

9.2 The prediction of infiltration and ventilation rates for heat loss calculations

9.2.1 The methodologies currently available for predicting infiltration rates in buildings, are of two types; those using the air change method and those based on the crack method. Of these the more objective and accurate are those based on the crack method. Fully computerised methodologies based on this method have been suggested (Nelson, 1971). However even with the more sophisticated analytical techniques significant errors will normally be produced because of the inaccuracies due to data errors and the simplifying assumptions made. Consequently in most situations simplified methodologies based on hand calculations or nomograms will be of sufficient accuracy. Of the methodologies noted, the most comprehensive method appropriate for simple design calculations is probably the crack method presented in the I.H.V.E. Guide (I.H.V.E., 1970). Consequently it was decided to use this method as a basis for discussing the limitations of the current methodologies and the areas in which realistic improvements to them may be made.

9.2.2 The I.H.V.E. method for predicting infiltration rates in buildings is described in section 2.4 and in

greater detail in paragraph 3.4.13. The use of the method for estimating design heat loss rates may be criticised in particular because significant errors are introduced due to over-simplification of the assumed meteorological design conditions. The method calculates a maximum likely infiltration rate, rather than an infiltration rate applicable to conditions of likely maximum heat loss. This rate is found assuming an extreme wind speed value and consequently it is assumed that stack effect is always of secondary significance. Heat losses are then estimated by calculating the heat loss due to the maximum infiltration rate, assuming a simultaneous occurrence of the maximum likely temperature difference. Because the frequency of occurrence of combined high wind speeds and low temperatures is relatively small significant overestimates of infiltration heat losses and underestimates of the importance of stack effect in design situations are made using this method.

9.2.3 In the above method one standard meteorological wind speed is assumed to be representative of conditions over the whole of the United Kingdom. The variation of meteorological wind speed in inland areas throughout the country is relatively small, ten percentile wind speeds for Kew, Abingdon, Keele and Renfrew being 7.2, 7.3, 6.8 and 7.7 m/s. respectively (M.O., 1968) a variation of the order of $\pm 10\%$. Consequently this approximation may be made with reasonable justification. However considerably

higher wind speeds are noted at coastal sites, for example at South Shields and Fleetwood the corresponding speeds are 8.8 m/s. and 9.3 m/s. respectively, due to the increased exposure of the sites. These should be allowed for by increasing the exposure rating for areas of this type if systematic errors in site wind speed are to be avoided. The effect of building orientation is disregarded in calculating the maximum infiltration rate. This would also seem to be justified as meteorological mean wind speeds are relatively constant as wind direction varies in most inland areas. At Kew, for example, the fifty percentile wind speed varies between a minimum of 3.5 m/s. for winds coming from $225^{\circ} - 315^{\circ}$ and a maximum of 3.8 m/s. for winds coming from $135^{\circ} - 225^{\circ}$, (Chandler, 1965). Considerably greater variations would normally be expected due to different local ground roughness conditions if this varied with direction around the building. Consequently the design meteorological wind speed may reasonably be assumed to come from whichever is the worst direction for the building being studied.

9.2.4 When considering infiltration heat losses both wind speed and temperature difference are important and the pattern of simultaneous variation of wind speed and external temperature will determine heat losses. Lacy (Lacy, 1972) recommends that bivariate analyses of wind speed and external temperature be used for determining meteorological design conditions. Bivariate analyses show which combinations of temperature and wind speed

occur preferentially, and, in relation to the calculation of heat loss, the frequency of occurrence of combinations of low temperatures and high wind speeds. In particular bivariate analyses show that combinations of low temperature and high wind speed occur relatively infrequently. This effect has been analysed empirically by Billington (Billington, 1966), who suggested that ventilation rates calculated ignoring this effect would represent significant overestimates of the actual rates. Full bivariate analyses are not suitable for simplified prediction techniques of the type being discussed as the data format is too complex to handle easily; they are much more suited to fully computerised predictive techniques. A more useful form for the meteorological information would be the provision of design wind speeds applicable to specified outside temperature ranges. Using this method a suitable design wind speed could be assumed for the external temperature range under consideration.

9.2.5 In Figure 9.1 the variation of three design hourly wind speeds with temperature are presented. The design wind speeds are fifty percentile, ten percentile and one percentile wind speeds for a site at Abbots Langley (Page, 1971). The curves shown are smoothed curves found by calculating, for each temperature, the mean of the appropriate wind speed values for that temperature and the two values at immediately adjacent temperatures. All three curves show similar behaviour with change in external temperature. In particular the design wind

speeds become much lower at very low external temperatures. Design temperatures used for calculating heat losses in the United Kingdom vary between -1°C and -6°C , and depend on the building shape and the overload capacity of the plant. Figure 9.1 clearly shows that in this region the assumption of a 9 m/s. design wind speed (which approximates to a one percentile wind for all conditions) in combination with a -1°C external temperature, as a basis for calculating infiltration heat losses, would result in very conservative plant sizing.

9.2.6 A more suitable design criteria might be the use of a design wind speed which is the npercentile wind speed for the temperature of -1°C (or alternatively for a range of temperatures below -1°C), as it is for conditions at or below this temperature that design heat loss calculations are made. It can be seen that in some cases, for example using a design temperature of -6°C , this method would still result in a conservative estimate, as the design speed at this temperature would be still lower. However, the amount of overdesign would be significantly reduced. The determination of a suitable reduced design wind speed is a complex task which is the problem of the meteorologist. However for the conditions $0^{\circ}\text{C} \geq T \geq -1.1^{\circ}\text{C}$ the fifty percentile, ten percentile and one percentile wind speeds at Abbots Langley are 0.83, 0.75 and 0.75 of the corresponding values for all temperature conditions. In the same way that arguments may be made for adopting single design

wind speeds and design temperatures throughout the country so these modified wind speeds may be typical of other areas. This may be confirmed to some extent, as estimated ten percentile wind speeds for the conditions $0^{\circ}\text{C} \geq T \geq -1.1^{\circ}\text{C}$ were found to be approximately 0.8, 0.8 and 0.6 of the corresponding values for all temperature conditions at Manchester Airport, London Airport and Renfrew respectively. Consequently it is suggested that, for calculating infiltration heat losses, a modified design wind speed could be used. An appropriate value for this would have to be determined from more detailed studies, but from the limited set of observations considered it would seem that a value of approximately 75% of the corresponding design wind for all temperature conditions might be suitable. The resulting design infiltration rates would be of the order of 0.67 of previously calculated values, which agrees reasonably well with Billington's conclusion that more realistic building heat loads could be calculated by halving the normal design rate of heat loss due to infiltration.

9.2.7 When calculating maximum infiltration rates the assumption that stack effect will have a negligible effect on the gross ventilation rate for the building is made. Allowance for stack effect is made, when assessing the distribution of heat loads throughout the building, by increasing the calculated infiltration rate by 20% on the lowest floor (the allowance reducing linearly until the building mid-height is reached). Above the mid-height

of the building no allowance for stack-induced infiltration is made as the stack effect will tend to cause exfiltration, which creates no additional heat load. The use of an approximation of this type, when considering infiltration at less extreme wind speeds, such as wind speeds at low temperatures or wind speeds typical of mean conditions, is no longer appropriate. In these conditions, when the relative importance of stack effect is much greater, the combined effect must be considered more carefully.

9.2.8 The prediction of gross ventilation rates and the distribution of ventilation under combined wind and stack effect conditions is complex. However acceptably accurate estimates of the combined ventilation can be made by calculating the ventilation due to each effect acting alone, and then combining the results. Consequently nomograms for predicting the ventilation due to wind acting alone and stack effect acting alone could be used to make a more realistic assessment of other design conditions. Suggested nomograms are presented in Figures 9.2 and 9.3.

9.2.9 A nomogram for predicting wind induced ventilation is presented in Figure 9.2. The form of the nomogram is based on the method given in the I.H.V.E. Guide, with the exception that the estimates may be made at different meteorological wind speeds, and can consequently be made for a greater range of conditions.

Also, the window cracks are assumed to have a flow exponent of 0.67 as this is thought to be more representative of actual values (see Figure 4.5). The chart is used to obtain a basic ventilation rate, which is found by estimating, initially, a design pressure difference, dependent upon the building's surroundings, it's height and the meteorological wind speed. From this pressure difference and the mean glazing leakage coefficient a basic ventilation rate can be found. Suggested values for meteorological wind speeds are given in Table 9.1.

TABLE 9.1 Suggested approximate meteorological wind speeds for infiltration rate calculations

Maximum infiltration rate	9.0 m/s.
Infiltration rate for maximum heat loss	6.5 m/s.
Mean infiltration rate	3.5 m/s.

Having found a basic infiltration rate the total infiltration rate could then be found using correction factors to allow for internal subdivision of the building, and a representative crackage length, in the same way as is recommended in the I.H.V.E. Guide method.

9.2.10 A nomogram suitable for predicting stack-induced ventilation, developed from a series of studies carried out using the natural ventilation analogue described in Chapter 5, is presented in Figure 9.3. The chart is of a similar form to that which predicts

wind-induced ventilation and is also used to estimate a basic ventilation rate. From a design pressure difference (found from the building height and design temperature difference) and assuming a relative stairwell door flow resistance value and the mean glazing leakage coefficient, the basic ventilation rate can be found. The magnitude of stack-induced ventilation is determined, to a large extent, by the resistance of the stairwell doors, as all the air flowing through the windows on one floor has to pass through the doors to travel to other floors. Stack effect may often be assumed to be less important than is realistic because the doors to vertical shafts, which are designed to be relatively air tight, are assumed to be always closed. In practice the vertical shafts are major circulation routes, particularly in tall buildings, and these doors will be open for significant proportions of the time that a building is in use. Consequently stack effect can only be accurately assessed by taking into account the likely pattern of use of the stairwell doors. To illustrate this effect estimated stairwell door resistances for different patterns of use are presented in Table 9.2. Having found the basic infiltration rate the total infiltration rate could easily be found using the correction factors as given in the Guide, and a representative crackage length of one half of the total crackage length for the building.

9.2.11 The total infiltration rate for conditions where combined wind-induced and stack-induced ventilation

TABLE 9.2 Effective stairwell door resistances for different patterns of use to illustrate the effect of door usage on vertical flow resistance.

(calculated using an assumed 4 second door opening)

Double door, 3 mm. gap, closed permanently	160 m ³ /hr. mm.wg. ^{0.5}
Double door, 5 mm. gap, closed permanently	250 m ³ /hr. mm.wg. ^{0.5}
Double door, one leaf opening, c. 20 times/hr.	750 m ³ /hr. mm.wg. ^{0.5}
Double door, one leaf opening, c. 50 times/hr.	1,500 m ³ /hr. mm.wg. ^{0.5}
Double door, permanently open	25,000 m ³ /hr. mm.wg. ^{0.5}

are acting simultaneously can be approximated by assuming that the combined rate is equal to the higher rate caused by one effect acting alone (Dick, 1950). This effect was investigated using the digital analogue for several building forms. The results suggested that the errors caused by the use of this assumption were small in most cases. The errors were greatest when the wind-induced ventilation rate was equal to the stack-induced ventilation rate; the assumed values being 10% - 20% smaller than the corresponding computed combined values. The errors rapidly reduced in size at other values. The distribution of maximum infiltration load on different floors may also be relatively easily estimated by comparing the total infiltration rates due to wind acting alone and stack effect acting alone. The variation of combined infiltration rate, at different floor levels,

with the relative magnitude of stack induced ventilation is shown in Figure 9.4. The increase in the combined infiltration rate decreases approximately linearly with height; a simplification which may be made with acceptable accuracy in estimating the variation of infiltration loads with height. It is hoped that the development of a design method based on these assumptions would produce significantly more accurate predictions without adding too greatly to the complexity of the methodology.

9.3 The prediction of possible ventilation rates in buildings.

9.3.1 The development of a methodology for predicting possible ventilation rates in buildings for assessing the degree of environmental control possible is very difficult. Whilst design infiltration rates are mainly dependent upon the air-tightness of elements of the building and the external meteorological conditions, ventilation rates are predominantly dependent on the pattern of use of the building by it's occupants. Two aspects of ventilation are of primary importance when considering the feasibility of natural ventilation for environmental control; the degree of individual control available and the maximum amount of ventilation possible in design situations without any compromise of other aspects of the use of the building.

9.3.2 Little advice is available to the designer concerning the evaluation of natural ventilation in these situations. The only applicable technique noted is that given in the I.H.V.E. Guide, 1970, and described in paragraph 2.4.4. The recommendations are inadequate for determining the feasible quality of natural ventilation in buildings for several reasons:

- a) the method disregards building exposure. Building height and location largely determine mean site wind speeds, and the wind speed determines the magnitude of the available motive forces.
- b) the method disregards the permissible open area available for ventilation. The likely ventilation rate obviously depends on the open area of ventilation opening. In many urban areas the permissible open area may be restricted due to problems of noise control or security and this factor will often affect the feasibility of using natural ventilation in these areas.
- c) the figures given are presented directly as air change rates. In a building with a constant area of ventilation opening the air change rate is dependent upon the building depth. Under any given conditions the air flow rate through the building will be relatively constant as building depth changes, but the air change rate

will decrease as the building depth increases. In many situations a designer is concerned with establishing a permissible building depth for given site conditions in order to compare the design constraints imposed by the use of natural ventilation with those of alternative methods of ventilation.

- d) the values found from the table are not related to the parameters which the designer can control and consequently the table gives no guidance as to how the performance can be altered by changes in design.

9.3.3 The development of an alternative methodology to predict the degree of individual control that can be obtained in a naturally ventilated building is not practicable at the present time. Individually an occupant may alter the window opening size in his room, and consequently alter the ventilation rate, however the precise rate and the effectiveness of the ventilation will depend upon the pattern of air flow throughout the building and the previous history of the ventilating air. Neither the accuracy of the digital analogue techniques nor the accuracy of the information available on likely detailed climatic conditions or patterns of use of buildings are sufficient to predict any meaningful performance figures of this type, and consequently the assessment of control can only be considered generally on a qualitative basis. A more practical concept for the

development of a methodology is the evaluation of a maximum ventilation rate for the whole building under normal summertime conditions. A design figure evaluated on this basis could be used to determine the practicability of natural ventilation for environmental control. If the maximum ventilation rate available under design conditions, and without interfering with other aspects of the use of the building, is sufficient to enable the mean thermal conditions of the building to be kept within acceptable limits then natural ventilation may be feasible. If not, then some mechanical control will be required.

9.3.4 An approach to a design methodology which might meet these requirements is suggested below. The method cannot be regarded as adequate to deal with all design situations, but it is hoped that it might form a more logical basis for further development than the method given in the I.H.V.E. Guide, 1970. The method is based on the use of a nomogram of a similar type to those used for predicting infiltration in buildings. A possible form of the nomogram is shown in Figure 9.5.

9.3.5 As an initial step in estimating the maximum ventilation rate possible an evaluation of the permissible open area of opening must be made. Window opening may be limited by many factors, some of which are security, safety, noise control, or the control of the ingress of dust or fumes. In many cases, particularly in urban

areas, the most serious of these factors will be noise, and this evaluation could be based on the required acoustical performance of the building facade. Consequently a simple nomogram is provided for calculating the approximate permissible open area of the facade. This nomogram is based on simple calculations of combined sound reduction indices for 70% solid wall, 30% single glazing and variable areas of open window. No allowances are made for transmission by other paths, and so the values found are only approximations of the actual likely performance of the building facade. Having found the permissible open area of facade the design meteorological conditions must be considered. The choice of design wind speed would be dependent upon the probability of occurrence of the other meteorological parameters considered in calculating the thermal loads on the building. In the case given a meteorological wind speed of 3.5 m/s. is assumed, which approximates to a mean wind speed for many areas. Other wind speeds could easily be used. In some cases, for example in sheltered areas, stack effect may be of greater significance than wind, and so the prediction of ventilation rates due to stack effect is also considered. Temperature differences of 4°C or 6°C are used. It is assumed that a maximum difference of 4°C might be appropriate to a high level of environmental control, (maximum mean daily internal temperature 23°C, assuming a maximum external daily temperature of 19°C), and that 6°C might be appropriate in

most cases for an acceptable standard of control.

9.3.6 It was found in the digital analogue studies that the mean ventilation rate per unit area of facade, averaged for all angles of incidence, was similar for both uniformly glazed building forms and forms glazed on two faces only. In both cases the mean ventilation rate for all angles of incidence was approximately 85% of the value calculated for a building glazed on two opposite faces at an angle of incidence of 0° . Consequently, when calculating the likely wind induced ventilation rate, this allowance for the effect of variation of angle of incidence is made.

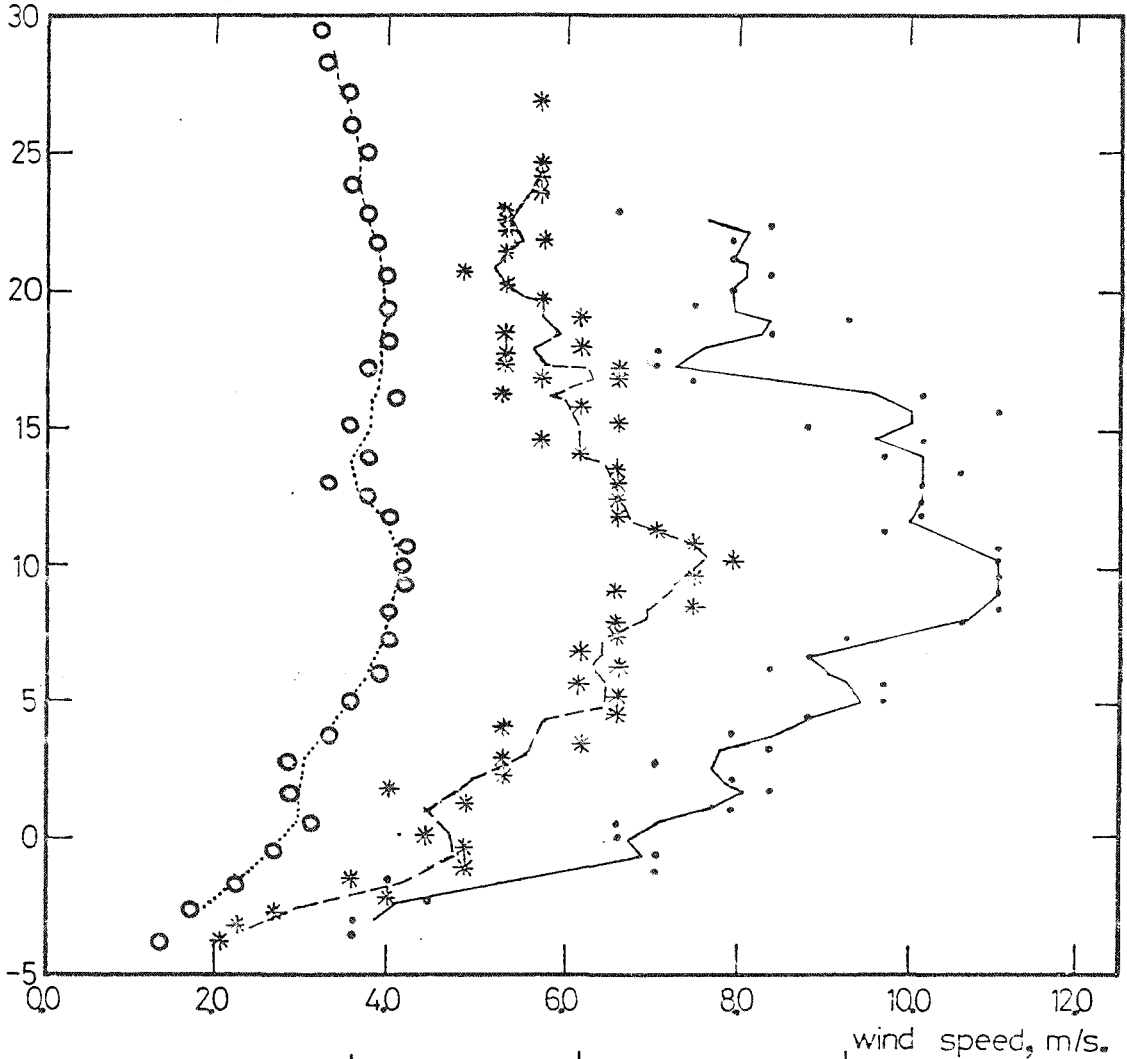
9.3.7 The nomogram could then be used in a similar manner to the ones used to predict building infiltration. By combining building height and location for wind-induced ventilation, or temperature difference for stack-induced ventilation, and considering whichever creates the greater ventilation rate, a pressure difference value could be found. From this figure, and knowing the permissible open area of facade, a maximum likely ventilation rate for the building per unit area of facade could be read off. The overall ventilation rate could be found by multiplying this figure by one half of the facade area of the building, and an air change rate found by dividing by the building volume. Finally it would be necessary to make allowance for the degree of internal subdivision of the building. It is likely that

this could be done using a series of simple factors, by which the basic ventilation rates could be modified, in a similar manner to the method suggested in the I.H.V.E. Guide infiltration calculation method. The development of a methodology of this type could not be regarded as completely acceptable as a technique for evaluating the adequacy of natural ventilation. One major limitation is that the methods, both for predicting infiltration rate and ventilation rate, caused by wind are really only applicable to relatively isolated buildings. In conditions where buildings are grouped closely the wind pressure acting across the building will normally be much lower. However this type of methodology probably offers a more realistic approach to the problem of assessing the feasibility of the use of natural ventilation in relation to the other design parameters which affect, or are affected by, ventilation in buildings.

Figure 9.1. Variation of design wind speed with external temperature at Abbots Langley.

1 %ile wind speed at specified temperature
10 %ile wind speed at specified temperature	-*-*-*-*
50 %ile wind speed at specified temperature	o-o-o-o-o

external temperature, °C.



50%ile wind speed all conditions

10%ile wind speed all conditions

1%ile wind speed all conditions

Figure 9.2. Nomogram for predicting wind induced infiltration.

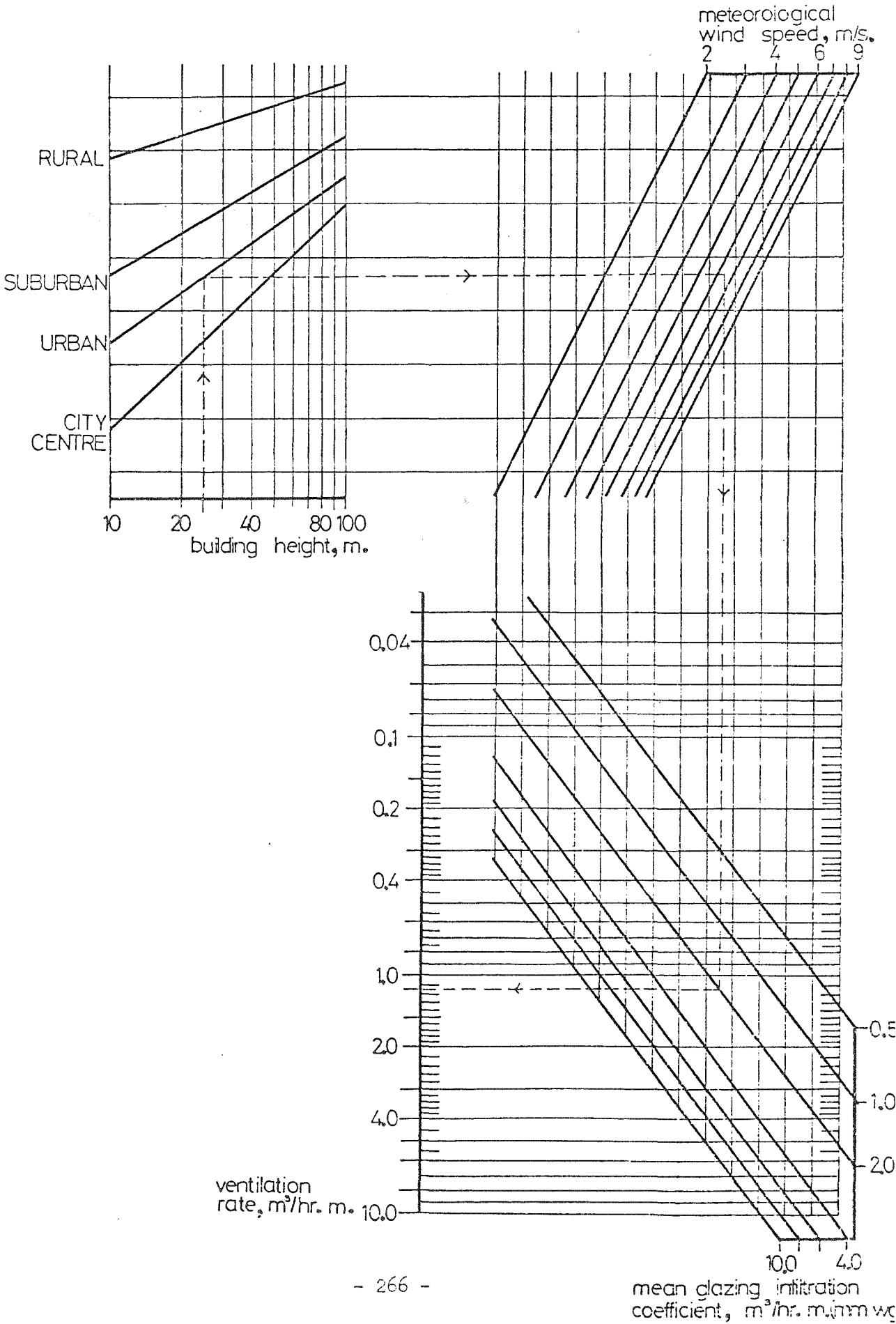


Figure 9.3. Nomogram for predicting stack induced infiltration.

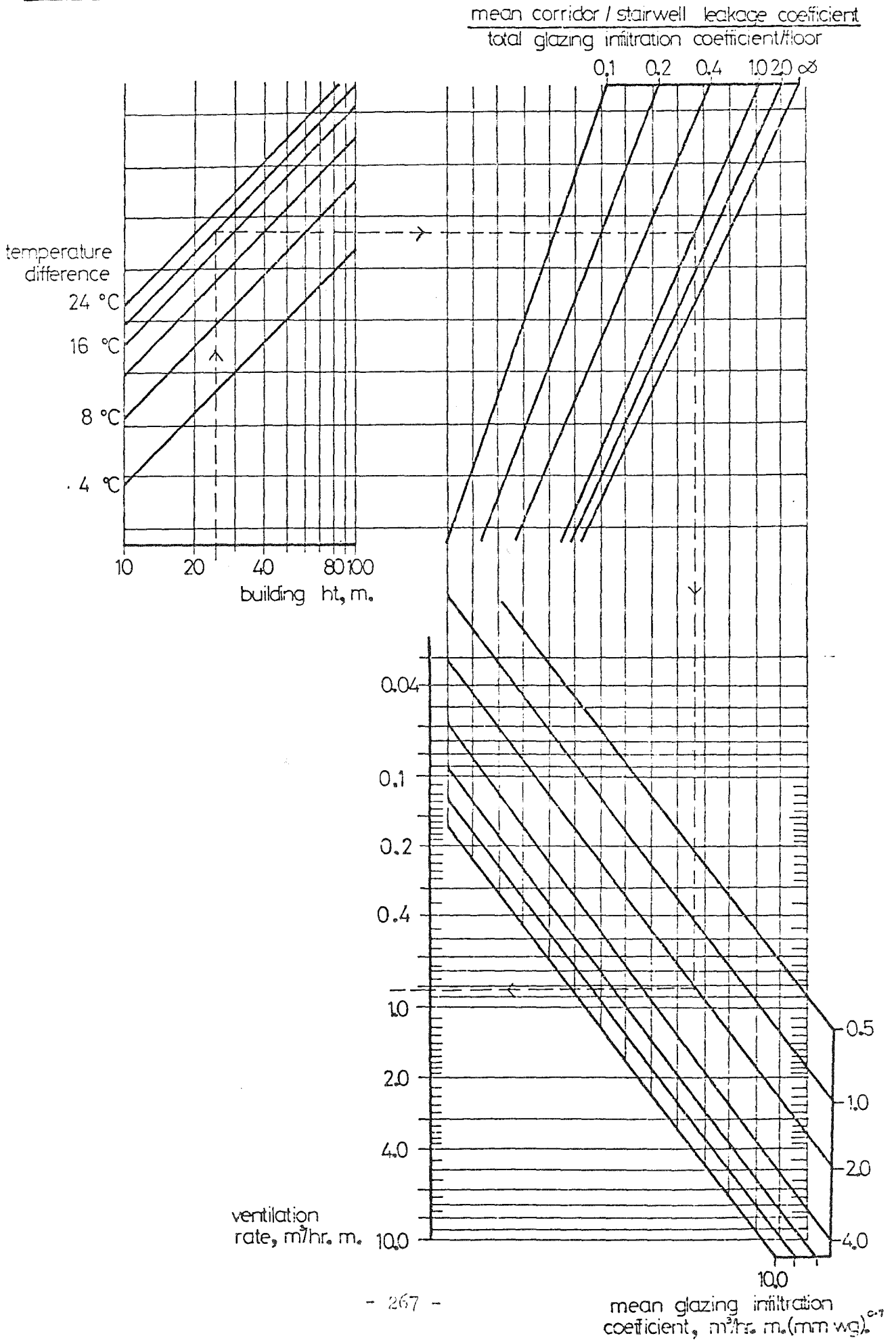


Figure 9.4, Variation of maximum combined ventilation rate with position and relative magnitude of wind and stack effects.

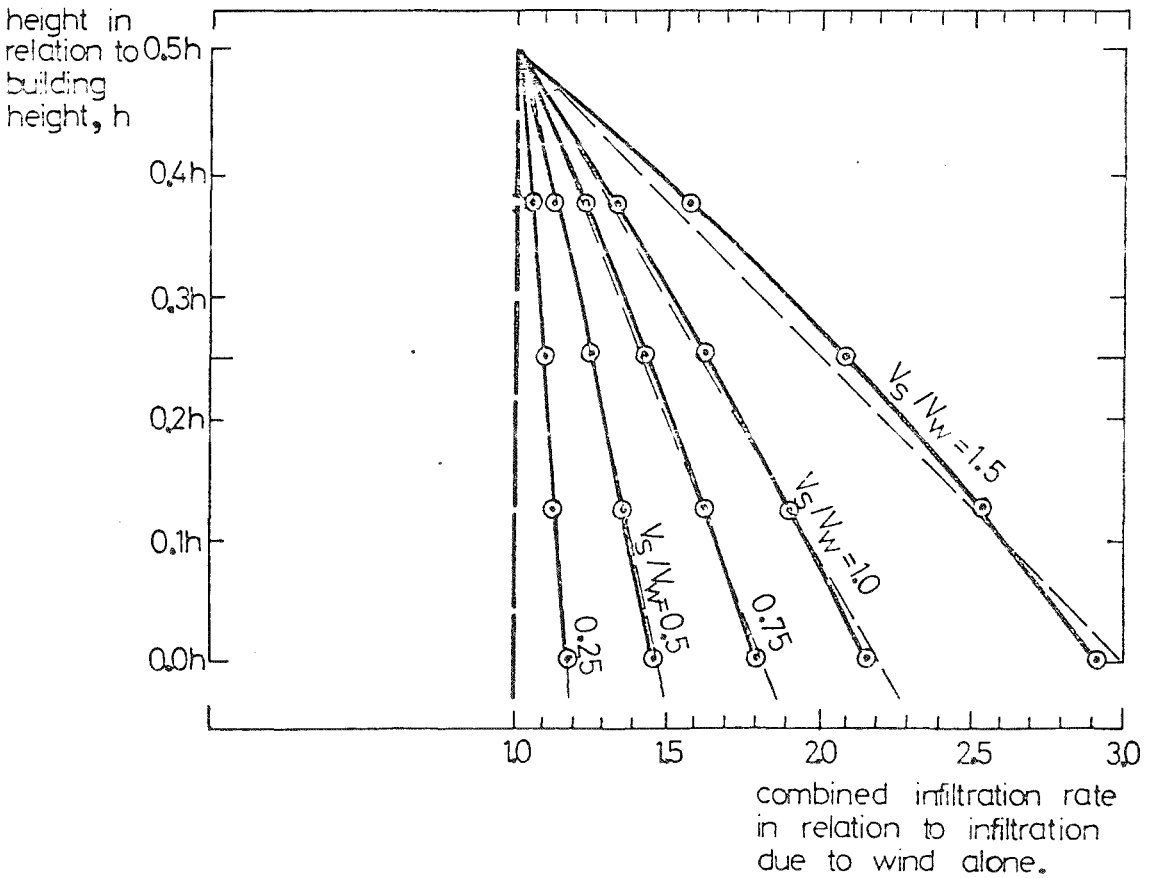
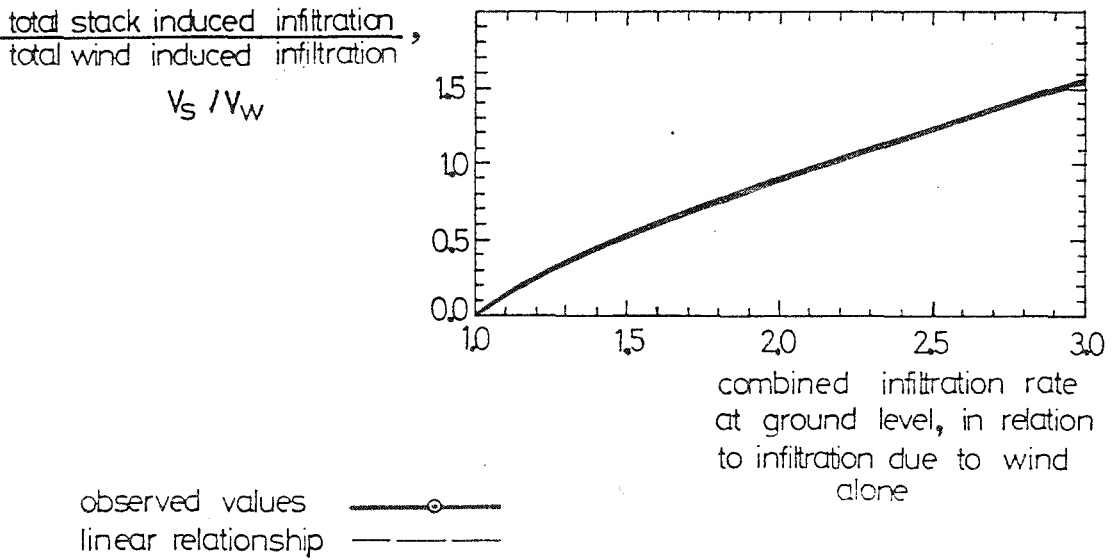


Figure 9.5.

Suggested nomogram for estimation of maximum ventilation rates available for environmental control in summertime.

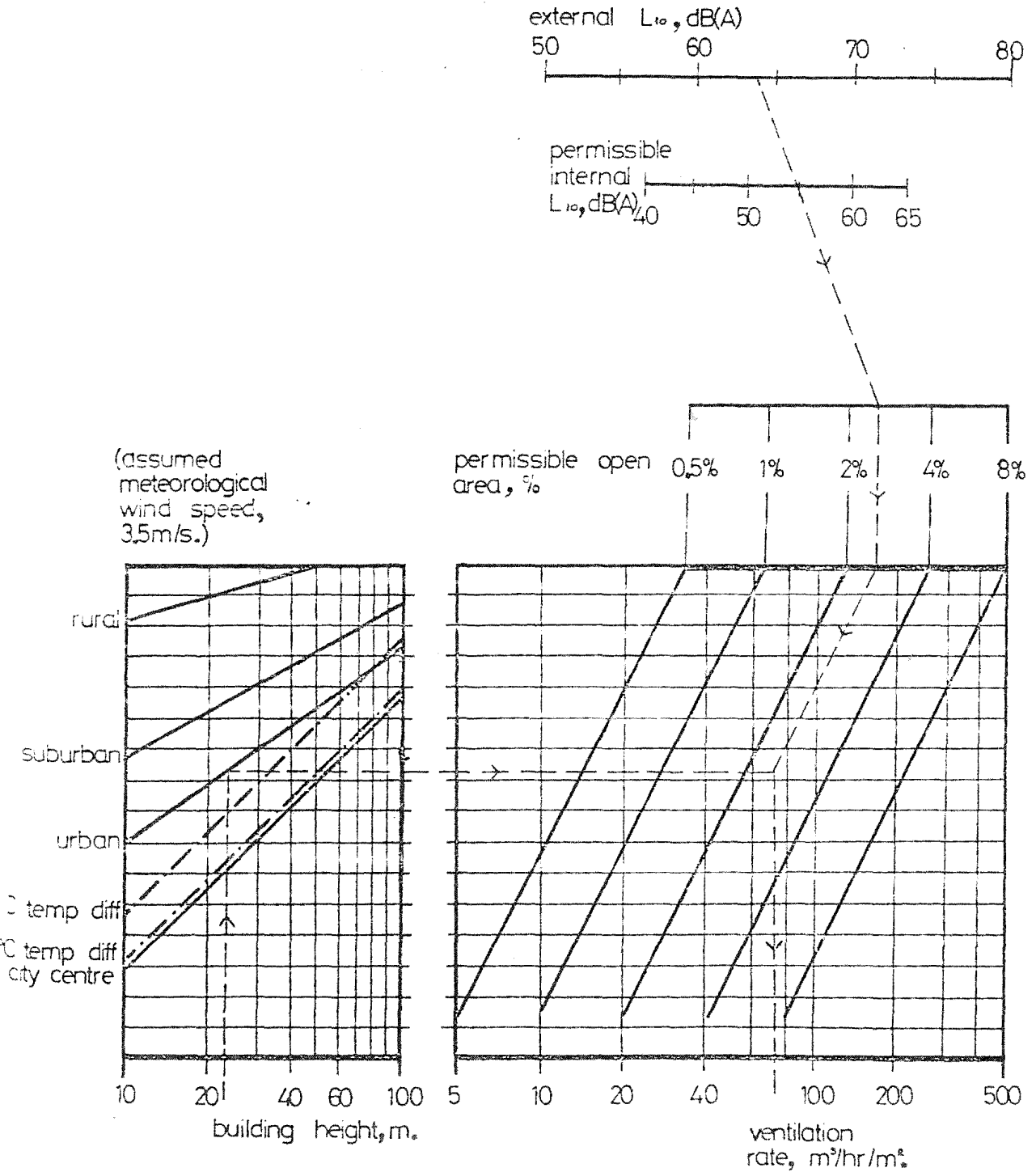
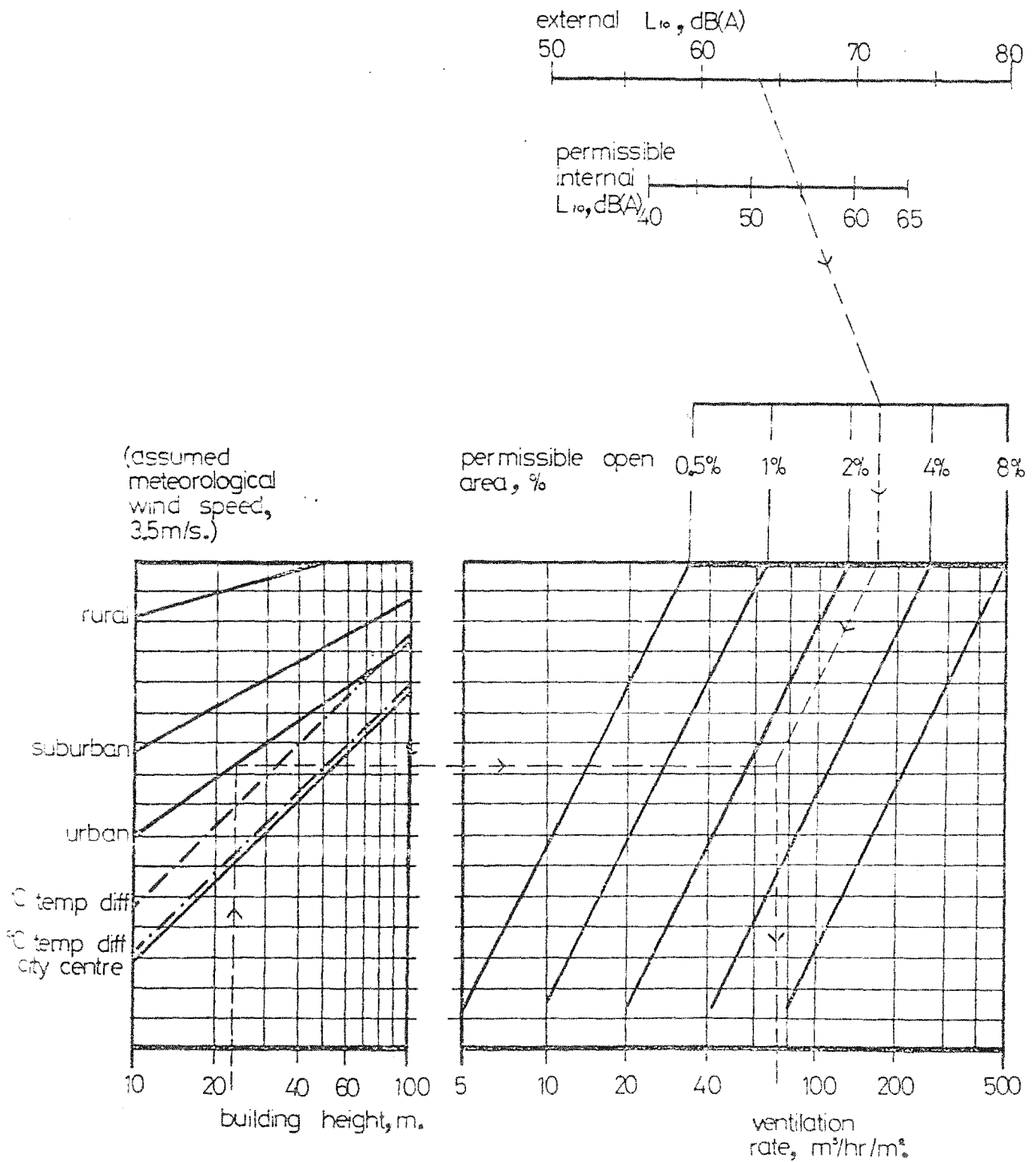


Figure 9.5.

Suggested nomogram for estimation of maximum ventilation rates available for environmental control in summertime.



10. CONCLUSIONS

10.1 The present analysis of techniques for predicting natural ventilation rates in buildings has been divided into two aspects; a consideration of the information required in order to carry out the calculations and an investigation of the validity of the assumptions made in the calculation procedures. These two aspects inter-relate as the accuracy of the operation of one aspect dictates the accuracy required of the other. A knowledge of both parts of the problem are needed if a balanced consideration of the feasibility of developing predictive methodologies is to be made.

10.2 A review of some previous studies of natural ventilation in buildings was made. It was found that most studies fell into one of two categories; full scale studies and digital analogue studies. Neither type of study was entirely adequate for assessing or developing detailed quantitative predictive techniques. In particular it was found that:

1. Full scale studies have established the relationships between ventilation rate and the major meteorological factors causing ventilation; wind speed and direction and temperature difference.
2. The ventilation rates measured in the full scale studies have been useful in terms of demonstrating the wide range of ventilation rates which might be found in these buildings under normal conditions.

However they are of insufficient accuracy to establish the influence of other design parameters, such as porosity or building shape, which are required to establish general predictive techniques.

3. The full scale studies have been carried out in a very limited range of building types (generally small domestic buildings), and consequently the infiltration rates measured are not representative of many other types of construction.
4. In the analogue work a number of simplifications have been made in order to calculate ventilation rates. In particular it is assumed that the aerodynamic forces, which act on the building, produce a series of quasi-static forces over the surfaces of the building, and that the internal temperature distributions are uniform throughout the building. Ventilation rates are then calculated assuming the building to be made up of a simple network of cells with specific flow resistances at the cell boundaries and no internal flow resistance.
5. None of the analogue studies which were reviewed have been compared with any full scale or model scale studies and so the significance of these simplifications has not been assessed.
6. There are considerable differences in the values of external pressure coefficients and typical window infiltration coefficients used in the various studies reviewed.

10.3 The major information requirements for calculating natural ventilation rates are wind speed, temperature difference, appropriate pressure coefficient values and air leakage characteristics of the building fabric and interior. Inaccuracies in wind speed and air leakage characteristic values were found to be of greatest significance in affecting the calculated ventilation rates as ventilation rates are approximately proportional to the assumed wind speed and air leakage coefficient values. Errors in assumed pressure coefficient values or temperature differences are less significant as the ventilation rates calculated are proportional to the square roots of these values. The likely accuracy levels of the major information requirements for natural ventilation calculations were investigated and are summarised below:

1. The largest errors in estimating ventilation rates are probably caused by the uncertainties in estimating site wind speeds. Wind speeds can be estimated above broad categories of generalised terrain using a logarithmic wind velocity profile. These estimates are not strictly appropriate in the general roughness height, within which most buildings are located, and are not correct where groups of buildings, situated close together, create a combined distortion of the mean wind conditions in the area. Waller et al (Waller, 1968) suggested that extreme site wind speeds can be estimated to an accuracy of

the order of $\pm 50\%$. Less extreme speeds can probably be estimated to a higher level of accuracy, but it is likely that relatively large uncertainties will still be involved in site wind speed estimates.

2. Large errors may also be caused by errors in assumed air leakage characteristics. Errors are largest in the assessment of infiltration leakage coefficients. The use of average coefficient values for generalised window types may lead to quite large errors as the variation within each type, due to differences in design, material and standard of construction is large. The use of test values for specific window units would result in much smaller errors although no figures for possible accuracy are available. The inaccuracies are probably less than those caused by the estimation of site wind speeds.
3. Errors caused by the use of incorrect pressure coefficient values are likely to be relatively small in most cases. The variation in values used by different workers show a range of the order of $\pm 20\%$. This range might cause errors in ventilation rate of about $\pm 10\%$, which is considerably less than the errors caused by the previously discussed mechanisms.

It was concluded, considering all information requirements, that it is unlikely that ventilation rates for a particular building can be predicted to an accuracy better than approximately $\pm 30\%$ because of errors in the data used.

10.4 A series of comparative studies were carried out in order to ascertain the validity of the assumptions used in natural ventilation theory and the accuracy of the calculations made using these assumptions. Two types of study were attempted; a comparison with the results of a small full scale study and with a series of model studies. In both cases comparisons of observed and calculated gross wind-induced ventilation rates were made. The major points from these studies may be summarised as follows:

1. The observed and calculated ventilation rates in the full scale study showed relatively large differences. It was thought that the differences between the observed and computed rates were largely due to errors in the observed ventilation rates, caused by diffusion of tracer gas and action of simultaneous stack effect, and to errors in estimating the leakage characteristics of the building. Because of the possible presence of errors due to these effects it was not possible to make an accurate assessment of the validity of the assumptions used in the calculations.
2. The results of the comparative model studies suggest that ventilation rates calculated using the digital analogue technique produce overestimates of the actual ventilation rates occurring. Measurements of the internal pressures in the models indicated that the errors in the computed ventilation rates were

caused mainly by reductions in the working efficiency of the openings in the windward face of the model.

The openings in the leeward face of the model appeared to operate at, or near to, their calibrated efficiency measured under steady conditions.

3. The reductions in operating efficiency of the openings in the model studies were thought to have been caused by two major mechanisms; the effect of lateral air flows travelling across the faces of the model interfering with the flow patterns at the air inlet positions, and the effect of fluctuations in mean pressure across the openings. Corrections made to the computed ventilation rates and pressure distributions, to allow for these phenomena, showed very good agreement with the observed ventilation rates and reasonable agreement with the observed pressure distributions.
4. The effect of data simplification was considered in the comparative studies. The use of mean pressure coefficients for a building face, rather than individual coefficients, which vary with position over the face, for calculating ventilation rates did not cause significantly greater inaccuracies in calculated ventilation rates. The presence of small-scale surface features on the model did not produce large changes in observed ventilation rates. It was concluded that these surface features may also be ignored without significantly affecting the accuracy

of the computed ventilation rates.

10.5 From these studies it was concluded that the use of a simplified ventilation theory, which assumes that a network of quasi-static forces acts over a building, will not accurately model conditions in a real building. In full-scale buildings with known air leakage characteristics and assuming known meteorological conditions it is possible that the errors between the actual and computed gross ventilation rates will be of a similar order of magnitude to those observed in the model studies, in which the computed rates were up to 20% higher than the observed rates. Insufficient information on lateral flow velocities and pressure fluctuations and the effect of these on full-scale ventilation openings is available, at the present time, for corrections to allow for these effects to be feasible in design calculations. However the digital analogue methods are of sufficient accuracy, when compared to the accuracy of the available input information, to be used to predict gross ventilation rates in complex buildings.

10.6 In relation to the errors caused by the accuracy levels of the input information available at the present time and simplifications made in the assumptions used in ventilation calculations, the development of more sophisticated analytical methods are not likely to produce more accurate design methodologies. The practical levels of accuracy which can be attained in predictive techniques are limited because ventilation rates are largely decided.

by the patterns of use of a building by its occupants, and these cannot be accurately predetermined. The prediction of maximum or normal infiltration heat loads in buildings could be improved by the use of design wind speeds which are related to their likelihood of occurrence with cold weather conditions, and by a more detailed consideration of the influence of stack-induced ventilation. No fully adequate methodology for evaluating the potential natural ventilation rates in buildings in summer conditions is available at the present time. A simple form of methodology could be developed by making an estimate of the potential ventilation rate under design meteorological conditions and with a maximum permissible open facade area, evaluated on a basis of acoustical or other relevant performance parameters of the building facade. The usefulness of the digital analogue may be greater in evaluating the performance of new ventilation systems; for example the practicality of combined mechanical and natural ventilation systems. A simple example of the use of the digital analogue for comparing the performance of a combined ventilation system with a totally naturally ventilated system is given in Appendix A7.

10.7 Some important limitations of the present work must be recognised. The most important restriction, which was imposed because most of the experimental work was carried out at model scale, was that the results were applicable to wind-induced gross ventilation rates only. Specific ventilation rates through small areas of the model

may vary considerably more from the computed rates than the total rate for the complete model did. This may be particularly important in situations where wind and stack effect are acting simultaneously. Under these conditions, particularly where wind and stack effect act locally in opposition to each other, the secondary effects due to lateral flow or pressure fluctuations may have greater influence in amending the actual ventilation rates. Consequently, although the computed gross ventilation rates have been shown to approximate reasonably to actual rates, the air flow distribution through a building may be considerably less accurately represented.

10.8 The comparative model studies have shown that ventilation rates cannot be accurately represented by an analysis assuming quasi-static forces to act at the building surfaces. Before the relevance of the model studies can be firmly established with relation to conditions in full-scale buildings further evidence of the validity of the model conditions in representing the appropriate full-scale conditions must be established. More detailed information on lateral air flow rates across building surfaces, pressure fluctuations at building faces and the influence of both these effects on changes in operating efficiency of full-scale ventilation openings is required. One aspect of flow conditions around the model which was not investigated was the effect of changes in wind direction around the model and the influence of these on the pattern of pressure fluctuations at the model surface.

The effect of additional disturbance due to the wakes from other buildings might also be expected to affect the air flow conditions around the model. As these conditions are representative of urban situations the importance of this aspect of the grouping of buildings must be evaluated before the quantitative results of the model work can be related realistically to full-scale conditions.

10.9 The results of the model studies are of particular significance in relation to some aspects of the wind loading of structures. Wind loads on building cladding are determined by the external aerodynamic forces which act on a building and also by the distribution of the pressure differences throughout the elements of the building. Several investigations of wind loads on building cladding have found that, relatively, very high wind loads are carried by the windward face. This phenomenon was observed in the model studies. The effect of changes in efficiency of the ventilation openings due to the secondary effects noted in the studies can be used to explain the wind loading distribution on the windward and leeward faces of full-scale buildings.

10.10 Some other aspects of natural ventilation were not investigated in the present study and require further study before fully adequate predictive methods can be established. A study or studies of these aspects would form a logical extension of the work. Probably the most significant area of uncertainty is in the ventilation of

spaces through one opening or openings in one wall only. In these conditions ventilation rates are probably determined largely by pressure fluctuations and turbulent diffusion, which makes the use of an analogue of the type used to predict cross ventilation in buildings inappropriate. A second aspect which requires further refinement, in order to improve predictive techniques, is the prediction of wind speeds and pressure coefficient values in urban conditions, where close grouping of buildings means that the standard wind speed prediction techniques are no longer applicable. In some naturally ventilated buildings the effect of non-uniform temperature distributions on ventilation patterns or the effect of air movement patterns in accentuating non-uniform temperature distributions, due to uncontrolled vertical air movement, is of considerable significance to the thermal comfort of the occupants. In order to study these situations with greater certainty the validity of the simple resistance network analogues which have been studied here must be established with greater accuracy in relation to the prediction of air movement patterns inside buildings.

APPENDICES

APPENDIX A1 A print-out of the Digital Analogue Programme
Developed to Determine Building Ventilation
Rates

A1.1 In this appendix a print-out of the digital analogue programme, as compiled for use on the Sheffield University I.C.L. 1907 Computer, is given. The programme is written in Fortran 1900 language. In the comparative model studies the programme was used as presented, except that the input wind speed was assumed to be the on-site wind speed. In order to do this card 68 was replaced by another card:

WIND = WINDMET

In all other respects the programme was identical. A typical set of results from the programme is presented in Appendix A5.

A1.2 The following are the major abbreviations used in the programme:

N(J)	Number of rooms on floor J
M	Room number
K	Number of floors in building
J	Floor number
FLTOFL	Floor to floor height, m.
HT	Building height, m.
WINDMET	Meteorological wind speed, m/s., at 10 m. height in open country
WIND	Site wind speed, at building roof height, m/s

TDIFF Interior/exterior temperature difference,
°C

SP Pressures generated by stack effect,
mm.wg./m/°C

VE(J,M) or VE1(J,M) Volumetric flow rate through the external opening in room M, floor J, m³/hr.

PDE(J,M) or PDE1(J,M) Pressure difference acting across the external opening in room M, floor J, mm.wg.

PCOEFPE(J,M) Pressure difference acting across the external opening in room M, floor J, expressed as a pressure coefficient

CL1(J,M) Total leakage coefficient for the external opening in room M, floor J, m³/hr/mm.wg.^{1/n}

ZI(J,M) Reciprocal of the flow exponent for the external opening in room M, floor J

PE(J,M) External pressure outside room M, floor J, caused by the wind speed, mm.wg.

PI(J,M) Total pressure outside room M, floor J, caused by wind and stack effect combined, mm.wg.

CE(J,M) External pressure outside room M, floor J, caused by the wind, expressed as a pressure coefficient relative to the free stream wind speed at the building roof height

VC(J,M) or VC1(J,M) Volumetric flow rate through the internal opening in room M, floor J, m³/hr.

PDC(J,M) or PDC1(J,M) Pressure difference acting across the internal opening in room M, floor J, m³/hr.

PCOEFFC(J,M) Pressure difference acting across the internal opening in room M, floor J, expressed as a pressure coefficient

CL2(J,M) Total leakage coefficient for the internal opening in room M, floor J, $m^3/hr/mm.wg.^{1/n}$

Z2(J,M) Reciprocal of the flow exponent for the internal opening in room M, floor J

VSTAIR(J) Volumetric flow rate through the corridor/stairwell opening, floor J, $m^3/hr.$

PSTAIR(J) Pressure in the stairwell, mm.wg.

CLS(J) Total leakage coefficient for the corridor/stairwell opening, $m^3/hr/mm.wg.^{1/n}$

ZS(J) Reciprocal of flow exponent for the corridor/stairwell opening, floor J

PDCS(J) Pressure difference acting across the corridor/stairwell opening, floor J, mm.wg.

PW(J) Corridor pressure, floor J, due to wind acting alone, mm.wg.

PC(J) Corridor pressure, floor J, due to wind and stack effect combined, mm.wg.

ZTOTVENT Sum of ventilation rates for all rooms, $m^3/hr.$

ZINFILT Sum of ventilation rates for all rooms where the flow direction is into the building, $m^3/hr.$

ZAVVENT Average room ventilation rate, $m^3/hr.$

ZSTDEV Standard deviation of all room ventilation rates, $m^3/hr.$

Appendix A1 Digital analogue programme to determine natural ventilation in buildings.

Line.	Column.	10	20	30	40	50	60	70	80
1									
2		JOB	BT5VENT4,	1807BT5C,	BILSBORROW				
3		FORTRAN	1, CR0(BT5VENT4PROG),	CR0(BT5VENT4DATA),	500,5000				
4		****							
5		DOCUMENT	BT5VENT4PROG						
6		PROGRAM	(BT5V1807BT5C)						
7		INPUT	1=CR0						
8		OUTPUT	2=LPO						
9		END							
10									
11		MASTER	VENTPLOT4						
12	C	THE PROGRAM	COMPUTES VENTILATION RATES AND PRESSURES BASED ON THE						
13	C	EQUATION FOR FLOW THROUGH AN ORIFICE	$V=CL * ((PD) ** 1/2)$						
14	C	EITHER FOR AN ARRAY OF CLIMATIC VARIABLES OF VALUE;							
15	C	WIND SPEED 0.001 1.0 2.0 4.0 6.0 8.0	TEMP DIFF 0.0 8.0 16.0 24.0						
16	C	WHERE INITIAL VALUES SHOULD BE 0.001 M/S. AND 8.0 DC.							
17	C	OR FOR ANY SPECIFIC CASE WHERE THE VALUES OF THE VARIABLES ARE NOT							
18	C	ANY OF THOSE OCCURRING IN THE CLIMATIC ARRAY							
19	C								
20	C	INDEPENDENT FLOOR BY FLOOR ANALYSIS GIVING PW(J)							
21	C								
22	C	N(J) IS NO. OF ROOMS ON FLOOR J	M IS ROOM NUMBER						
23	C	K IS NO. OF FLOORS	J IS FLOOR NUMBER						
24	C	VE OR VE1 IS VOLUME FLOW CMH. FROM EXTERIOR TO ROOM M							
25	C	VC OR VC1 IS VOLUME FLOW CMH. FROM ROOM M TO CORRIDOR							
26	C	VSTAIR IS VOLUME FLOW RATE CMH. FROM STAIR TO CORRIDOR							
27	C	PE OR PT IS EXT. PRESSURE MM.WG. OUTSIDE ROOM M							
28	C	CE IS PRESSURE COEFFICIENT OUTSIDE ROOM M							
29	C	PDE OR PDE1 IS PRESSURE DIFFERENCE MM.WG. FROM EXTERIOR TO ROOM M							
30	C	PCOEFFE IS PRESSURE DIFFERENCE FROM OUTSIDE TO ROOM M							
31	C	IN PRESSURE COEFFICIENT FORM							
32	C	PDC OR PDC1 IS PRESSURE DIFFERENCE MM.WG. FROM ROOM M TO CORRIDOR							
33	C	PCOEFFC IS PRESSURE DIFFERENCE ROOM M TO CORRIDOR							
34	C	IN PRESSURE COEFFICIENT FORM							
35	C	PC OR PW IS PRESSURE IN CORRIDOR MMWG.							
36	C	PSTAIR OR PSTAIR1 IS PRESSURE IN STAIRWELL MMWG.							

- 274 -

Appendix A1 Digital analogue programme to determine natural ventilation in buildings.

Line.	Column.	10	20	30	40	50	60	70	80	
37		DIMENSION PT (10,20),PW(10)								
38		DIMENSION VE(10,20),PDE(10,20),PDC(10,20),VC(10,20),PE(10,20)								
39		DIMENSION VF1(10,20),PDE1(10,20),PDC1(10,20),VC1(10,20),CE(10,20)								
40		DIMENSION Z1(10,20),CL1(10,20),Z2(10,20),CL2(10,20),PC(10),N(10)								
41		DIMENSION PSTAIR(10),VSTAIR(10),CLS(10),ZS(10),PDCS(10)								
42		DIMENSION PSTAIR1(10),PDCS1(10),PCOEFFE(10,20),PCOEFFC(10,20)								
43		READ(1,101)K								
44		READ(1,104)FLTOFL								
45		HT=FLTOFL*K								
46	101	FORMAT(12)								
47		DO 40 J=1,K								
48		READ(1,101)N(J)								
49		DO 41 M=1,N(J)								
50		READ(1,102)CL1(J,H),CL2(J,M),Z1(J,M),Z2(J,M)								
51	102	FORMAT(4F0.0)								
52	41	CONTINUE								
53		READ(1,103)CLS(J),ZS(J)								
54	40	CONTINUE								
55		READ(1,104)((CE(J,M),H=1,N(J)),J=1,K)								
56	104	FORMAT(20F0.0)								
57		READ(1,103)WINDMET,TDIFF								
58	103	FORMAT(2F0.0)								
59		DO 44 J=1,K								
60		WRITE(2,105)J,CLS(J),ZS(J)								
61		WRITE(2,106)								
62		DO 45 M=1,N(J)								
63	45	WRITE(2,107)CE(J,H),CL1(J,M),CL2(J,M),Z1(J,M),Z2(J,M)								
64	44	CONTINUE								
65	105	FORMAT(1H0,10HFLOOR NO.=,12,10X,4HCLS=,F6.1,5X,3HZS=,F5.2)								
66	106	FORMAT(20X,2HPE,10X,3HCL1,10X,3HCL2,10X,2HZ1,10X,2HZ2)								
67	107	FORMAT(20X,F4.2,6X,F7.1,6X,F7.1,8X,F4.2,8X,F4.2)								
68		WIND=WINDMET*1.62*((HT/500.0)**0.33)								
69		PWTOT=0.0								
70		DO 46 J=1,K								
71		DO 47 M=1,N(J)								
72	47	PE(J,M)=CE(J,H)*0.0624*WIND*WIND								

Appendix A1 Digital analogue programme to determine natural ventilation in buildings.

Line.	Column.	10	20	30	40	50	60	70	80	
73	46	CONTINUE								
74		D) 29 I=1,K								
75		CYCLE=1.0								
76		PETOT=0.0								
77		D) 18 M=1,N(J)								
78	18	PETOT=PETOT+PE(J,H)								
79		PEAVG=PETOT/N(J)								
80		D) 27 M=1,N(J)								
81		PDE(J,M)=(PE(J,M)-PEAVG)/2.0								
82		PDC(J,M)=(PE(J,M)-PEAVG)/2.0								
83		IF(PDE(J,M).EQ.0.0)PDE(J,H)=0.01								
84		IF(PDC(J,M).EQ.0.0)PDC(J,H)=0.01								
85	27	CONTINUE								
86	17	ALIM1=PDE(J,1)								
87		ALIM2=PDE(J,N(J))								
88		D) 11 M=1,N(J)								
89		IF(PDE(J,M).GE.0.0)VE(J,M)=CL1(J,M)*(PDE(J,M)**(1/Z1(J,M)))								
90		IF(PDE(J,M).LT.0.0)VE(J,M)=-CL1(J,M)*								
91	1	((ABS(PDE(J,M)))**((1/Z1(J,M))))								
92		IF(PDC(J,M).GE.0.0)VC(J,M)=CL2(J,M)*(PDC(J,M)**(1/Z2(J,M)))								
93	11	IF(PDC(J,M).LT.0.0)VC(J,M)=-CL2(J,M)*								
94	1	((ABS(PDC(J,M)))**((1/Z2(J,M))))								
95	20	D) 12 M=1,N(J)								
96		VE(J,M)=(VE(J,M)+VC(J,M))/2.0								
97	12	VC(J,M)=VE(J,H)								
98		H=0.0								
99		D) 25 M=1,N(J)								
100	23	H=H+VC(J,M)								
101		D) 19 M=1,N(J)								
102	19	VC(J,M)=VC(J,H)-H/N(J)								
103		IF(ABS(ABS(VC(J,1))-ABS(VE(J,1))).GT.								
104	1	(ABS(VC(J,1)/1000.0)))GO TO 20								
105		D) 13 M=1,N(J)								
106		IF(VE(J,M).GE.0.0)PDE(J,M)=(VE(J,M)/CL1(J,M))**Z1(J,M)								
107		IF(VE(J,M).LT.0.0)PDE(J,M)=-(((ABS(VE(J,M)))/CL1(J,M))**Z1(J,M))								
108		IF(VC(J,M).GE.0.0)PDC(J,M)=(VC(J,M)/CL2(J,M))**Z2(J,M)								

Appendix A1 Digital analogue programme to determine natural ventilation in buildings.

Line.	Column.	10	20	30	40	50	60	70	80	
109	13	IF(VC(J,M).LT.0.0)PDC(J,M)=-(((ABS(VC(J,M)))/CI2(J,M))**72(J,M))								
110		D) 14 M=1,N(J)/2								
111		F1=PDE(J,M)+PDC(J,M)-PDC(J,N(J)/2+M)-PDE(J,N(J)/2+M)								
112		F2=PE(J,M)-PE(J,N(J)/2+M)								
113		IF(F1.EQ.0.0)F1=F1+0.001								
114		IF(PE(J,M)-PE(J,N(J)/2+M))21,22,21								
115	22	PDE(J,M)=PDE(J,M)-F1*PDE(J,M)/((PDF(J,M)+PDC(J,M))*2.0)								
116		PDC(J,M)=PDC(J,M)-F1*PDC(J,M)/((PDF(J,M)+PDC(J,M))*2.0)								
117		PDC(J,N(J)/2+M)=PDC(J,N(J)/2+M)+F1*PDC(J,N(J)/2+M)/								
118	1	(PDF(J,N(J)/2+M)+PDC(J,N(J)/2+M))*2.0)								
119		PDE(J,N(J)/2+M)=PDE(J,N(J)/2+M)+F1*PDE(J,N(J)/2+M)/								
120	1	(PDE(J,N(J)/2+M)+PDC(J,N(J)/2+M))*2.0)								
121		GO TO 24								
122	21	F=F2/F1								
123		PDE(J,M)=PDF(J,M)*F								
124		PDC(J,M)=PDC(J,M)*F								
125		PDC(J,N(J)/2+M)=PDC(J,N(J)/2+M)*F								
126		PDE(J,N(J)/2+M)=PDE(J,N(J)/2+M)*F								
127	24	CONTINUE								
128	14	CONTINUE								
129		D) 15 M=1,N(J)-1								
130		G=(PE(J,M)-PDE(J,M)-PDC(J,M)-PE(J,M+1)+PDE(J,M+1)+PDC(J,M+1))/2.0								
131		PDE(J,M)=PDF(J,M)+G*PDF(J,M)/(PDE(J,M)+PDC(J,M))								
132		PDC(J,M)=PDC(J,M)+G*PDC(J,M)/(PDE(J,M)+PDC(J,M))								
133		PDC(J,M+1)=PDC(J,M+1)-G*PDC(J,M+1)/(PDC(J,M+1)+PDE(J,M+1))								
134	15	PDE(J,M+1)=PDE(J,M+1)-G*PDE(J,M+1)/(PDC(J,M+1)+PDE(J,M+1))								
135		CYCLE=CYCLE+1.0								
136		IF(CYCLE.GT.50.5)GO TO 31								
137		IF(ABS(ALIM1-PDE(J,1)).LT.ABS(PDE(J,1)/1000.0))GO TO 16								
138		GO TO 17								
139	16	IF(ABS(ALIM2-PDE(J,N(J))).LT.ABS(PDE(J,N(J))/1000.0))GO TO 28								
140		GO TO 17								
141	31	WRITE(2,108)								
142	108	FORMAT(1H1,30HCURRENT VALUES AFTER 50 CYCLES)								
143	28	PW(J)=((PE(J,1)-PDE(J,1)-PDC(J,1))+(PE(J,N(J))								
144	1	-PDE(J,N(J))-PDC(J,N(J))))/2.0								

Appendix A1 Digital analogue programme to determine natural ventilation in buildings.

Line.	Column.	10	20	30	40	50	60	70	80
145		PWTOT	=PWTOT	+PW(J)					
146		PWAVG	=PWTOT/K						
147		D) 30	M=1,N(J)						
148		VE1(J,M)	=VE(J,M)						
149		PDE1(J,M)	=PDE(J,M)						
150		PDC1(J,M)	=PDC(J,M)						
151	30	VC1(J,M)	=VC(J,M)						
152	29	CONTINUE							
153	C								
154	C								
155	C	CALCULATION	OF NFUTRAL	ZONE	HEIGHT				
156	C								
157	218	ZN=HT/2.0							
158		SP=0.0044*TDIFF							
159		D) 211	J=1,K						
160	211	PSTAIR(J)	=-(ZN-((J-1)*FLTOFL)-1.0)*SP						
161		VSTOT=0.0							
162		D) 212	J=1,K						
163		IF(PSTAIR(J),GE,0.0)	VSTAIR(J)=CLS(J)*(PSTAIR(J)**(1/7S(J)))						
164		IF(PSTAIR(J),LT,0.0)	VSTAIR(J)=-CLS(J)*(ABS(PSTAIR(J))**(1/7S(J)))						
165	212	VSTOT=VSTOT+VSTAIR(J)							
166		IF(VSTOT)240,299,242							
167	240	ZN=ZN-(HT/500.0)							
168		D) 213	J=1,K						
169	213	PSTAIR(J)	=-(ZN-((J-1)*FLTOFL)-1.0)*SP						
170		VSTOT=0.0							
171		D) 214	J=1,K						
172		IF(PSTAIR(J),GE,0.0)	VSTAIR(J)=CLS(J)*(PSTAIR(J)**(1/7S(J)))						
173		IF(PSTAIR(J),LT,0.0)	VSTAIR(J)=-CLS(J)*(ABS(PSTAIR(J))**(1/7S(J)))						
174	214	VSTOT=VSTOT+VSTAIR(J)							
175		IF(VSTOT)240,299,243							
176	243	ZN=ZN+(HT/1000.0)							
177		G) TO 299							
178	242	ZN=ZN+(HT/500.0)							
179		D) 215	J=1,K						
180	215	PSTAIR(J)	=-(ZN-((J-1)*FLTOFL)-1.0)*SP						

Line.	Column.	10	20	30	40	50	60	70	80	
181		VSTOT=0.0								
182		D) 216 J=1,K								
183		IF(PSTAIR(J),GE,0.0)VSTAIR(J)=CLS(J)*(PSTAIR(J)**(1/ZS(J)))								
184		IF(PSTAIR(J),LT,0.0)VSTAIR(J)=-CLS(J)*(ABS(PSTAIR(J))**(1/ZS(J)))								
185	216	VSTOT=VSTOT+VSTAIR(J)								
186		IF(VSTOT)244,299,242								
187	244	Z1=ZN-(HT/1000.0)								
188		G) TO 299								
189	299	D) 217 J=1,K								
190		PC(J)=PW(J)+((ZN-((J-1)*FLTOFL)-1.0)*SP								
191	217	PSTAIR(J)=PWAVG								
192		D) 220 J=1,K								
193		D) 219 M=1,N(J)								
194	219	PT(J,M)=PE(J,M)+(ZN-((J-1)*FLTOFL)-1.0)*SP								
195	220	CONTINUE								
196	C									
197	C									
198	C	CALCULATION OF COMBINED VENTILATION								
199	C									
200		D) 320 J=1,K								
201		PSTAIR1(J)=PSTAIR(J)								
202		PDCS(J)=PSTAIR1(J)-PC(J)								
203		DENOM=10.0								
204	399	PC(J)=PC(J)+PDCS(J)/DENOM								
205		PDCS1(J)=PSTAIR1(J)-PC(J)								
206		D) 321 M=1,N(J)								
207		PDE1(J,M)=(PDE(J,M)/(PDE(J,M)+PDC(J,M)))*(PT(J,M)-PC(J))								
208		RATIO=PDE1(J,M)/PDE(J,M)								
209		IF(RATIO,LT,0.0)GO TO 340								
210		PDC1(J,M)=PDC(J,M)*(RATIO**((Z2(J,M)/Z1(J,M))))								
211		G) TO 338								
212	340	PDC1(J,M)=-((PDC(J,M)*((ABS(RATIO))**((Z2(J,M)/Z1(J,M))))								
213	338	PDE1(J,M)=(PDE1(J,M)/(PDE1(J,M)+PDC1(J,M)))*(PT(J,M)-PC(J))								
214		RATIO=PDE1(J,M)/PDE(J,M)								
215		IF(RATIO,LT,0.0)GO TO 341								
216		PDC1(J,M)=PDC(J,M)*(RATIO**((Z2(J,M)/Z1(J,M))))								

Appendix A1 Digital analogue programme to determine natural ventilation in buildings.

Line.	A1 Column.	10	20	30	40	50	60	70	80	
217		GO TO 342								
218	341	PDC1(J,M)=- (PDC(J,M))*((ABS(RATIO))** (Z2(J,M)/Z1(J,M))))								
219	342	CONTINUE								
220		IF(PDE1(J,M),GE,0,0)GO TO 322								
221		VE1(J,M)=-CL1(J,M)*((ABS(PDE1(J,M))))** (1/Z1(J,M)))								
222		GO TO 323								
223	322	VE1(J,M)=CL1(J,M)*(PDE1(J,M))* (1/Z1(J,M))								
224	323	IF(PDC1(J,M),GE,0,0)GO TO 324								
225		VC1(J,M)=-CL2(J,M)*((ABS(PDC1(J,M))))** (1/Z2(J,M)))								
226		GO TO 325								
227	324	VC1(J,M)=CL2(J,M)*(PDC1(J,M))* (1/Z2(J,M))								
228	325	VE1(J,M)=(VE1(J,M)+VC1(J,M))/2.0								
229	321	VC1(J,M)=VF1(J,M)								
230		DO 326 M=1,N(J)								
231		IF (VE1(J,M),GE,0,0)GO TO 327								
232		PDE1(J,M)=-(((ABS(VE1(J,M)))/CL1(J,M))**Z1(J,M))								
233		GO TO 328								
234	327	PDE1(J,M)=(VE1(J,M)/CL1(J,M))**Z1(J,M)								
235	328	IF(VC1(J,M),GE,0,0)GO TO 329								
236		PDC1(J,M)=-(((ABS(VC1(J,M)))/CL2(J,M))**Z2(J,M))								
237		GO TO 326								
238	329	PDC1(J,M)=(VC1(J,M)/CL2(J,M))**Z2(J,M)								
239	326	CONTINUE								
240		WTOT=0.0								
241		DO 330 M=1,N(J)								
242	330	WTOT=WTOT+VE1(J,M)								
243		IF(PDCS1(J),GE,0,0)GO TO 331								
244		VSTAIR(J)=-CLS(J)*((ABS(PDCS1(J))))** (1/ZS(J))								
245		GO TO 332								
246	331	VSTAIR(J)=CLS(J)*(PDCS1(J))* (1/ZS(J))								
247	332	CONTINUE								
248		WTOT=WTOT+VSTAIR(J)								
249		IF(PDCS(J),GE,0,0.AND.WTOT,GE,0,0)GO TO 399								
250		IF(PDCS(J),LT,0,0.AND.WTOT,LT,0,0)GO TO 399								
251		PC(J)=PC(J)-PDCS(J)/DENOM								
252		IF(DENOM,GE,999,0)GO TO 398								

Appendix A1 Digital analogue programme to determine natural ventilation in buildings.

Line.	Column.	
253		DENOM=DENOM*10.0
254		GO TO 399
255	398	PC(J)=PC(J)+PDCS(J)/DENOM
256	320	CONTINUE
257		VELHEAD=0.0624*WIND*WIND
258		ZINFILT=0.0
259		ZNOROOM=0.0
260		ZTOTVENT2=0.0
261		ZTOTVENT=0.0
262		ZAVVENT=0.0
263		DO 336 J=1,K
264		DO 335 M=1,N(J)
265		PCOEFFE(J,M)=PDE1(J,M)/VELHEAD
266		IF(ABS(PCOEFFE(J,M)),GE.10.0)PCOEFFE(J,M)=0.0
267		PCOEFFC(J,M)=PDC1(J,M)/VELHEAD
268		IF(ABS(PCOEFFC(J,M)),GE.10.0)PCOEFFC(J,M)=0.0
269		ZTOTVENT2=ZTOTVENT2+(VE1(J,M)**2)
270		ZTOTVENT=ZTOTVENT+ABS(VE1(J,M))
271	335	IF(VE1(J,M),GT.0.0)ZINFILT=ZINFILT+VE1(J,M)
272	336	ZNOROOM=ZNOROOM+N(J)
273		ZAVVENT=ZTOTVENT/ZNOROOM
274		ZSTDEV=SQRT((ZTOTVENT2/ZNOROOM)-(ZAVVENT*ZAVVENT))
275	C	
276	C	
277	C	PRINTOUT OF RESULTS
278	C	
279		WRITE(2,301)WINDHET,TDIFF
280		WRITE(2,302)ZINFILT
281		WRITE(2,303)ZAVVENT
282		WRITE(2,304)ZSTDEV
283		DO 310 J=1,K
284		WRITE(2,305)
285		DO 311 M=1,N(J)-1,2
286		MM=M+1
287	311	WRITE(2,306)J,M,VE1(J,M),PCOEFFE(J,M),PDE1(J,M),PDC1(J,M)
288	1	,J,MM,VE1(J,MM),PCOEFFE(J,MM),PDE1(J,MM),PDC1(J,MM)

Appendix A1 Digital analogue programme to determine natural ventilation in buildings.

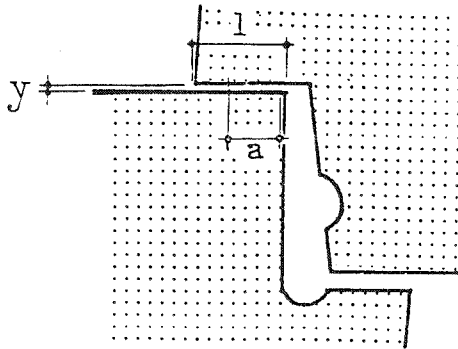
Line.	Column.	10	20	30	40	50	60	70	80	
289	310	CONTINUE								
290		WRITE(2,307)								
291		D) 339 J=1,K								
292	339	WRITE(2,308)J,VSTAIR(J),PSTAIR(J),PC(J)								
293	301	FORMAT(1H1,22HRESULTS FOR WIND SPEED,F5.2,								
294	1	29HM/S. TEMPERATURE DIFFERENCE,F5.2,3HDC.)								
295	302	FORMAT(1H0,29HTOTAL INFILTRATION RATE, CMH.,21X,F8.2)								
296	303	FORMAT(1H0,35HAVERAGE ROOM VENTILATION RATE, CMH.,15X,F8.2)								
297	304	FORMAT(1H0,46HSTANDARD DEVN. OF ROOM VENTILATION RATES, CMH.,								
298	1	4X,F8.2)								
299	305	FORMAT(1H0,10HFLOOR ROOM,5X,7HVE(CMH),5X,7HPDE(CP.,5X,3HMM),5X,								
300	1	7HPDC(MM),9X,10HFLOOR ROOM,5X,7HVE(CMH),5X,7HPDE(CP.,5X,3HMM),								
301	2	5X,7HPDC(MM))								
302	306	FORMAT(I4,3X,I2,5X,F8.2,5X,F5.2,3X,F7.3,5X,F7.3,9X,I4,3X,I2,5X,								
303	1	F8.2,5X,F5.2,3X,F7.3,5X,F7.3)								
304	307	FORMAT(1H0,5HFLOOR,10X,6HVSTAIR,6X,6HPSTAIR,12X,9HPCORRIDOR)								
305	308	FORMAT(I4,10X,F8.2,4X,F7.3,13X,F7.3)								
306	C									
307	C									
308	C	RECYCLING OF WIND AND TEMPERATURE VALUES								
309	C									
310		TDIFF1=1000.0								
311		IF(TDIFF.EQ.0.0)TDIFF1=8.0								
312		IF(TDIFF.EQ.8.0)TDIFF1=16.0								
313		IF(TDIFF.EQ.16.0)TDIFF1=24.0								
314		IF(TDIFF.EQ.24.0)GO TO 337								
315		TDIFF=TDIFF1								
316		IF(TDIFF.EQ.8.0.OR.TDIFF.EQ.16.0.OR.TDIFF.EQ.24.0)GO TO 218								
317		WIND1=1000.0								
318	337	TDIFF=0.0								
319		IF(WINDMET.EQ.0.001)WIND1=1.00								
320		IF(WINDMET.EQ.1.00)WIND1=2.00								
321		IF(WINDMET.EQ.2.00)WIND1=4.00								
322		IF(WINDMET.EQ.4.00)WIND1=6.00								
323		IF(WINDMET.EQ.6.0)WIND1=8.00								
324		IF(WINDMET.EQ.8.00)GO TO 400								

Appendix A1 Digital analogue programme to determine natural ventilation in buildings.

Line.	Column.	
	10	
	20	
	30	
	40	
	50	
	60	
	70	
	80	
325		WINDMET=WIND1
326		IF(WINDMET.EQ.1.00.OR.WINDMET.EQ.2.00.OR.WINDMET.EQ.4.00)GO TO 44
327		IF(WINDMET.EQ.6.00.OR.WINDMET.EQ.8.00)GO TO 44
328	400	STOP
329		EVD
330		FINISH
331		****

A2.1 If it is assumed that all diffusion of tracer gas in the full scale building studied by Tamura and Wilson, and used for the comparative study in Chapter 6, takes place through the window openings then it is possible to make an estimate of the order of magnitude of this effect.*

A2.2 Considering the crackage through which the helium will diffuse a simplified analysis may be made by considering only that part of the crackage where major resistance to flow occurs. This will be that part of the crack where the width is smallest. One may consider this as a channel of uniform width y , length l , and total channel length of L .



The helium gas concentration at one end of the crack will be approximately equal to the mean internal concentration, c_0 while the outer end may be assumed to have a concentration near to zero.

A2.3 At any point in the crack, a distance, a , from the outer end, considering a thin element, under steady state

conditions, and over a time scale which is short in comparison to the rate of decrease in the mean internal level in concentration of the tracer gas.

the net flow into the element =
the net flow out of the element

or $\frac{dc}{dt} = 0$

but by Fick's law

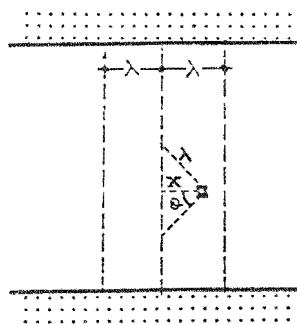
$$\frac{dc}{dt} = \frac{d^2c}{da^2}$$

then $c \propto ka$

or $c_a = \frac{a}{l} c_0$ (A2.1)

where c_a is the concentration of helium at a .

A2.4 Now if two adjacent elements are taken, of width λ and distances a and $(a - \lambda)$ from the outer edge where λ is the mean free path length of helium at N.T.P.



One can consider a small volume in the inner element of dimensions, dx, dy, dz and a distance x from the interface. The solid angle subtended at the interface by molecules travelling over their mean free path lengths can be

computed as:

$$\begin{aligned}
 &= \frac{\int_0^{\cos^{-1} x/\lambda} 2\pi \lambda \cdot \sin \theta \cdot d\lambda}{\lambda^2} \\
 &= \frac{\int_0^{\cos^{-1} x/\lambda} 2\pi \lambda \cdot \sin \theta \cdot \lambda d\theta}{\lambda^2} \\
 &= - (2\pi \cdot \cos \theta)_0^{\cos^{-1} x/\lambda} \\
 &= 2\pi (1 - x/\lambda) \quad \dots\dots (A2.2)
 \end{aligned}$$

A2.5 Then the probability of molecules crossing the interface from this volume

$$= \frac{2\pi (1 - x/\lambda)}{4\pi}$$

and the number of molecules escaping will be

$$= \frac{1}{2} (1 - x/\lambda) c_a \cdot dV$$

where dV is the element volume

$$= \frac{1}{2} (1 - x/\lambda) c_a \cdot dx \cdot dy \cdot dz$$

and the total number escaping from the element throughout the building crackage

$$\begin{aligned}
 &= \int_0^\lambda \int_0^y \int_0^L \frac{1}{2} (1 - x/\lambda) c_a \cdot dx \cdot dy \cdot dz \\
 &= \frac{1}{2} \left[x - \frac{x^2}{2\lambda} \right]_0^\lambda \cdot y \cdot L \cdot c_a \\
 &= \frac{1}{4} \cdot \lambda \cdot y \cdot L \cdot c_a = \frac{1}{4} \cdot y \cdot L \cdot \frac{a}{1} \cdot c_0 \quad \dots\dots (A2.3)
 \end{aligned}$$

but the number of molecules moving from the second element back to the first will be

$$\frac{1}{4} \cdot \lambda \cdot y \cdot L \cdot \frac{(a - \lambda)}{1} c_0$$

and the net loss of molecules will be

$$\frac{1}{4} \cdot \lambda \cdot y \cdot L \cdot \frac{\lambda}{1} c_0 \quad \dots\dots (A2.4)$$

but these will move at a speed V_m , where V_m is the mean molecular velocity. Thus the rate of loss of molecules will be

$$\frac{1}{4} \cdot \lambda \cdot y \cdot L \cdot \frac{\lambda}{1} \cdot c_0 \cdot \frac{V_m}{\lambda}$$

but the rate of loss of molecules of helium from the building is also equivalent to

$$- V_0 \cdot \frac{dc_0}{dt}$$

where V_0 is the building volume.

which gives an equivalent air change rate (c.f. equation 3.1)

$$= \frac{\lambda \cdot y \cdot L \cdot V_m}{4 \cdot l \cdot V_0} \quad \dots\dots (A2.5)$$

A2.6 In particular when the units of y and l are in mm., and L in m., V_0 in m^3 ., and V_m in m/s., then the apparent air change rate, /hr.

$$= \frac{900 \cdot \lambda \cdot y \cdot L \cdot V_m}{l \cdot V_0} \quad \dots\dots (A2.6)$$

In the full scale building

$$L = 10^2 \text{ m.}$$

$$y \approx 0.4 \text{ mm.}$$

$$l \approx 2.5 \text{ mm. (assumed)}$$

$$V_o = 3.4 \times 10^2 \text{ m}^3$$

$$V_m \text{ helium} = 12 \times 10^2 \text{ m/sec.}$$

$$\lambda \text{ NTP helium} = 17 \times 10^{-8} \text{ m.}$$

and the apparent air change rate, due to diffusion of helium through the building openings, = 0.009 air changes/hr.

Note: Insufficient information concerning the construction of the building was available to enable an estimation of the apparent ventilation rate due to diffusion through the building fabric to be made; consequently only an estimate of the apparent ventilation rate through the open areas of the building could be made. This figure will represent an underestimate of the total apparent ventilation rate due to diffusion.

APPENDIX A3 Calibration of Ventilation Openings used in the Model Ventilation Studies.

A3.1 Two types of opening were used in the model studies to simulate building ventilation. These openings were circular holes of diameter 1.0 mm. and 2.5 mm., drilled in perspex plate of thickness 3 mm. The smaller openings were arranged in groups of four, in square formations at 2.0 mm. centres. These openings had to be accurately calibrated over the working range of pressures in order that the comparative calculated ventilation rates could be found.

A3.2 Plates, containing varying numbers of the openings being calibrated, were fixed over the end of a small air duct and the joints sealed. Air was drawn through the duct from the opposite end, and then through a "Gapmeter" flow rate meter, by a small suction pump. The air flow rate from the air duct was measured by the air flow rate meter, which is capable of measuring air flow rates in the range 0.06 to 3.00 m³/hr. The pressure difference acting across the plate was measured using an inclined tube manometer. One pressure tapping was situated in the wall of the duct, approximately 100 mm. away from the plate; the second was located immediately adjacent to and in front of the plate.

A3.3 An initial set of tests with the plates containing 2, 4 and 6 openings was carried out. With each plate a series of ten readings of flow rate and pressure

difference were taken. The complete set of results was analysed by least squares analysis to find the best fit calibration curve. The results of this set are given in Table A3.1. The line of best fit for these points was found to be:

$$V = 0.0508 (\text{dP})^{0.528} \dots\dots (\text{A3.1})$$

A3.4 It was found however, analysing the results from the three sets separately, that the value of the coefficient varied. The best values, analysing the results separately were found to be:

- for 2 openings, coefficient = 0.0515
- for 4 openings, coefficient = 0.0507
- for 6 openings, coefficient = 0.0501

The variation was interpreted as being due to a constant rate of leakage from other sources in each of the three sets of tests. An estimated expression for the leakage and corrected calibration was found by analysing the results as a set of three simultaneous equations of the form:

$$\begin{aligned} & \text{number of holes} \times \text{apparent coefficient} \\ = & \text{number of holes} \times \text{real coefficient} + \text{leakage} \\ 2 \times 0.0515 & = (2 \times \text{coefficient}) + \text{leakage} \\ 4 \times 0.0507 & = (4 \times \text{coefficient}) + \text{leakage} \\ 6 \times 0.0501 & = (6 \times \text{coefficient}) + \text{leakage} \end{aligned}$$

Using this technique a value for the corrected coefficient of 0.0493 was found. The expression for the leakage

being:

$$V = 0.0050 (\text{dP})^{0.528} \quad \dots\dots (\text{A3.2})$$

A3.5 In order to check the accuracy of this interpretation the procedure was repeated with the air duct joints more heavily sealed. The results from this set of observations are shown in Table A3.2. The calibration line for these results was found to be:

$$V = 0.0504 (\text{dP})^{0.528} \quad \dots\dots (\text{A3.3})$$

The coefficients obtained by analysing the results separately were as shown below:

for 1 opening, coefficient = 0.0512

for 2 openings, coefficient = 0.0500

for 3 openings, coefficient = 0.0501

Analysing these results in the same way the best value for the corrected coefficient was found to be 0.0494, and the best expression for the rate of leakage:

$$V = 0.0016 (\text{dP})^{0.528} \quad \dots\dots (\text{A3.4})$$

A3.6 Thus the corrected calibration for the 2.5 mm. diameter openings is assumed to be:

$$V = 0.0494 (\text{dP})^{0.528} \quad \dots\dots (\text{A3.5})$$

The corrected calibration curve for all sets of readings taken is shown in Figure A3.1, with flow rates corrected for the assumed rates of leakage. The 95% certainty limits of the points plotted gives values of approximately $\pm 4\%$

of the coefficient value.

A3.7 A similar procedure was followed with the 1.0 mm. diameter openings, the results being presented in Tables A3.3 and A3.4. An initial set of readings was analysed, for which the line of best fit was found to be:

$$V = 0.00621 (dP)^{0.605} \quad \dots\dots (A3.6)$$

Analysing the three sets of results separately the best values of the coefficients were found to be:

for 12 openings, coefficient = 0.00641

for 24 openings, coefficient = 0.00613

for 36 openings, coefficient = 0.00606

Using these coefficients in three simultaneous equations, as in paragraph 3.4, the best value of the corrected coefficient, allowing for leakage, was found to be 0.00588, and the leakage expressed by the equation:

$$V = 0.0061 (dP)^{0.605} \quad \dots\dots (A3.7)$$

A3.8 A second set of results was analysed, again with a very small rate of leakage occurring. For these results the best calibration curve is given by:

$$V = 0.00618 (dP)^{0.587} \quad \dots\dots (A3.8)$$

The results, analysed separately give values of the coefficient of:

for 12 openings, coefficient = 0.00624

for 24 openings, coefficient = 0.00617

for 36 openings, coefficient = 0.00612

After allowing for the assumed leakage the best value of the corrected coefficient was estimated as 0.00606, and the leakage expressed by the equation:

$$V = 0.0025 (dP)^{0.587} \quad \dots (A3.9)$$

A3.9 From these two sets of observations the calibration curves found are:

$$V = 0.00588 (dP)^{0.605} \quad \dots (A3.10)$$

$$V = 0.00606 (dP)^{0.587} \quad \dots (A3.11)$$

The final calibration line was chosen by assuming an exponent intermediate in value between the two calculated. For each curve an amended coefficient was found, assuming the new exponent value and equating the flow rate values at a pressure difference of 10 mm.wg., which is in the centre of the working range. Thus the two calibration curves are amended:

$$0.00588(10)^{0.605} \rightarrow c.(10)^{0.596}: c = 0.00598$$

$$0.00606(10)^{0.587} \rightarrow c.(10)^{0.596}: c = 0.00595$$

From these values the final calibration curve for the 1.00 mm. diameter openings is taken to be:

$$V = 0.00597 (dP)^{0.596} \quad \dots (A3.12)$$

The corrected calibration curve, for all sets of readings taken, is shown in Figure A3.2, with flow rates corrected for the assumed rates of leakage. Again the 95% confidence limits are approximately equivalent to $\pm 4\%$ of the calibration coefficient value.

TABLE A3.1 Flow Calibration 2.5 mm diameter Openings

No. of openings	Observed Flow Rate, l/min.	Pressure Difference, mm.wg.	Observed Flow Rate/Opening, m ³ /hr.	Corrected Flow Rate allowing for leakage, m ³ /hr.
2	3.18	3.15	0.095	0.090
	3.80	4.35	0.114	0.109
	4.45	5.90	0.134	0.128
	5.05	7.60	0.151	0.144
	5.66	9.65	0.170	0.162
	6.28	11.60	0.188	0.179
	6.90	14.10	0.207	0.197
	7.50	16.50	0.225	0.215
	8.12	19.55	0.244	0.233
	8.72	22.40	0.262	0.250
4	5.66	2.62	0.085	0.083
	6.28	3.16	0.094	0.092
	6.90	3.75	0.104	0.102
	7.50	4.40	0.112	0.109
	8.12	5.25	0.122	0.119
	8.72	6.00	0.131	0.128
	9.35	6.90	0.140	0.137
	10.0	7.90	0.150	0.147
	10.6	8.85	0.159	0.155
11.2	10.15	0.168	0.164	
6	6.00	1.45	0.060	0.059
	8.30	2.75	0.083	0.082
	10.6	4.15	0.106	0.104
	12.9	5.95	0.129	0.127
	15.3	8.20	0.153	0.151
	17.6	10.60	0.176	0.173
	20.0	13.55	0.200	0.197
	22.4	16.90	0.224	0.221
	24.6	20.00	0.246	0.242
26.8	23.70	0.268	0.264	

TABLE A3.2 Flow Calibration 2.5 mm diameter Openings

No. of openings	Observed Flow Rate, l/min.	Pressure Difference, mm.wg.	Observed Flow Rate/Opening, m ³ /hr.	Corrected Flow Rate allowing for leakage, m ³ /hr.
1	4.44	22.1	0.266	0.259
	4.12	19.4	0.247	0.240
	3.80	16.6	0.228	0.222
	3.16	12.0	0.190	0.185
	2.57	8.00	0.154	0.150
	1.95	4.70	0.117	0.114
	1.66	3.50	0.099	0.096
	1.32	2.45	0.079	0.077
2	7.50	17.7	0.225	0.222
	6.90	15.0	0.207	0.204
	6.28	12.6	0.188	0.185
	5.68	10.25	0.170	0.167
	5.07	8.10	0.152	0.150
	4.44	6.30	0.133	0.131
	3.80	4.55	0.114	0.112
	3.20	3.30	0.095	0.094
3	8.70	10.55	0.174	0.172
	8.15	9.50	0.163	0.161
	7.50	8.05	0.150	0.149
	6.90	6.80	0.138	0.137
	6.25	5.65	0.125	0.124
	5.65	4.65	0.113	0.112
	5.00	3.70	0.100	0.099
	4.45	2.90	0.089	0.088

TABLE A3.3 Flow Calibration 1.0 mm diameter Openings

No. of openings	Observed Flow Rate, l/min.	Pressure Difference, mm.wg.	Observed Flow Rate/Opening, m ³ /hr.	Corrected Flow Rate allowing for leakage, m ³ /hr.
36	24.6	23.3	0.0410	0.0399
	22.4	20.2	0.0373	0.0363
	20.0	16.65	0.0333	0.0324
	17.6	13.65	0.0293	0.0285
	15.3	10.70	0.0255	0.0248
	13.1	8.15	0.0217	0.0211
	10.7	6.00	0.0178	0.0173
	8.30	4.10	0.0138	0.0134
	6.14	2.32	0.0102	0.0999
	4.94	1.67	0.0082	0.0080
24	15.3	21.0	0.0383	0.0368
	13.0	16.0	0.0325	0.0312
	10.6	11.6	0.0265	0.0254
	9.36	9.35	0.0234	0.0225
	8.12	7.25	0.0203	0.0195
	6.91	5.45	0.0173	0.0166
	5.69	3.98	0.0142	0.0136
	4.45	2.60	0.0111	0.0107
	3.80	2.03	0.0095	0.0091
	3.21	1.55	0.0080	0.0077
12	8.10	21.8	0.0405	0.0373
	7.50	18.85	0.0375	0.0345
	6.92	16.3	0.0346	0.0319
	6.28	13.8	0.0314	0.0290
	5.68	11.6	0.0284	0.0262
	5.08	9.70	0.0254	0.0234
	4.44	7.70	0.0222	0.0205
	3.80	5.95	0.0190	0.0175
	3.20	4.45	0.0160	0.0148
	2.58	3.20	0.0129	0.0119

TABLE A3.4 Flow Calibration 1.0 mm diameter Openings

No. of openings	Observed Flow Rate, l/min.	Pressure Difference, mm.wg.	Observed Flow Rate/Opening, m ³ /hr.	Corrected Flow Rate allowing for leakage, m ³ /hr.
36	24.6	24.95	0.0410	0.0406
	22.4	21.50	0.0373	0.0369
	20.0	17.50	0.0333	0.0330
	17.6	14.35	0.0293	0.0290
	15.3	11.25	0.0255	0.0252
	12.7	8.45	0.0211	0.0209
	10.7	6.30	0.0178	0.0176
	8.30	4.15	0.0138	0.0136
	24	15.3	22.80	0.0383
13.0		17.00	0.0325	0.0320
10.6		12.50	0.0265	0.0261
9.36		9.75	0.0234	0.0230
8.12		7.55	0.0203	0.0200
6.91		5.55	0.0173	0.0170
5.69		4.00	0.0142	0.0140
4.40		2.70	0.0110	0.0108
12		8.10	24.35	0.0405
	7.50	21.60	0.0375	0.0364
	6.92	18.55	0.0346	0.0336
	6.28	15.60	0.0314	0.0305
	5.68	13.20	0.0284	0.0276
	5.04	10.80	0.0252	0.0244
	4.40	8.40	0.0220	0.0213
	3.80	6.65	0.0190	0.0184

Figure A3.1. Calibration of 2.5mm, diameter openings.

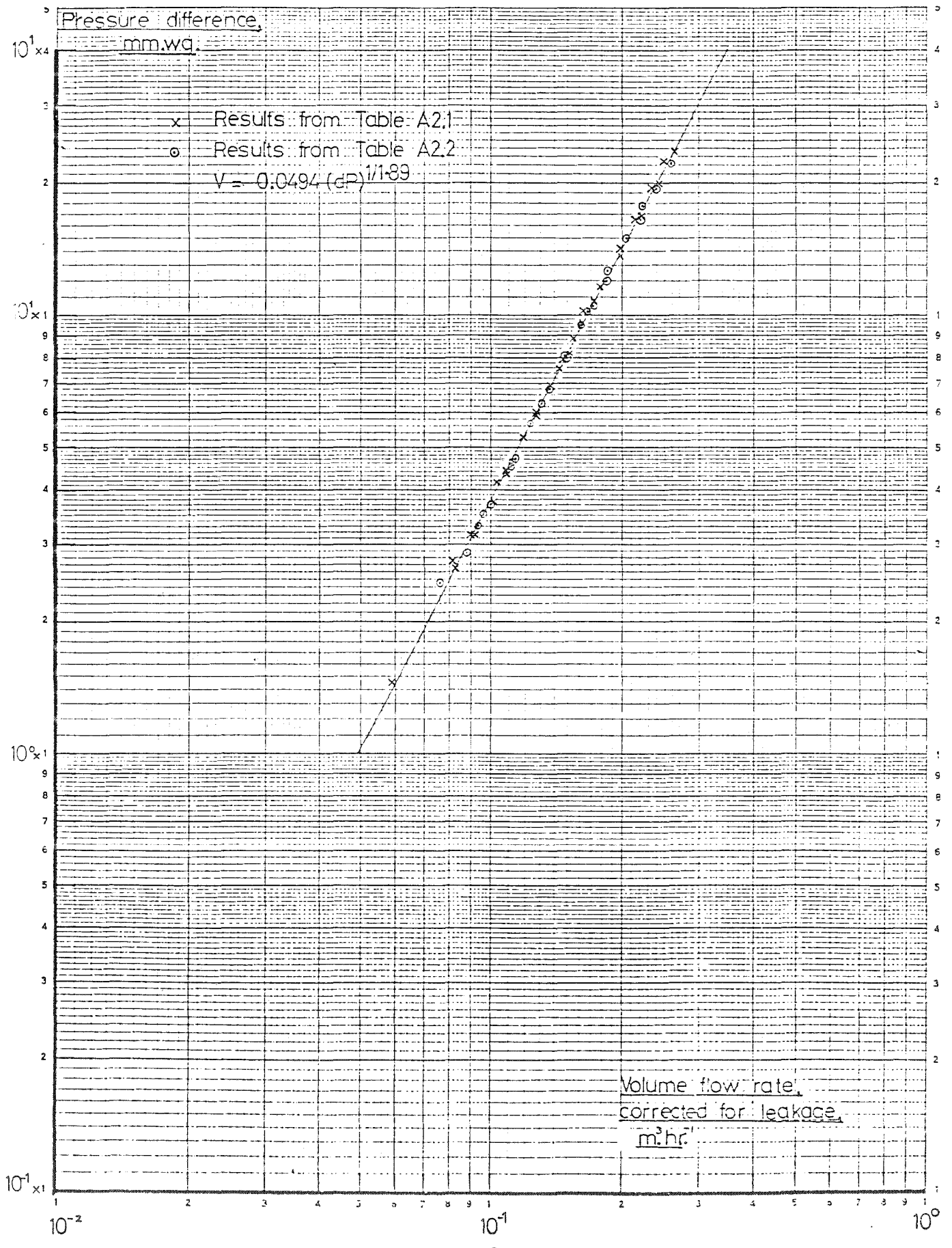
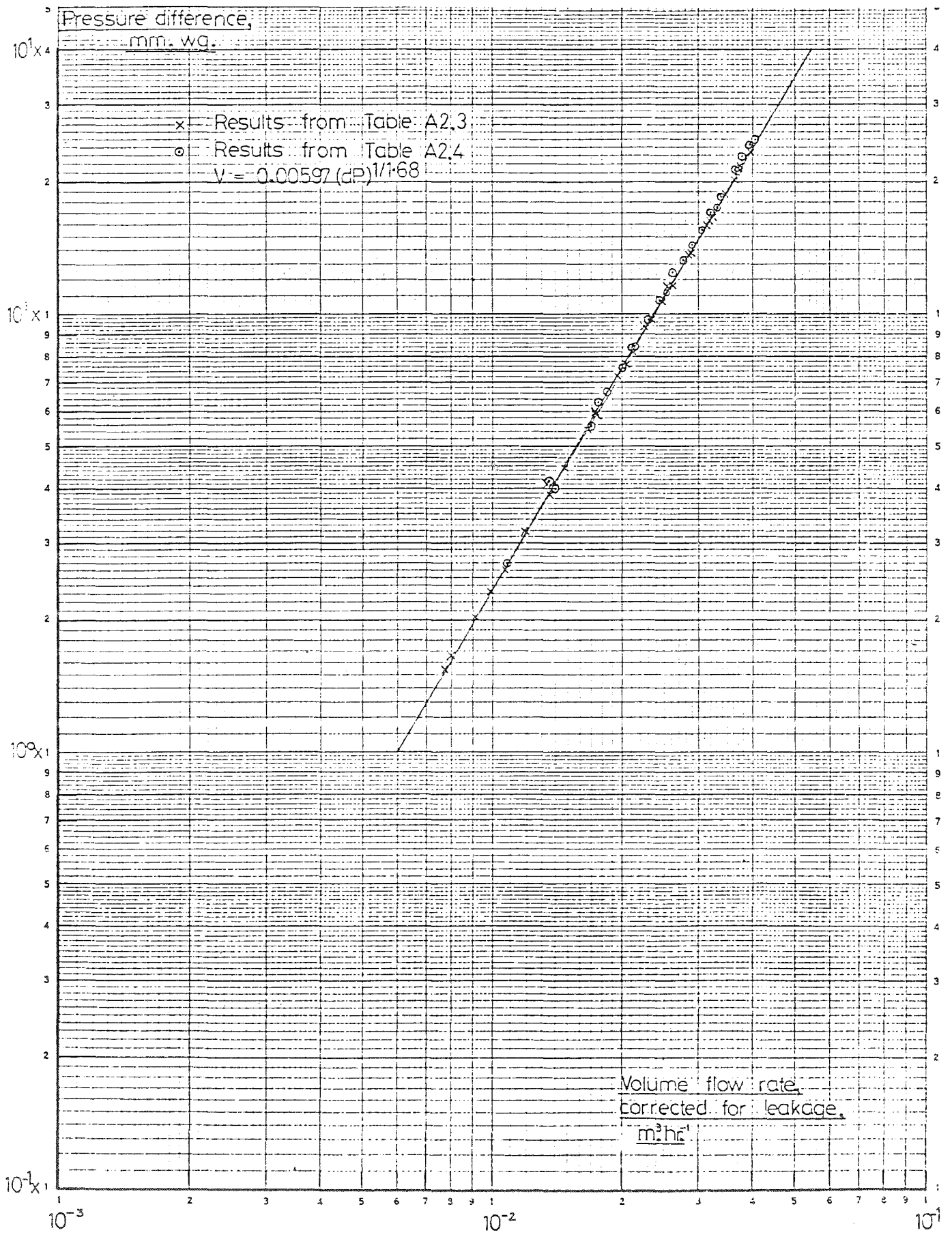


Figure A3.2. Calibration of 1.0mm. diameter openings.



A4.1 In order to carry out the comparative ventilation rate calculations in the model studies it was first necessary to find the pressure distributions over the models. Pressure coefficients were calculated from measurements made at representative positions over the surfaces of the model, and are recorded in this appendix. Measurements were made in the two boundary layers used in the model tests, which are described in paragraph 7.6.2.

A4.2 Mean pressures were measured at each of twelve pressure tappings distributed over one model face. The tappings were spread in a 30 mm. x 30 mm. grid over the model face, at heights of 15 mm., 45 mm. and 75 mm., and numbered 1-12, as shown in Figure 7.3. Angles of incidence of air flow were measured with respect to the normal from the model face being considered. Measurements were made at 15° intervals between 0° and 345°.

A4.3 The observed pressure coefficients are presented in Tables A4.1 and A4.2. For each angle of incidence the mean pressure coefficient for the whole face is given, and also the mean pressure coefficient at each of the twelve tapping positions. The individual tapping pressure coefficients are presented, in the Tables, in a matrix which corresponds to the actual tapping configuration on

the model, as shown below:

$$\theta = 0^\circ; \quad C_p \text{ mean} = x$$

1	2	3	4
5	6	7	8
9	10	11	12

TABLE A4.1 Measured model external pressure coefficients,
boundary layer I

$\theta = 0^\circ$; C_p mean = 0.76							
0.81	0.85	0.85	0.81				
0.78	0.87	0.85	0.75				
0.52	0.79	0.75	0.50				
$\theta = 15^\circ$; C_p mean = 0.76				$\theta = 345^\circ$; C_p mean = 0.73			
0.68	0.78	0.83	0.87	0.92	0.79	0.76	0.64
0.67	0.86	0.89	0.86	0.89	0.84	0.81	0.59
0.46	0.73	0.79	0.66	0.65	0.74	0.65	0.42
$\theta = 30^\circ$; C_p mean = 0.62				$\theta = 330^\circ$; C_p mean = 0.57			
0.42	0.54	0.72	0.83	0.81	0.62	0.57	0.37
0.41	0.60	0.78	0.91	0.83	0.70	0.58	0.35
0.29	0.58	0.69	0.68	0.67	0.62	0.51	0.24
$\theta = 45^\circ$; C_p mean = 0.43				$\theta = 315^\circ$; C_p mean = 0.36			
0.22	0.27	0.47	0.62	0.57	0.35	0.33	0.16
0.19	0.41	0.57	0.72	0.63	0.49	0.35	0.15
0.11	0.36	0.52	0.64	0.53	0.41	0.31	0.08
$\theta = 60^\circ$; C_p mean = 0.15				$\theta = 300^\circ$; C_p mean = 0.10			
0.03	0.01	0.17	0.24	0.19	0.07	0.09	0.02
0.02	0.17	0.26	0.32	0.17	0.20	0.13	-0.01
-0.03	0.13	0.22	0.26	0.10	0.18	0.09	-0.03
$\theta = 75^\circ$; C_p mean = -0.28				$\theta = 285^\circ$; C_p mean = -0.32			
-0.10	-0.16	-0.08	-0.92	-0.95	-0.22	-0.12	-0.11
-0.12	-0.04	-0.12	-0.80	-0.83	-0.26	-0.07	-0.13
-0.12	-0.05	-0.07	-0.75	-0.76	-0.21	-0.07	-0.12
$\theta = 90^\circ$; C_p mean = -0.65				$\theta = 270^\circ$; C_p mean = -0.65			
-0.33	-0.71	-0.80	-0.75	-0.75	-0.84	-0.69	-0.36
-0.38	-0.67	-0.83	-0.78	-0.77	-0.85	-0.65	-0.35
-0.29	-0.54	-0.83	-0.89	-0.83	-0.82	-0.57	-0.29

TABLE A4.1 contd.

$\theta = 105^\circ$; Cp mean = -0.57	$\theta = 255^\circ$; Cp mean = -0.57
-0.62 -0.62 -0.58 -0.53	-0.54 -0.60 -0.61 -0.62
-0.62 -0.59 -0.56 -0.50	-0.50 -0.56 -0.58 -0.59
-0.55 -0.55 -0.56 -0.52	-0.57 -0.54 -0.56 -0.53
$\theta = 120^\circ$; Cp mean = -0.52	$\theta = 240^\circ$; Cp mean = -0.57
-0.58 -0.58 -0.55 -0.49	-0.57 -0.59 -0.60 -0.62
-0.56 -0.56 -0.53 -0.46	-0.53 -0.59 -0.60 -0.59
-0.48 -0.51 -0.52 -0.45	-0.51 -0.56 -0.54 -0.50
$\theta = 135^\circ$; Cp mean = -0.45	$\theta = 225^\circ$; Cp mean = -0.48
-0.47 -0.47 -0.49 -0.43	-0.45 -0.50 -0.48 -0.48
-0.48 -0.46 -0.46 -0.41	-0.45 -0.51 -0.52 -0.50
-0.42 -0.44 -0.43 -0.42	-0.46 -0.49 -0.46 -0.42
$\theta = 150^\circ$; Cp mean = -0.36	$\theta = 210^\circ$; Cp mean = -0.37
-0.41 -0.38 -0.35 -0.31	-0.33 -0.36 -0.40 -0.43
-0.41 -0.38 -0.36 -0.32	-0.34 -0.38 -0.39 -0.40
-0.35 -0.36 -0.34 -0.33	-0.34 -0.36 -0.35 -0.34
$\theta = 165^\circ$; Cp mean = -0.32	$\theta = 195^\circ$; Cp mean = -0.31
-0.43 -0.34 -0.29 -0.26	-0.26 -0.28 -0.32 -0.41
-0.41 -0.34 -0.30 -0.27	-0.28 -0.29 -0.33 -0.39
-0.31 -0.30 -0.28 -0.26	-0.25 -0.27 -0.28 -0.30
$\theta = 180^\circ$; Cp mean = -0.23	
-0.27 -0.29 -0.27 -0.27	
-0.26 -0.22 -0.22 -0.25	
-0.22 -0.17 -0.16 -0.19	

TABLE A4.2 Measured model external pressure coefficients,
boundary layer II

$\theta = 0^\circ$; C_p mean = 0.52							
0.65	0.73	0.68	0.59				
0.45	0.59	0.55	0.37				
0.34	0.52	0.50	0.28				
$\theta = 15^\circ$; C_p mean = 0.49				$\theta = 345^\circ$; C_p mean = 0.45			
0.47	0.60	0.70	0.70	0.75	0.66	0.57	0.46
0.31	0.49	0.55	0.49	0.54	0.52	0.44	0.26
0.23	0.45	0.50	0.38	0.40	0.48	0.41	0.18
$\theta = 30^\circ$; C_p mean = 0.40				$\theta = 330^\circ$; C_p mean = 0.36			
0.30	0.41	0.59	0.67	0.66	0.50	0.41	0.28
0.18	0.38	0.47	0.52	0.49	0.41	0.30	0.13
0.12	0.34	0.43	0.41	0.39	0.37	0.28	0.08
$\theta = 45^\circ$; C_p mean = 0.27				$\theta = 315^\circ$; C_p mean = 0.23			
0.16	0.21	0.38	0.54	0.45	0.31	0.27	0.15
0.08	0.24	0.33	0.43	0.35	0.29	0.19	0.05
0.04	0.21	0.30	0.35	0.29	0.24	0.18	0.03
$\theta = 60^\circ$; C_p mean = 0.13				$\theta = 300^\circ$; C_p mean = 0.08			
0.07	0.05	0.19	0.25	0.15	0.13	0.12	0.04
0.01	0.15	0.17	0.21	0.08	0.12	0.10	-0.01
0.00	0.11	0.16	0.19	0.06	0.12	0.08	-0.02
$\theta = 75^\circ$; C_p mean = -0.08				$\theta = 285^\circ$; C_p mean = -0.15			
-0.02	-0.07	0.01	-0.27	-0.47	-0.08	-0.01	-0.04
-0.04	-0.01	0.00	-0.28	-0.42	-0.12	-0.04	-0.06
-0.05	-0.01	-0.01	-0.21	-0.32	-0.09	-0.04	-0.07
$\theta = 90^\circ$; C_p mean = -0.34				$\theta = 270^\circ$; C_p mean = -0.38			
-0.11	-0.22	-0.39	-0.79	-0.77	-0.52	-0.24	-0.14
-0.11	-0.19	-0.43	-0.67	-0.63	-0.47	-0.26	-0.15
-0.10	-0.16	-0.35	-0.61	-0.57	-0.42	-0.21	-0.13

TABLE A4.2 contd.

$\theta = 105^\circ$; C_p mean = -0.46	$\theta = 255^\circ$; C_p mean = -0.46
-0.35 -0.50 -0.57 -0.57	-0.53 -0.57 -0.50 -0.41
-0.32 -0.45 -0.53 -0.50	-0.50 -0.52 -0.46 -0.37
-0.27 -0.40 -0.51 -0.49	-0.49 -0.50 -0.41 -0.30
$\theta = 120^\circ$; C_p mean = -0.48	$\theta = 240^\circ$; C_p mean = -0.46
-0.51 -0.50 -0.49 -0.48	-0.45 -0.48 -0.48 -0.51
-0.48 -0.51 -0.50 -0.46	-0.45 -0.49 -0.49 -0.47
-0.39 -0.41 -0.50 -0.43	-0.42 -0.48 -0.46 -0.38
$\theta = 135^\circ$; C_p mean = -0.38	$\theta = 225^\circ$; C_p mean = -0.35
-0.39 -0.40 -0.38 -0.35	-0.32 -0.35 -0.37 -0.36
-0.38 -0.42 -0.41 -0.35	-0.32 -0.36 -0.37 -0.36
-0.32 -0.38 -0.39 -0.36	-0.31 -0.37 -0.35 -0.31
$\theta = 150^\circ$; C_p mean = -0.26	$\theta = 210^\circ$; C_p mean = -0.25
-0.30 -0.27 -0.25 -0.24	-0.22 -0.24 -0.25 -0.30
-0.31 -0.28 -0.27 -0.22	-0.22 -0.24 -0.26 -0.30
-0.27 -0.26 -0.25 -0.22	-0.21 -0.23 -0.25 -0.27
$\theta = 165^\circ$; C_p mean = -0.19	$\theta = 195^\circ$; C_p mean = -0.19
-0.24 -0.20 -0.17 -0.15	-0.15 -0.18 -0.20 -0.23
-0.24 -0.21 -0.18 -0.16	-0.16 -0.18 -0.21 -0.24
-0.22 -0.20 -0.17 -0.15	-0.15 -0.17 -0.21 -0.22
$\theta = 180^\circ$; C_p mean = -0.14	
-0.14 -0.14 -0.13 -0.14	
-0.14 -0.13 -0.13 -0.14	
-0.15 -0.13 -0.12 -0.14	

A5.1 In this appendix one set of observations and computed results, taken from the comparative model studies, is presented in detail. The results given are those for the following model conditions:

 window opening configuration C (two opposite porous walls),
 9 openings per face,
 2.5 mm. diameter openings,
 boundary layer I,
 angle of incidence of air flow, 45° .

A5.2 The results describing the observed and computed internal pressures are not strictly comparable with those describing the observed and computed ventilation rates because the two models used to measure these values had slight differences in detailed design. The internal pressure measurement model was subdivided by two intermediate floors, and the mean internal pressure was calculated as the mean pressure from the three levels of the model. The ventilation rate measurement model could not be similarly subdivided because of the presence of the orifice plate, and consequently the computed ventilation rates were recalculated assuming a model form with no appreciable internal resistance to vertical flow.

A5.3 Mean internal pressure measurements are presented in Table A5.1, and the comparative computed results are

presented in Table A5.2. The experimental procedure describing the use of the internal pressure measurement model is outlined in Chapter 7, paragraphs 7.6.6 and 7.6.7. The measurements were made at three velocities, 13 m/s., 19 m/s., and 25 m/s., and the results from the three sets of measurements are presented. One set of observed mean air flow rates through the ventilation rate measurement model is presented in Table A5.3, and the comparative computed results are presented in Table A5.4. The experimental procedure describing the use of this model is explained in Chapter 7, paragraphs 7.6.8 to 7.6.10. For this set of model conditions the observed internal pressure coefficient and ventilation rate were found to be -0.161 and 1.410 m³/hr. respectively; the corresponding computed values were found to be -0.039 and 1.560 m³/hr.

TABLE A5.1 Model internal pressure measurements, observed results.

Nominal air velocity; 13 m/s.

Wind tunnel centreline velocity pressures, mm.wg.		12.1, 11.9, 11.85
Mean wind tunnel centreline velocity pressure, mm.wg.		11.95
Corrected velocity pressure, mm.wg.		11.45
Observed internal pressures, mm.wg.	Mean pressure, mm.wg.	
Floor 1 -1.75 -1.75 -1.75 -1.75		-1.75
Floor 2 -1.55 -1.75 -1.65 -1.60		-1.64
Floor 3 -1.60 -1.75 -1.80 -1.60		-1.69
Mean internal pressure, mm.wg.		-1.69
Mean internal pressure coefficient, $C\bar{p}_i$,		<u>-0.149</u>

Nominal air velocity; 19 m/s.

Wind tunnel centreline velocity pressures, mm.wg.		24.1, 23.8, 23.6
Mean wind tunnel centreline velocity pressure, mm.wg.		23.85
Corrected velocity pressure, mm.wg.		22.9
Observed internal pressures, mm.wg.	Mean pressure, mm.wg.	
Floor 1 -3.30 -3.35 -3.75 -3.70		-3.53
Floor 2 -3.10 -2.90 -3.90 -3.85		-3.44
Floor 3 -3.30 -3.25 -4.15 -4.00		-3.68
Mean internal pressure, mm.wg.		-3.55
Mean internal pressure coefficient, $C\bar{p}_i$,		<u>-0.155</u>

TABLE A5.1 contd.

Nominal air velocity: 25 m/s.

Wind tunnel centreline velocity pressures, mm.wg.		38.0, 37.7, 38.0
Mean wind tunnel centreline velocity pressure, mm.wg.		37.9
Corrected velocity pressure, mm.wg.		36.4
Observed internal pressures, mm.wg.	Mean pressure, mm.wg.	
Floor 1 -6.60 -6.60 -5.90 -5.90		-6.25
Floor 2 -6.25 -6.05 -6.65 -6.50		-6.46
Floor 3 -6.50 -6.60 -7.35 -7.30		-6.94
Mean internal pressure, mm.wg.		-6.55
Mean internal pressure coefficient, $C_{\bar{p}_i}$,		<u>-0.179</u>
Average internal pressure coefficient, all velocities		<u>-0.161</u>

TABLE A5.2 Model internal pressure measurement, computed results.

Input data summary

(Full data requirements and nomenclature may be seen in Appendix A1)

Exterior/room openings, flow characteristics (CL1, Z1);

Corridor/stairwell openings, flow characteristics (CLS, ZS);

As calibration for 2.5 mm. diameter openings;

Infiltration coefficient, CL1 or CLS = 0.049

Flow exponent reciprocal, Z1 or ZS = 1.89

Room/corridor openings, flow characteristics (CL2, Z2):

As there was no internal resistance to horizontal flow in the model, dummy values were used in the programme with very high infiltration coefficient values.

Infiltration coefficient, CL2 = 10.00

Flow exponent reciprocal, Z2 = 2.00

Assumed external pressure coefficients (CE):

	Room 1	Room 2	Room 3	Room 4	Room 5	Room 6
Floor 1	0.22	0.40	0.53	-0.44	-0.46	-0.45
Floor 2	0.28	0.46	0.60	-0.49	-0.49	-0.46
Floor 3	0.25	0.35	0.50	-0.47	-0.49	-0.47

Computed results

Velocity pressure 24.96 mm.wg., Wind speed 20.00 m/s.

Floor	Room	VE(m ³ /hr)	PDE(mm.wg.)	PDE(Cp)	PDC(mm.wg.)
1	1	0.133	6.47	0.26	0.00
1	2	0.175	10.96	0.44	0.00
1	3	0.201	14.20	0.57	0.00
1	4	-0.167	-10.01	-0.40	0.00
1	5	-0.172	-10.51	-0.42	0.00
1	6	-0.169	-10.26	-0.41	0.00

TABLE A5.2 contd.

Floor	Room	VE(m ³ /hr)	PDE(mm.wg.)	PDE(Cp)	PDC(mm.wg.)
2	1	0.147	7.84	0.31	0.00
2	2	0.187	12.34	0.49	0.00
2	3	0.213	15.83	0.63	0.00
2	4	-0.179	-11.38	-0.46	0.00
2	5	-0.179	-11.38	-0.46	0.00
2	6	-0.173	-10.63	-0.43	0.00
3	1	0.142	7.35	0.29	0.00
3	2	0.166	9.85	0.39	0.00
3	3	0.197	13.60	0.54	0.00
3	4	-0.172	-10.62	-0.43	0.00
3	5	-0.177	-11.12	-0.45	0.00
3	6	-0.172	-10.62	-0.43	0.00

Floor	VSTAIR (m ³ /hr.)	PSTAIR (mm.wg.)	PCORRIDOR (mm.wg.)	PCORRIDOR (Cp.)
1	-0.001	-0.973	-0.973	-0.039
2	-0.016	-0.973	-0.851	-0.034
3	0.017	-0.973	-1.120	-0.044

VE represents the air flow rate through each external opening,

PDE represents the pressure difference acting across each opening,

PDC represents the pressure difference acting across each dummy opening,

PCORRIDOR represents the internal pressure on each floor of the model, as the internal pressure is uniform throughout each floor of the model.

Consequently the computed mean internal pressure, expressed as a pressure coefficient was found to be -0.039.

TABLE A5.3 Model ventilation rate measurements, observed results.

Wind tunnel centreline velocity pressures, mm.wg.,	17.4, 17.4
Mean wind tunnel centreline velocity pressure, mm.wg.,	17.4
Corrected velocity pressure, mm.wg.	16.9
Wind speed, m/s.,	16.64
Micromanometer output calibration/pressure difference, mm.wg./mV.	97.2

Micromanometer zero pressure difference output voltages, mV.

before orifice plate pressure difference measurement:

19.3 19.3 19.3 19.3 19.3

after orifice plate pressure difference measurement:

19.7 19.7 19.7 19.7 19.7

Mean micromanometer zero pressure difference voltage, mV. 19.5

Micromanometer orifice plate pressure difference output voltages, mV.

3.7	4.9	2.4	5.2	1.8
6.8	4.5	2.5	1.6	3.1
3.0	1.3	3.7	6.0	3.5
3.9	6.1	1.6	2.1	2.5

Micromanometer orifice plate readings, voltage difference values, mV.

15.8	14.6	17.1	14.3	17.7
12.7	15.0	17.0	17.9	16.4
16.5	18.2	15.8	13.5	16.0
15.6	13.4	17.9	17.4	17.0

TABLE A5.3 contd.

Computed volume flow rates, m³/hr.

1.155	1.110	1.202	1.099	1.223
1.036	1.126	1.198	1.230	1.177
1.180	1.240	1.155	1.068	1.162
1.148	1.064	1.230	1.212	1.198

Mean observed ventilation rate, m³/hr.

1.161

Ventilation rate corrected to 20 m/s. wind speed, m³/hr.

1.410

TABLE A5.4 Model ventilation rate measurements, computed results.

Input data summary

(Full data requirements and nomenclature may be seen in Appendix A1).

Exterior room openings, flow characteristics (CL1, Z1)

As calibration for 2.5 mm. diameter openings:

Infiltration coefficient, CL1 = 0.049

Flow exponent reciprocal, Z1 = 1.89

Room/corridor openings, flow characteristics (CL2, Z2)

Corridor/stairwell openings, flow characteristics (CLS, ZS)

As there was no internal resistance to flow in the model, dummy values were used in the programme with with very high infiltration coefficient values.

Infiltration coefficient, CL2, CLS = 10.00

Flow exponent reciprocal, Z2, ZS = 2.00

Assumed external pressure coefficients (CE):

	Room 1	Room 2	Room 3	Room 4	Room 5	Room 6
Floor 1	0.22	0.40	0.53	-0.44	-0.46	-0.45
Floor 2	0.28	0.46	0.60	-0.49	-0.49	-0.46
Floor 3	0.25	0.35	0.50	-0.47	-0.49	-0.47

Computed results

Velocity pressure 24.96 mm.wg. Wind speed 20.00 m/s.

Floor	Room	VE(m ³ /hr)	PDE(mm.wg.)	PDE(Cp)	PDC(mm.wg.)
1	1	0.133	6.47	0.26	0.00
1	2	0.175	10.96	0.44	0.00
1	3	0.201	14.21	0.57	0.00
1	4	-0.167	-10.01	-0.40	0.00
1	5	-0.172	-10.51	-0.42	0.00
1	6	-0.169	-10.26	-0.41	0.00

TABLE A5.4 contd.

Floor	Room	VE(m ³ /hr)	PDE(mm.wg.)	PDE(Cp)	PDC(mm.wg.)
2	1	0.148	7.96	0.32	0.00
2	2	0.188	12.46	0.50	0.00
2	3	0.214	15.95	0.64	0.00
2	4	-0.178	-11.26	-0.45	0.00
2	5	-0.178	-11.26	-0.45	0.00
2	6	-0.172	-10.51	-0.42	0.00
3	1	0.141	7.22	0.29	0.00
3	2	0.165	9.71	0.39	0.00
3	3	0.196	13.46	0.54	0.00
3	4	-0.174	-10.76	-0.43	0.00
3	5	-0.178	-11.26	-0.45	0.00
3	6	-0.174	-10.76	-0.43	0.00

Floor	VSTAIR (m ³ /hr.)	PSTAIR (mm.wg.)	PCORRIDOR (mm.wg.)	PCORRIDOR (Cp.)
1	0.000	-0.973	-0.973	-0.039
2	0.000	-0.973	-0.973	-0.039
3	0.000	-0.973	-0.973	-0.039

VE represents the air flow through each external opening,

PDE represents the pressure difference acting across each opening,

PDC represents the pressure difference acting across each dummy opening,

PCORRIDOR represents the internal pressure on each floor of the model.

The computed total ventilation rate through the model was found to be 1.560 m³/hr. at a wind speed of 20 m/s.

APPENDIX A6

A suggested function to describe the variation of mean pressure coefficient with angle of incidence.

A6.1 The information available which describes the variation of mean pressure coefficients on building surfaces with angle of incidence of the wind is limited. In design guides values of pressure coefficient are normally quoted only for the four wind directions perpendicular to the main faces of the building. In many cases this information will be sufficient to carry out design calculations. In certain cases, in particular in computer based calculations, where many detailed calculations can be quickly repeated, more detailed information on the variation of pressure coefficients at other angles may be useful. One function for describing the variation of pressure coefficient with angle of incidence, (Nelson, 1971) was discussed in paragraph 3.4:14. It was noted that values calculated using this function did not agree well with the measured model pressure coefficients and consequently an alternative function, which is derived from model observations, has been suggested. The function is put forward, tentatively, as a technique suitable for further development, as the results on which it is based are from a very limited series of model studies. However it is possible that a function of the type suggested may provide a more adaptable method of quantifying this effect.

A6.2 The effect of building shape and boundary layer conditions on mean pressure coefficient values is complex.

Design guides (B.R.S, 1970), normally allow for these factors in the design pressure coefficients quoted for the wind directions perpendicular to the building faces. The present function was developed to interpolate pressure coefficient values at intermediate angles of incidence, using the pressure coefficient values measured or quoted for the major wind directions.

A6.3 It was found that the variation of mean pressure coefficient could be adequately described for the two test conditions measured by using two secondary variables; the mean pressure differences across the opposite faces of the model, C_{pd} , and the average of the mean pressures on opposite faces of the model, C_{pm} . These variables were chosen because, for the cases studied, both showed maximum and minimum values at or near the major wind directions, and so they were suitable for combining with known pressure coefficient values at these angles. The variation of the pressure difference value C_{pd} was found to approximate to $(\cos \theta)^{0.5}$, (where θ is the angle between the direction of the air flow and a normal to the face being considered). The mean pressure function, C_{pm} , was found to possess a minimum value at $\theta = 90^\circ$ and a maximum value at $\theta = 0^\circ$, and to vary approximately as:

$$C_{pm_\theta} = (C_{pm})_{\min} + ((C_{pm})_{\max} - (C_{pm})_{\min}) \cdot \cos \theta$$

A6.4 Using these functions the value of the mean pressure coefficient at angles of incidence θ° and

$(180 + \theta)^\circ$ could be found using equations of the form:

$$Cp_\theta = Cpm_\theta + 0.5.Cpd_\theta \quad \dots\dots (A6.1)$$

$$Cp_{\theta+180} = Cpm_\theta - 0.5.Cpd_\theta \quad \dots\dots (A6.2)$$

where the suffix θ indicates the variable value at an angle of incidence, θ .

Substituting Cpm and Cpd in equations A6.1 and A6.2 by the relationships noted in paragraph A6.3, the function (expressed in terms of the known pressure coefficient values at angles of incidence 0° , $90^\circ (= 270^\circ)$ and 180°) becomes:

$$Cp_\theta = Cp_{90} + 0.5(Cp_0 + Cp_{180} - 2Cp_{90}). \cos \theta + 0.5(Cp_0 - Cp_{180}).(\cos \theta)^{0.5} \quad \dots\dots (A6.3)$$

$$Cp_{\theta+180} = Cp_{90} + 0.5(Cp_0 + Cp_{180} - 2Cp_{90}). \cos \theta - 0.5(Cp_0 - Cp_{180}).(\cos \theta)^{0.5} \quad \dots\dots (A6.4)$$

for conditions $0^\circ \leq \theta \leq 90^\circ$ and $270^\circ \leq \theta \leq 360^\circ$

Comparisons of the observed mean pressure coefficient values at different angles of incidence and the corresponding computed values for the wind tunnel model shown in Figure 7.2 are presented in Figures A6.1 and A6.2.

A6.5 Although the values of pressure coefficient calculated using the function agree moderately well with the observed values for the model in both boundary layers studied certain limitations must be recognised. In

particular the function has been derived from results using a model with a 1:1 plan ratio only, as this was the only model form used in the experimental work, and the function has not been compared with measured values for models having different plan ratios. The function is also only appropriate for a building in a relatively isolated position, where the air flow pattern is not significantly influenced by adjacent buildings. Under such conditions the variation of the pressure coefficient values will normally alter because of the distortion of the air flow pattern caused by the neighbouring buildings.

Figure A6.1.

Comparison between suggested function (to allow for variation of angle of incidence on mean pressure coefficients) and observed results, boundary layer I.

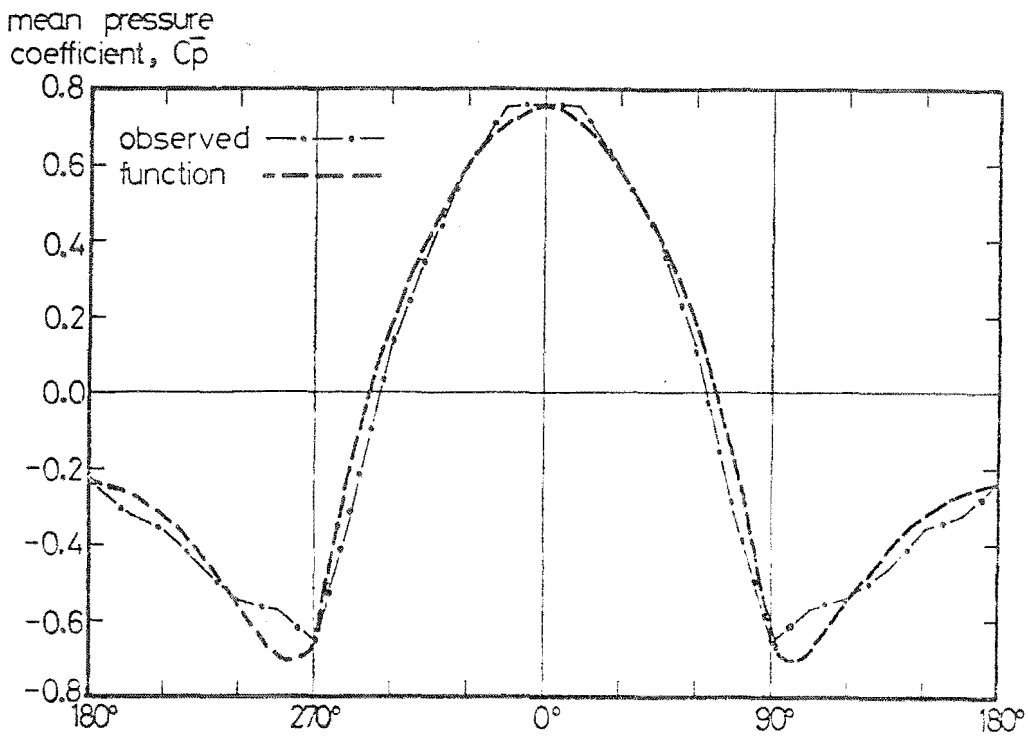
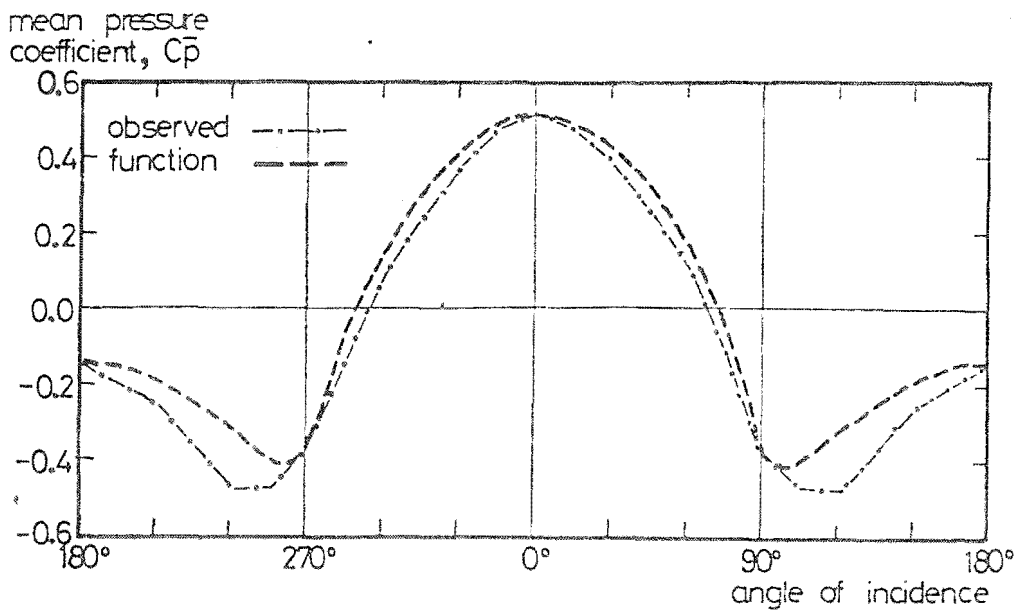


Figure A6.2.

Comparison between suggested function (to allow for variation of angle of incidence on mean pressure coefficients) and observed results, boundary layer II.



APPENDIX A7 The Use of the Digital Analogue in Analysing
the Performance of a Combined Natural and
Mechanical Ventilation System.

A7.1 The comparative model studies which have been carried out have shown that ventilation rates cannot be predicted accurately if the normally used simplifying assumptions are made. In general this conclusion suggests that the use of simple calculation methods, such as simple nomograms, are of ample sophistication for design calculations. There are some circumstances in which fully-computerised calculations are of particular use. Two circumstances in which such methods may be more useful are in the analysis of the pattern of behaviour of a ventilation system over a large range of meteorological conditions or the analysis of more complex ventilation systems; for example in the analysis of the feasibility of combined mechanical and natural ventilation systems.

A7.2 A simple analysis of this type, which uses the digital analogue to show the change of behaviour of a naturally ventilated building, due to the addition of a simple mechanical ventilation system, is presented, as an example, below. A simple notional building form is used as a subject of the analysis, and is described in Figure A7.1. Mean pressure coefficient values of +0.7 and -0.25 are assumed to act on the two major faces of the building. Wind speeds have been calculated from the meteorological wind speeds, assuming the building to be located in an urban area. The air leakage coefficient values are given

in Figure A7.1; and are approximately equivalent to an open facade area of 0.5%.

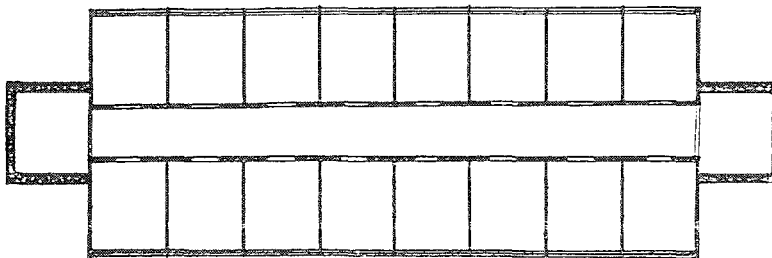
A7.3 In the alternative ventilation system background mechanical ventilation is assumed to be provided by a simple mechanical system which, under the conditions described, is able to maintain the stairwell at a positive pressure of +0.5 mm.wg. relative to other areas of the building. (This is a simplification of the real situation, as the performance of the fan used to provide the mechanical ventilation would be affected by changes in the external wind speed). This type of system might be derived as a development of the stairwell pressurisation systems used in some buildings for fire safety. The use of ventilators in the stairwell doorways, which would allow free air movement under normal conditions and would close automatically in the case of fire to allow pressurisation to take place, could, for example, be used to allow pressurisation fans to provide background ventilation for the building.

A7.4 In Figure A7.2 average room ventilation rates are given for the naturally ventilated building. In Figure A7.3 the average room ventilation rates are given, for the same range of meteorological conditions, for the alternative system. The figures show how the introduction of the additional mechanical ventilation reduces the variability of the ventilation rate due to external climatic conditions. In the illustration given, for example, the 10% and 90% ventilation rates in summertime

conditions would be approximately 5 m³/hr. and 25 m³/hr. in the naturally ventilated building; and 12 m³/hr. and 25 m³/hr. with the background ventilation. A system of this type could provide significantly more dependable ventilation rates under unfavourable meteorological conditions, than a naturally ventilated system, without incurring the full cost of total mechanical ventilation. The investigation of the relative performance of proposed ventilation systems using different amounts of mechanical ventilation is complex as, for each case, the full range of climatic conditions and patterns of use of the building needs to be considered to assess objectively the merits of the different solutions. It is in these types of situation, where approximate answers are required for a large number of conditions, that computerised techniques are likely to be of greatest use to the designer.

Figure A7.1. Building form used in illustrative analysis.

Typical floor plan;



General characteristics ;

Number of floors	8
Nominal room size	4.0x3.0x2.4m.
Floor to floor height	2.7m.

Leakage coefficients assumed;

External wall / room	300m ³ /hr./mm.wg.
Internal doors	600m ³ /hr./mm.wg.
Stairwell doors	1500m ³ /hr./mm.wg.

Exponent values assumed;

External wall	0.55
Doorways	0.67

Figure A7.2. Variation of average room ventilation rate with meteorological conditions, natural ventilation system.

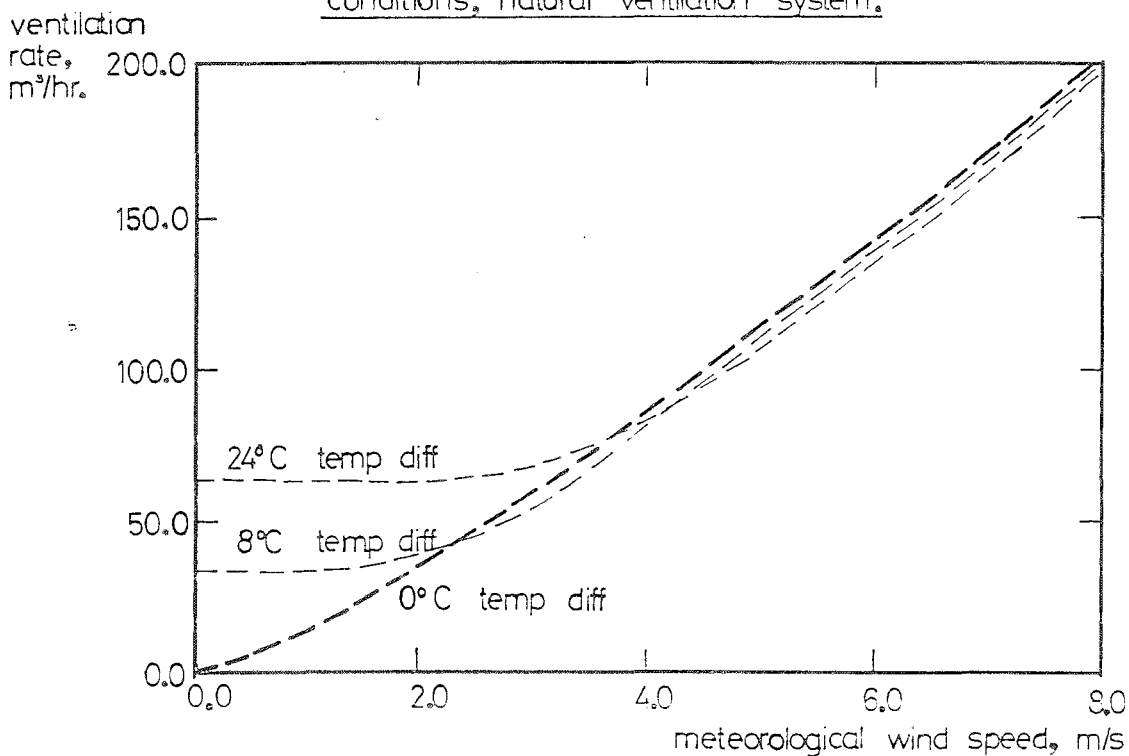
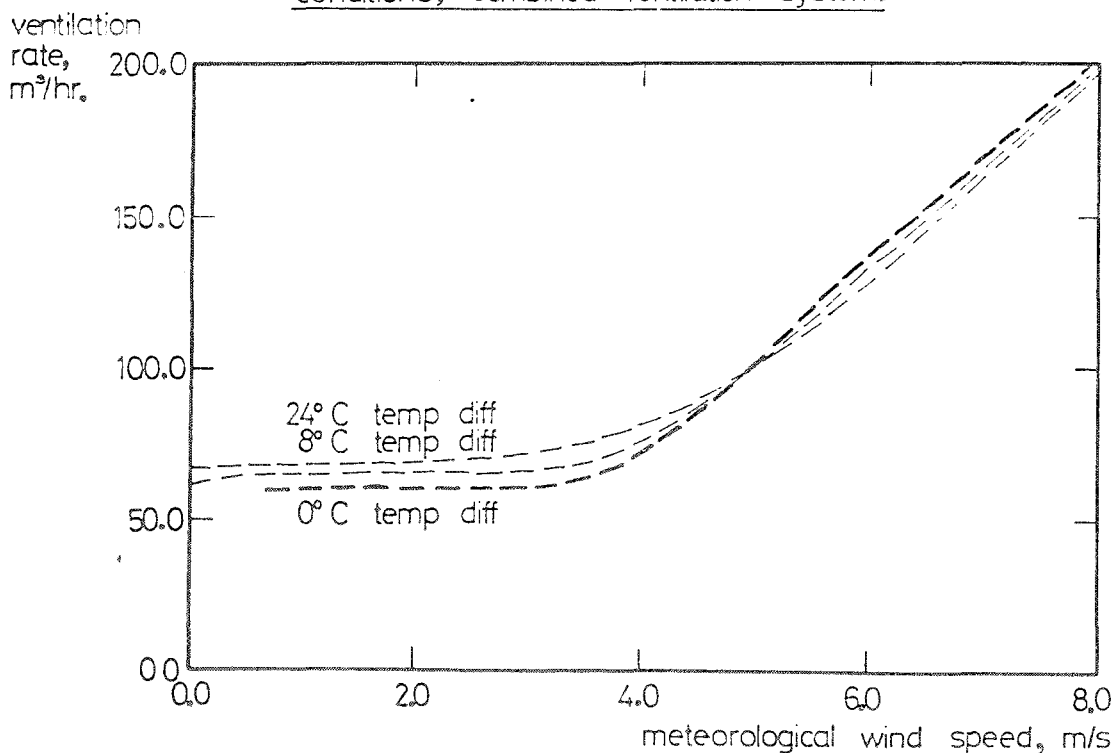


Figure A7.3. Variation of average room ventilation rate with meteorological conditions, combined ventilation system.



REFERENCES

- A.S.H.R.A.E.,
1972
AMERICAN SOCIETY OF HEATING,
REFRIGERATING and AIR CONDITIONING
ENGINEERS,
"Handbook of Fundamentals",
American Society of Heating,
Refrigerating and Air Conditioning
Engineers, New York, 1972.
- A.S.M.E.,
1959
AMERICAN SOCIETY of MECHANICAL
ENGINEERS,
"Fluid Meters, their Theory and
Application",
American Society of Mechanical
Engineers, New York, 1959.
- Bahnfleth,
1957
BAHNFLETH, D.R., MOSELEY, T.D. and
HARRIS, W.S.,
"Measurements of Infiltration in Two
Residences",
A.S.H.A.E. Trans., Vol. 63, 1957.
- Pailey,
1943
BAILEY, A. and VINCENT, N.D.G.,
"Wind Pressure on Buildings Including
the Effects of Adjacent Buildings",
Jnl. Inst. C.E., Vol. 20(8), 1943.
- Baines,
1965
BAINES, W.D.
"Effects of Velocity Distribution on
Wind Loads and Flow Patterns on
Buildings",
Conference proceedings, "Wind Effects
on Buildings and Structures", National
Physical Laboratory, 26-28 June, 1963.
- Bedford,
1943
BEDFORD, T, WARNER, C.G. and
CHRENKO, F.A.,
"Observations on the Natural
Ventilation of Dwellings",
R.I.B.A. Jnl., Vol. 51, 1943-44.
- Best,
1952
BEST, A.C., KNIGHTING, E., PEDLOW, R.
and STORMONT, K.,
"Temperature and Humidity Gradients in
the First 100 Metres Over South-East
England",
Meteorological Office, Geophysical
Memoirs, No. 89, 1952.
- Billington,
1966
BILLINGTON, N.S.,
"Some Aspects of Heating Design",
H.V.R.A., Laboratory Report, No. 35,
Oct. 1966.

Bogoslovskii,
1967

BOGOSLOVSKII, V.N. and TITOV, V.P.,
"Air Conditioning of Buildings and Allowance for Air Penetration in Calculation of the Heating Duty",
Kuibyshev Institute of Building,
Moscow, Collection 52, 1967 and
H.V.R.A. Translation No. 134.

B.R.S.,
1970

BUILDING RESEARCH STATION,
"The Assessment of Wind Loads",
B.R.S. Digest 119, July 1970.

B.S.I.,
1964

BRITISH STANDARDS INSTITUTION,
"Methods of Measurement of Fluid Flow in Pipes - Orifice Plates, Nozzles and Venturi Tubes",
B.S. 1042, Part 1, 1964.

B.S.I.,
1971

BRITISH STANDARDS INSTITUTION,
"Recommendations for the Grading of Windows",
Draft for Development, 4:1971.

Carne,
1945

CARNE, J.B.,
"The Natural Ventilation of Unheated Closed Rooms",
Jnl. Hygiene, Vol. 44, 1945-46.

Chandler,
1965

CHANDLER, T.J.,
"The Climate of London",
Hutchinson, London, 1965.

Chien,
1951

CHIEN, N., FENG, Y., WANG, H. and SIAO, T.,
"Wind Tunnel Studies of Pressure Distribution on Elementary Building Forms",
Iowa Institute of Hydraulic Research,
Iowa City, U.S.A., 1951.

Coblentz,
1963

COBLENTZ, C.W. and ACHENBACH, P.R.,
"Field Measurements of Air Infiltration in Ten Electrically Heated Houses",
A.S.H.R.A.E. Jnl., Vol. 5, 1963.

Dalgleish,
1967

DALGLEISH, W.A., WRIGHT, W. and SCHRIEVER, W.R.,
"Wind Pressure Measurements on a Full-Scale High-Rise Office Building",
Conference proceedings, "Wind Effects on Buildings and Structures", Ottawa, Canada, 11-15 Sept., 1967.

- Davenport,
1965 a DAVENPORT, A.G.,
"The Relationship of Wind Structure
to Wind Loading",
Conference proceedings, "Wind Effects
on Structures", National Physical
Laboratory, 1965.
- Davenport,
1965 b DAVENPORT, A.G.,
"Wind Loads on Structures",
Div. of Building Research, Ottawa,
Canada, Technical Paper No. 88.
- Davenport,
1967 DAVENPORT, A.G.,
"The Dependence of Wind Loads on
Meteorological Parameters",
Conference proceedings, "Wind Effects
on Buildings and Structures", Ottawa,
Canada, Sept. 1967.
- Dick,
1949 DICK, J.B.,
"Experimental Studies in the Natural
Ventilation of Houses",
J.I.H.V.E., Vol. 17, 1949.
- Dick,
1950 DICK, J.B.,
"The Fundamentals of Natural
Ventilation of Houses",
J.I.H.V.E., Vol. 18, 1950.
- Dick,
1951 DICK, J.B.,
"Ventilation Research in Occupied
Houses",
J.I.H.V.E., Vol. 19, 1951.
- Dick,
1953 DECK, J.B. and THOMAS, D.A.,
"Air Infiltration Through Gaps Around
Windows",
J.I.H.V.E., Vol. 21, 1953.
- Ford,
1973 FORD, R.D. and KERRY, G.,
"The Sound Insulation of Partially
Open Double Glazing",
Applied Acoustics, Vol. 6, 1973.
- Gabriellson,
1968 GABRIELLSON, J. and PORRA, P.,
"Calculation of Infiltration and
Transmission Heat Loss in Residential
Buildings by Digital Computer",
J.I.H.V.E., Vol. 35, 1968.
- Geiger,
1966 GEIGER, R.,
"The Climate Near the Ground",
Harvard University Press, Cambridge,
Massachusetts, 1966.

- Givoni, 1962 GIVONI, B.,
"Basic Study of Ventilation Problems in Hot Countries - Final Report", Israel Institute of Technology, Building Research Station, Technion City, 1962.
- Harris, 1970 HARRIS, R.I.,
"The Nature of Wind", Inst. C.E., Seminar Proceedings, "The Modern Design of Wind Sensitive Structures", June 1970.
- Harris, 1972 HARRIS, R.I.,
"Measurements of Wind Structure", Proceedings of Symposium on External Flows, University of Bristol, July 1972.
- Harrison, 1962 HARRISON, E.,
H.V.R.A. Technical Report
"The Heating of Buildings by Off-Peak Electricity Supplies", Appendix 2, "Air Infiltration into Heated Buildings", J.I.H.V.E., Vol. 29, 1961.
- Hitchin, 1967 HITCHIN, E.R. and WILSON, C.B.,
"A Review of Experimental Techniques for the Investigation of Natural Ventilation in Buildings", Building Science, Vol. 2, 1967.
- Howard, 1966 HOWARD, J.S.,
"Ventilation Measurements in Houses and the Influence of Wall Ventilators", Building Science, Vol. 1, 1966.
- Humphreys, 1970 a HUMPHREYS, M.A. and NICOL, J.F.,
"An Investigation into the Thermal Comfort of Office Workers", J.I.H.V.E., Vol. 38, 1970 and B.R.S. Current Paper 14/71.
- Humphreys, 1970 b HUMPHREYS, M.A.,
"A Simple Derivation of Thermal Comfort Conditions", J.I.H.V.E., Vol. 38, 1970 and B.R.S. Current Paper 14/71.
- I.H.V.E., 1970 INSTITUTION OF HEATING AND VENTILATING ENGINEERS,
"I.H.V.E. Guide, 1970, Book A; Design Data", I.H.V.E., London, 1971.

Jackman, 1968 JACKMAN, P.J. and DEN OUDEN, H.,
 "The Natural Ventilation of Tall Office Buildings",
 Research Institute for Public Health Engineering, T.N.O., Delft, Publication 304.

Jackman, 1969 JACKMAN, P.J.,
 "A Study of the Natural Ventilation of Tall Office Buildings",
 H.V.R.A. Laboratory Report, No. 53, 1969.

Jackman, 1971 JACKMAN, P.J.,
 Private Communication with Professor J.K. Page,
 December 1971.

Jensen, 1963 JENSEN, M. and FRANCK, N.,
 "Model-Scale Tests in Turbulent Wind",
 Part 1, The Danish Technical Press, Copenhagen, 1963.

Johnson, 1948 JOHNSON, N.K.,
 "The Vertical Gradient of Wind Velocity in the Lowest Layers of the Atmosphere",
 Meteorological Office, Professional Notes, No. 91, 1948.

Jordan, 1963 JORDAN, R.C., ERICKSON, G.A. and LEONARD, R.R.,
 "Infiltration Measurements in Two Occupied Houses",
 A.S.H.R.A.E. Jnl., Vol. 5, 1963.

Karulek, 1970 KARULEK, J.,
 "Air Exchange in Multi-Storey Buildings",
 Ciep. Ogr. Went. March 1970 and H.V.R.A. Translation No. 216.

Kibblewhite, 1967 KIBBLEWHITE, D. and STEWART, L.J.,
 "A Survey of the Thermal Environment of Naturally Ventilated Offices",
 J.I.H.V.E., Vol. 35, 1967.

Kreith, 1957 KREITH, F. and EISENSTADT, R.,
 "Pressure Drop and Flow Characteristics of Short Capillary Tubes at Low Reynolds Numbers",
 A.S.M.E. Trans., Vol 79(2), July 1957.

Kurek, 1965 KUREK, E.J.,
 "Pressurisation, Convection and Air Flow Inside Buildings",
 A.S.H.R.A.E. Jnl., Vol. 7, 1965.

Lacy,
1972 LACY, R.E.,
"Survey of Meteorological Information
for Architecture and Building",
B.R.S. Current Paper 5/72.

Langdon,
1965 LANGDON, F.J.,
"Thermal Conditions in Offices",
R.I.B.A. Jnl., Vol. 72, 1965.

Langdon,
1970 LANGDON, F.J. and LOUDON, A.G.,
"Discomfort in Schools from Overheating
in Summer",
J.I.H.V.E., Vol. 37, 1970 and B.R.S.
Current Paper 19/70.

Lawson,
1968 LAWSON, T.,
"Architects Journal Handbook of
Building Environment, Section 3, Air
Movement and Natural Ventilation",
Architects Journal, Nov. 1968.

Lenkei,
1965 LENKEI, A.,
"Close Clearance Orifices",
Product Engineering, April 1965.

Lidwell,
1960 a LIDWELL, O.M.,
"The Evaluation of Ventilation",
Jnl. Hygiene, Vol. 58, 1960.

Lidwell,
1960 b LIDWELL, O.M. and WILLIAMS, R.E.,
"The Ventilation of Operating Theatres",
Jnl. Hygiene, Vol. 58, 1960.

Loudon,
1968 LOUDON, A.G.,
"Summertime Temperatures in Buildings",
I.H.V.E./B.R.S. Symposium, "Thermal
Environment in Modern Buildings",
February 29, 1968 and B.R.S. Current
Paper 47/68.

Malinowski,
1971 MALINOWSKI, H.K.,
"Wind Effect on Air Movement Inside
Buildings",
3rd International Conference on Buildings
and Structures, Tokyo, 1971.

Meckler,
1967 MECKLER, M.,
"How to Determine Building Infiltration
Rates at Low Reynolds Numbers",
Heating, Piping and Air Conditioning,
March 1967.

M.O.,
1968 METEOROLOGICAL OFFICE,
"Tables of Surface Wind Speed and
Direction over the United Kingdom",
Meteorological Office, H.M.S.O., London,
1968.

- Nelson,
1971
- NELSON, L. (LOKMANHEKIM, Ed.),
Procedure for Determining Heating and
Cooling Loads for Computerised Energy
Calculations "An Algorithm for
Infiltration Rate Calculations",
A.S.H.R.A.E. Task Group on Energy
Requirements for Heating and Cooling,
1971.
- Newberry,
1968
- NEWBERRY, C.W., EATON, K.J. and
MAYNE, J.R.,
"Wind Loading of a Tall Building in an
Urban Environment",
Conference proceedings, "Wind Effects
on Buildings and Structures",
Loughborough, 2-4 April, 1968 and B.R.S.
Current Paper 59/68.
- Page,
1971
- PAGE, J.K.,
Unpublished manuscript presenting results
of bivariate analysis of hourly wind
speed and hourly temperature for a
site at Abbots Langley, 1949-1950.
- Rajagopalan,
1963
- RAJAGOPALAN, P.R. and RAO, K.R.,
"Studies on the Natural Ventilation of
Buildings by the Hydraulic Analogue
Method",
Jnl. Indian Architect, Feb. 1963.
- Rogelein,
1967
- ROGELEIN, W.,
"Determination of the Ventilation Heat-
Load Caused by Wind on Tall Buildings",
Heiz. Luft. Haustechn., Vol. 18, 1967
and H.V.R.A. Translation No. 139.
- Sasaki,
1965
- SASAKI, J.R. and WILSON, A.G.,
"Air Leakage Values for Residential
Windows",
A.S.H.R.A.E., 72nd Annual Meeting,
Portland, Ore., July 1965.
- Smith,
1951
- SMITH, E.G.,
"The Feasibility of Using Models for
Pre-determining Natural Ventilation",
Texas Engineering Experimental Station,
Research Report No. 26, 1951.
- Svetlov,
1966
- SVETLOV, K.S.,
"Computers for Calculating Air Exchange
in Multi-Storey Buildings",
Vodos. Sanit. Tech., Vol. 11, 1966 and
H.V.R.A. Translation No. 122.

- Tamura, 1963 TAMURA, G.T. and WILSON, A.G.,
"Air Leakage and Pressure Measurements
on Two Occupied Houses",
A.S.H.R.A.E. Jnl., Vol. 5, 1963.
- Tamura, 1969 TAMURA, G.T.,
"Computer Analysis of Smoke Movement
in Tall Buildings",
A.S.H.R.A.E. Trans., Vol. 75, 1969.
- Tamura, 1970 TAMURA, G.T. and WILSON, A.G.,
"Natural Venting to Control Smoke
Movement in Buildings via Vertical
Shafts",
A.S.H.R.A.E. Trans., Vol. 76, 1970.
- Van Ackere, 1970 VAN ACKERE, C.P.,
"L'elancheite des Chassis de Fenêtres",
C.S.T.C. Revue, Jan. 1970.
- Van den Hoven, 1957 VAN DEN HOVEN, I.,
"Power Spectrum of Horizontal Wind
Speed.....",
Jnl. Meteorology, Vol. 14, 1957.
- Waller, 1968 WALLER, R., DUKES, T. and DALLEY, E.,
"A Comparison Between the Quality of
the Techniques and the Data Available
to the Environmental Designer With
Regard to Wind Loading",
Conference proceedings "Wind Effects on
Buildings and Structures", Loughborough,
1968.
- Wannerberg, 1957 WANNERBERG, J.S. and VAN STRAATEN, J.F.,
"Wind Tunnel Tests on Scale Model
Buildings",
J.I.H.V.E., Vol. 24, 1957.
- Whitbread, 1965 WHITBREAD, R.E.,
"Model Simulation of Wind Effects on
Structures",
Conference proceedings, "Wind Effects
on Buildings and Structures", National
Physical Laboratory, 26-28 June, 1965.
- Wilson, 1963 WILSON, SIR A. (Chairman),
"Noise, Final Report of the Committee on
the Problem of Noise",
H.M.S.O., London, 1963.
- Wise, 1973. WISE, A.F.E.,
"Designing Offices Against Traffic Noise -
Environmental Standards, Design Principles
and Engineering Requirements",
Building Services Engineer, Vol. 40,
1973 and B.R.S. Current Paper, 6/73.